Ph.D CHEMISTRY

W. R. Summers

REACTIONS OF GASEOUS HALOCARBONS WITH CLEAN TITANIUM SURFACES

A B S T R A C T

The reactions of several series of alkyl halides with atomically clean titanium films have been investigated. Two groups of reactions have been found.

Reactions of the first group occurred extremely rapidly on virgin films at low temperature. Reactions of the second group occurred subsequent to an initial, virgin film reaction, and normally proceeded at elevated temperatures.

The second group was divided into two subgroups. The first subgroup consisted of the noncatalytic reactions of alkyl halides to produce mixtures of olefin and paraffin with loss of halide and some hydride into the bulk of the film. The second subgroup consisted of catalytic, dehydrohalogenation reactions of alkyl halides to give gaseous hydrogen halide and olefin. In the case of certain reactants, these reactions proceeded on a competitive basis.

Kinetics were determined and apparent activation energies were measured for most reactions.

short title

GASEOUS HALOCARBON REACTIONS ON CLEAN TITANIUM SURFACES

W. R. SUMMERS

REACTIONS OF GASEOUS HALOCARBONS WITH CLEAN TITANIUM SURFACES

by

Wayne Richard Summers
B.Sc. (Hons), University of British Columbia, 1965

A thesis submitted to the Faculty of Graduate Studies and Research in partial fulfilment of the requirements for the degree of Doctor of Philosophy

Department of Chemistry,
McGill University,
Montreal, Canada

June, 1970

ACKNOWLEDGEMENTS

I wish to express my gratitude to Dr. J. F. Harrod for his constant interest and encouragement during the course of this work.

Financial assistance from The National Research Council of Canada during 1968-1969 and 1969-1970 is also gratefully acknowledged.

Ph.D CHEMISTRY

W. R. Summers

REACTIONS OF GASEOUS HALOCARBONS WITH CLEAN TITANIUM SURFACES

A B S T R A C T

The reactions of several series of alkyl halides with atomically clean titanium films have been investigated. Two groups of reactions have been found.

Reactions of the first group occurred extremely rapidly on virgin films at low temperature. Reactions of the second group occurred subsequent to an initial, virgin film reaction, and normally proceeded at elevated temperatures.

The second group was divided into two subgroups. The first subgroup consisted of the noncatalytic reactions of alkyl halides to produce mixtures of olefin and paraffin with loss of halide and some hydride into the bulk of the film. The second subgroup consisted of catalytic, dehydrohalogenation reactions of alkyl halides to give gaseous hydrogen halide and olefin. In the case of certain reactants, these reactions proceeded on a competitive basis.

Kinetics were determined and apparent activation energies were measured for most reactions.

TABLE OF CONTENTS

page

I. INTRODUCTION

II. APPARATUS AND EXPERIMENTAL TECHNIQUES

page

page

page

page

VIII. REFERENCES

LIST OF FIGURES

Figure page

Figure page

LIST OF TABLES

INTRODUCTION

I - 1. Origin of the Problem

In 1965, Matlack and Breslow reported that ballmilling certain transition metals, metal hydrides, divalent metal halides or metal oxides produced active catalysts for polymerization of ethylene (1). Linear, high density polymers, similar to those produced by Ziegler catalysts, were obtained. A reasonable interpretation of these results is that ballmilling produces atomically clean surfaces which, either directly or after reaction with solvent, become active polymerization catalysts. Metals which lack catalytic activity often become active catalysts when an alkyl halide is added to the ballmilling mixture. Others, which are active catalysts, have their catalytic activity enhanced by the addition of an alkyl halide (1). Ray and Ruehlen have reported that titanium metal catalyzes the polymerization of ethylene during ballmilling (2). However, Matlack and Breslow have observed that titanium metal catalyzes the polymerization of ethylene only if an alkyl halide is added to the ballmilling mixture (1).

If the enhancement of catalytic activity which occurs when an alkyl halide is present is the result of oxidation of the clean metal to an alkyl metal halide, then this chemistry obviously should provide a novel approach to Ziegler catalysts. The latter are more conventionally produced by treating a transition metal halide in a high oxidation

state with a reducing, alkylating agent (3).

The present study of reactions of gaseous alkyl halides with titanium films was initiated to try to gain an understanding of the chemical nature of the active polymerization sites proposed by Matlack and Breslow (1). It rapidly became apparent that the reactions of organic halides with metal films would be interesting in their own right and would relate to studies of corrosion and boundary lubrication as well as to Ziegler catalysis. Emphasis therefore was shifted from applications of titanium species to polymer chemistry to a general survey of the chemistry and kinetics of the reactions of several groups of alkyl halides with titanium surfaces. Thus three definable areas and their inter-relationships became pertinent. These were;

i) reactions and interactions at solid-gas interfaces,

ii) the reactivity of the carbon-halogen bond, and

iii) the chemistry of titanium.

I - 2. The Metal-Gas Interface

a) Factors controlling Surface Reactivity

The chemical activity of a surface is dependent on its cleanliness, its area and its chemical nature.

i) Cleanliness

A surface whose composition is representative of bulk material must be and remain, essentially free of contamination for the duration of any study of its physical or chemical

properties. An excellent definition, presented by Allen et al., describes such a surface as, "One free of all but a few percent of a single monolayer of foreign atoms, either adsorbed onto or substitutionally replacing surface atoms of the parent lattice." (4).

The simplest of several methods for producing such a surface is by evaporation of a chemically pure substance and condensation onto a suitable substrate. Evaporation is usually accomplished by some form of heating or by sputtering with inert gas ions.

Once deposited, a film has a clean lifetime which is dependent upon the rate of impingement of gas molecules onto its surface, and therefore upon the pressure of gas above the surface. An equation for calculating the clean lifetime of a surface was derived by Roberts and Vanderslice (5).

$$t_c = \alpha n_m / \beta \nu \qquad (I - 1$$

where t_c is the clean lifetime of the surface in seconds, α is the tolerable contamination level expressed as a fraction of a monolayer (typically about 0.05), n_m is the number of surface sites per monolayer per unit area, and ν is the number of molecules striking a unit area of surface per second. The sticking coefficient, β, is the fraction of molecules striking the surface that remain on it. Typical values of β vary between 0.1 and 1.0.

When ν is converted to a pressure value in torr

and plotted against clean lifetime for a surface, a graph such as that reproduced in figure (I-1) results (6). In this figure, both α and β are equal to 1.0. It can be seen that a vacuum of about 10^{-9} torr is required to maintain a clean surface for a period of a few hours.

Work in this ultrahigh vacuum range necessitates exclusion of high vapour pressure materials such as mercury, manometer oils, and even most sealing greases from the reaction system.

Although it is probable that pressures in this range were achieved as early as 1935 (7), it was not until 1950 that a method for measuring pressures lower than 10^{-8} torr was devised by Bayard and Alpert (8). The inverted or Bayard-Alpert ion gauge measures pressures down to 10^{-11} torr and makes definite statements on surface cleanliness possible. Its introduction undoubtedly is a major cause of the recent marked expansion in the literature of surface chemistry and physics.

ii) Surface Area

Surface area, the second major factor which affects the activity of vapour deposited metal films, has also been extensively investigated.

Although there is no real limit, typical geometric surface areas of metal films usually range from 50 cm.^{2} to 500 cm.^{2}. However, the real or specific area of a film may be many times greater than the geometric area because of surface roughness. A roughness factor may then be defined as the ratio of the

FIGURE (I - 1)

Variation of Clean Surface Time with Pressure.

Reproduced from R. W. Roberts and L. E. St. Pierre, Science, 147, 1529, (1965).

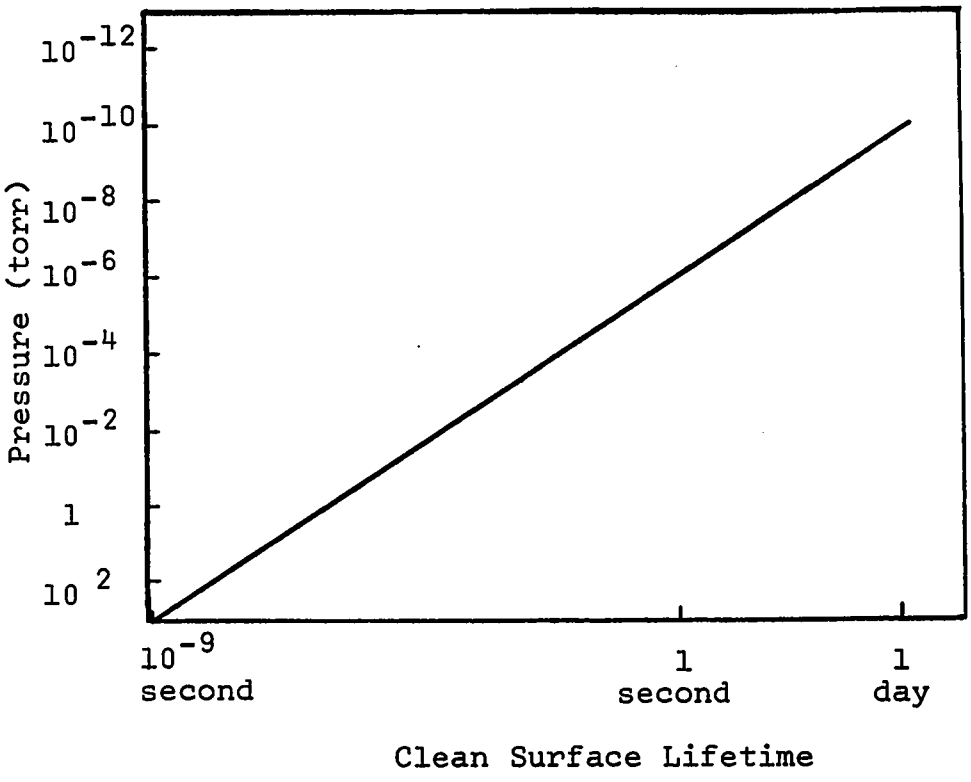
Pressure (torr)
10^-12
10^-10
10^-8
10^-6
10^-4
10^-2
1
10^2
10^-9 second
1 second
1 day
Clean Surface Lifetime

specific area upon the geometric area. The magnitude of the roughness factor depends on many variables. It will be close to unity for a low melting metal such as sodium, and if other variables are held constant, will increase with increasing melting point through a series of metals. For example, on an ambient temperature substrate, one will find roughness factors of 2.5 for aluminum, 9.0 for rhodium (9), 7.5 for nickel and 14.0 for tungsten (10). Roughness factors tend to decrease with increased rates of film deposition as is illustrated in figure (I-2) (10). With higher melting point metals, increases are also noted with increasing film thickness and with lower melting point metals, decreases are noted with increasing substrate temperature.

The specific surface area of a metal is also sensitive to exposure to reactive gases, which will cause considerable decrease (11). Films that are deposited with large roughness factors are in a metastable state and annealing causes such a film to sinter and hence reduce its specific area. Anderson et. al. (10, 12) have found that nickel films deposited on a pyrex substrate at 273^{o}K have a roughness factor of about 7.5, but after sintering for twenty minutes at 468^{o}K, this reduces to a constant value of 3.5.

Use of electron microscopy to investigate sintering (10) has shown that three mechanisms are involved. Initially, gaps between micro-crystals rapidly disappear, shutting off lower surfaces to access. Secondly, and more slowly,

FIGURE (I - 2)

Variation of Specific Surface Area of Evaporated Metal Films with Rate of Deposition.

o - Nickel

Δ - Tungsten

Reproduced from J. R. Anderson, R. B. Baker and J. V. Sanders, J. Catalysis, 1, 443, (1962).

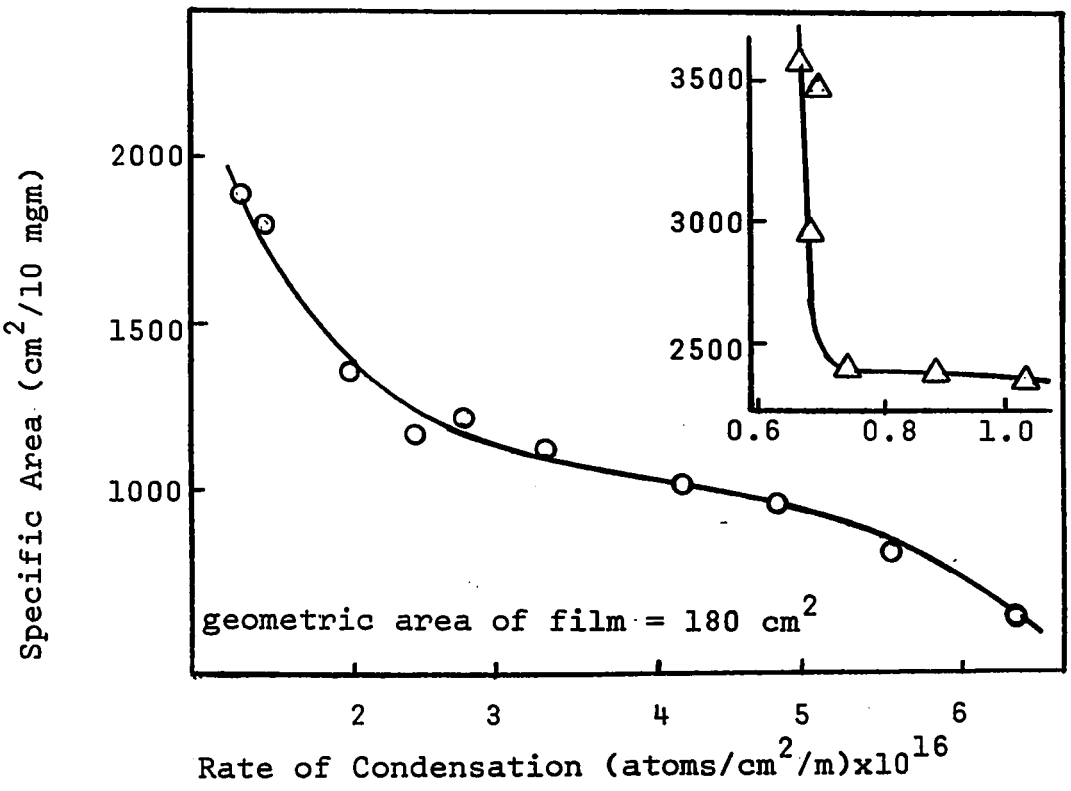
Specific Area (cm^2/10 mgm)
2000
1500
1000
3500
3000
2500
0.6
0.8
1.0
geometric area of film = 180 cm^2
2
3
4
5
6
Rate of Condensation (atoms/cm^2/m)x10^{16}

sintering causes the removal of asperities and probably also of some steps and terraces on crystal faces. Lastly, crystal growth occurs. The first mechanism causes a rapid and marked reduction in specific area, the second causes a slower and less pronounced reduction and the third does not appreciably affect the specific area.

Knowledge of the exact nature of surface sites is slight. There is still controversy concerning whether or not reactivity is possessed uniformly by surface atoms or whether it is associated with surface point defects, edge dislocations, grain boundaries and so forth. On a more macroscopic scale, it has been demonstrated that adsorption will occur preferentially on certain crystal planes rather than on others and that the chemical nature of the adsorption differs on different crystal planes. For example, studies of nitrogen adsorption on tungsten single crystals (13, 14) have shown that different energies of desorption exist for different crystal planes.

b) Classification of Surface Interactions and Reactions

Classification of elementary reactions has been useful in the study of the mechanisms of both inorganic and organic reactions. Such elementary reactions include S_N1 and S_N2 substitution reactions, four centre reactions, radical combinations and so forth.

A restricted classification of elementary surface reactions has been presented by Burwell (15) and provides

a useful terminology for comparing and constrasting proposed mechanisms of surface reactions. The classification is considered to be restricted because it does not distinguish between making (or breaking) a σ-bond and a π-bond; nor is a distinction made between a gas phase molecule and one which is physically adsorbed to the surface.

Five elementary classes are listed with examples.

i) Non-dissociative adsorption, and its reverse, desorption,

e.g., $S + NH_3 \rightleftarrows S\text{-}NH_3$. (I - 2

ii) Dissociative adsorption, and its reverse, associative desorption,

e.g., $2\,S + H_2 \rightleftarrows 2\,S\text{-}H$. (I - 3

iii) Dissociative surface reaction, and its reverse, associative surface reaction,

e.g., $2\,S + S\text{-}CH_2CH_3 \rightleftarrows S\text{-}H + S\text{-}CH_2CH_2\text{-}S$. (I - 4

iv) Reactive adsorption, and its reverse, reactive desorption,

e.g., $S\text{-}H + CH_2{=}CH_2 \rightleftarrows S\text{-}CH_2CH_3$ (I - 5

v) Quasisorbed reaction,

e.g., $2\,S\text{-}H + CH_2{=}CH_2 \rightleftarrows CH_3\text{-}CH_3 + 2\,S$. (I - 6

The only term which may require clarification is quasisorbed, which refers to the direct reaction of a gas molecule with a surface species without preliminary chemisorption of the molecule. It is associated with the surface only in a transition state complex which desorbs as it forms.

c) Scope of Studies of Surface Interactions and Reactions

Interactions which occur between metal surfaces and their ambient atmospheres include many phenomena of considerable academic and technological importance. A large volume of literature exists relating to areas such as;

i) adsorption, desorption and chemical exchange studies (16);

ii) boundary lubrication studies (17);

iii) oxidation and corrosion studies (18, 19);

iv) catalytic reactions such as cracking, hydrogenation, isomerization and hydrogenolysis (20);

v) comparative studies of various metals within each of the above areas (16-20).

It is interesting to note that rather few references exist relating to dehydrohalogenation reactions on metal surfaces, and those that do, are usually to dehydrohalogenation as a side reaction during hydrogenolysis of carbon-halogen bonds.

d) General Studies of Surface Interactions and Reactions

Trapnell has investigated the chemisorption activity of twenty-two main group and transition metals, including titanium, with a series of six gases, and has established an order of affinity of gases which is common to all metal surfaces (21). The ordering of affinities is

$$O_2 > C_2H_2 > C_2H_4 > C{\equiv}O > H_2 > N_2.$$

It was found, with one exception, that if a metal chemisorbs

a particular gas, it will also chemisorb all gases higher in the ordering; if it does not chemisorb a gas, it will not chemisorb any gas lower in the ordering. Titanium was found to chemisorb all gases tested instantaneously and irreversibly at room temperature so that more than fifty percent of the geometric area of the film was covered and an immeasurably low gas pressure resulted. Except for oxygen chemisorption, which was thought to be controlled by the metal work function, Trapnell related chemisorptive activity to the presence of energetically available, but unoccupied, d-orbitals. Thus titanium, with its many available, empty d-orbitals, chemisorbs all gases; nickel adsorbed all except nitrogen (metals between titanium and nickel in the first transition series were not examined); copper adsorbed all but nitrogen and hydrogen; and zinc adsorbed only oxygen.

The adsorption and, in some cases, decomposition of methane and ethane have been studied on various transition metals, including titanium. Trapnell has measured adsorption of methane and ethane on titanium (22) throughout a temperature cycle from -78°C to +70°C and then back to -78°C. Adsorption of both gases was increased by increased temperatures but was not decreased by a subsequent temperature decrease. Ethane was more extensively adsorbed than methane, reaching a maximum θ of about 0.35 compared to a maximum of about 0.25 for methane, where θ is defined as the covered fraction of available surface sites. No hydrogen or other gas phase

products were detected.

In a similar study, Roberts reported that titanium adsorbed ethane at both 27°C and 100°C but yielded no gas phase products at either temperature (23). It is interesting to note that Roberts did detect hydrogen as a decomposition product during the adsorption of ethane on vanadium at 100°C but not at 27°C. He also found that adsorption was enhanced by increased temperature. Metals which decomposed ethane were divided into two classes. Tungsten, molybdenum and vanadium, all of which form carbides, gave hydrogen as a decomposition product. Rhodium, iridum and rhenium, which do not form carbides, gave methane as a major decomposition product.

Roberts suggested that for the cases where adsorption occurred but no decomposition products appeared (titanium, nickel, iron, palladium and platinum), all adsorbed species must be strongly bonded to the surface. Both Trapnell and Roberts suggested the possibility of hydride diffusion into the metal lattice in the case of titanium (22, 23).

A study of oxygen adsorption on titanium films at 25°C has shown that the limiting amount of oxygen adsorbed is dependent on film thickness. At 1.8×10^{-7} torr, the rate of oxygen uptake is fast initially but rapidly levels to a value near zero (24).

Several studies of the reactions of halogens with titanium have been reported. From a technological point of

view the reactions of iodine with titanium and other metals are of particular interest. Iodine, dissolved in n-butylbenzene, forms a charge transfer complex which will act as a boundary lubricant by reacting with a fresh titanium surface, generated by wear, to produce titanium(II) iodide (25, 26). Lubrication is a result of the lamellar structure of the metal iodide. In fact, metals which do not form lamellar metal iodides are not lubricated by iodine. The n-butylbenzene serves as a hydrophobic agent to protect the lubricating layer from decomposition by atmospheric moisture. A study of friction coefficient as a function of temperature has shown that the metal iodide acts as an efficient lubricant until about 400°C at which temperature the friction coefficient rises sharply. Loss of the lubricating titanium iodide lamellar structure was attributed to the preferred formation of a volatile titanium(IV) iodide species at the latter temperature (26).

Because of their deliquescent nature, metal iodides had not been positively identified at worn interfaces until a recent X-ray diffraction study of a carefully protected wear track on a nickel specimen revealed the presence of $NiI_2 \cdot 6H_2O$ (27).

A study of adsorption isotherms for iodine on evaporated tungsten films by Campbell et. al. (28) at 0°C, 150°C and 300°C indicated that at 300°C some process other than adsorption was occurring. Campbell suggested that a bulk iodide may have been forming at this temperature.

Halogen and oxygen interactions with metal surfaces have also been studied by following changes in the metal work function. The work function of a metal, the energy required to remove an electron from its surface, will change when gas is adsorbed onto the surface. The chemisorbed species has a dipole, and if the negative pole is outward, then the work function increases, if the positive pole is outward, then the work function decreases. Thus one would expect the adsorption of oxygen, or a halogen, to increase the work function. This increase is found at high coverage, but in many cases, not before the work function initially undergoes a significant decrease at low coverage. The decrease in work function, caused by a positive surface dipole, is attributed to penetration beyond the metal surface, into the lattice, by the adsorbed electronegative species. The eventual build up of true surface species causes the later increase in work function.

Using field emission microscopy, Duell et. al. (29, 30) observed initial work function decreases followed by increases during the adsorption of chlorine and bromine on tungsten. The results were the same whether the surface chloride originated from molecular chlorine or from carbon tetrachloride or chloroform. It was also observed that adsorbed chloride could be removed by reaction with methane although the desorbed product was not identified. Initial work function decreases have also been observed during the

adsorption of chlorine on nickel films (31) and on titanium films (32).

The concept of the penetration of electronegative gases below the surface layers of metals originated with Burshtein, Surova and Shurmovskaya, who noted that the phenomenon is sensitive to the size of the penetrating species (33, 34). For example, the adsorption of oxygen or fluorine on iron produces an initial positive surface potential whereas chlorine and iodine produced only negative surface potentials. Surface penetration must also be temperature dependent since those species that are too large for penetration at one temperature are able to do so at higher temperatures. An example of this behaviour is reported by Quinn and Roberts for oxygen on nickel, copper and iron in the temperature range -195°C to +25°C (35).

e) Reactions of Alkyl Halides with Metals

i) Direct Reactions

The most fundamental preparative method in organometallic chemistry, upon which depends the synthesis, either directly or indirectly, of many organometallic compounds, is the reaction of an electropositive metal with an organic halide to yield a product containing a carbon to metal bond (36).

$$2\,M + n\,R\text{-}X \rightarrow R_n\text{-}M + M\text{-}X_n \text{ (or } 2\,R_n\text{-}M\text{-}X_n) \quad \text{(I - 7}$$

As a general rule, in order to be useful, such reactions must yield a product that is soluble or sufficiently easily

detached from the metal surface to allow complete reaction.

This reaction has provided an important, direct route to many main group organometallic compounds. In fact, the first organometallic compounds ever prepared, ethylzinc iodide and diethylzinc were made by this method (37). Organo-derivatives of lithium, aluminum and magnesium, which are very important in synthetic organic chemistry are usually prepared by this reaction. The reaction can be extended to many other main group metals and metalloids by using metal couples and alloys. Thus, alkylsilicon halides may be prepared in the presence of copper at elevated temperatures where it is postulated that a transient cuprous alkyl is first formed and the alkyl group is subsequently transferred to the silicon. Evidence for the existence of a volatile transient Cu(I)-CH_3 species has been presented by Hurd and Rochow who demonstrated that a copper mirror may be transported along a glass tube by a stream of methyl chloride at 250°C (38). Lead tetraalkyls are prepared by reaction of an alkyl halide with a lead-sodium alloy, where the highly exothermic heat of formation for the sodium halide provides the thermo-dynamic force for the reaction.

The generally high reactivity of transition metals towards other molecules leads to the expectation that they should react readily with organic halides. When these reactions are attempted, any alkylmetal halide which might form is of limited stability and almost always short-lived (39, 40).

Some interesting exceptions to this statement exist. For example, refluxing allyl bromide on palladium sponge, under nitrogen, forms di-μ-bromobis(π-allyl)dipalladium (41).

Few surface studies of direct, gaseous alkyl halide reactions with metals have been reported. Simple hydrocarbon coupling products were reported for reactions of gaseous alkyl halides with lithium (42) and magnesium (43) surfaces.

Studies of the adsorption of methyl chloride and methylene chloride and of their desorption products have been reported by McConkney and Anderson for a variety of metal films, but with particular emphasis on sodium (44), and titanium and palladium (45). They found that the principal desorption products from adsorption on a virgin sodium film were methane and ethane for methyl chloride, and methane and ethylene for methylene chloride. All chloride was lost to the film. At temperatures between 20°C and 60°C and at pressures between 0.3 and 1.2 torr, extensive reaction of gaseous methyl chloride occurred giving ethane as the principal product and only small amounts of methane. All the chloride and about half the carbon was lost to the film during this reaction.

At temperatures between 0°C and 250°C, the products resulting from the reactions between methyl chloride and films of nickel, copper, platinum, cobalt, manganese, aluminum or silver were methane and hydrogen. The reaction between methyl chloride and titanium or palladium films produced

methane but no hydrogen. Methyl chloride on titanium also produced quantities of ethane and ethylene, and on palladium produced traces of ethane. However, methylene chloride on palladium produced methane and as much as one third ethane, whilst on titanium the products were methane, ethylene and a residual organic polymeric film. With both reactants, considerable carbon was lost to the films, although further product desorption could be enhanced by treatment with hydrogen.

ii) Hydrogenolysis Reactions

An extensive calorimetric study of the hydrogenolysis of several alkyl chlorides and fluorides over a palladium on carbon catalyst has been reported by Lacher et. al. (46). Although the heats of reactions of the fluorides were found to be more exothermic than those of the corresponding chlorides by four or five kilocalories, their reactions nonetheless proceeded more slowly and with greater difficulty than the reactions of the chlorides. The slower rates of the fluorides were attributed to a greater activation energy associated with the higher carbon-fluorine bond strength.

Deuteriolyses of n-propyl chloride and isopropyl chloride, using deuterium to propyl chloride ratios of about 10 and 23, over a palladium-pumice catalyst have been reported by Addy and Bond (47). Deuterium pressures of 135±6 torr were used and reactions were followed to a maximum 25 percent conversion. In both cases, the reaction was found to be first order in propyl chloride concentration, with isopropyl chloride

reacting about four times faster than n-propyl chloride.

Hydrogenolyses of ethyl chloride and ethyl bromide over evaporated metal films of platinum, palladium, nickel, iron, tungsten and rhodium have been reported by Kemball and Campbell (48). They have also reported a study of the hydrogenolysis of t-butyl chloride on platinum, palladium, nickel and iron films (49). On platinum and palladium all reactants produced their corresponding alkane and hydrogen halide. On nickel and iron, t-butyl chloride reacted to give isobutylene and hydrogen chloride. The reverse process, isobutylene and hydrogen chloride reacting on nickel to give t-butyl chloride, was also reported. Ethyl bromide and ethyl chloride on nickel, iron, tungsten or rhodium, produced mixtures of ethane, ethylene and hydrogen halide.

Deuteriolysis studies indicated that different modes of adsorption occurred on different metals and for different reactants. Ethyl bromide on nickel, or iron, gave almost exclusively monodeuterioethane with minor amounts of dideuterioethane. Rhodium, platinum and palladium produced large amounts of dideuterioethane, and little or none of the monodeuterio- product. Ethyl chloride also reacted over nickel or iron films to form primarily monodeuterioethane. However it produced larger quantities of the dideuterio- product than were formed by ethyl bromide. Both rhodium and palladium produced large amounts of dideuterioethane. Platinum however, produced equal amounts of mono- and dideuterioethane. All

surfaces also produced minor amounts of tri-, tetra-, penta- and hexadeuterioethanes.

In all cases, the dideuterio product was analyzed as about 90 percent 1,1-dideuterioethane. Rates of disappearance of all reactants were first order in alkyl halide concentration. The rate was also found to be approximately proportional to the reciprocal of the hydrogen halide concentration. Reaction of t-butyl chloride was much more rapid than that of ethyl chloride or bromide.

In studies of the hydrogenolysis of methyl chloride on titanium, McConkney and Anderson (45) found a first order dependence on the concentrations of both hydrogen and methyl chloride. Neither caused the rate to pass through a maximum. They concluded that the reaction most probably proceeds by a path in which the reactants do not compete for the same surface sites.

Deuteriolysis of methyl chloride over palladium or titanium gave methane d_1. Methylene chloride gave methyl chloride d_0 initially and then methane d_1.

iii) Halide Exchange Reactions

As a result of their study of methyl chloride reactions on titanium, McConkney and Anderson concluded that a mixture of ^{35}Cl enriched methyl chloride and ^{13}C methyl chloride at 300°C did not undergo isotopic scrambling. For this reason they suggested that carbon-chlorine bond rupture was irreversible.

Exchange reactions of halide in methyl chloride or

bromide with halide chemisorbed on metal films have also been studied by Coeckelbergs et al. using radio-tracer techniques (50-53). Exchange was found to occur between methyl chloride and ^{36}Cl-hydrogen chloride on tungsten (50, 51) and molybdenum films (52). Exchange was also observed between ^{80}Br which was chemisorbed on aluminum or gold films, and methyl bromide (53).

During the investigation of the exchange of ^{36}Cl on tungsten films, it was found that a mixture of hydrogen chloride and methyl chloride, or hydrogen chloride alone, reacted on the film at 262°C to produce hydrogen. Methyl chloride, over tungsten at 262°C, in the absence of hydrogen chloride, produced methane. Coeckelbergs proposed that the exchange reaction may have occurred by either of two possible mechanisms. One possible alternative which he suggested was a Hinschelwood mechanism. This mechanism proposes a dissociative adsorption and an associative desorption of the methyl chloride molecule. The other possible alternative was a quasisorbed mechanism wherein gaseous or physisorbed hydrogen chloride or methyl chloride interact with a chemisorbed chloride species.

On nickel or iron films, the reaction of t-butyl chloride produced isobutylene and hydrogen chloride, even in the presence of hydrogen (49). Since the reverse process also occurs (49), there can be little doubt that, in these cases, rupture of the carbon-chlorine bond is reversible.

f) Analogies between Surface and Homogeneous Species

It has already been stated that transition metal alkyls, formed by the direct reaction of an alkyl halide with a transition metal surface, are of limited stability and short-lived (39, 40). Such metal alkyl complexes do exist, however, in the presence of stabilizing ligands. It is not unreasonable to expect that transient organometallic surface species should have a chemistry which, in many respects, resembles that of transition metal-alkyl complexes in solution. Such similarities have been noted for more stable surface species. In fact, the identification of chemisorbed surface species by infra-red spectroscopy, particularly carbonyls, hydrides and olefins has been helped, in many cases, by comparison with the spectra of analogous molecular species in solution (54, 55). Rooney has invoked π-bonding of olefins and arenes to metals in molecular complexes as a model for surface intermediates of several catalytic exchange reactions on metal films (56).

More recently, Collman has commented on the similarity between oxidative additions to square planar d^8 complexes and dissociative chemisorption at transition metal surfaces as key steps in several catalytic processes (57). Indeed, the great number of transient complexes between hydrocarbon fragments and transition metal surfaces being proposed to explain heterogeneous reactions has been matched by a similar proliferation of transition metal complexes in solution.

Examples of such complexes result when methyl iodide undergoes oxidative addition to $IrCl(CO)\{(C_6H_5)_3P\}_2$ or $RhCl(CO)\{(C_6H_5)_3P\}_2$ (58).

Burwell and Peri, although in agreement with the usefulness of intercomparison of surface and solution reactions, point out that metal surfaces with their wide array of surface orbitals, provide opportunities for polynuclear bonding which are not available in mononuclear complexes. Therefore identical chemistry should not necessarily be expected from both systems (59).

I - 3. Trends in Carbon-Halogen Bond Reactivity

Campbell and Kemball have shown that the ease of hydrogenolysis of alkyl chlorides on palladium follows the order, t-butyl >> isopropyl > n-propyl ≈ ethyl (49).

Coates et al. have made some useful deductions from thermochemical considerations of the reactions of methyl halides with main group elements (60). Since most transition metals are at least as reactive as main group metals, these deductions should also be applicable to them. The primary difference between the two groups should be the stability of the metal alkyl products.

Coates et al. considered the reaction of methyl chloride with various elements in the manner illustrated by equation (I-8.

$$2\ M + n\ CH_3\text{-}Cl \rightarrow M\text{-}(CH_3)_n + M\text{-}Cl_n \qquad (I - 8$$

It was recognized that other products, as illustrated by equation (I-9, may have been thermodynamically more favourable.

$$2\ M + n\ CH_3Cl \rightarrow Cl_m\text{-}M\text{-}(CH_3)_{n-m} + Cl_{(n-m)}\text{-}M\text{-}(CH_3)_m \qquad (I - 9$$

However, for purposes of simplicity, Coates ignored the possibility that mixed products might occur. Within the main group elements, reaction (I-8 is exothermic except for carbon, nitrogen, oxygen, mercury, thallium, lead and bismuth. The primary driving force for the reaction is the strongly exothermic formation of the metal chloride. This is particularly true for the II-B group, zinc, cadmium and mercury where in each case the methyls are endothermic compounds. In fact, the methyls of mercury, thallium, lead and bismuth are so strongly endothermic that their unfavourable heats of formation are not outweighed by the exothermic formation of the metal chloride and they therefore do not react directly with methyl chloride.

The many mechanisms of the various reactions and the variety of conditions under which they occur, indicate that kinetic as well as thermodynamic factors must be considered. Calculated heats of reactions of methyl halides with metals suggest that the fluoride should react most exothermically. In practice however, methyl fluoride has been found to react by far the most reluctantly. The activation energies of these reactions are most likely related to strength of the carbon-halogen bond which must be broken. Thus as bond strength decreases, reactivity increases and the observed relative

reactivities for the methyl halides are fluoride << chloride < bromide < iodide (60). It is well known that the ease of formation of Grignard reagents follows this sequence. Maccoll has pointed out that unimolecular decomposition reactions of alkyl halides also follow this sequence (61). Large increases in reactivity occur as methyl groups replace hydrogens α to the halide species. Maccoll has also noted that small but real increases in reactivity also result when methyl groups replace hydrogens β to the halide species (61).

I - 4. Organotitanium Chemistry

Since it may be expected that alkyls on titanium surfaces will have a chemistry similar to their solution counterparts (56-59), a brief outline of organotitanium chemistry is in order.

Cotton (39) has reviewed eleven unsuccessful attempts to prepare organotitanium compounds prior to 1952, which cast doubt on the possibility of their existence. However, in 1952 a systematic investigation by Herman and Nelson resulted in the preparation and isolation of phenyltriisopropoxytitanium (62, 63), and a considerable number of compounds containing titanium-carbon σ or π-bonds have been prepared and characterized in subsequent years.

Organometallic compounds of titanium(II), titanium(III) and titanium(IV) are known. These may be covalent compounds, sandwich compounds or mixed sandwich-covalent compounds(64).

Sandwich compounds of titanium are cyclopentadienyl complexes.

As might be expected, the chemical properties of organotitanium compounds depend strongly on the nature of the ligand species and on the oxidation state of the titanium. One feature of covalent titanium(IV) organometallics is their thermal instability. Both tetramethyltitanium and tetraphenyltitanium will spontaneously decompose above -20°C giving more thermally stable titanium(II) derivatives. Diphenyltitanium is stable to about 200°C. Sandwich and mixed sandwich-covalent compounds are more thermally stable than covalent compounds. This stabilizing effect is also observed with amine, ether and phosphine ligands, and is thought to be a result of the effective increase of electron density on the metal.

All covalent titanium alkyl compounds are easily oxidized. Titanium(II) compounds react pyrophorically with oxygen or moisture. Bis(π-cyclopentadienyl)titanium(IV) compounds tend to be more resistant to oxidation.

Organotitanium(II) and (IV) species both react vigourously with organic halides with scission of titanium-carbon σ-bonds; π-bonds however, are considerably more stable. The final titanium products are the same whether organic or inorganic halides are used. The reaction of methyltitanium trichloride with carbon tetrachloride results in large quantities of methyl chloride and titanium tetrachloride (64). Tetramethyltitanium or tetraphenyltitanium react with carbon tetrachloride at -80°C. In the tetraphenyltitanium reaction,

diphenyl, chlorobenzene, hexachloroethane and titanium tetrachloride are produced. All can be explained by a free radical mechanism (64). Reactions with more complex organic halides are analogous and benzyl chloride for example, will react with generation of dibenzyl.

Bis(π-cyclopentadienyl)titanium reacts with carbon tetrachloride to give bis(π-cyclopentadienyl)titanium dichloride, hexachloroethane and other products. Diphenyltitanium reacts with carbon tetrachloride or chloroform to give benzene, diphenyl and titanium tetrachloride, but no titanium(II) or (III) derivatives (64).

LaLau analyzed the infra-red spectrum of methyl-titanium trichloride and its deuterium analogue. Comparison of the metal-carbon stretching frequencies of these compounds with those of methyl-trichloro compounds of silicon, germanium and tin led to the conclusion that the carbon-titanium bond is significantly weaker than the metal-carbon bonds of the group IV-a elements (66).

Two important consequences result from the weak metal-carbon bond in titanium alkyls. Firstly, the bond is unstable, especially if the alkyl group contains a β-hydrogen and olefin may be eliminated, leaving a titanium-hydride species. This type of elimination has been observed by Brintzinger (67). Secondly, insertion reactions, analogous to reactive adsorption, make possible olefin polymerization by a mechanism such as that proposed by Cossee(70). DeVries

has observed the insertion of isobutylene into methyltitanium trichloride to give neopentyltitanium trichloride (68). Rodriquez and VanLooy have proposed the disproportionation of methyltitanium trichloride and n-propyltitanium trichloride to give propylene and methane during ethylene polymerization by methyltitanium trichloride. The first ethylene insertion gives n-propyltitanium trichloride. The product propylene is postulated to copolymerize with ethylene and therefore is not isolated. However, careful use of deuterated reactants and analysis of the infra-red spectra of the copolymers which are produced, provide good evidence for the presence of propylene in the reaction mixture (69). The mechanism is identical with that proposed by deVries (68) to explain the decomposition of ethyltitanium trichloride to ethylene, ethane and titanium trichloride.

On the basis of the solution chemistry of known alkyltitanium compounds, four types of reactions might be expected to occur with alkyltitanium surface intermediates.

i) Homolysis,

e.g., $Ti\text{-}CH_2CH_3 \rightarrow Ti\cdot + \cdot CH_2CH_3$ (I - 10

ii) β-hydride elimination (transfer of hydride to surface),

e.g., $Ti\text{-}CH_2CH_3 \rightarrow Ti\text{-}H + CH_2{=}CH_2$ (I - 11

iii) Disproportionation,

e.g., $2\ Ti\text{-}CH_2CH_3 \rightarrow 2\ Ti + CH_2{=}CH_2 + CH_3\text{-}CH_3$ (I - 12

iv) Insertion,

e.g., $Ti\text{-}CH_2CH_3 + CH_2{=}CH_2 \rightarrow Ti\text{-}CH_2CH_2CH_2CH_3$ (I - 13

The work which is presented in this thesis will point out some similarities between unstable alkyltitanium surface species and alkyltitanium solution species. It will also demonstrate that the chemistry of the surface species is, in some respects, different from that of the homogeneous species.

APPARATUS AND EXPERIMENTAL TECHNIQUES

II - 1. Description of Apparatus

a) General

All experimental work was performed in a reaction system which is represented schematically in figure (II-1). To ensure maximum activity and reproducibility of titanium films, the system was designed and built in accordance with standard techniques for generation and maintainance of ultra-high vacuum (6, 71, 72, 73). The system, except for those parts lying outside the dashed line enclosure in figure (II-1), was built within an oven frame and could be heated to about 400°C. The oven temperature however, was always thermostated at 300°C or 350°C. Pumping was performed by a three stage mercury diffusion pump and mechanical backing pump. The pumps were separated from the reaction system during experiments, by two liquid nitrogen traps in series. The second trap (figure (II-1), T-2) was included in the oven during bake-out and was immersed in liquid nitrogen only after the heating cycle was complete.

The reaction system was primarily pyrex glass with stainless steel and Kovar metal components attached by glass-metal seals and vacuum flanges with copper gaskets. Because heating pyrex glass to 350°C may cause considerable strain, several Mason Renshaw Inc. stainless steel flex tubes were incorporated into the system.

FIGURE (II - 1)

Schematic Representation of Reaction System

C.M. = Capacitance Manometer

C.V.L. = Calibrated Variable Leak

G.P. = Glass Port

G.S. = Gas Source

I.G. = Ionization Gauge

M.S. = Mass Spectrometer

R.B. = Reaction Bulb

T. = Trap

V. = Valve

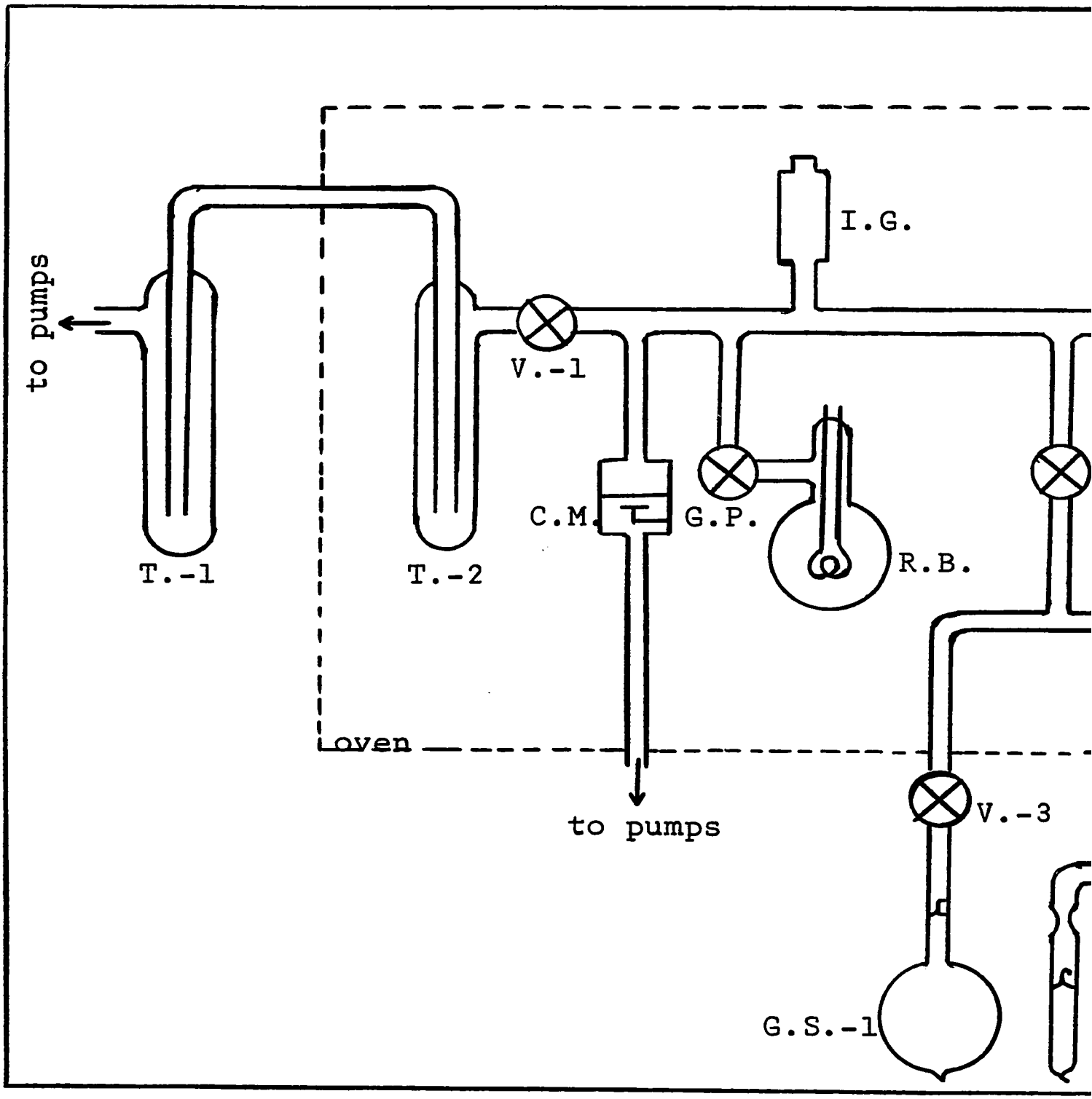
to pumps
T.-1
T.-2
V.-1
I.G.
C.M.
G.P.
R.B.
oven
to pumps
V.-3
G.S.-1

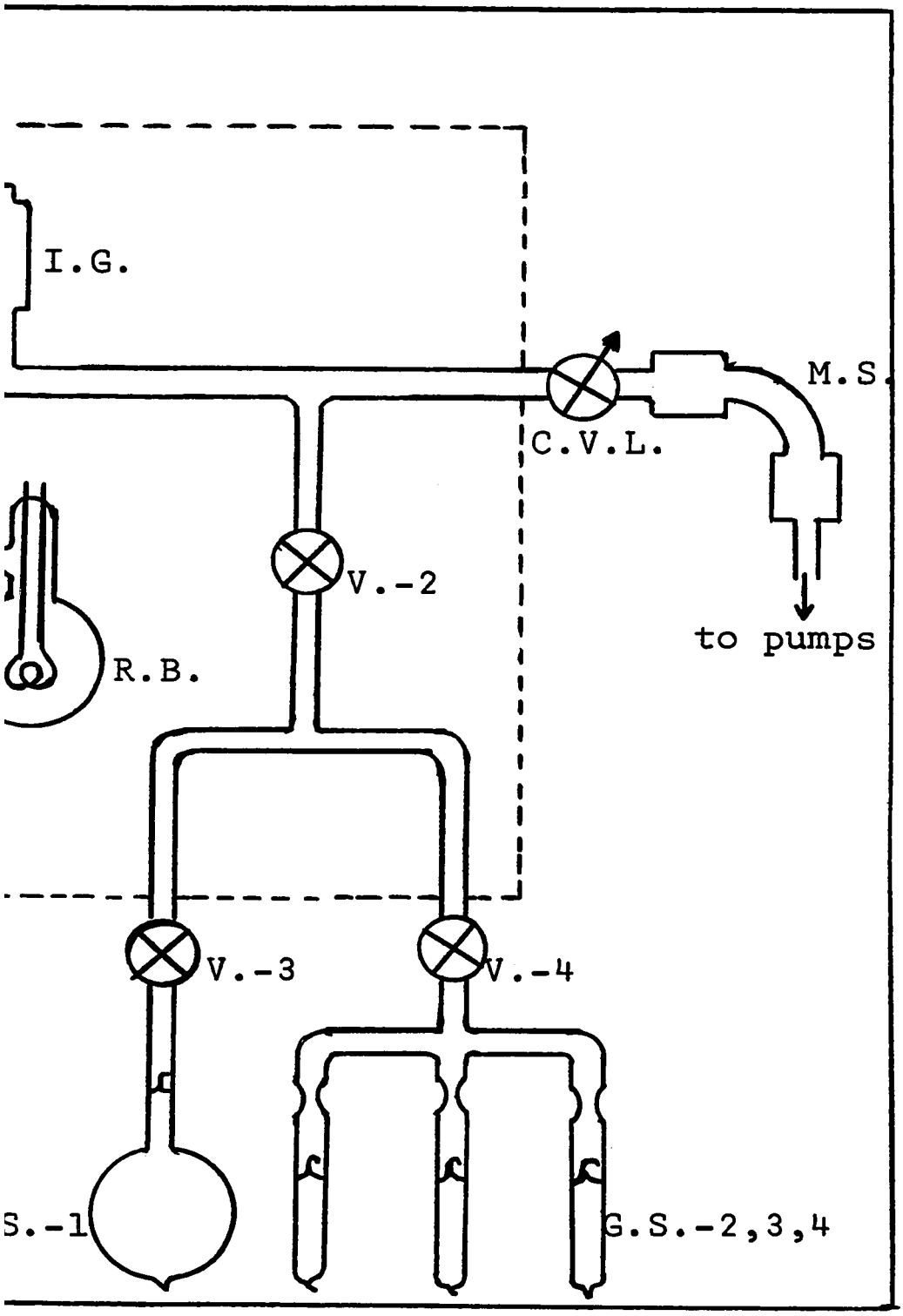
I.G.
M.S.
C.V.L.
V.-2
to pumps
R.B.
V.-3
V.-4
S.-1
G.S.-2,3,4

b) Valves

All valves in the system (figure (II-1), V_1 - V_4) were Granville Phillips Company Type 'C', bakeable, all metal valve bodies with manual drivers. Standard drivers (used for V_1, V_3 and V_4) operated the valves in a completely insensitive manner so that a valve was either open or closed. A special low torque driver was used on the valve which admitted gas into the reaction manifold (figure (II-1), V_2). Exceptionally fine leak control was achieved with this device and leak rates resulting in reactant pressures of 10^{-2} torr were obtained routinely.

c) Pressure Measurement

Two pressure measuring devices were used in this system. Pressures during pumping to an acceptable vacuum were monitored by a General Electric Model 22-GT-114 Bayard-Alpert ionization gauge (figure (II-1), I.G.) in conjunction with a General Electric Model 22-GC-130 control unit. The operating range of this gauge was from 10^{-3} to 10^{-11} torr.

Pressure of reactant and product gases was measured by a Granville Phillips Model 03, Series 212, capacitance manometer (figure (II-1), C.M.). This apparatus includes a bakeable sensing head and an electronic balancing unit. Differential pressure across a deflectable nickel diaphragm was measured as a change in capacitance between the nickel diaphragm and another plate. This instrument was rated to measure differential pressure from 0 to 10 torr, with a rated minimum detectable

pressure differential of less than $5x10^{-3}$ torr.

Calibration of the capacitance manometer was achieved by use of a McLeod gauge. The calibration procedure showed that the capacitance manometer was usuable at differential pressures of less than 10^{-3} torr. Dry nitrogen was used as a calibrating gas and care was taken to eliminate the possibility of diffusional effects (74, 75) which are associated with use of McLeod gauges. The performance of the capacitance manometer in its lower range was checked against a National Research Corporation Type 524-F cold cathode ionization gauge and Model 851 control unit. Agreement was excellent. The operating range of the cold cathode gauge was from 10^{-1} to $5x10^{-5}$ torr.

d) Analytical Devices

Analysis of reactant and product gases was performed mass spectrometrically with a Consolidated Electrodynamics Corporation Type 21-615 residual gas analyzer (figure (II-1), M.S.). This small mass spectrometer was pumped by a single stage diffusion pump which was separated from the spectrometer by two liquid nitrogen traps in series. This unit could be set to scan through any part of, or all of its mass range, which was 2 - 100 A.M.U. It also could be tuned to any mass of particular interest. Spectra were obtained dynamically by bleeding gas into the unit at a constant rate through a Granville Phillips Series 203, calibrated, variable leak (figure (II-1), C.V.L.), while the mass peaks of interest were scanned by the residual gas analyzer. Reproducibility of mass spectra was excellent,

although resolution became troublesome above mass 50. In all cases, sampling by the residual gas analyzer removed immeasureably small amounts of the gaseous reaction mixture.

The effect of the calibrated leak on peak heights, recorded by the residual gas analyzer, was investigated with the following results. For a constant calibrated leak opening, peak height was directly proportional to the gas pressure in the reaction manifold as illustrated by figure (II-2). For a constant gas pressure in the reaction manifold, the logarithm of the peak height was directly proportional to the opening of the calibrated leak as illustrated by figure (II-3). The proportionality constant relating peak height to gas pressure in the reaction manifold for a constant calibrated leak opening, was different for different gases and could be related to the relative sensitivity of each gas in the residual gas analyzer. The proportionality constant relating logarithm of peak height to calibrated leak opening was the same for all gases and gas pressures investigated. The change of slope in figure (II-3) at calibrated leak opening 122 is attributed to some asperity on the sealing surfaces and occurred for all gases.

Gas adsorption data on clean metal films were obtained by separating the reaction bulb (figure (II-1), R.B.) containing the film from the manifold, to which the capacitance manometer was attached, by a magnetically operated ground glass port (figure (II-1), G.P.). This port was a modification of a design by Dekker (76). The volume of the manifold and of the reaction

FIGURE (II - 2)

Variation of Mass Spectra Peak Heights with Gas Pressure for a constant Calibrated Variable Leak Opening

O - mass 15 peak of methane for a C.V.L. opening of 115.

Δ - mass 42 peak of n-propyl chloride for a C.V.L. opening of 122.

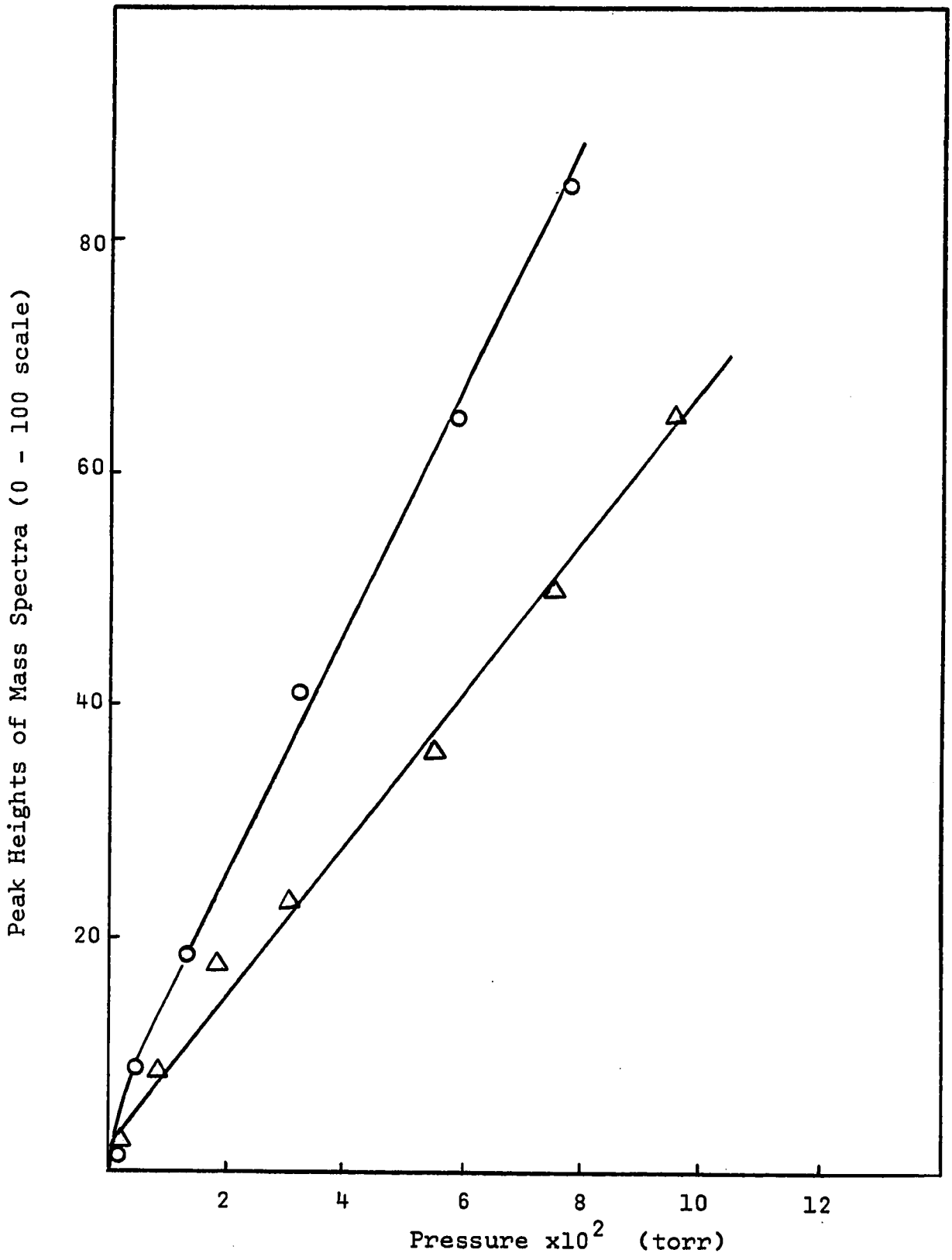
Peak Heights of Mass Spectra (0 - 100 scale)
80
60
40
20
2
4
6
8
10
12
Pressure x10^2 (torr)

FIGURE (II - 3)

Variation of Mass Spectra Peak Heights with Calibrated Variable Leak Opening for constant Gas Pressure

○ - mass 41 peak of n-propyl chloride at 0.1 torr pressure.

△ - mass 15 peak of methyl chloride at 0.1 torr pressure.

▽ - mass 15 peak of methane at 0.1 torr pressure.

● - mass 15 peak of methane at 0.08 torr pressure.

▲ - mass 15 peak of methane at 0.01 torr pressure.

□ - mass 15 peak of methane at 0.005 torr pressure.

◇ - mass 15 peak of methane at 0.001 torr pressure.

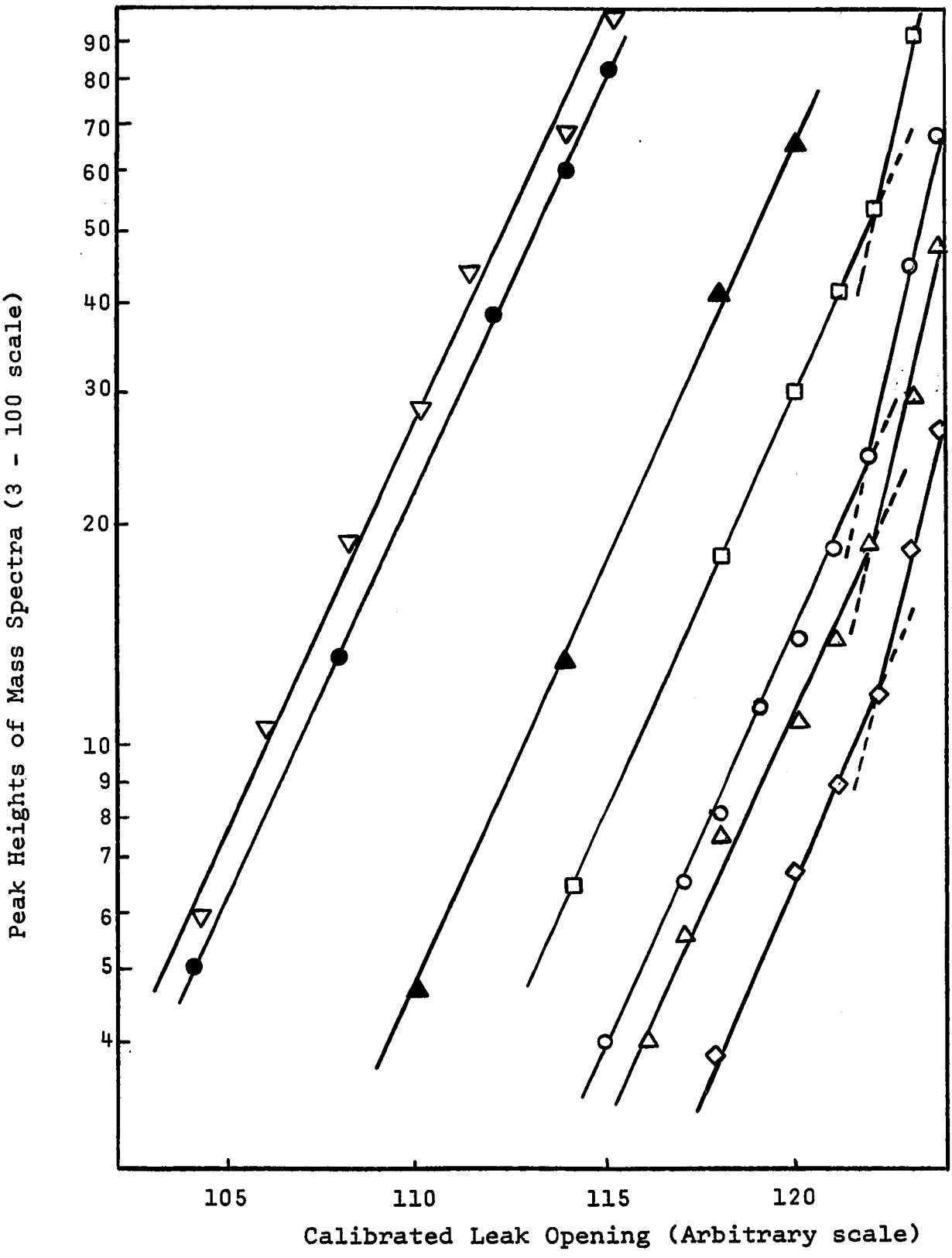
Peak Heights of Mass Spectra (3 - 100 scale)
90
80
70
60
50
40
30
20
10
9
8
7
6
5
4
105
110
115
120
Calibrated Leak Opening (Arbitrary scale)

bulb were calibrated. Thus an expected and an actual pressure decrease when the glass port was opened, allowed the number of molecules removed from the gas phase by adsorption, to be calculated.

e) Reaction Vessel

The reaction bulbs (figure (II-1), R.B.) were 300 ml. round bottom flasks which were attached to the system by a side arm. Three tungsten rods (50 mil diameter), supplied by A. D. Mackay Inc., were sealed through pyrex glass in the neck of the flask and suspended two titanium filaments (10 mil diameter), also supplied by A. D. Mackay Inc., in the centre of the bulb. Filaments were attached to the tungsten rods by spot welding. Use of two filaments provided a safeguard against loss of an experiment because of premature filament burnout. A standard 7 inch length of titanium wire was used to make a pair of filaments which had a typical weight of 40 milligrams.

The titanium wire used for all experimental work was at least 99.5 percent pure according to an ingot analysis supplied by A. D. Mackay Inc. Major impurities were carbon (0.08% max.), nitrogen (0.05% max.), hydrogen (0.015% max.) and iron (0.250% max.).

Temperatures of the reaction bulb were maintained by thermostated baths. From ambient temperature to 120°C, an oil bath was used, and from 120°C to 250°C, a molten wax bath was used. Both baths were controlled to better than ±1°C.

f) Protective Circuitry

The General Electric ionization gauge control provided protection for the ionization gauge. If a pressure greater than twice full scale deflection on the pressure readout was detected, the gauge was automatically shut off. The control also provided a relay, fused at two amps. which tripped when the ionization gauge was shut off. This relay was used to control a system of secondary relays with 25 amp. ratings. Power to the diffusion pumps, the oven heaters and the powerstats controlling filament outgassing was fed through these secondary relays during a bake-out. The ionization gauge control was set so that a pressure greater than 2×10^{-3} torr would activate the circuitry to shut off the ionization gauge, the heaters, the filament and the diffusion pump. Thus a strain-induced crack in any of the glass components of the reaction system during a bake-out would not result in extensive damage.

Secondary relays were bypassed at times other than bake-out so that the diffusion pumps and the powerstats for the filament could remain in use even though the ionization gauge was not operating.

II - 2. Experimental Procedure

a) Initial Preparations

A new reaction bulb was attached to the reaction manifold, leak-checked, and calibrated for volume. Using an auxiliary vacuum system, a reactant alkyl halide was condensed into a

glass vial to which a breakseal was attached, thoroughly outgassed and sealed under vacuum. The vial (figure (II-1), G.S.-1) was then attached to the reaction system behind a metal valve (figure (II-1), V_2). After checking for leaks at the point of attachment, the breakseal was broken and the reactant source was again outgassed using the large diffusion pump. Again using the auxiliary system, gases expected as products were also condensed into vials, with breakseals, thoroughly outgassed and sealed under vacuum. These gas sources (figure (II-1), G.S.-2,3,4) were attached to the reaction system behind a metal valve (figure (II-1), V_3). A glass constriction was placed beyond the breakseal of each product source. Each product source, in sequence, could be introduced by breaking its breakseal, used, condensed back into its vial and glassblown off the system at its constriction.

All chemicals were reagent grade materials. Gas sources were supplied by Matheson of Canada Ltd., Columbia Organic Chemicals or Phillips Petroleum Company. Liquids were supplied by K. & K. Laboratories Inc., Matheson, Coleman and Bell Inc. or Aldrich Chemical Company. All liquids were vacuum distilled from phosphorous pentoxide.

b) Calibration Procedures

After completion of initial preparations, and before starting outgassing of the filaments, the residual gas analyzer was calibrated with the reactant and expected product gases. This involved obtaining mass spectra of the pure gases and

determining the relative sensitivity of the analyzer to the various gases. Relative sensitivities were obtained by two independent methods. Base peak heights of various pure gas samples were measured for a constant calibrated variable opening and gas pressure. The most insensitive range multiplier setting of the analyzer was used to minimize the effect on peak height of variations of leak rate into the analyzer.

The second method for determining relative sensitivities was to obtain mass spectra of gas mixtures of known composition. These mass spectra, in conjunction with pure gas mass spectra, make possible the calculation of relative sensitivities.

c)Filament Outgassing

After the calibration of the residual gas analyzer was completed, the gas sources were valved off (figure (II-1), V_3 and V_4 were closed) and the reaction system was pumped onto the 10^{-5} torr scale. At this point, filament outgassing was started by resistive heating. Voltage into the filaments was slowly increased and initially large quantities of gas were desorbed from the filaments. The filaments were maintained below their evaporation temperature but at red heat for at least 24 hours. At the end of this period the pressure in the system should have decreased onto the 10^{-7} torr scale.

d) Bake-out

While continuing to outgas the filaments, the driving mechanisms from the pump valve and the manifold valve (figure (II-1), V_1 and V_2) were removed and bake-out clamps were attached

locking the valve bodies into the open position. The electronics were also removed from the capacitance manometer sensing head. The protective circuitry, previously described, was activated and the oven frame was installed. Heating was started and thermostatted at 300°C or 350°C.

Typically, the pressure in the system might now rise as high as 10^{-3} torr and then begin to decrease to a minimum of about 2×10^{-6} torr. The system was usually baked for 15 hours. A timing device was used to turn the oven off at an appropriate time so that the reaction system was returned to ambient temperature at a convenient hour. The pressure in the system at this time might be as low as 2×10^{-8} torr and would decrease onto the 10^{-9} torr scale when the trap (figure (II-1), T_2), which had been baked in the oven, was immersed in liquid nitrogen.

e) Film Deposition

After the pieces removed from the system during bake-out were replaced, the protective circuitry deactivated, and all parts of the reaction system had returned to ambient temperature, resistive heating of the titanium filaments was increased until they reached their evaporation temperature. If the filaments had been properly outgassed, this procedure did not increase the pressure in the system above about 5×10^{-9} torr. Filament evaporation was finely controlled by using two powerstats in series so that rates of deposition remained essentially constant from experiment to experiment. Substrate temperature was not controlled and may have been as high as 60°C during

film deposition.

Contrary to indications in the literature (9, 77), no difficulty was experienced in resistively evaporating titanium filaments.

Typical geometric area of a film was about 200 cm.^{2}. If the filaments had been properly centred in the reaction bulb, films appeared to have a uniform distribution. Weights of several films were determined and ranged from 9 to 15 milligrams per film (0.045 to 0.075 milligrams per cm.^{2}). In general however, film weights were not determined.

f) Reactions and Analyses

When deposition of a titanium film was complete, the ionization gauge was immediately shut off and the reaction bulb was immersed in an ice-water mixture, or left to equilibrate to ambient temperature. A period of ten minutes was allowed for the bulb temperature to equalize and for the ionization gauge to cool. During this period, reactant was admitted up to the manifold valve (figure (II-1), V_2). After this period, the exit valve (figure (II-1), V_1) was closed to separate the pumps from the reaction system, and the magnetic, glass port (figure (II-1), G.P.) was also closed. Using the capacitance manometer, 2×10^{-2} torr of reactant was admitted. The latter corresponded to about 3.5×10^{17} molecules or about one monolayer coverage on the film, if a typical roughness factor of 10 was assumed. The magnetic glass port was then opened, admitting reactant gas onto the clean titanium film. Pressure decrease

was monitored by the capacitance manometer and the reactant-product gas mixture was sampled periodically by the residual gas analyzer until reaction had ceased. The system was then pumped out and this procedure was repeated to check for further adsorptivity or reactivity. When films had ceased to be active at low temperature, the reaction bulb was heated in a thermostatted bath.

Three methods were used to follow kinetics.

i) Mass spectra of reactant-product mixtures were recorded during reactions and computer analyzed for composition. A typical computer program and its derivation from mass spectrometric calibration data is presented in Appendix I.

ii) If a unique reactant mass fragment peak existed, and if the reaction were rapid, then the residual gas analyzer was tuned to that peak and a decay curve was recorded.

iii) In the case where one mole of reactant gave two moles of product, it was possible to follow the progress of the reaction with the capacitance manometer.

When a series of reactions were run at various temperatures to generate Arrhenius data, either of two procedures were used to ensure that no irreversible changes in film activity occurred.

In one method, a sequence of reactions at various temperatures was performed in a random manner and then the reaction rate at the first temperature was rechecked. In the second method, an intermediate temperature in a sequence was

run initially and was followed by step-wise increases in reaction temperature to a maximum and then step-wise decreases to a minimum. Any progressive, irreversible change in film activity would then manifest itself as a characteristic curve in a plot of the Arrhenius data. Reproducibility of rates at any given temperature was also checked from time to time when this method was used. In general, film activity was found to be suprisingly constant throughout numerous reactions, run at several temperatures, over many hours.

g) Limitations on Experimental Procedure

The limiting response rate of the reaction system was investigated and was found to obey conditions which support the hypothesis that response was limited by interdiffusion of reactant and product molecules; that is, by the diffusion of reactant to the metal surface, or by diffusion of product to the detectors.

In a typical reaction where interdiffusion of product and reactant was fast compared to reaction rate, it was possible to generate sawtooth decay curves of reactant concentration as shown in figure (II-4) by periodically isolating the reaction bulb from the detectors. This was done by closing and reopening the magnetically operated glass port.

Since rates of diffusion are insensitive to temperature and also because the reaction bulb is isolated from the detectors by a manifold at ambient temperature, it would be expected that when the rate of interdiffusion was much slower than the rate of reaction, the apparent activation energy should level to zero.

FIGURE (II - 4)

Variation of Reactant Concentration with Time when Glass Port is Periodically Closed and Opened

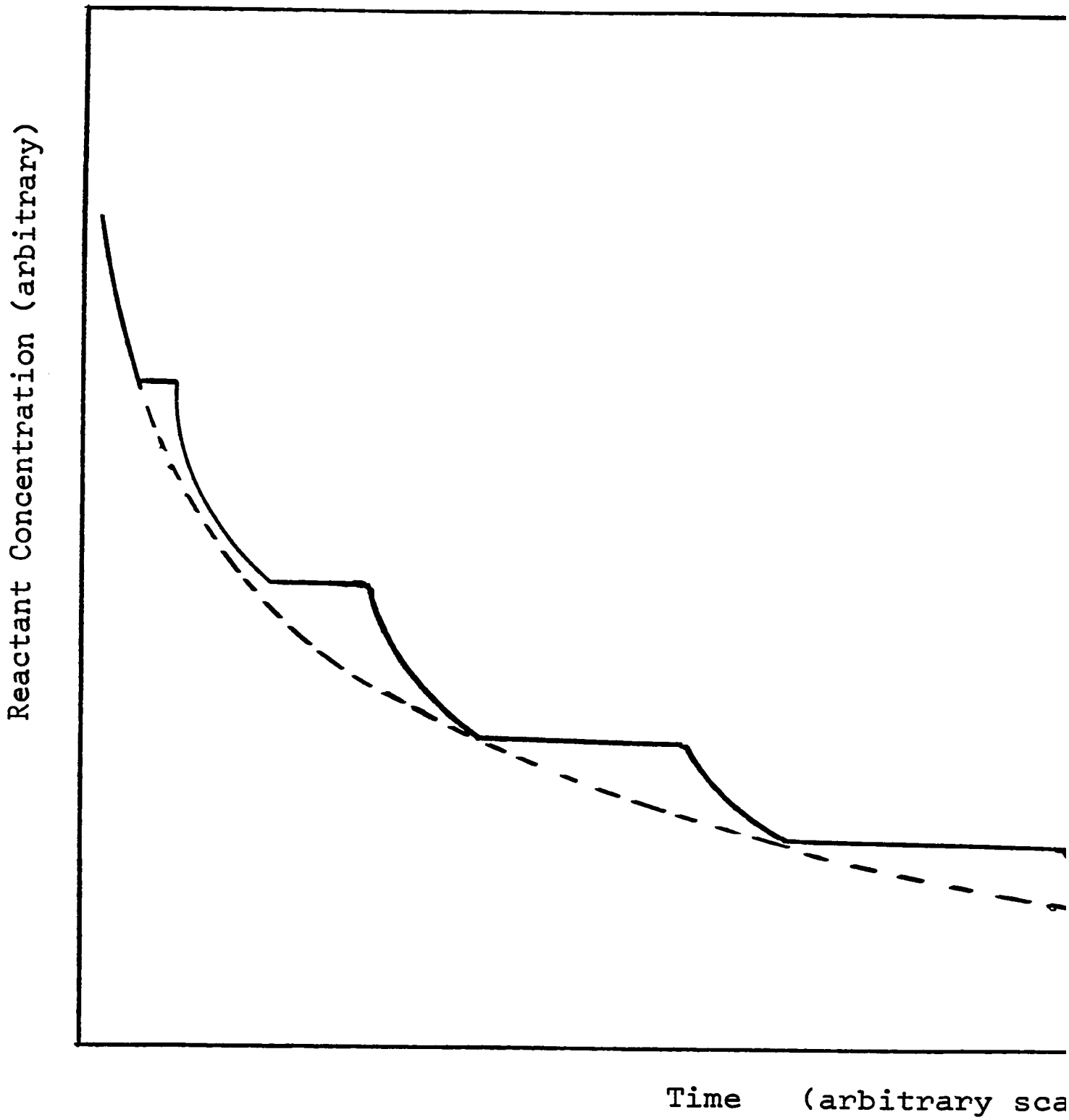
Reactant Concentration (arbitrary)
Time (arbitrary sca

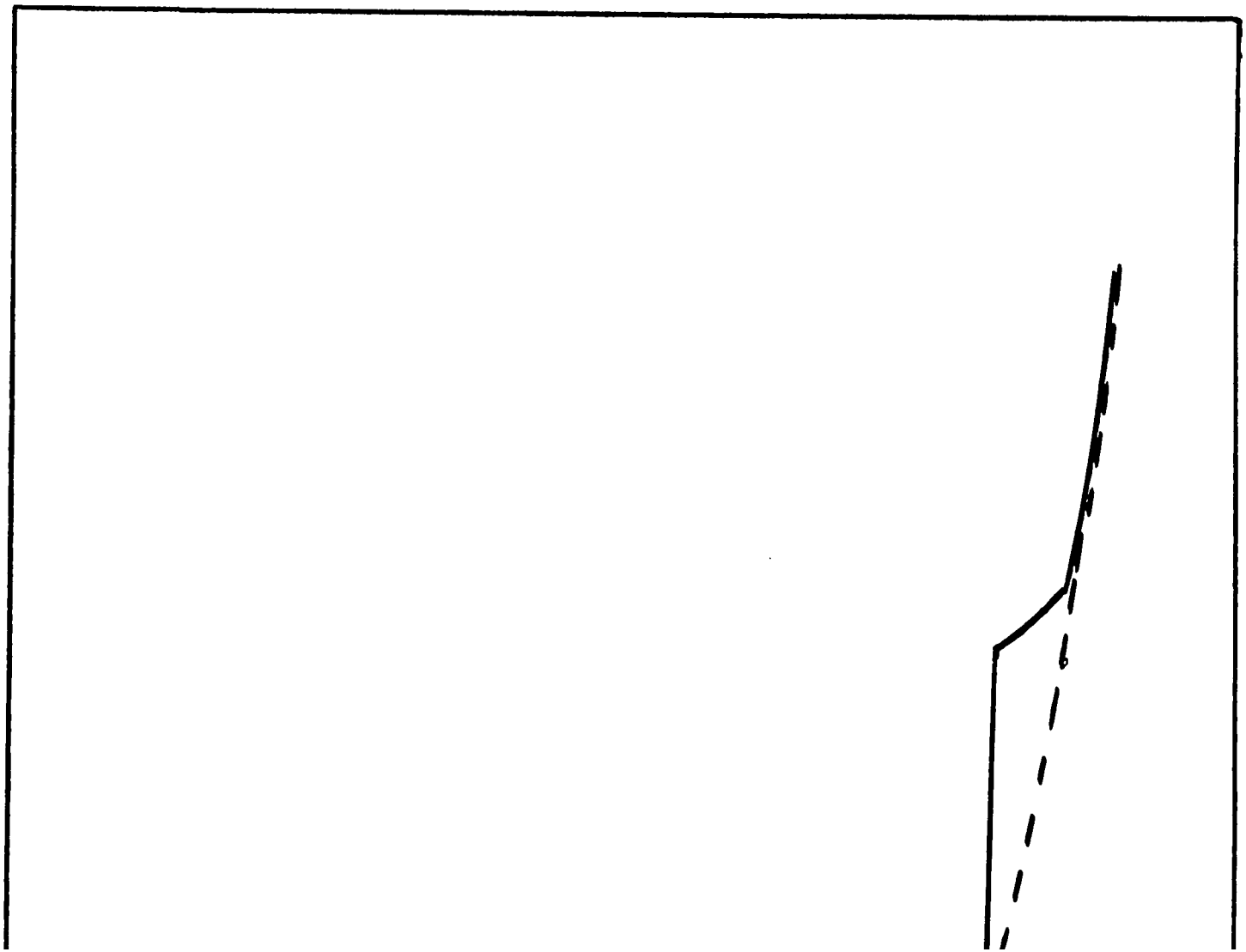
(arbitrary scale)

This type of behaviour has been found in the reactions of t-butyl chloride and isopropyl chloride on titanium and is illustrated by figure (III-36) and figure (III-34).

The limiting response rate has also been found to be inversely proportional to the gas pressure in the reaction system, giving further support to the hypothesis that it is a diffusion phenomenon. The response rates of the system detectors are known to be greater than the observed limiting response rates.

Observed limiting response rate constants were about 6.9×10^{-3} sec.$^{-1}$ at 5×10^{-2} torr for the t-butyl chloride reaction and 7.6×10^{-4} sec.$^{-1}$ at 5×10^{-1} torr for the isopropyl chloride reaction. The slightly less than ten fold increase of rate constant for a ten fold decrease in pressure is accounted for almost exactly by the square root of the inverse ratio of reactant molecular weights, which also supports the diffusion hypothesis.

The expected limiting response rate constant for a reaction at 10^{-2} torr would be about 3.5×10^{-2} sec.$^{-1}$. None of the reactions studied at this pressure have had rate constants which approach this value and no sudden levelling of Arrhenius plots to a zero slope would be expected. This phenomenon was not observed for any of these reactions.

EXPERIMENTAL RESULTS

III - 1. Introductory Comments

The direct reactions of four series of halocarbons with titanium films have been investigated. These series are identified as follows.

i) The halide series: This set of reactants was used to investigate the effects upon reactivity of the various halides, attached to the same alkyl group. Included in this series were n-propyl fluoride, chloride, bromide and iodide.

ii) The α-methyl series: This set of reactants was used to investigate reactivity effects resulting from α-methylation of ethyl chloride. Included in this series were ethyl chloride, isopropyl chloride and t-butyl chloride.

iii) The β-methyl series: This group of reactants was used to investigate reactivity effects resulting from β-methylation of ethyl chloride. This series of reactants included ethyl chloride, n-propyl chloride, isobutyl chloride and neopentyl chloride.

iv) The dichloro- series: This group of reactants was used to investigate the effects of having more than one chloride in the reactant molecule. Reactants included in this series are 1,2-dichloropropane, 1,3-dichloropropane and 1,3-dichloro-2,2-dimethylpropane.

In addition, the reactions of hydrogen chloride and methyl chloride were investigated, although not in detail.

Two types of reactions were observed for all halocarbons. The first was a very rapid reaction with adsorption on a virgin film at low temperature. This reaction normally did not proceed beyond the order of one monolayer equivalent, and was too rapid to allow meaningful kinetic measurements.

The second type of reaction which was observed for all halocarbons, was performed subsequent to a low temperature, virgin film reaction. This reaction, which occurred at higher temperatures, was easily controlled. Useful kinetic measurements could be made and the reactions proceeded with reproducible rates through many monolayer equivalents of reactant. Depending upon the reactant halocarbon being studied, these reactions can be divided into two subgroups.

Halocarbons of the first subgroup reacted to give mixtures of corresponding olefin and paraffin with loss of hydride and halide into the film. For the second subgroup of halocarbons, the film became an active dehydrohalogenation catalyst, so that the reaction products were gaseous hydrogen halide and olefin. It was possible in some dehydrohalogenation reactions to adjust reaction conditions and obtain minor amounts of side products.

The bulk of the experimental work which will be presented relates to the high temperature reactions.

Throughout the text of this thesis, unless otherwise defined, 'P_o' refers to initial reactant pressure and 'P' refers to reactant pressure at time 't'. All reaction orders have

been determined by following disappearance of reactant and not by studies of initial rate slopes.

III - 2. Blank Runs and Effect of Film Contamination

The possible reactivity or adsorptivity of n-propyl chloride on pyrex glass was investigated. A typical reaction bulb was attached to the system, which was then pumped and baked overnight at 350°C. To ensure that no traces of titanium were present on the reaction bulb walls, at no time was the filament outgassed. A slightly poorer than normal vacuum was attained, but still on the 10^{-9} torr scale. When reactant n-propyl chloride was admitted to the reaction bulb, no adsorption or reaction was observed. The bulb was heated to 100°C, 200°C and 240°C without observable adsorption or reaction.

It was also demonstrated that neither isobutyl chloride nor 1,3-dichloro-2,2-dimethylpropane react on pyrex glass at 225°C over a period of several hours.

Film contamination and its effect on reactivity were investigated. A titanium film which had been used extensively for kinetic studies of the reaction of n-propyl chloride was exposed to atmosphere for an extended period. It was then pumped overnight and heated at 200°C for several hours. Quantities of nitrogen or carbon monoxide, water and carbon dioxide were desorbed. The film, however, remained completely unreactive toward n-propyl chloride at 200°C.

A virgin film, deposited at 10^{-9} torr, was exposed

to a mixture of air and n-propyl chloride at 0°C. Oxygen was preferentially adsorbed from the gas mixture and no product propylene or propane was detected. The film remained unreactive with n-propyl chloride at 200°C.

III - 3. Interactions of Alkyl Halides with Virgin Films

a) n-Propyl Halides

At low temperatures, all n-propyl halides were adsorbed by virgin films. The residual gas phase contained mixtures of propylene, propane and, in most cases, n-propyl halide. On a film at 0°C, n-propyl chloride was more extensively adsorbed, and also reacted to give almost twice the quantity of gas phase products than were observed for reaction on a film at 20°C. However, product ratio did not vary signifigantly.

For all reactants, adsorption and initial appearance of gas phase products were very rapid. The adsorption and reaction of approximately one monolayer equivalent (which was 3.5×10^{17} molecules or about 10^{-2} torr) of n-propyl chloride, bromide or iodide with virgin films was always incomplete and always resulted in complete film deactivation toward subsequent reactant doses at low temperature. Although the bulk of the gas phase products was rapidly produced before the first mass spectrometric analysis could be completed, small amounts continued to be produced over a longer time. After a period of one or two hours even this residual reaction ceased. The residual reaction produced larger amounts of propylene than the initial

reaction, so that the gas phase product ratio changed with time. This therefore provided a method of determining the probable product ratio at the instant of initial reaction by extrapolation to zero time. This extrapolation is illustrated in figure (III-1).

Although n-propyl fluoride resembled the other halides in that it was strongly adsorbed and gave mixtures of propane and propylene, in two important respects it was different. Admission of approximately one monolayer equivalent of reactant n-propyl fluoride onto a virgin film resulted in its complete disappearance, either by reaction or by adsorption. The effect of this reactant dose on activity of the film was negligible. In fact, four doses of n-propyl fluoride, each approximately equal to one monolayer equivalent successively reacted to completion within a period of several minutes. Another dose, equal to about ten monolayer equivalents, then reacted completely in a period of about three hours. The propane:propylene product ratio, within experimental error, did not differ for any of these n-propyl fluoride reactions.

Loss of reactant by adsorption occurred only for the first monolayer equivalent dose. Even after the reaction of the ten monolayer equivalent dose, the film retained significant reactivity, although somewhat diminished from its virgin reactivity.

The rate of reaction of the ten monolayer equivalent dose was sufficiently slow so that it was possible to obtain meaningful kinetics. The disappearance of n-propyl fluoride was found to occur with first order dependence and is illustrated

FIGURE (III - 1)

Change of Mole Percent Propylene in Product Mixture (balance is Propane) with Time during Reactions of n-Propyl Halides with Virgin Films

○- n-propyl bromide at 0°C

△- n-propyl chloride at 0°C

□- n-propyl chloride at 20°C

▽- n-propyl iodide at 0°C

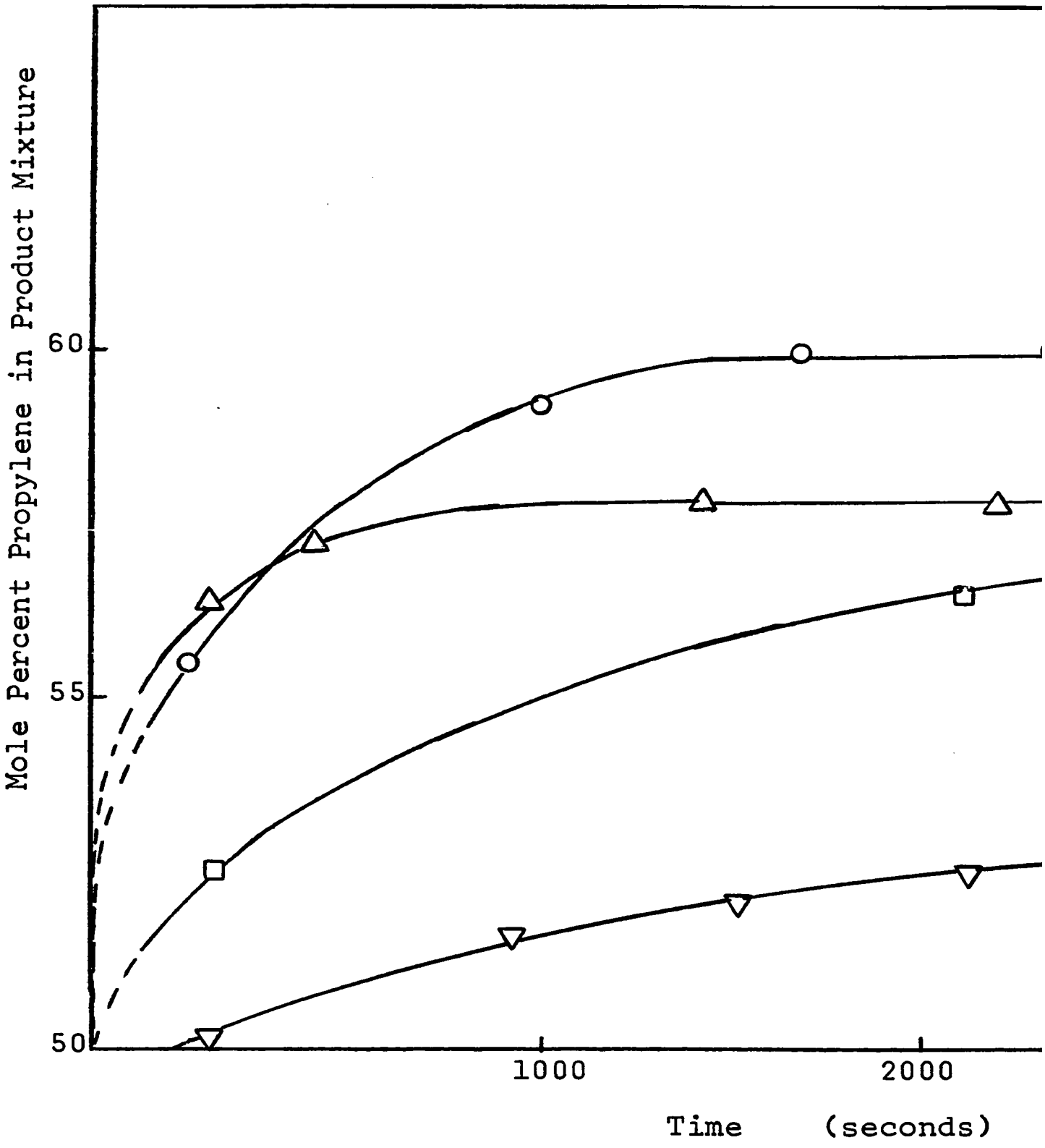
Mole Percent Propylene in Product Mixture
60
55
50
1000
2000
Time (seconds)

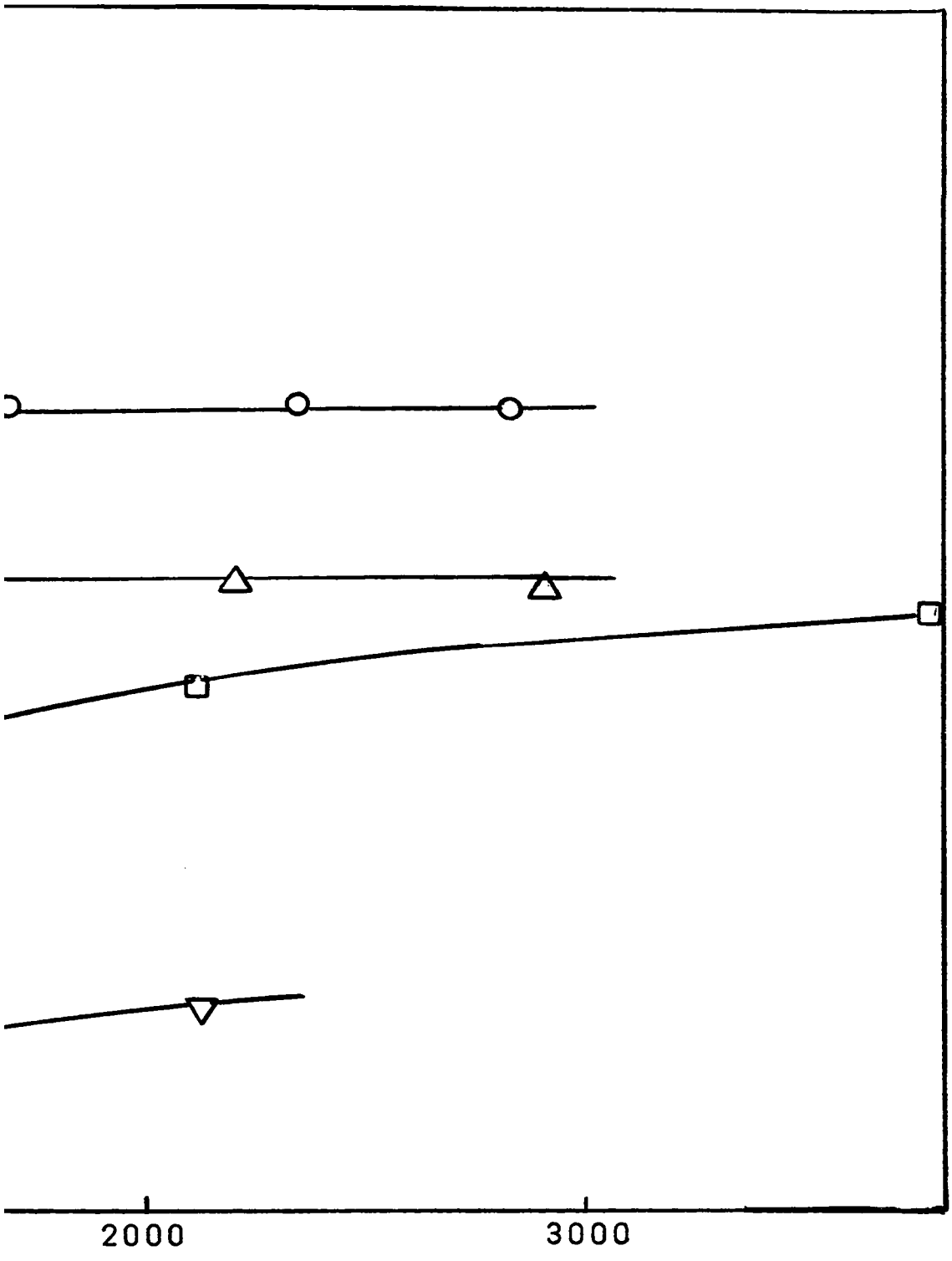
2000
3000
(seconds)

by figure (III-2).

The interactions of all n-propyl halides with virgin films are summarized in Table (III-1). 'Mole percent reacted' and 'mole percent adsorbed' values were recorded 300 seconds after admission of reactant to the film. 'Product ratio' values were obtained by extrapolation to zero time as previously explained. In the case of n-propyl fluoride where complete loss of reactant by adsorption or reaction had occurred before the first mass spectrometric analysis could be performed, the product ratio value cited is that observed from the first analysis.

b) α-Methyl Series

The interactions of ethyl chloride, isopropyl chloride and t-butyl chloride with virgin films were investigated.

The adsorption and reaction of a monolayer equivalent of ethyl chloride with a virgin film at 20°C was incomplete and resulted in deactivation of the film toward subsquent doses of reactant at low temperature.

The adsorption and reaction of a monolayer equivalent of isopropyl chloride was rapid and complete on a film at 0°C, and caused substantial but incomplete film deactivation for a second reactant dose at 0°C. The second dose did not react to completion over a four hour period and caused almost complete film deactivation. The film deactivation during reaction of the second and third doses is demonstrated by plots of isopropyl chloride disappearance in figure (III-3).

When the data for the reactions of the second and third

FIGURE (III - 2)

First Order Disappearance of 0.1 torr of n-Propyl Fluoride by Reaction on a Titanium Film at $0^{o}C$

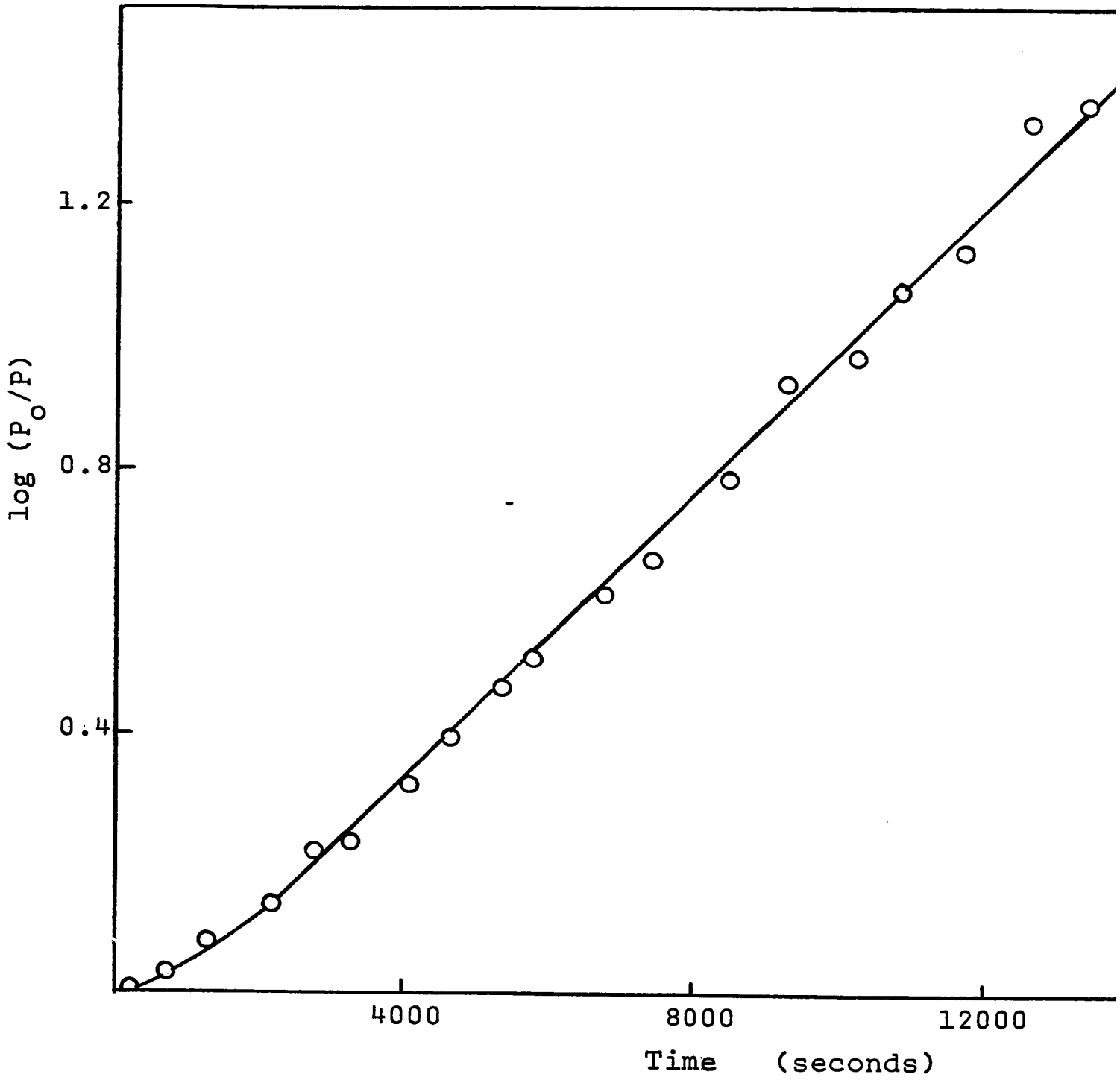
1.2
0.8
0.4
log (P_o/P)
4000
8000
12000
Time (seconds)

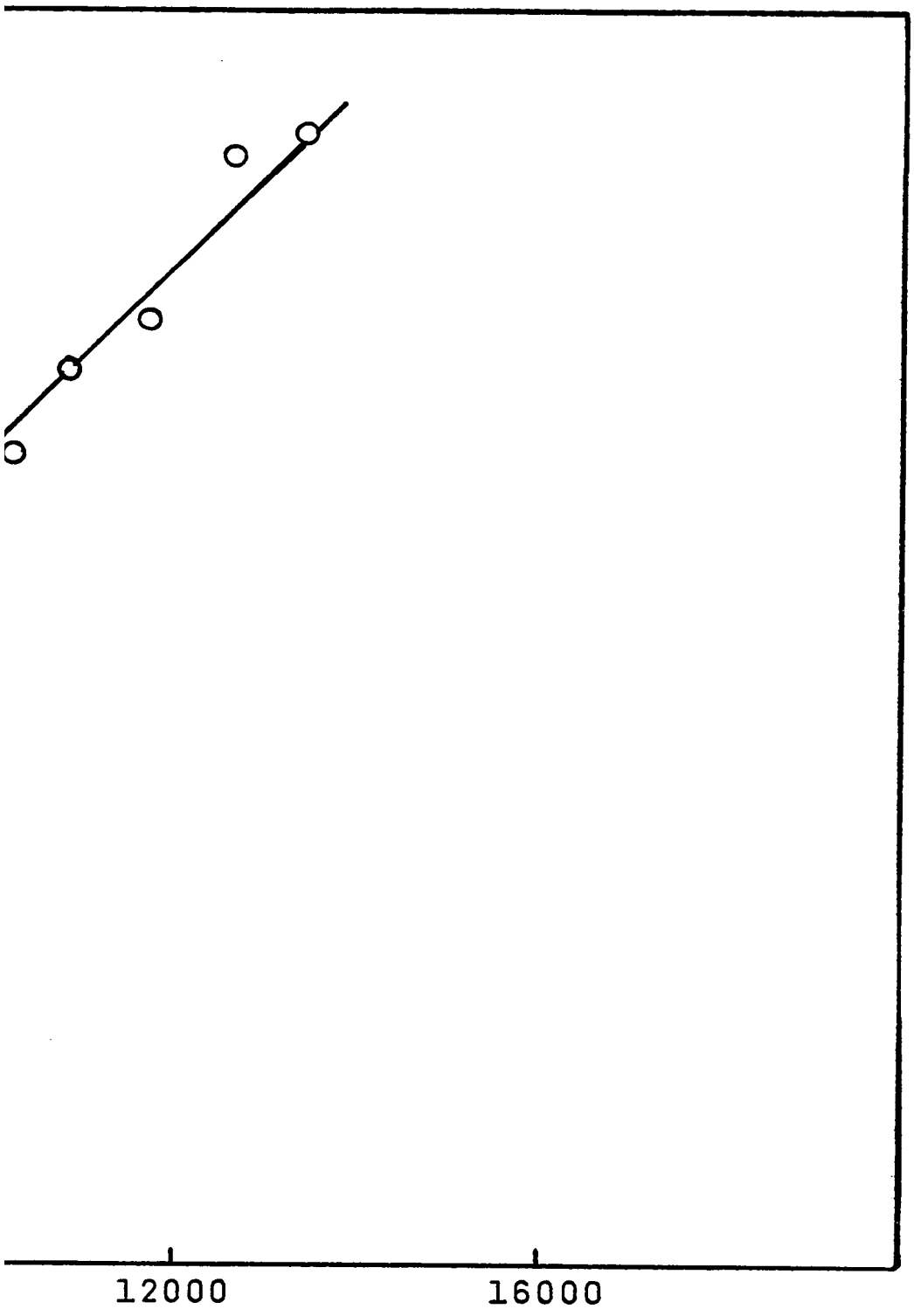

onds)

TABLE (III - 1)

n-Propyl Halide Interactions with Vi

reactant	number of reactant molecules $\times 10^{17}$	pressure equivalent (torr)$\times 10^{2}$	film temp. ^{o}C	reactant	
				mole % adsorbed	mole % reacted
n-propyl fluoride	3.7	1.0	0.0	70.4	29.6
n-propyl chloride	3.7	1.0	0.0	64.0	26.6
n-propyl chloride	3.7	1.0	20.	17.5	15.3
n-propyl bromide	3.7	1.0	0.0	41.0	18.5
n-propyl iodide	3.7	1.0	0.0	61.0	15.0

I - 1)

tions with Virgin Films

reactant			gaseous products and product ratios
e % orbed	mole % reacted	mole % unaffected	
4	29.6	0.0	propane:propylene 20:80
0	26.6	9.4	propane:propylene 50:50
5	15.3	67.2	propane:propylene 50:50
)	18.5	40.5	propane:propylene 50:50
	15.0	24.0	propane:propylene 50:50

FIGURE (III - 3)

Film Deactivation during Reaction of Isopropyl Chloride at 0°C

$(P_o - P)$ vs. Time

○ - second monolayer equivalent dose

□ - third monolayer equivalent dose

$(P_o - P)^2$ vs. Time

△ - second monolayer equivalent dose

◇ - third monolayer equivalent dose

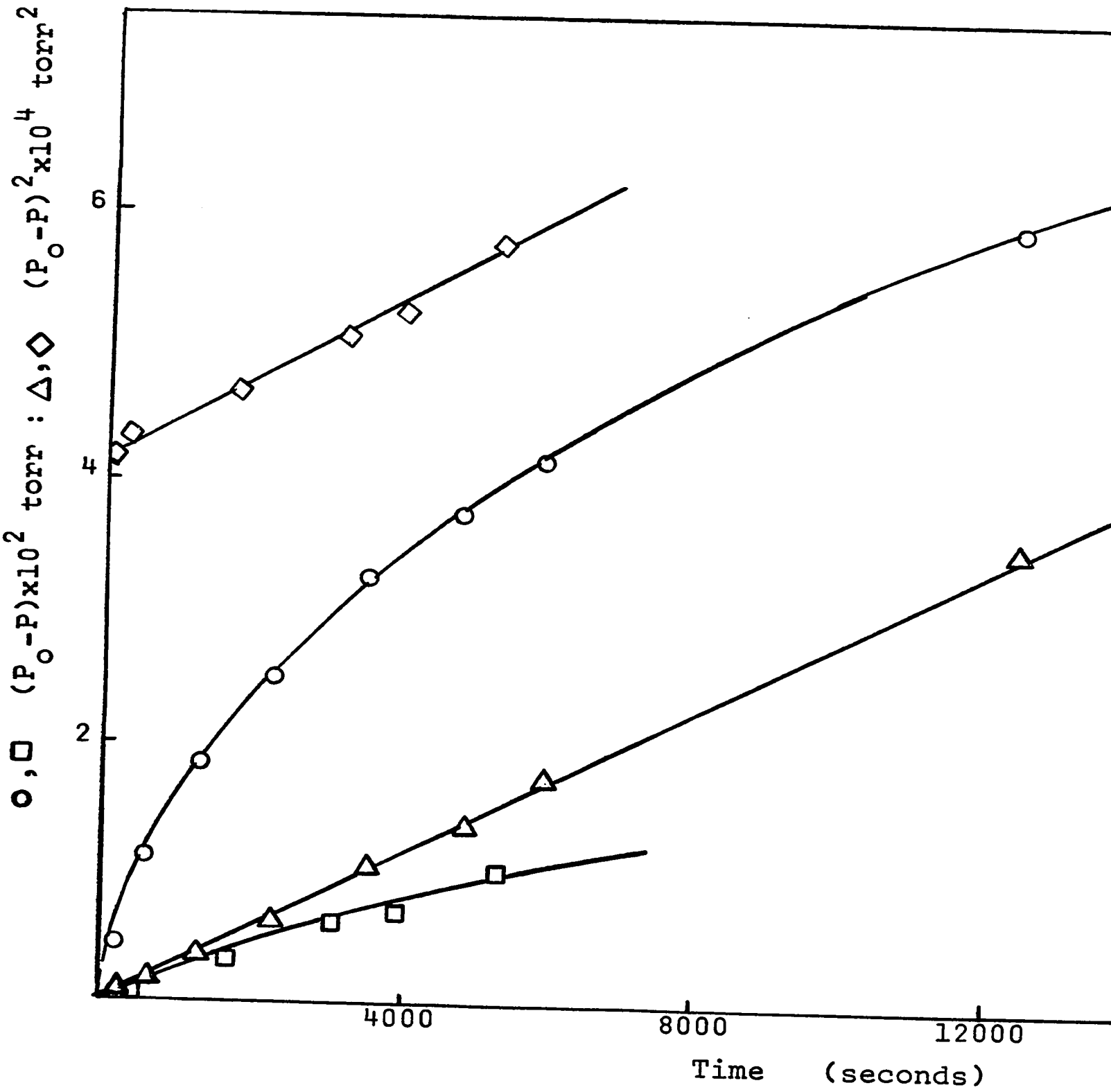
○,□ $(P_o-P)x10^2$ torr : △,◇ $(P_o-P)^2x10^4$ torr^2
6
4
2
4000
8000
12000
Time (seconds)

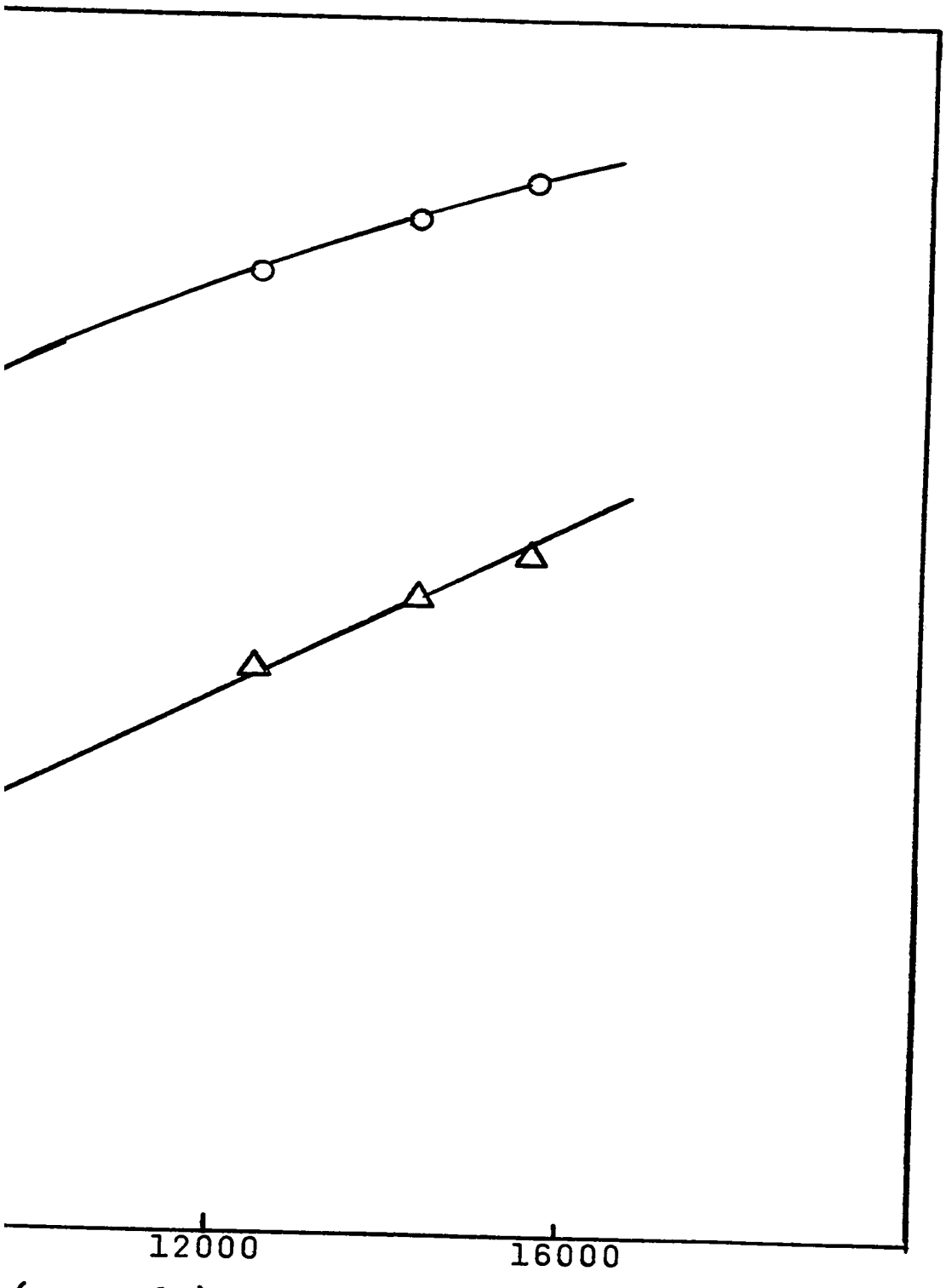
12000
16000
(seconds)

doses of isopropyl chloride are plotted according to equation (III-2, which is the integrated form of equation (III-1, the straight line plots in figure (III-3) result.

$$\frac{d(P_o-P)}{dt} = \frac{k}{(P_o-P)} \qquad \text{(III - 1}$$

$$(P_o-P)^2 = kt + C_o \qquad \text{(III - 2}$$

These equations express the well known parabolic law which is a typical kinetic expression for diffusion controlled reactions. In figure (III-3), P_o for the third dose has been equated to (P_o-P) for the second dose plus the initial reactant pressure of the third dose for the diffusion control kinetics plots. Thus, for both the second and the third dose, (P_o-P) represents the combined total of isopropyl chloride which has been reacted on the film, and equation (III-1 then states that the rate of disappearance of reactant is inversely proportional to the total amount of reactant consumed.

The adsorption and reaction of a monolayer equivalent of t-butyl chloride on a film at 0°C was rapid and complete. A subsequent dose continued to react, much more rapidly than the second dose of isopropyl chloride had reacted. During the reaction of the second dose of t-butyl chloride, gaseous hydrogen chloride was detected. For this reason, no attempt was made to plot this data as a diffusion controlled reaction.

Reactions of ethyl chloride and isopropyl chloride gave mixed olefin and paraffin products. Reaction of t-butyl chloride gave only olefin. Adsorption and reaction data for

this series is summarized in Table (III-2).

c) β-Methyl Series

The interactions of ethyl chloride, n-propyl chloride, isobutyl chloride and neopentyl chloride with virgin films was investigated.

The interactions of ethyl chloride and n-propyl chloride have been reported in the previous series but are again summarized in Table (III-3) with data for isobutyl chloride and neopentyl chloride.

The only product from the reaction of isobutyl chloride with a virgin film at 0°C was isobutylene. A three monolayer equivalent dose of isobutyl chloride was admitted to the film. The number of molecules which reacted was scarcely greater than the number of n-propyl chloride molecules which had reacted when a one monolayer equivalent dose of that reactant was studied under identical conditions. The reaction and adsorption of the initial isobutyl chloride dose resulted in complete film deactivation toward the second dose.

A one monolayer equivalent dose of neopentyl chloride was completely adsorbed by a virgin film at 0°C. Analysis of residual gas species revealed the presence of neopentane, a minor amount of isobutylene and a trace of methane.

No detectable adsorption of isobutyl chloride or of neopentyl chloride occurred when the reactants were admitted to virgin films at 200°C.

TABLE (III - 2)*

α-Methyl Series Interactions with Virgin

reactant	number of reactant molecules $x10^{17}$	pressure equivalent (torr)$x10^{2}$	film temp. ^{o}C	reactant		
				mole % adsorbed	mole % reacted	mol una
ethyl chloride	3.7	1.0	20.	32.5	18.5	49
ethyl chloride	3.7	1.0	20.	23.0	9.0	68
i-propyl chloride	3.7	1.0	0.0	21.0	79.0	0
t-butyl chloride	3.7	1.0	0.0	20.0	80.0	0

* All data were recorded 300 seconds after admission of react

- 2)*

ns with Virgin Films

reactant			gaseous products and product ratios
% bed	mole % reacted	mole % unaffected	
	18.5	49.0	ethane:ethylene 20:80
	9.0	68.0	ethane:ethylene 30:70
	79.0	0.0	propane:propylene 20:80
	80.0	0.0	isobutylene

nission of reactant to film.

TABLE (III - 3)*

β-Methyl Series Interactions with Vir

reactant	number of reactant molecules $x10^{17}$	pressure equivalent (torr)$x10^{2}$	film temp. °C	reactant		
				mole % adsorbed	mole % reacted	m u
ethyl chloride	3.7	1.0	20	32.5	18.5	
	3.7	1.0	20	23.0	9.0	
n-propyl chloride	3.7	1.0	20	17.5	15.3	
	3.7	1.0	0.0	64.0	26.6**	
isobutyl chloride	11.5	3.1	0.0	37.0	10.0†	
	5.5	1.5	218.	0.0	19.0	
neopentyl chloride	3.7	1.0	0.0	100.	trace	
	3.7	1.0	200.	0.0	~15.	

* All data except n-propyl chloride product ratios were admission of reactant to film.

** $=0.99x10^{17}$ molecules

† $=1.15x10^{17}$ molecules

I - 3)*

ions with Virgin Films

reactant		gaseous products and product ratios
% ɔed	mole % reacted	mole % unaffected	
	18.5	49.0	ethane:ethylene 20:80
	9.0	68.0	ethane:ethylene 30:70
	15.3	67.2	propane:propylene 50:50
	26.6**	9.4	
	10.0†	53.0	isobutylene
	19.0	81.0	
	trace	0.0	neopentane:isobut- 90:10
	~15.	~85.	ylene:methane :trace

ratios were recorded 300 seconds after

d) Dichloro- Series

The interactions of 1,2-dichloropropane and 1,3-dichloropropane with virgin films were investigated.

Adsorption and reaction of a one monolayer equivalent dose of either reactant on a film at 20°C was incomplete. Both deactivated the films toward subsequent doses.

The 1,2-dichloropropane gave only propylene as product, the 1,3-dichloropropane gave principally cyclopropane and minor amounts of propylene. Adsorption and reaction data for this set are summarized in Table (III-4).

e) Miscellaneous Gases

Both hydrogen chloride and methyl chloride were strongly adsorbed by virgin films. Small amounts of methane were found after admission of methyl chloride. Both gases caused complete film deactivation toward subsquent doses.

The adsorption of ethylene by a film at 20°C was also investigated. It was found that ethylene was strongly adsorbed but that no product species were formed.

The interaction of a monolayer equivalent of propane with a virgin film at 20°C was minimal. No reaction products were formed and only small amounts of adsorption occurred. However, heating the film to 200°C resulted in more extensive adsorption, but no product formation.

Data for this section are summarized in Table (III-5).

TABLE (III - 4)*

Dichloro- Series Interactions with Virg

reactant	number of reactant molecules x10^{17}	pressure equivalent (torr)x10^{2}	film temp. °C	reactant	
				mole % adsorbed	mole % reacted
1,2-dichloropropane	3.7	1.0	20	10	25
	3.7	1.0	20	0.0	35
1,3-dichloropropane	4.25	1.15	20	25	16.5
	3.7	1.0	180	0.0	10

TABLE (III - 5)*

Miscellaneous Studies of Interactions on V

methyl chloride	3.7	1.0	20	38	4.5
ethylene	4.75	1.4	20	95	0.0
	14.0	3.35	20	49.5	0.0
propane	3.7	1.0	20†	5†	0.0

* All data were recorded 300 seconds after admission of

† When film temperature was increased to 200°C, 'mole %

- 4)*

ɔns with Virgin Films

reactant			gaseous products and product ratios
ɔle % i- ɔrbed	mole % reacted	mole % unaf- fected	
10	25	65	propylene
).0	35	65	
25	16.5	58.5	cyclo- propane:propylene major:minor
).0	10	90	

- 5)*

ɔactions on Virgin Films

38	4.5	57.5	methane
95	0.0	5	none
9.5	0.0	50.5	
5†	0.0	95	none

admission of reactant to film.

0°C, 'mole % adsorbed' increased to 68.

III - 4. Elevated Temperature Interactions of Alkyl Halides with Previously Reacted Titanium Films

a) n-Propyl Halide Series

i) n-Propyl Chloride

The reaction of n-propyl chloride, at elevated temperatures, with previously reacted titanium films, occurred smoothly through many monolayer equivalents of reactant with reproducible rates. The reactant disappeared with half order kinetics and gave a mixture of propylene and propane as products. Neither hydrogen nor hydrogen chloride were detected and no loss of carbon to the film was observed.

The reaction of 10^{-2} torr doses of n-propyl chloride occurred at convenient rates for kinetic investigation between $170^{o}C$ and $220^{o}C$. Figures (III-4) and (III-6) show the half order dependence of the reaction on reactant pressure for investigations on two different films. Apparent rate constants for these two sets of reactions vary somewhat. Those obtained from figure (III-6) are almost three times greater than those obtained from figure (III-4). The film used to generate the data illustrated by figure (III-6) was considerably heavier than the film used to generate the data illustrated by figure (III-4). However, both sets of reactants gave Arrhenius plots with almost identical slopes. These Arrhenius plots are shown in figures (III-5) and (III-7). The slopes of these graphs were calculated by the method of least squares and gave the apparent activation energy for the reaction of n-propyl chloride

FIGURE (III - 4)

Disappearance of n-Propyl Chloride

Plotted as a Half Order Reaction

for $P_o = 10^{-2}$ torr

○ - 220°C

△ - 210°C

◇ ,□ - 200°C

● - 190°C

▽ - 180°C

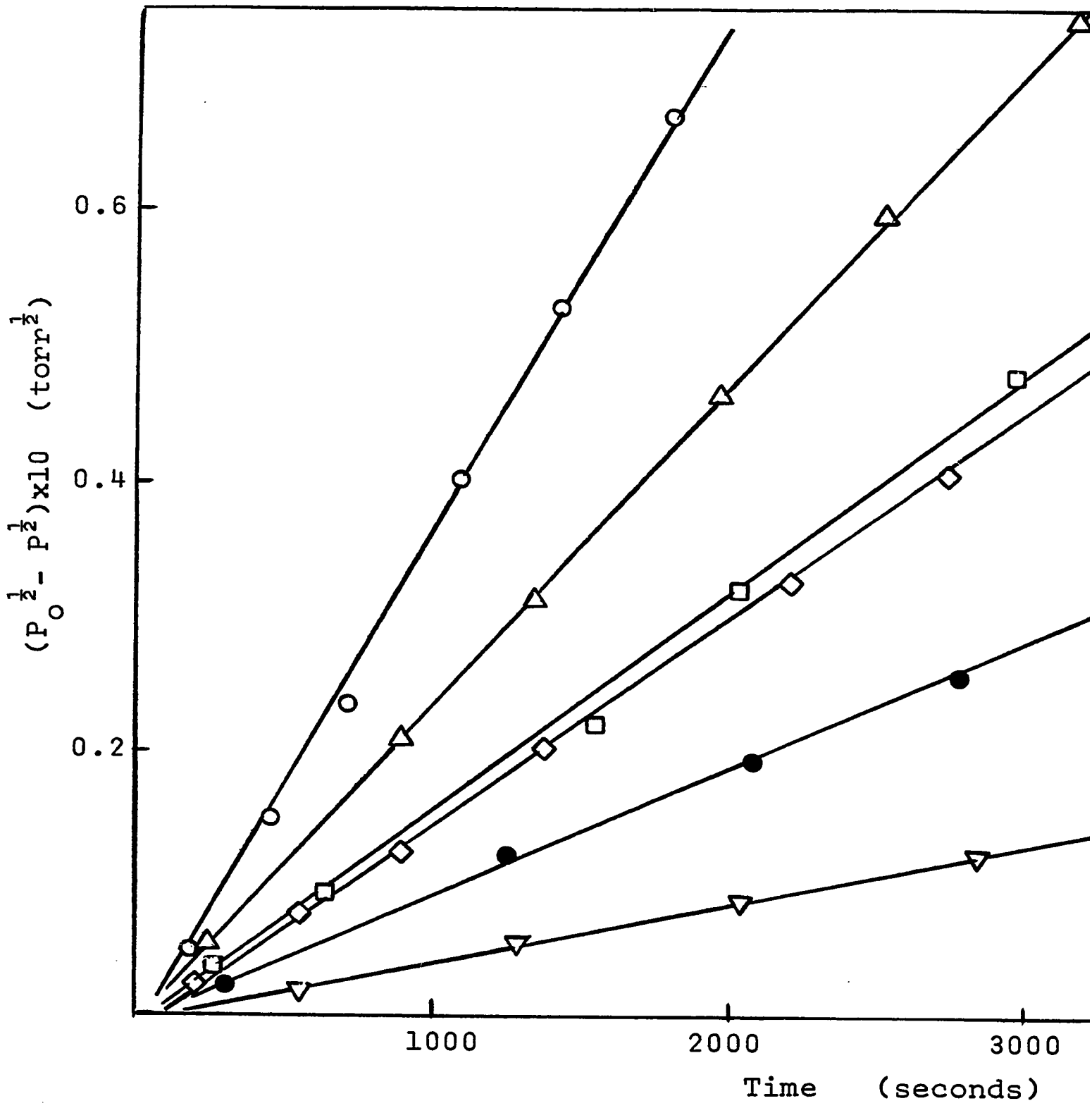
0.6
0.4
0.2
$(P_o^{\frac{1}{2}} - P^{\frac{1}{2}}) \times 10$ $(torr^{\frac{1}{2}})$
1000
2000
3000
Time (seconds)

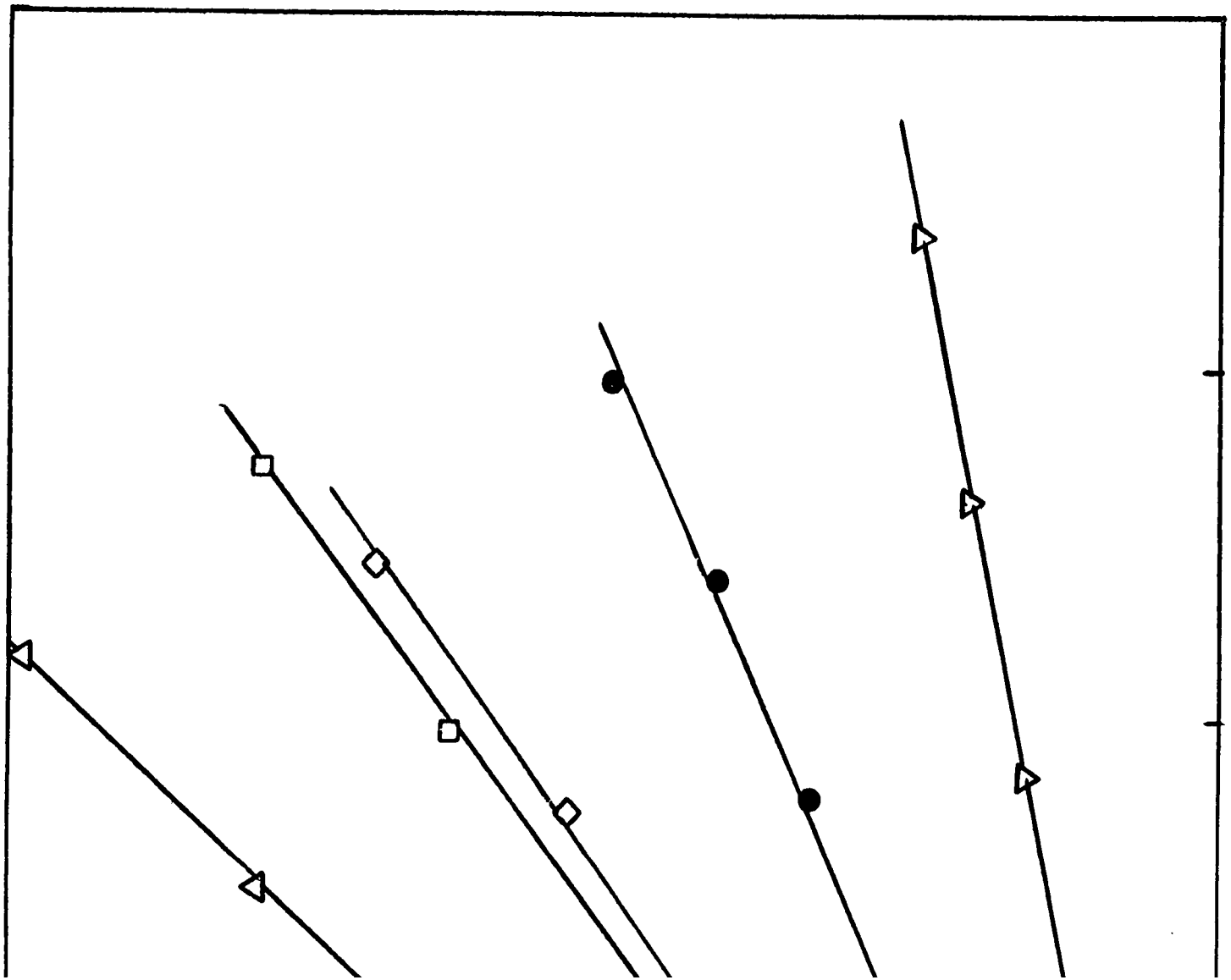
4000
3000
(seconds)

FIGURE (III - 5)

Arrhenius Plot of Rate Data from Half Order Disappearance

of n-Propyl Chloride in Figure (III-4)

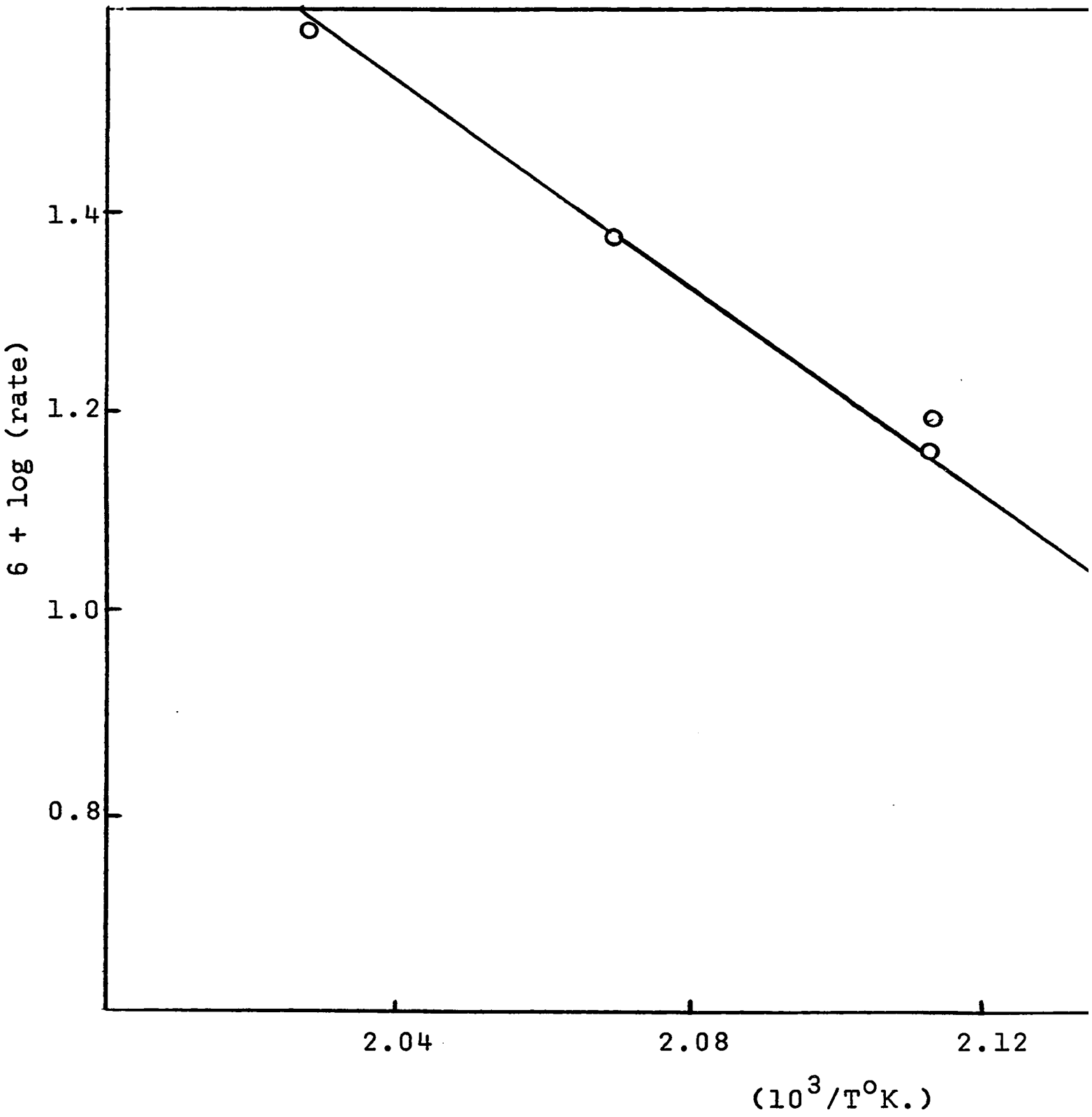
1.4
1.2
1.0
0.8
6 + log (rate)
2.04
2.08
2.12
(10³/T°K.)

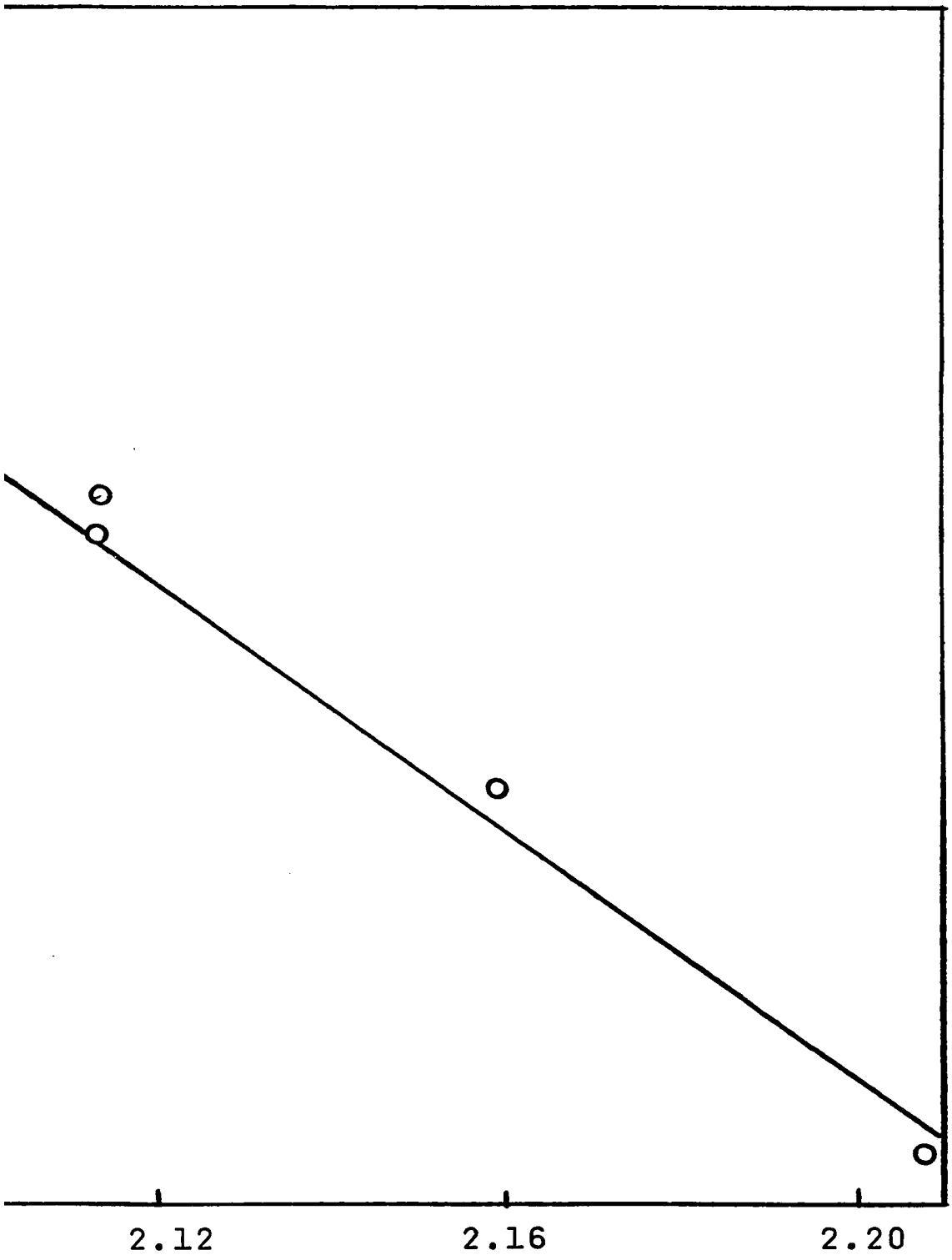

[°K.)

FIGURE (III - 6)

Disappearance of n-Propyl Chloride

Plotted as a Half Order Reaction

for $P_o = 10^{-2}$ torr

○ - 175.5°C

▽ - 182.5°C

□ - 190°C

△ - 200°C

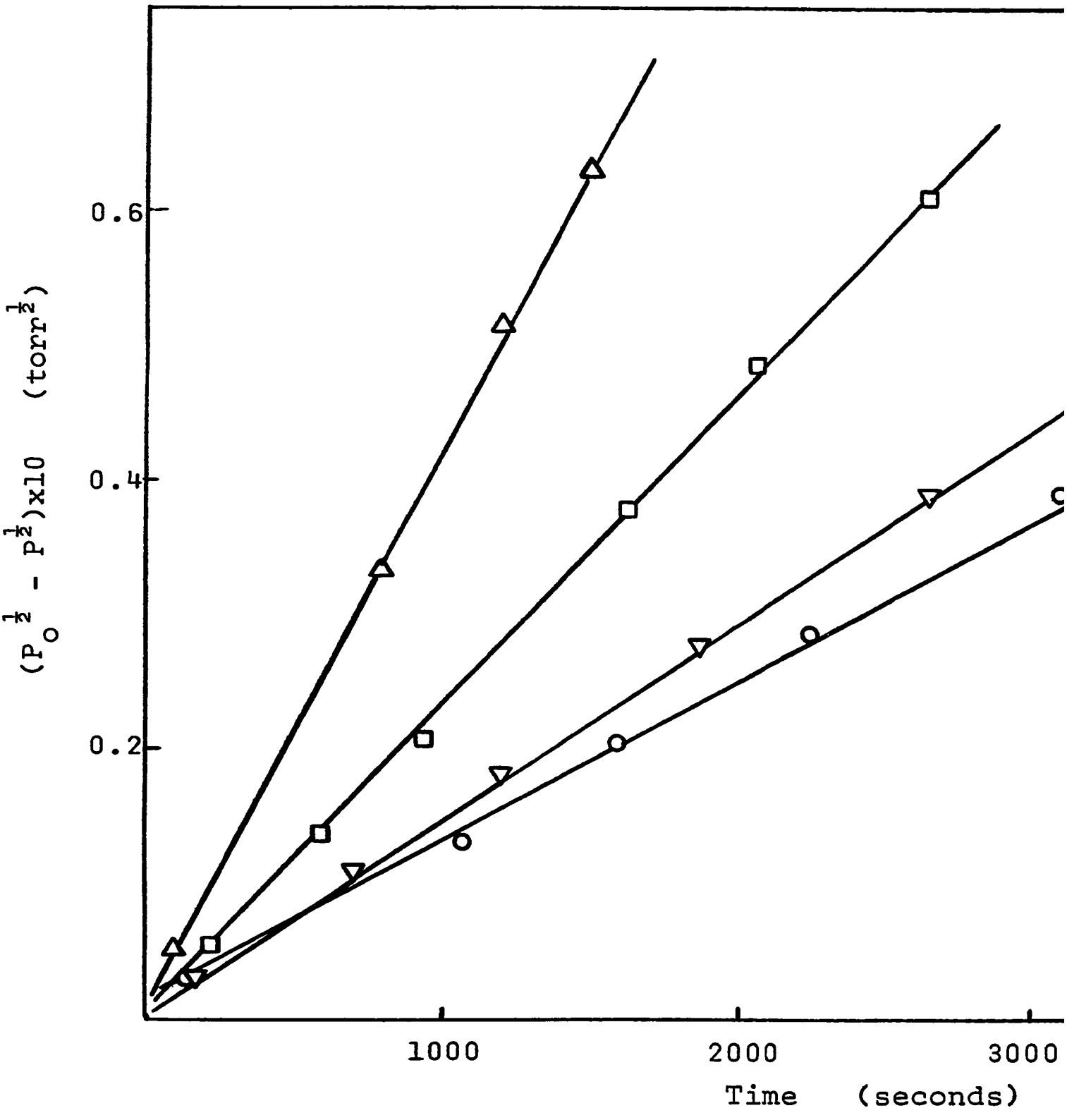
0.6
0.4
0.2
$(P_o^{\frac{1}{2}} - P^{\frac{1}{2}})x10$ (torr$^{\frac{1}{2}}$)
1000
2000
3000
Time (seconds)

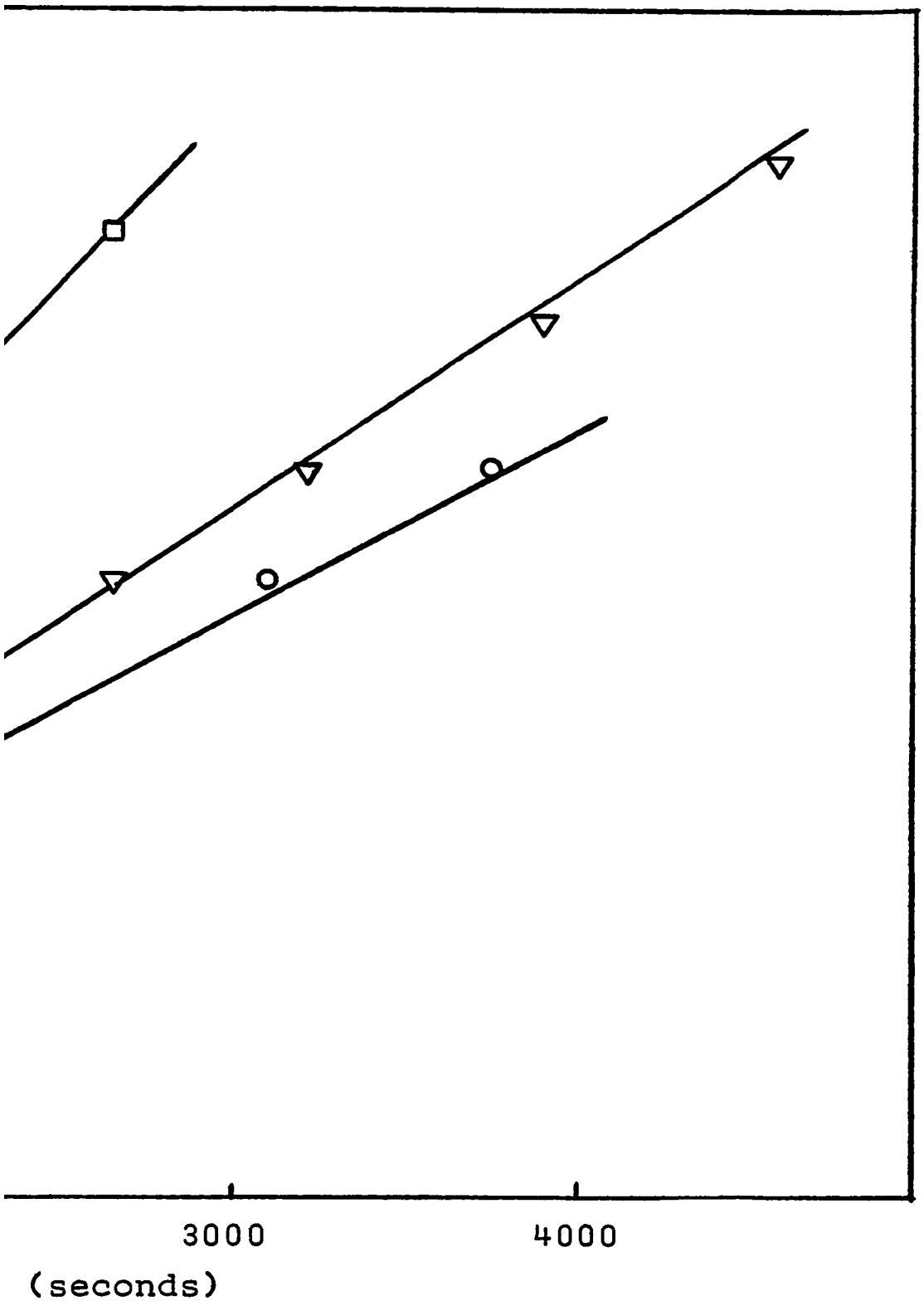
3000
4000
(seconds)

FIGURE (III - 7)

Arrhenius Plot of Rate Data from Half Order Disappearance

of n-Propyl Chloride in Figure (III-6)

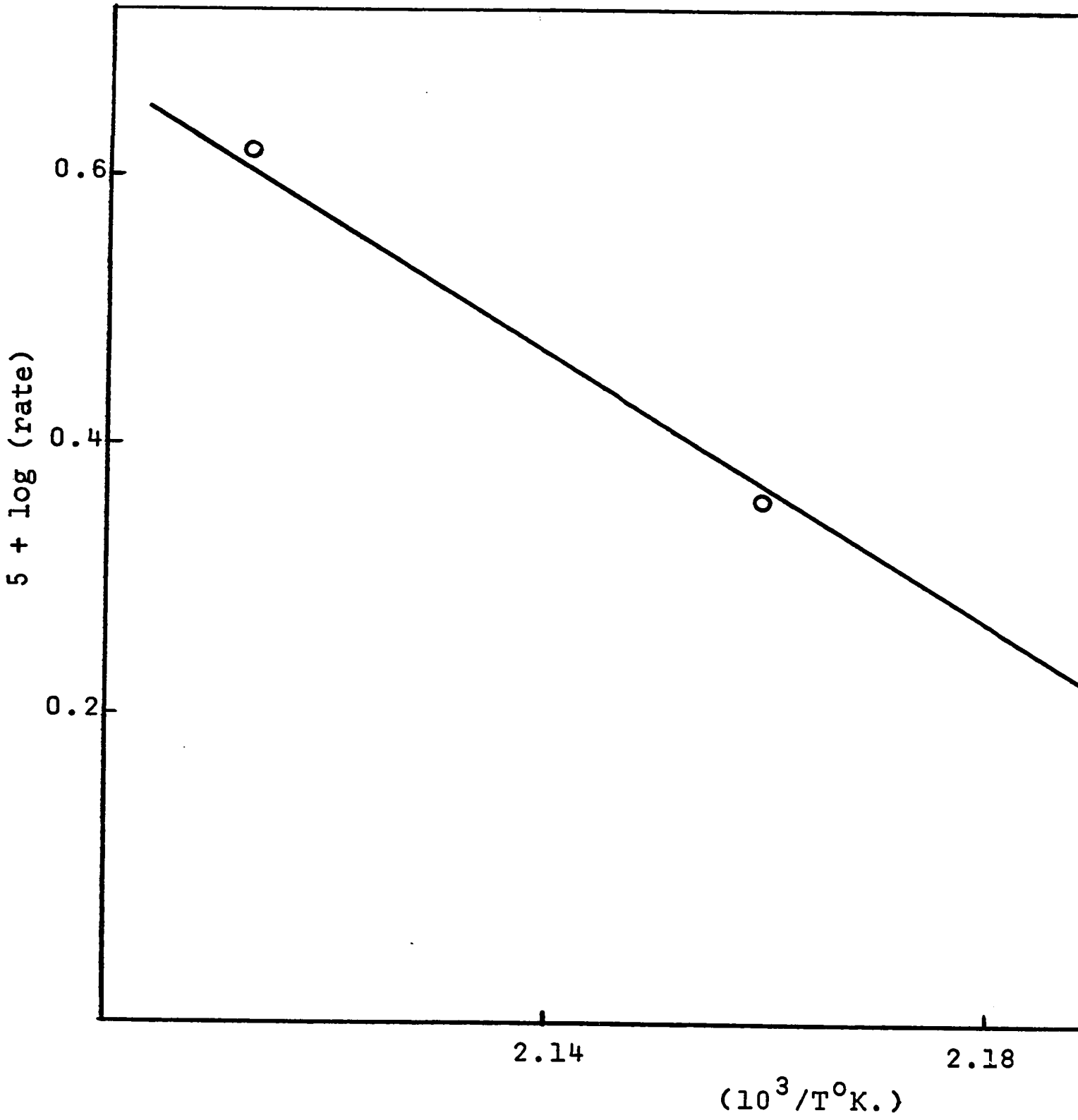
0.6
0.4
0.2
5 + log (rate)
2.14
2.18
(10³/T°K.)

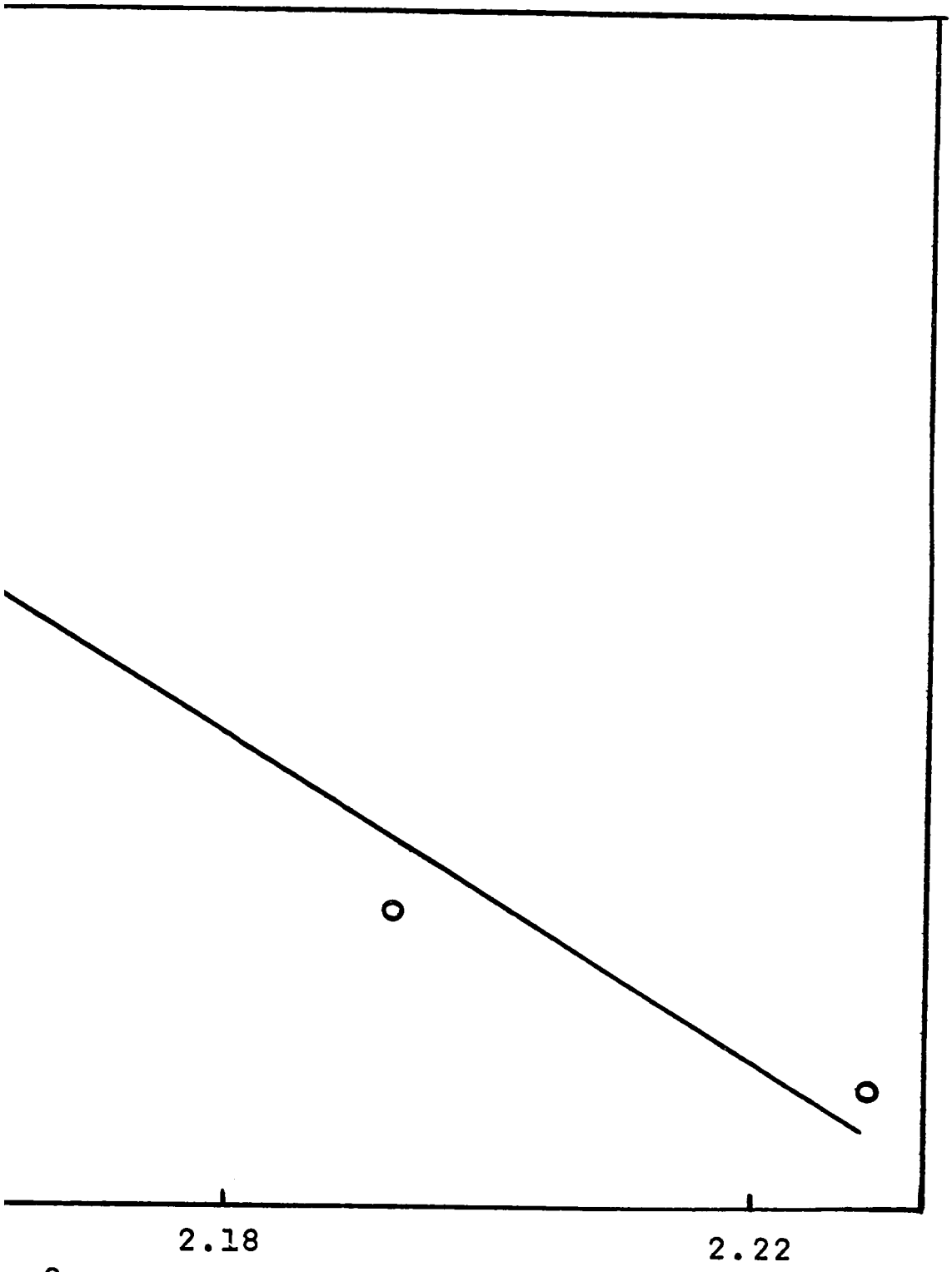
2.18
2.22
/T°K.)

as 23.4±0.9 kcal./mole and 22.6±1.3 kcal./mole respectively.

Rate reproducibility within a set of reactions on any one film was good as can be seen by examining the rate slopes of two reactions at the same temperature, (200°C) in figure (III-4).

An interesting feature of this reaction is an apparent activation of the film which occurs during the reaction of the first dose of reactant at elevated temperature. In figure (III-8), the rate slopes for reaction of 10^{-2} torr at 200°C are reproduced from figure (III-4). In addition, a kinetic plot of the first dose of reactant, also at 200°C, is shown. This reaction shows a period of activation, followed by a straight line plot with a slope having better than ±5% agreement with slopes of subsequent reactions at the same temperature.

It was found that increased initial reactant pressures tended to decrease the apparent rate constant. Three reactions of n-propyl chloride at an identical temperature but for different P_o's are shown in figure (III-9), illustrating this phenomenon.

It was also noted that the initial reactant pressure affected the ratio of propane to propylene in the gaseous products. An increase in P_o resulted in enhanced propane production. A second effect also influenced the product ratio. As a film was more and more extensively reacted, the propane to propylene ratio increased. These effects are both shown in figure (III-10) which also shows a direct proportionality between mole percent propane generated and mole percent n-propyl chloride reacted.

FIGURE (III - 8)

Half Order Disappearance of n-Propyl Chloride at 200°C, Showing Initial Film Activation (Δ), and Reproducibility of Rates for Reactions of Equal Reactant Doses at the same Temperature.

○ - Early Reaction

□ - Later Reaction

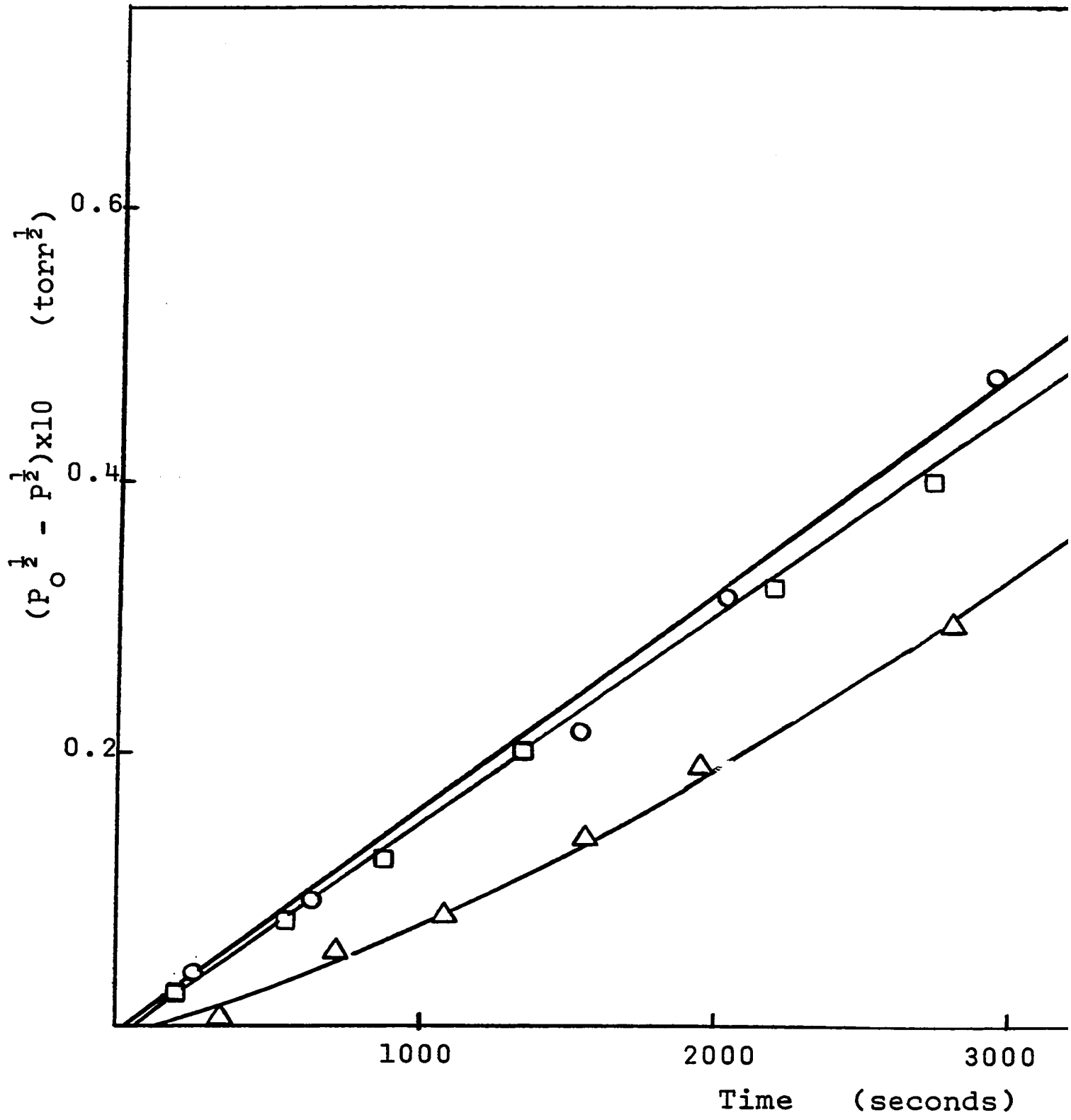
0.6
0.4
0.2
$(P_o^{\frac{1}{2}} - P^{\frac{1}{2}}) \times 10$ (torr$^{\frac{1}{2}}$)
1000
2000
3000
Time (seconds)

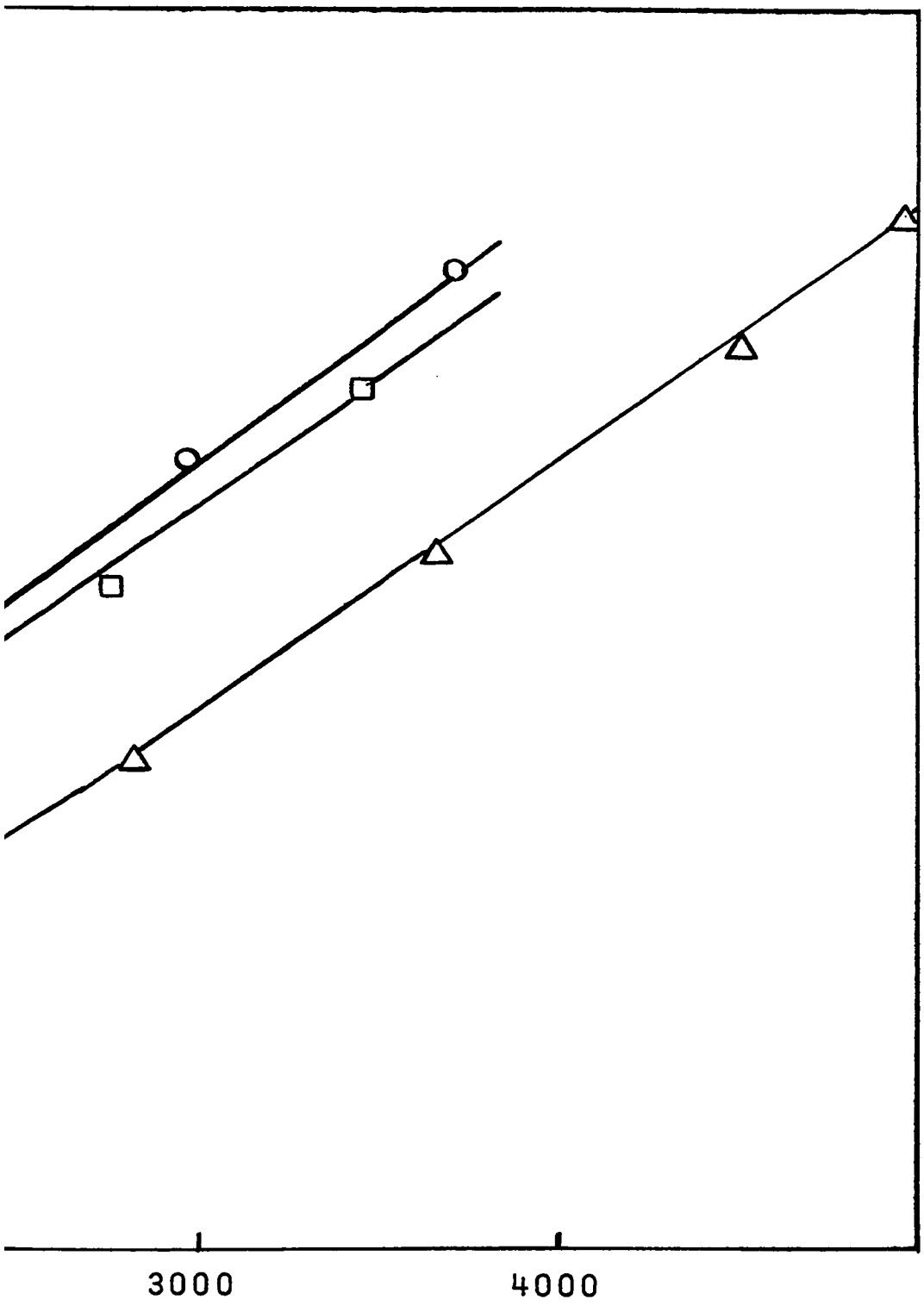
3000
4000
(seconds)

FIGURE (III - 9)

Rate Dependence on Initial Pressure of Reactant n-Propyl Chloride during Half Order Disappearance at 223°C

○ - $P_o = 1.1 \times 10^{-2}$ torr

△ - $P_o = 2.5 \times 10^{-2}$ torr

□ - $P_o = 6.5 \times 10^{-2}$ torr

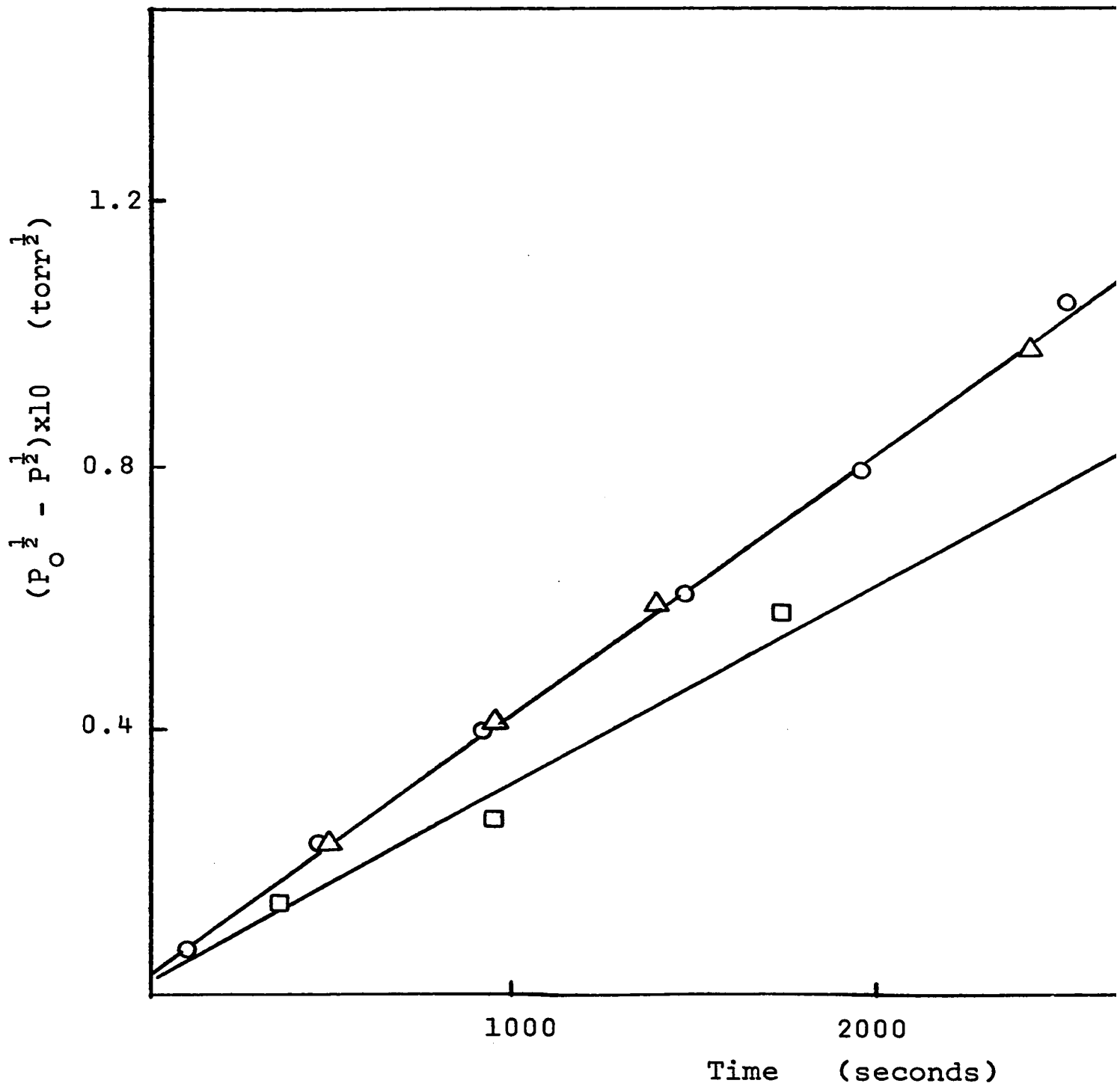
1.2
0.8
0.4
$(P_o^{\frac{1}{2}} - P^{\frac{1}{2}}) \times 10$ $(torr^{\frac{1}{2}})$
1000
2000
Time (seconds)

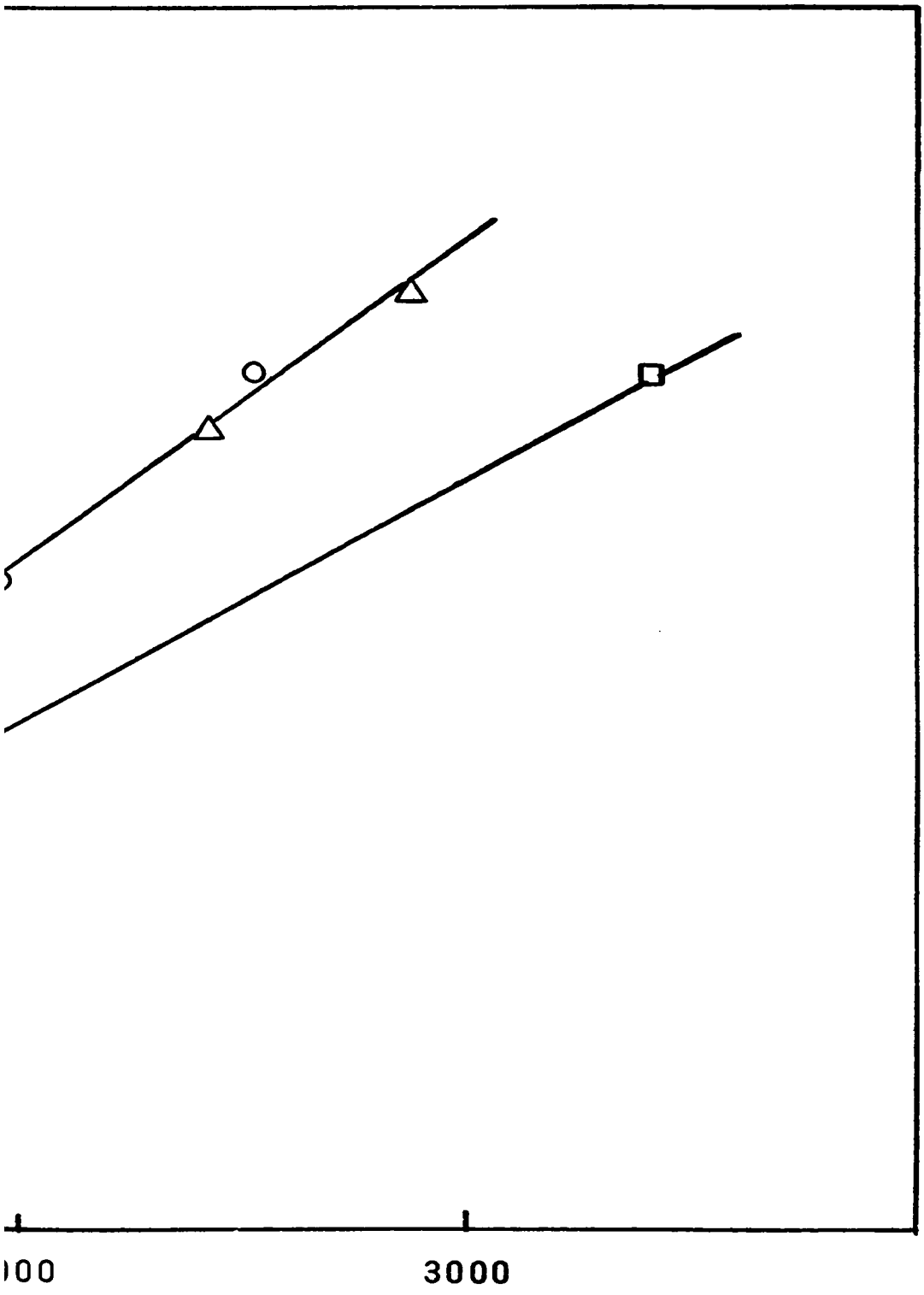
)00
3000
seconds)

FIGURE (III - 10)

Dependence of Mole Percent Propane Generated on Mole Percent n-Propyl Chloride Reacted for Various Initial Pressures of n-Propyl Chloride

□ - $P_o = 1.1 \times 10^{-2}$ torr on extensively reacted film

△ - $P_o = 2.5 \times 10^{-2}$ torr on extensively reacted film

○ - $P_o = 6.5 \times 10^{-2}$ torr on extensively reacted film

◇ - $P_o = 1.0 \times 10^{-2}$ torr on relatively unreacted film

at 223°C

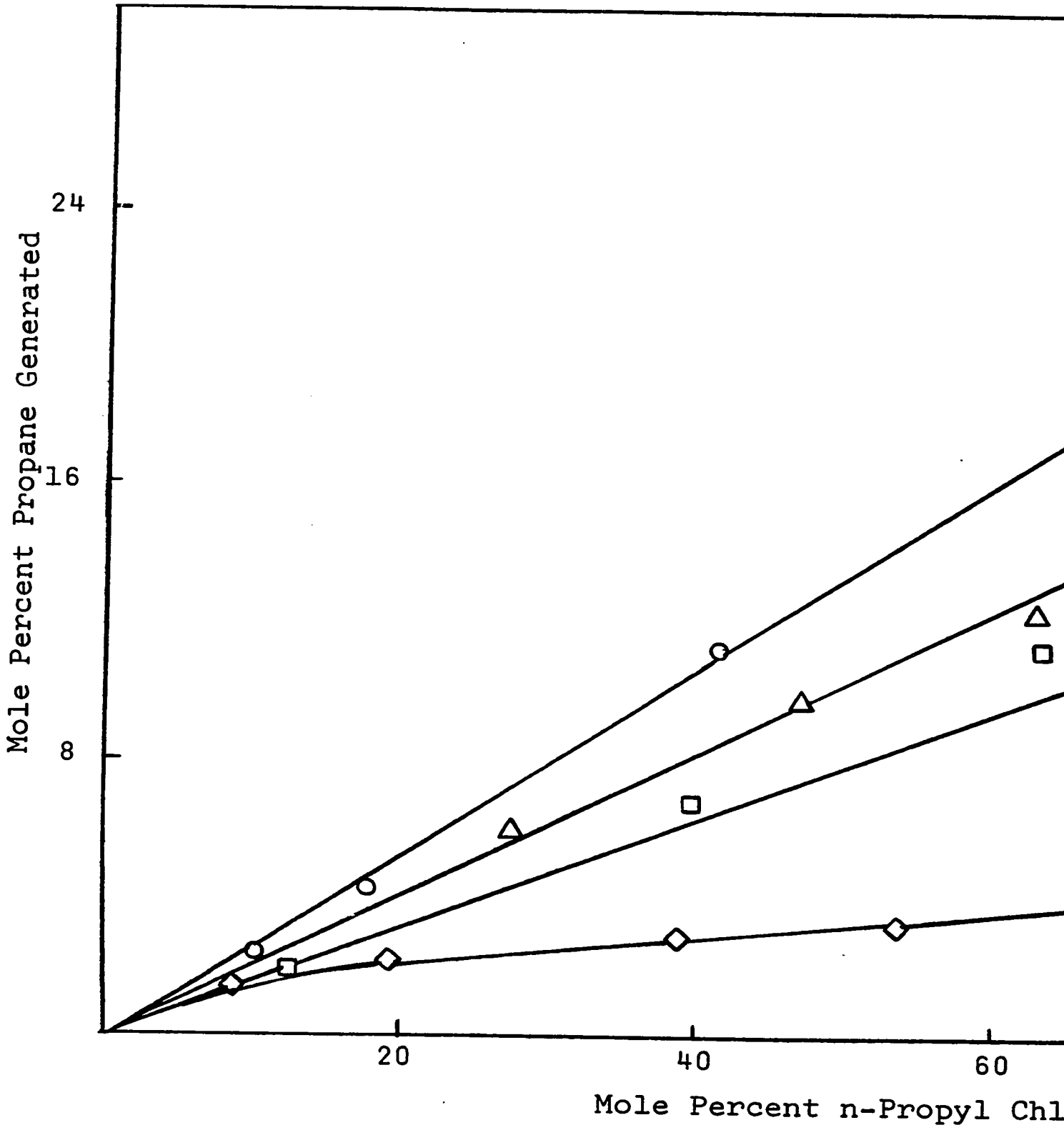
24
16
8
Mole Percent Propane Generated
20
40
60
Mole Percent n-Propyl Chl

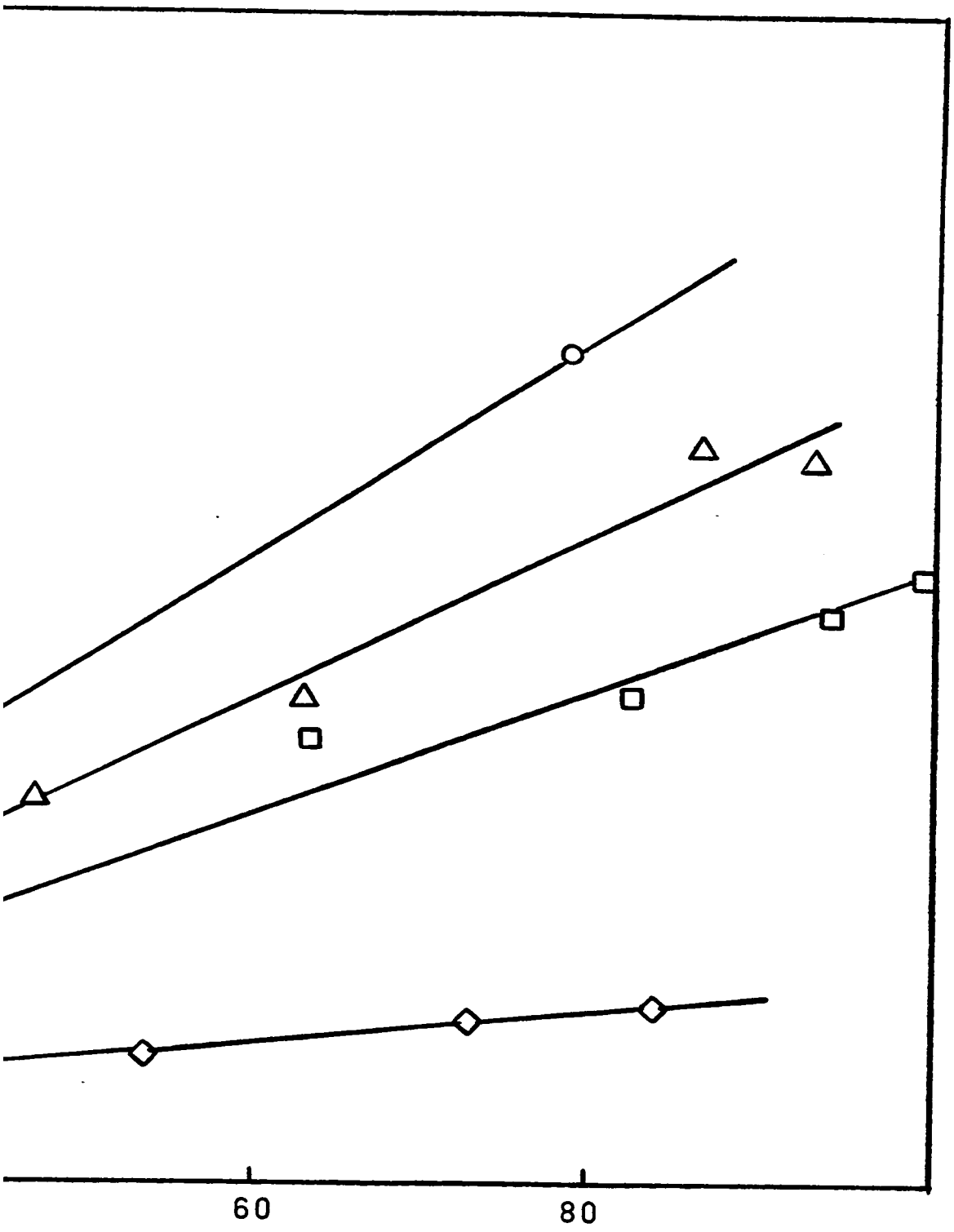

ent n-Propyl Chloride Reacted

This means that for any given reaction, the product ratio is invariant as reactant is consumed. Within the limits of this study, no variation of product ratio with temperature was found.

ii) n-Propyl Bromide

The reaction of n-propyl bromide at elevated temperatures, with previously reacted titanium films, occurred smoothly through many monolayer equivalents of reactant with reproducible rates. As in the case of n-propyl chloride, the reactant disappeared with half order kinetics and gave a mixture of propylene and propane as products. Neither hydrogen nor hydrogen bromide were detected and no loss of carbon to the film was observed.

The reaction of 10^{-2} torr and 3.3×10^{-2} torr doses occurred at convenient rates for kinetic investigation between 185°C and 225°C. Figures (III-11) and (III-12) illustrate the half order dependence of the reaction on reactant concentration for 10^{-2} torr doses and figure (III-13) shows the same dependence for 3.3×10^{-2} torr doses. Arrhenius plots for these three sets of reactions are shown in figure (III-14). Calculation of the slopes of the lines in figure (III-14) gave the apparent activation energy for the reaction of n-propyl bromide as 25.8±0.4 kcal./mole and 27.3±0.6 kcal./mole for the two sets of reaction data at $P_o = 10^{-2}$ torr and as 27.9±0.2 kcal./mole for the reaction data at $P_o = 3.3 \times 10^{-2}$ torr.

Rate reproducibility is illustrated by two reactions at 224.5°C in figure (III-11). The initial reactant pressure affected the propane to propylene ratio in the gaseous products

FIGURE (III - 11)

Disappearance of n-Propyl Bromide

Plotted as a Half Order Reaction

for $P_o = 10^{-2}$ torr

△ - 195°C

○ - 205°C

▽ - 214.5°C

◇, □ - 224.5°C

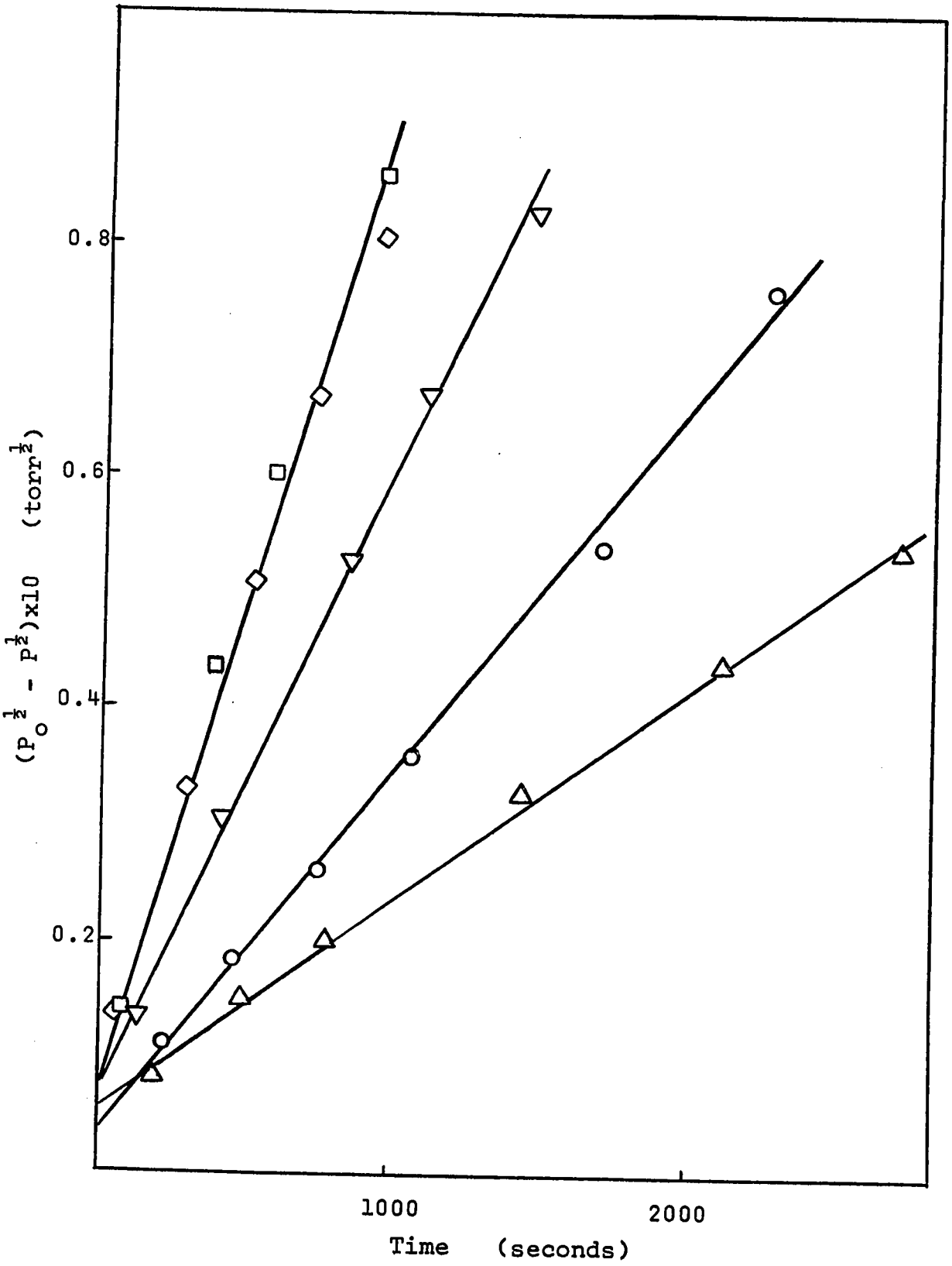
0.8
0.6
0.4
0.2
$(P_o^{\frac{1}{2}} - P^{\frac{1}{2}}) \times 10$ (torr$^{\frac{1}{2}}$)
1000
2000
Time (seconds)

FIGURE (III - 12)

Disappearance of n-Propyl Bromide

Plotted as a Half Order Reaction

for $P_o = 10^{-2}$ torr

△ - 188.5°C

□ - 203°C

○ - 211.5°C

▽ - 223.5°C

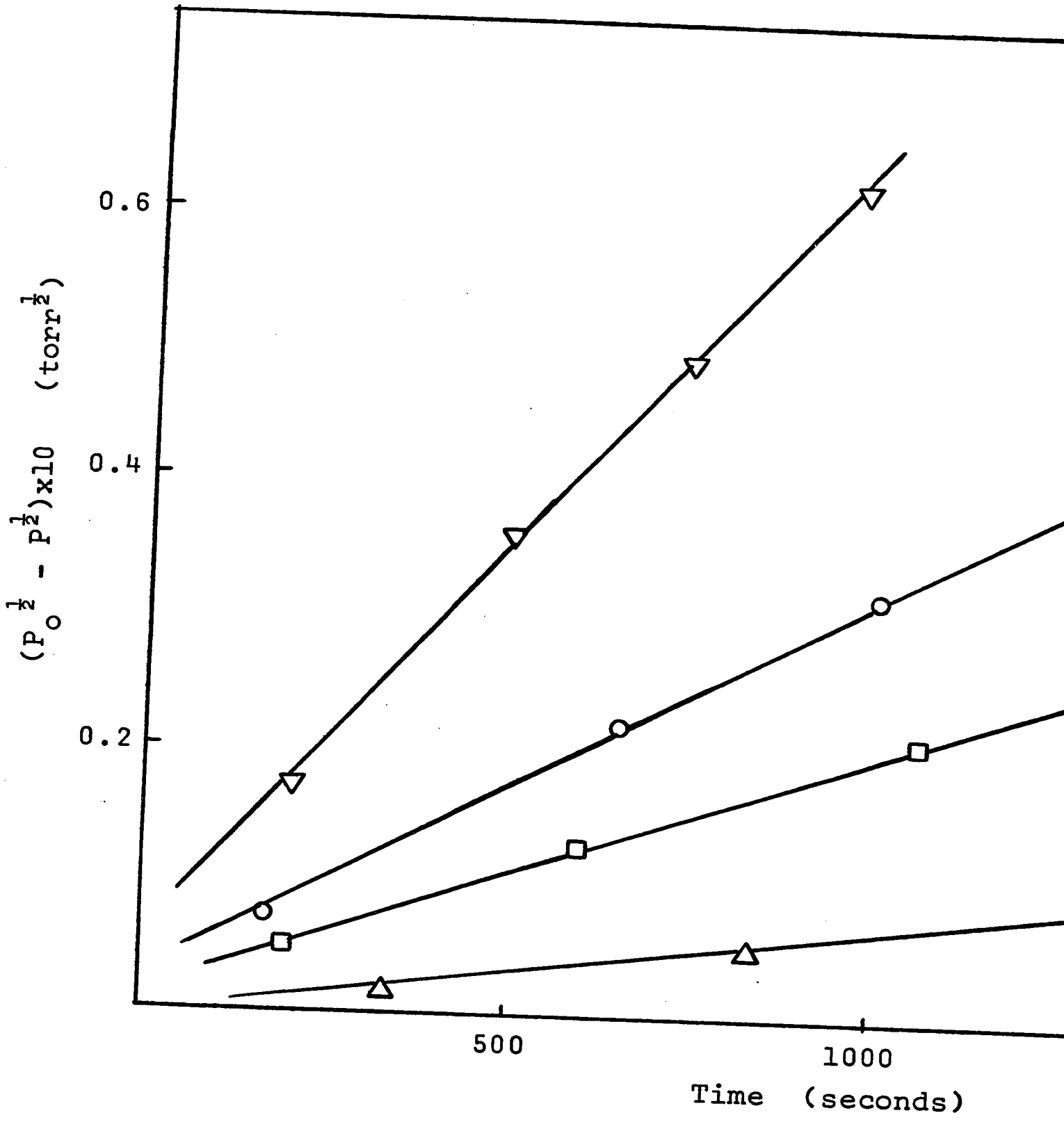
0.6
0.4
0.2
$(P_o^{\frac{1}{2}} - P^{\frac{1}{2}}) \times 10$ (torr$^{\frac{1}{2}}$)
500
1000
Time (seconds)

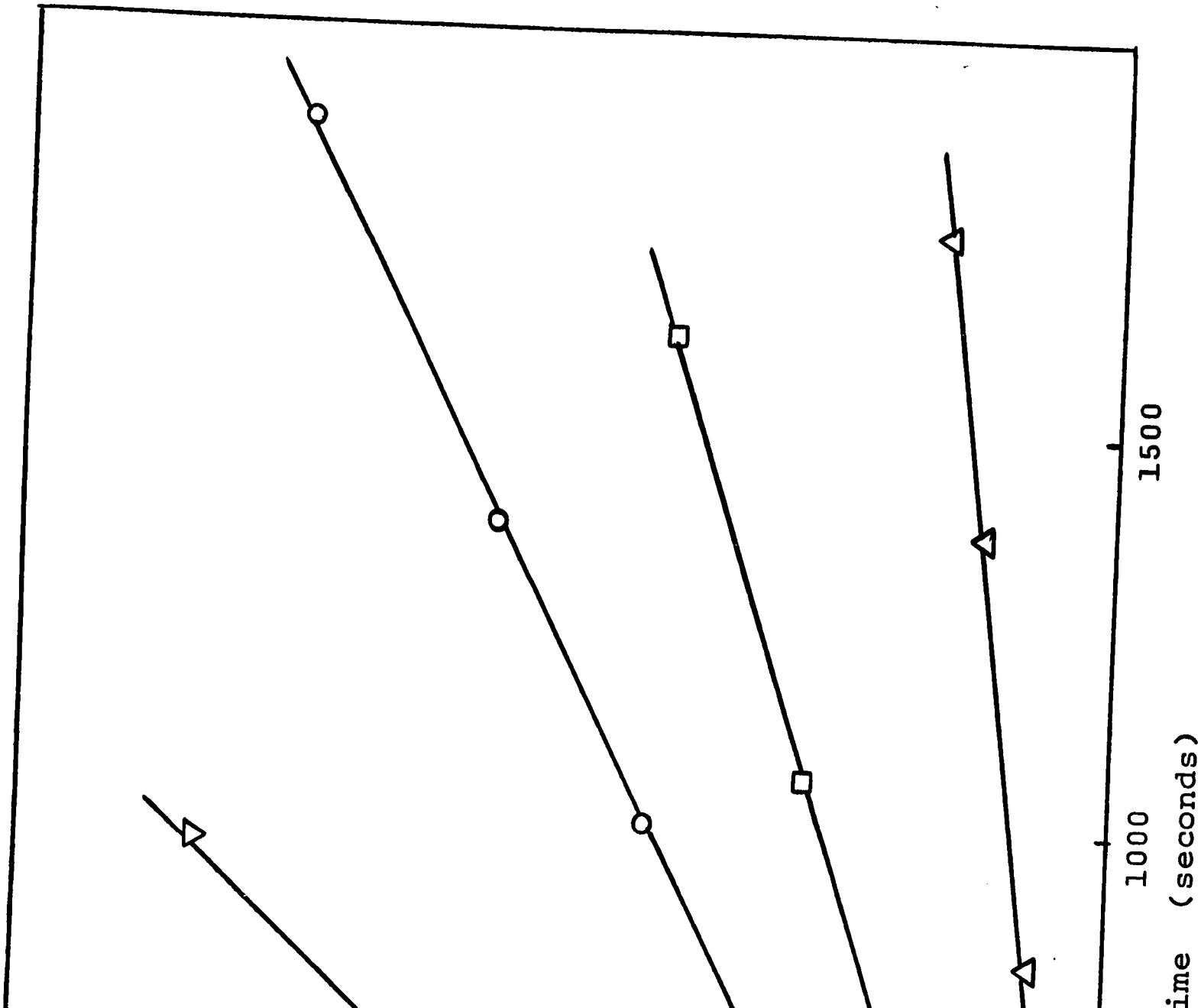
1500
1000
ime (seconds)

FIGURE (III - 13)

Disappearance of n-Propyl Bromide

Plotted as a Half Order Reaction

for $P_o = 3.3 \times 10^{-2}$ torr

□ - 203°C

○ - 211.5°C

△ - 223.5°C

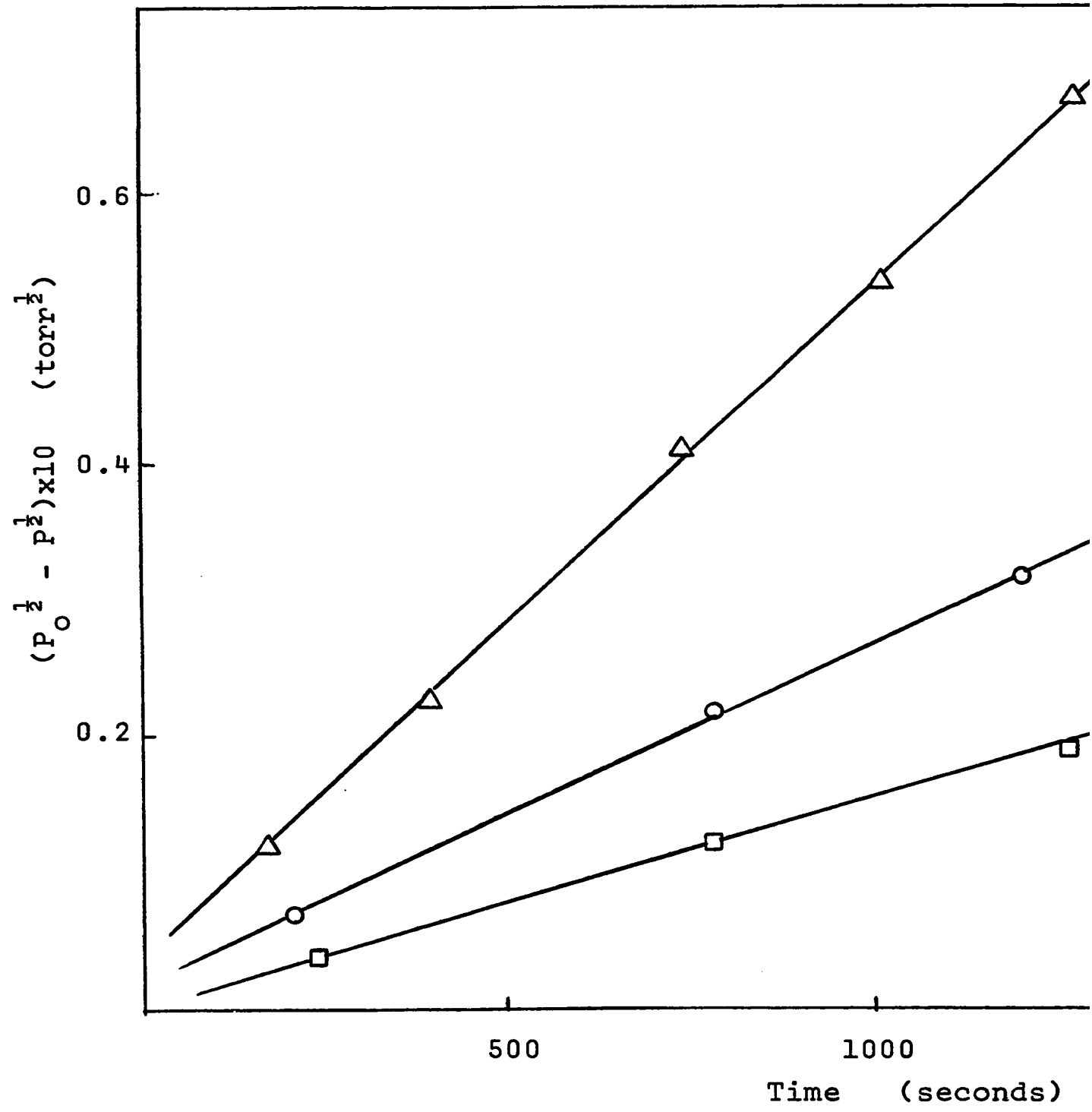
0.6
0.4
0.2
$(P_o^{\frac{1}{2}} - P^{\frac{1}{2}})x10$ $(torr^{\frac{1}{2}})$
500
1000
Time (seconds)

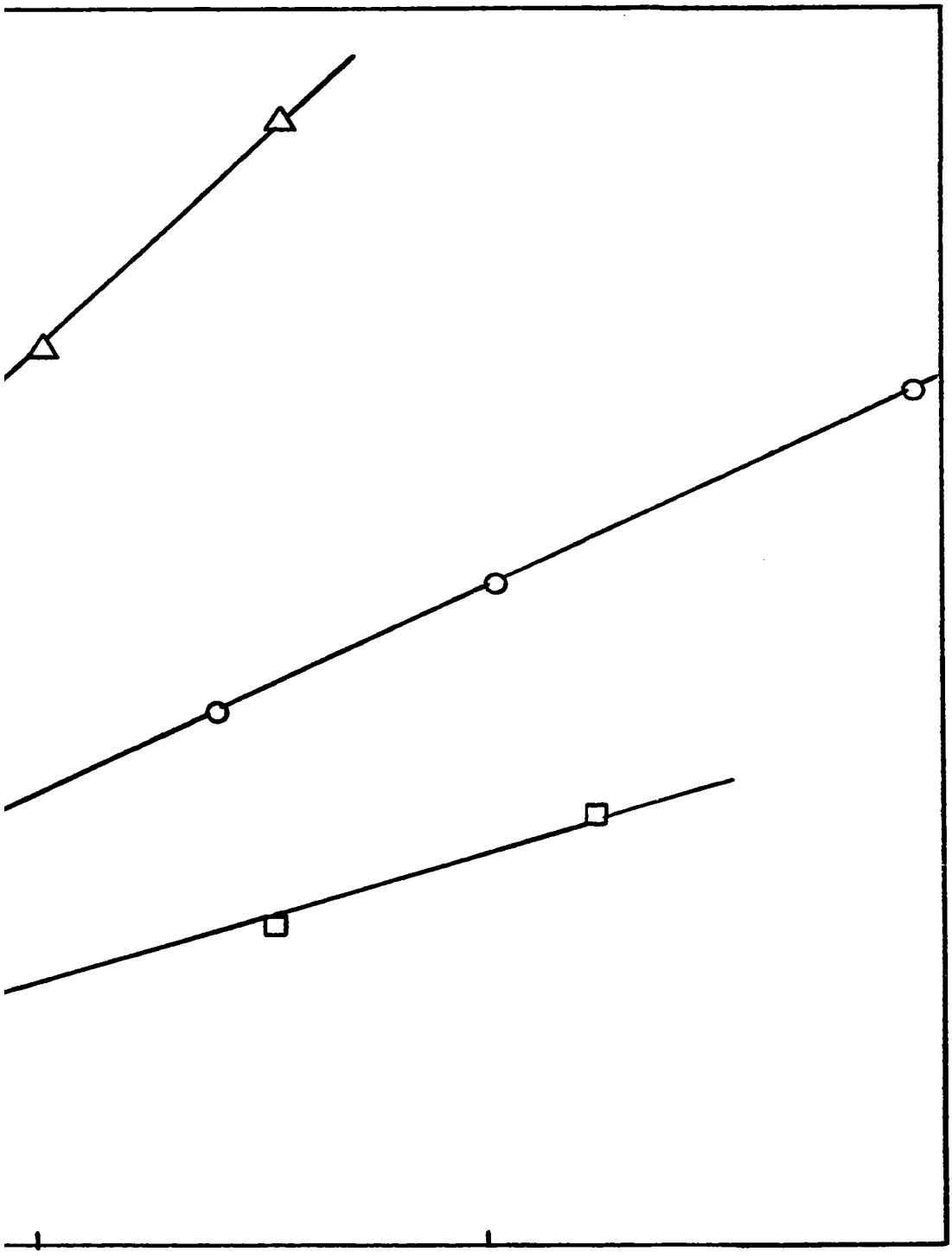
L000
1500
(seconds)

FIGURE (III - 14)

Arrhenius Plots of Rate Data from Half Order Disappearances

of n-Propyl Bromide

○ - Figure (III-11)

□ - Figure (III-12)

△ - Figure (III-13)

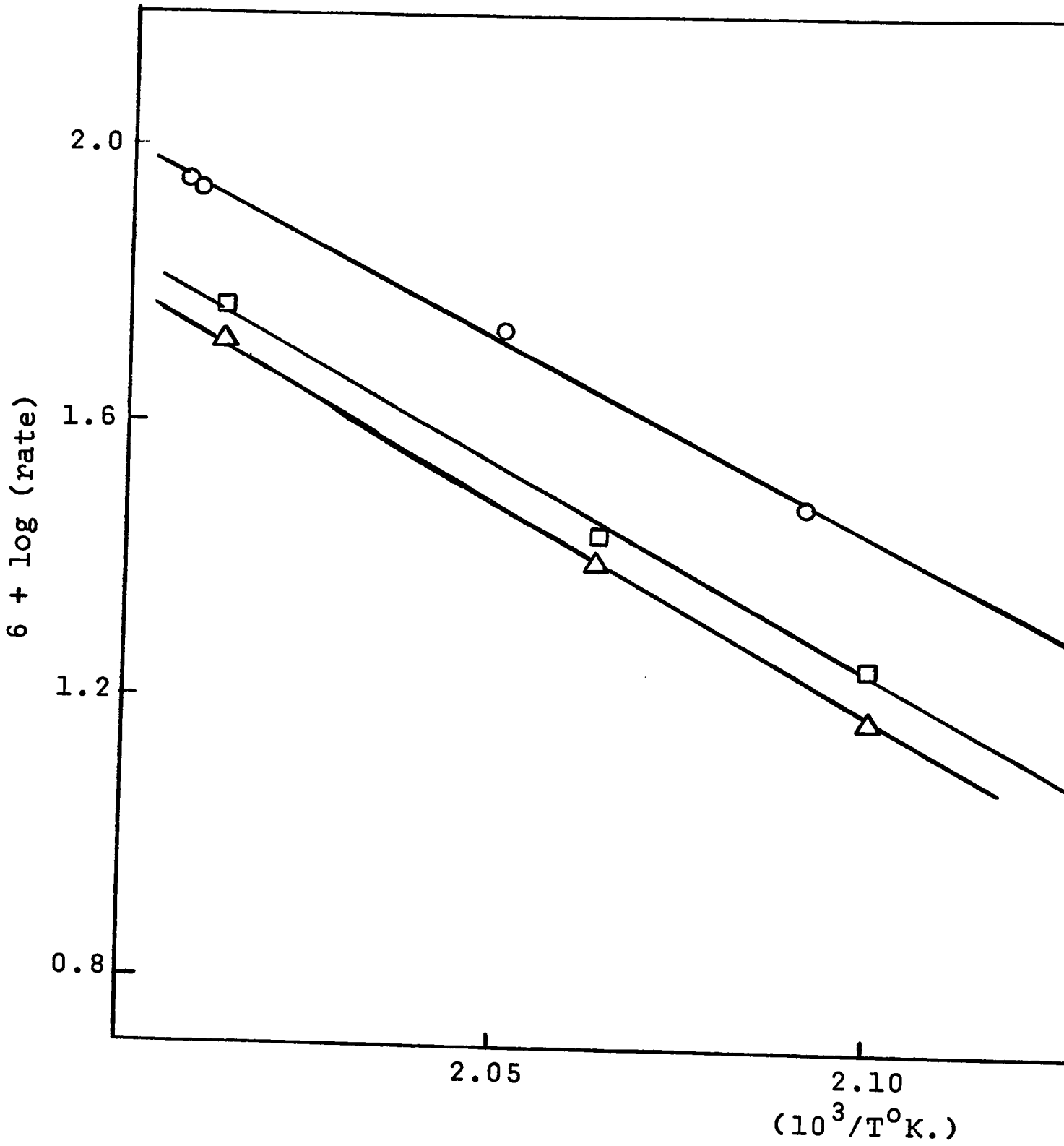
2.0
1.6
1.2
0.8
6 + log (rate)
2.05
2.10
(10³/T°K.)

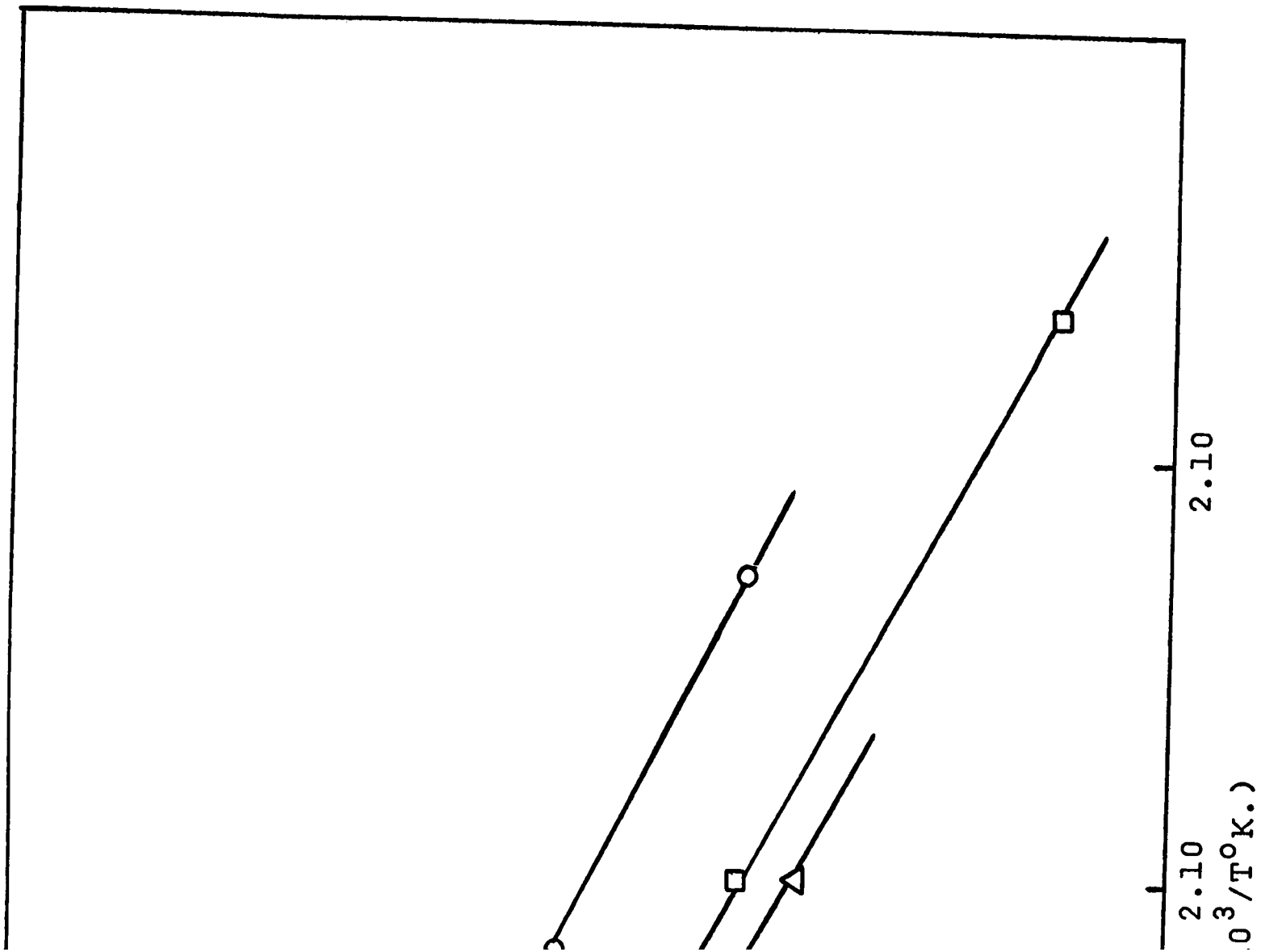
2.10
2.10
$10^3/T^oK.$)

in an identical manner to that noted for n-propyl chloride. This effect is illustrated in figure (III-15).

iii) n-Propyl Iodide

The reaction of n-propyl iodide at elevated temperatures with previously reacted titanium films, occurred smoothly through many monolayer equivalents of reactant with reproducible rates. As in the cases of n-propyl chloride and bromide, the reactant disappeared with half order kinetics and gave mixtures of propane and propylene as products. Neither hydrogen nor hydrogen iodide were detected and no loss of carbon to the film was observed.

The reaction of 10^{-2} torr and 3.3×10^{-2} torr doses occurred at convenient rates for kinetic investigation between $190^{\circ}C$ and $220^{\circ}C$. Figures (III-16) and (III-17) illustrate the half order dependence of the reaction on reactant concentration for 10^{-2} torr and 3.3×10^{-2} torr doses respectively.

Arrhenius plots for these two sets of reactions are shown in figure (III-18). Calculation of the slopes of the lines in figure (III-18) gave the apparent activation energy for the reaction of n-propyl iodide as 28.9 ± 0.3 kcal./mole at 10^{-2} torr and 29.8 ± 0.3 kcal./mole at 3.3×10^{-2} torr.

The initial reactant pressure affected the ratio of propane to propylene in the gas products in an identical manner to that noted for n-propyl chloride and bromide. This effect is shown in figure (III-19).

FIGURE (III - 15)

Dependence of Mole Percent Propane Generated on Mole Percent n-Propyl Bromide Reacted for Various Initial Pressures of n-Propyl Bromide

□ - $P_o = 1.25 \times 10^{-2}$ torr

○ - $P_o = 5.0 \times 10^{-2}$ torr

△ - $P_o = 10^{-1}$ torr

at 200°C

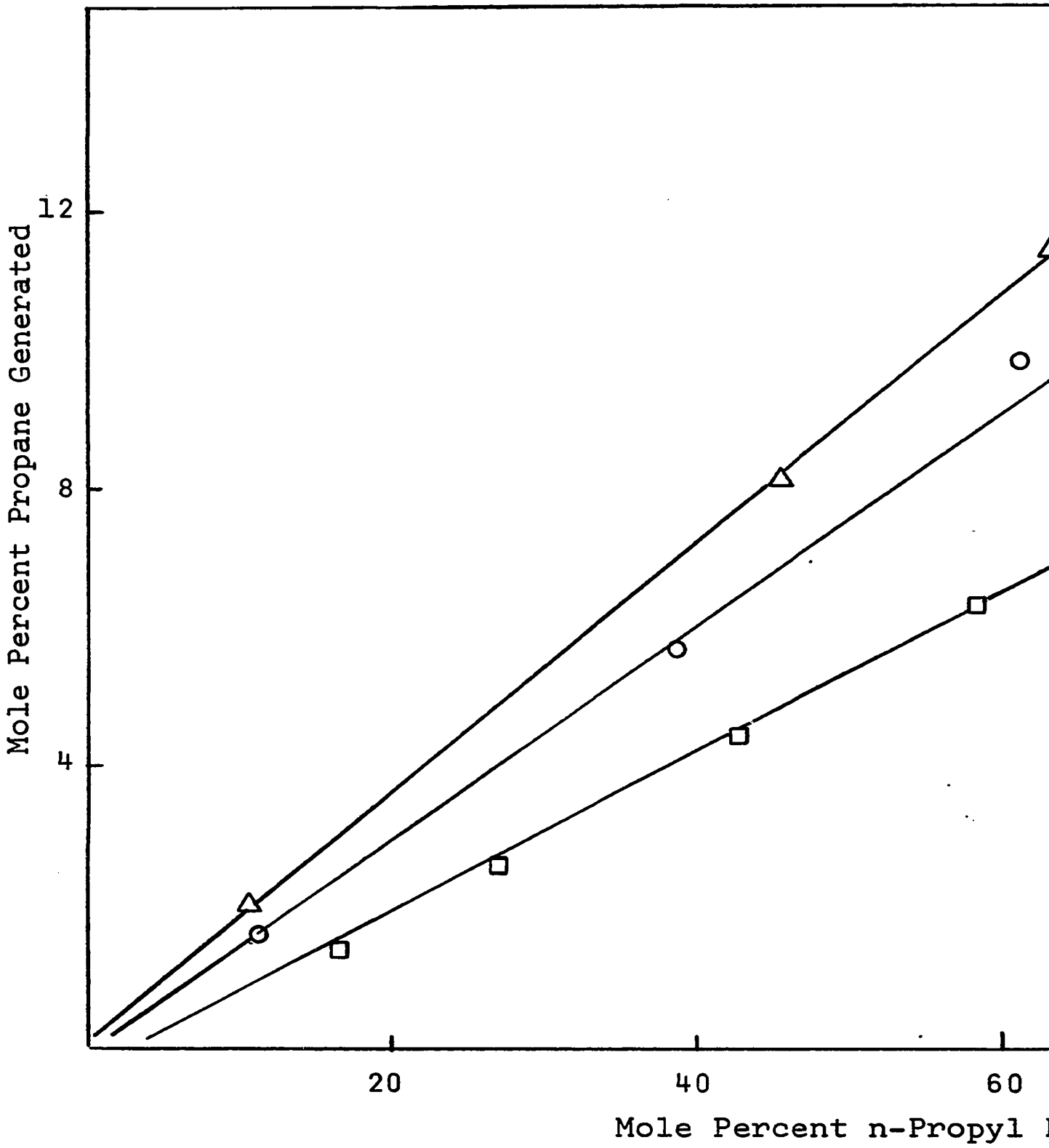
Mole Percent Propane Generated
12
8
4
20
40
60
Mole Percent n-Propyl

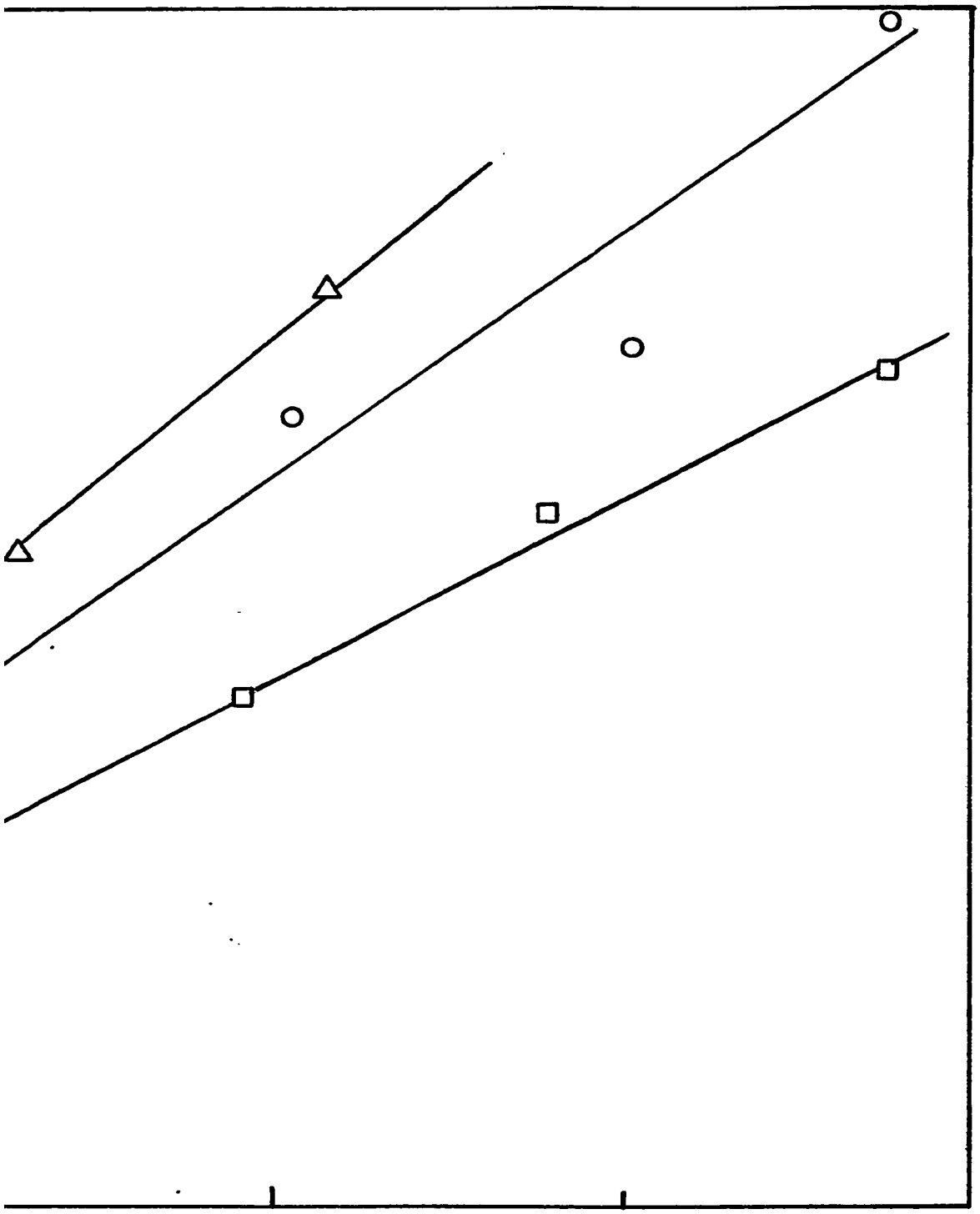

cent n-Propyl Bromide Reacted

FIGURE (III - 16)

Disappearance of n-Propyl Iodide

Plotted as a Half Order Reaction

for $P_o = 10^{-2}$ torr

▽ - 191°C

○ - 198.5°C

△ - 207.5°C

□ - 218.5°C

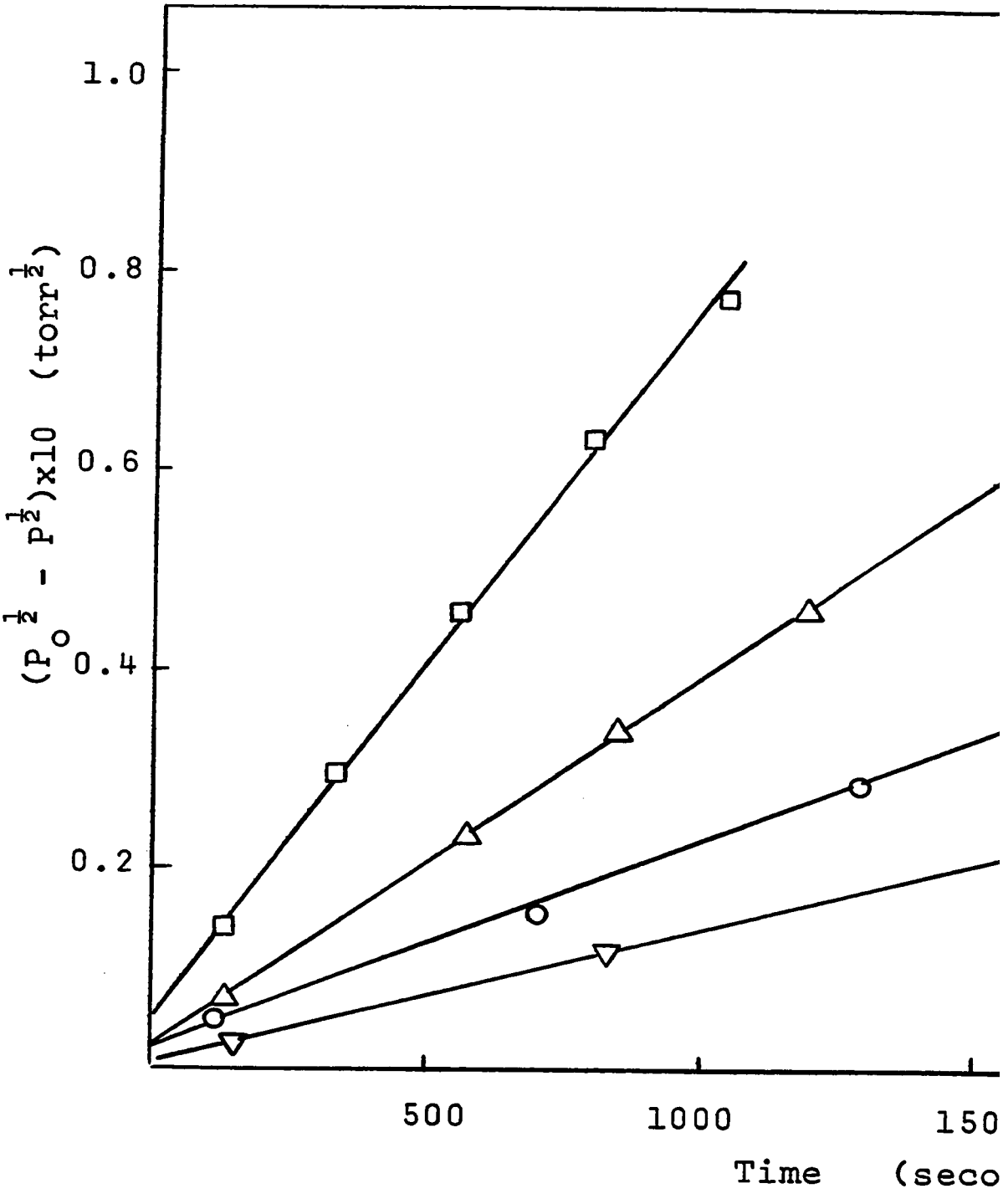
1.0
0.8
0.6
0.4
0.2
$(P_o^{\frac{1}{2}} - P^{\frac{1}{2}})x10$ (torr$^{\frac{1}{2}}$)
500
1000
150
Time (seco

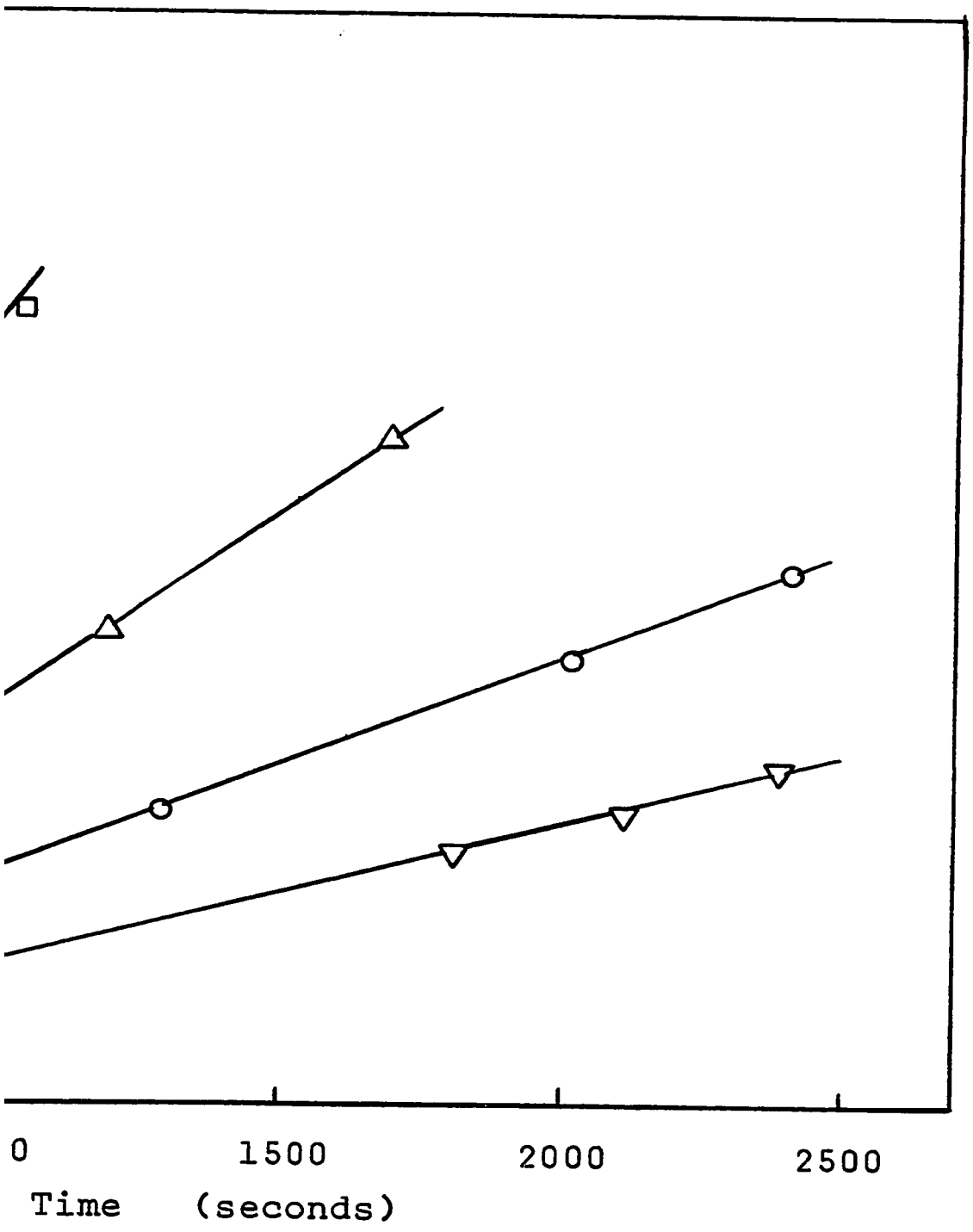
0
1500
2000
2500
Time (seconds)

FIGURE (III - 17)

Disappearance of n-Propyl Iodide

Plotted as a Half Order Reaction

for $P_o = 3.3 \times 10^{-2}$ torr

◇ - 191°C

△ - 198.5°C

□ - 207.5°C

○ - 218.5°C

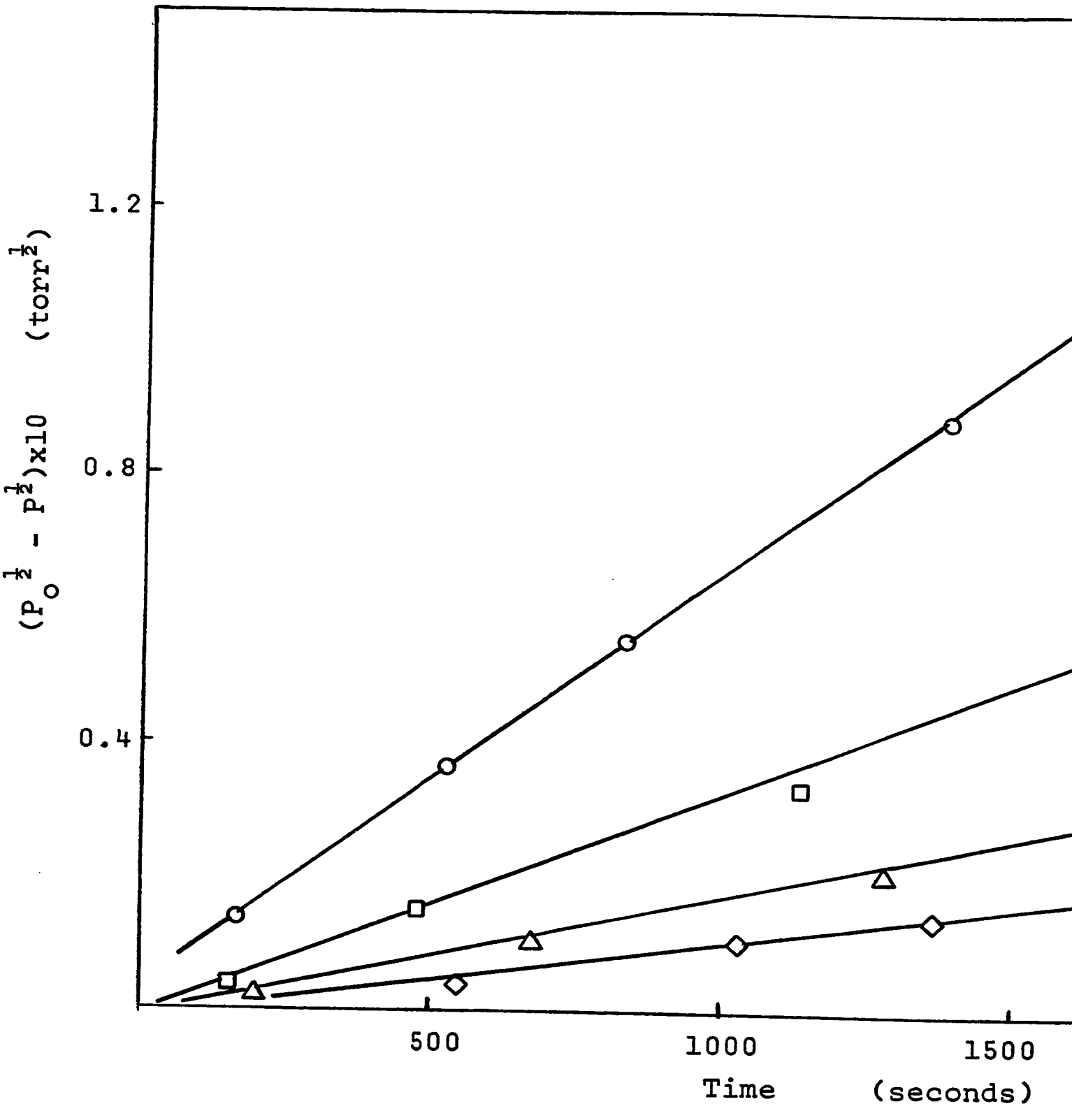
1.2
0.8
0.4
$(P_o^{\frac{1}{2}} - P^{\frac{1}{2}})x10$ (torr$^{\frac{1}{2}}$)
500
1000
1500
Time (seconds)

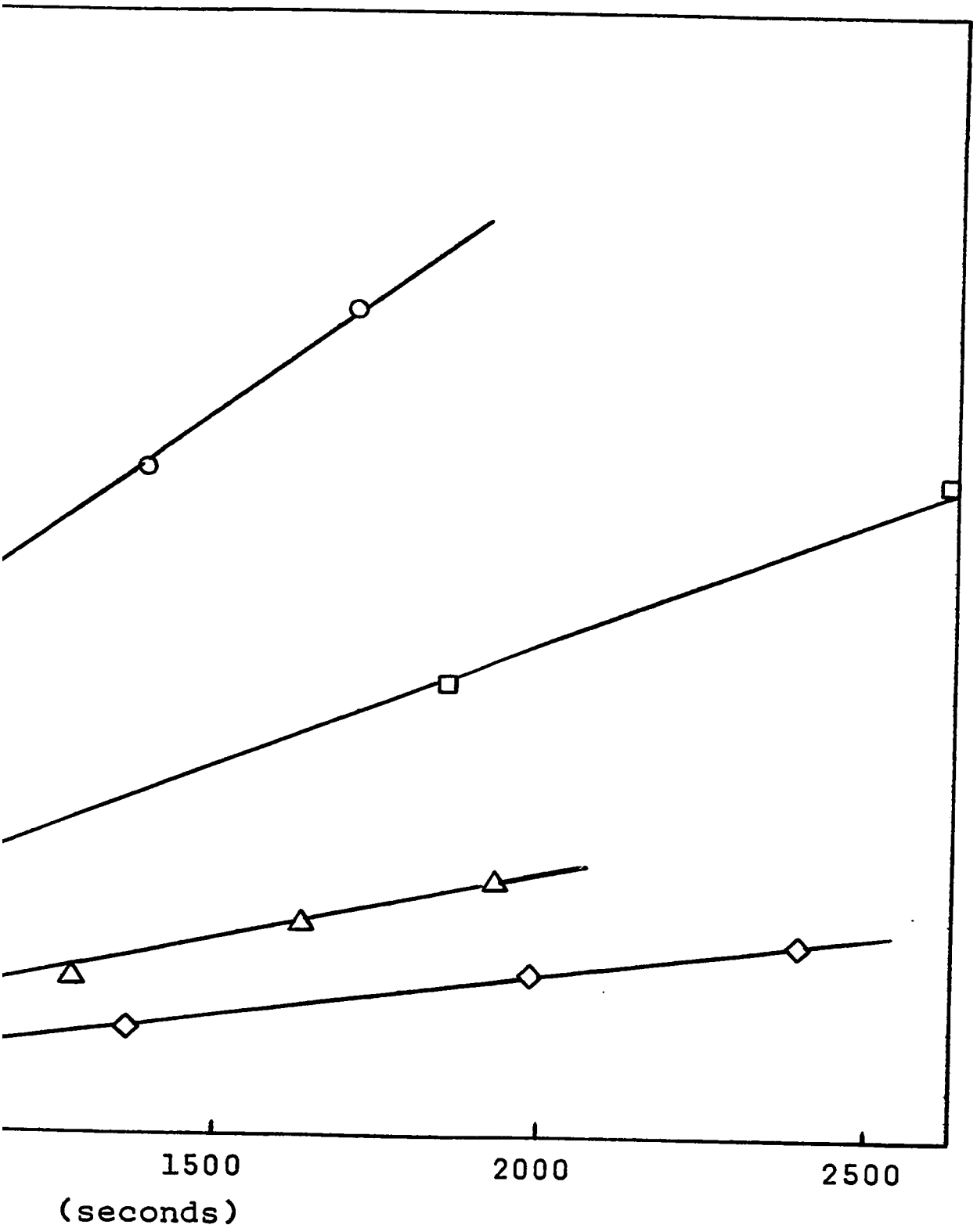
1500
2000
2500
(seconds)

FIGURE (III - 18)

Arrhenius Plots of Rate Data from Half Order Disappearances

of n-Propyl Iodide

□ - Figure (III-16)

△ - Figure (III-17)

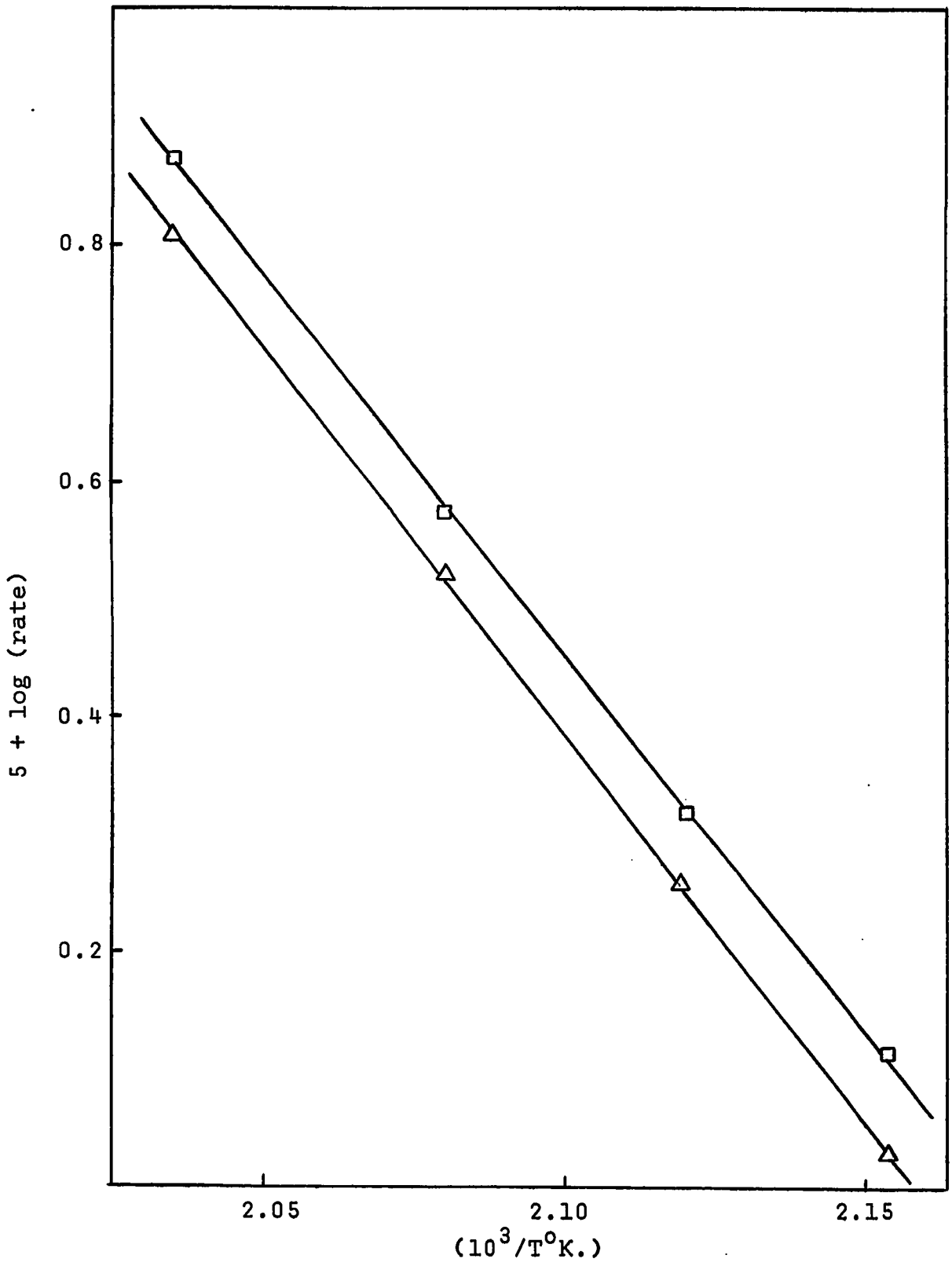
0.8
0.6
0.4
0.2
5 + log (rate)
2.05
2.10
2.15
(10³/T°K.)

FIGURE (III - 19)

Dependence of Mole Percent Propane Generated on Mole Percent n-Propyl Iodide Reacted for Various Initial Pressures of n-Propyl Iodide

O- $P_o = 10^{-2}$ torr

□- $P_o = 5 \times 10^{-2}$ torr

Δ- $P_o = 10^{-1}$ torr

at 200°C

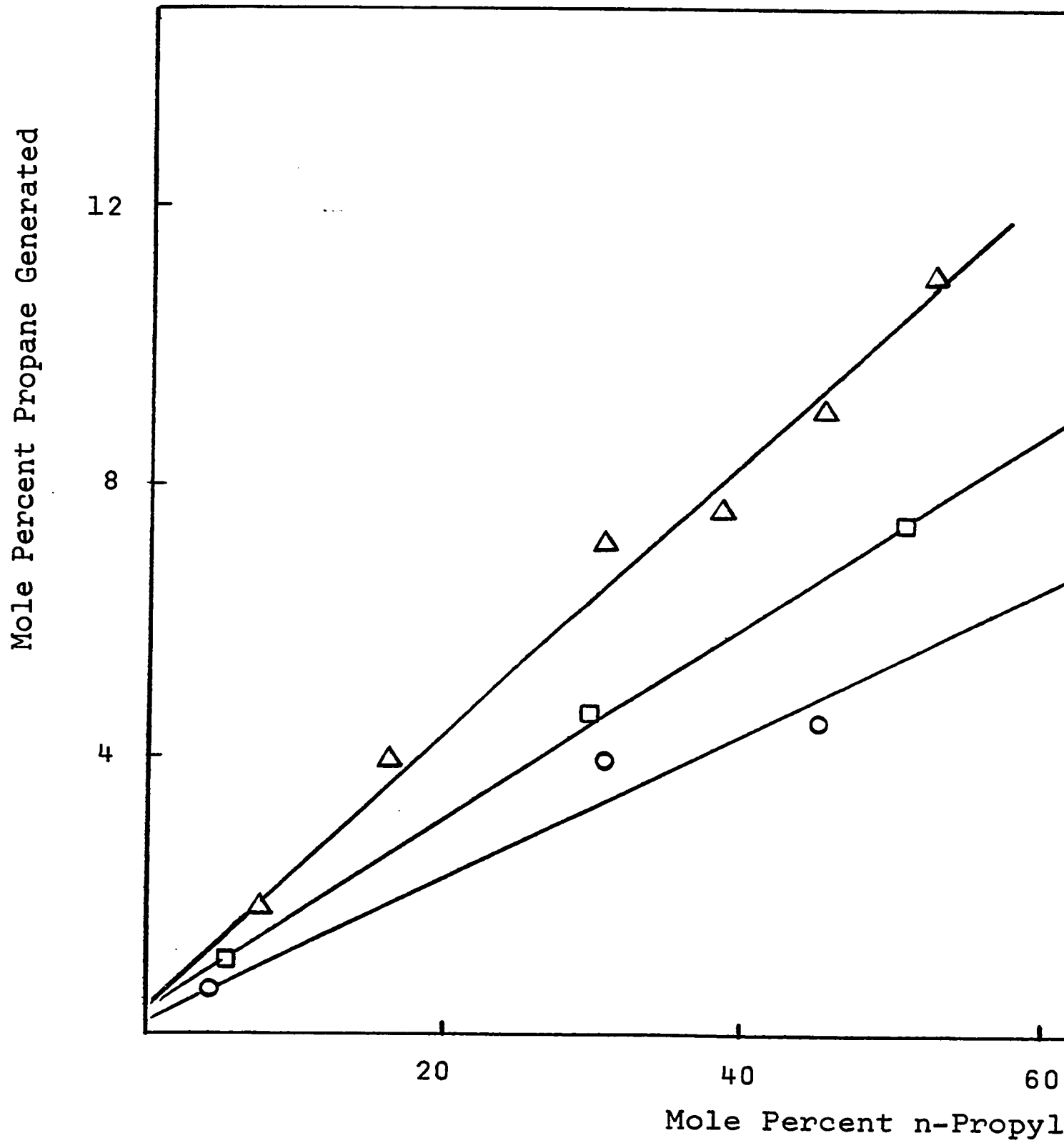
Mole Percent Propane Generated
12
8
4
20
40
60
Mole Percent n-Propyl

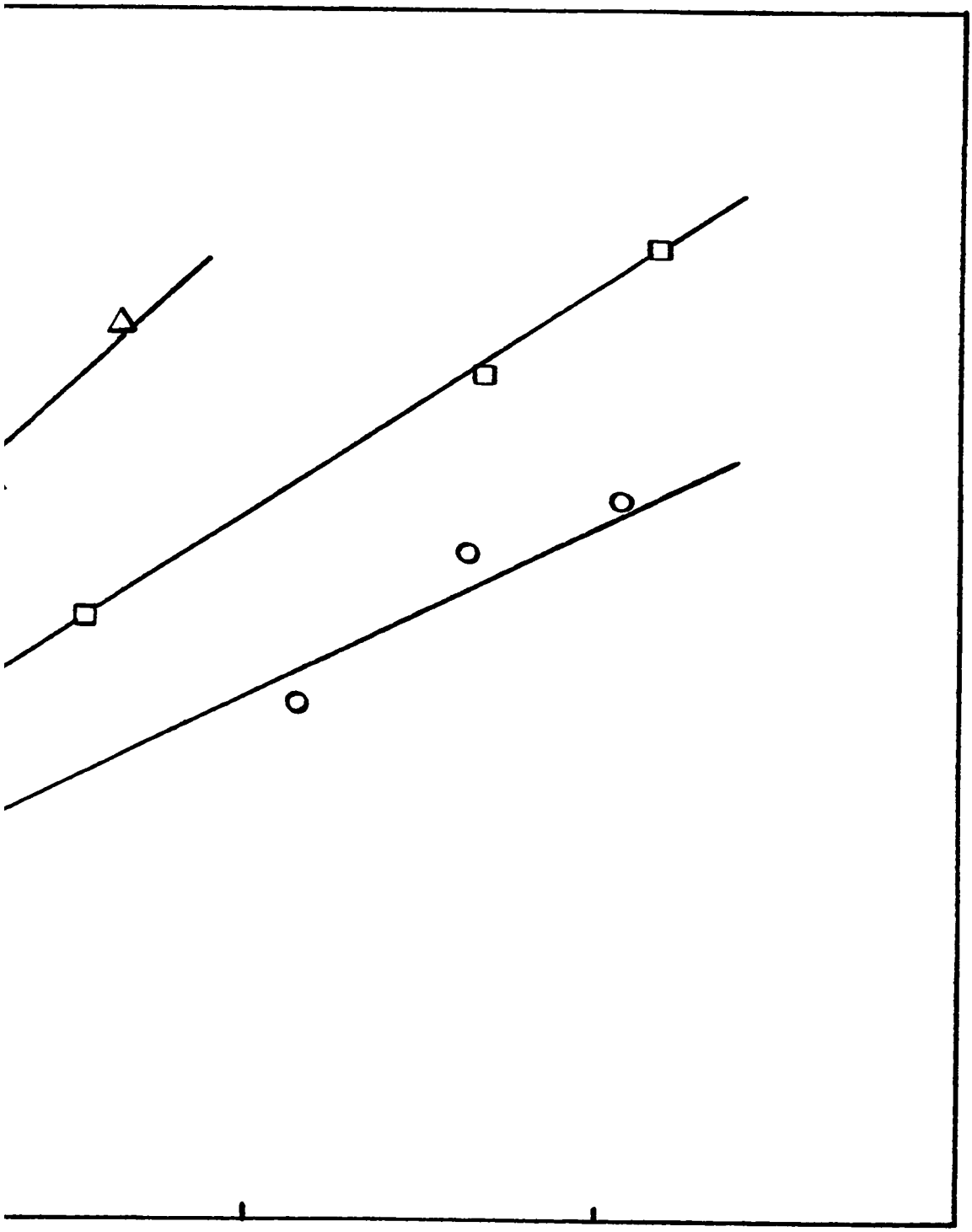

ent n-Propyl Iodide Reacted

iv) n-Propyl Fluoride

The reaction of n-propyl fluoride at elevated temperatures with previously reacted titanium films, occurred smoothly through many monolayer equivalents of reactant with reproducible rates. As in the cases of the other n-propyl halides, mixtures of propane and propylene occurred as products. Neither hydrogen nor hydrogen fluoride were detected and no loss of carbon to the film was observed.

In the n-propyl halide series, the reaction of n-propyl fluoride was unique. Disappearance of reactant occurred with first order kinetics. Rates for the disappearance were markedly more rapid than for the other n-propyl halides and the reaction of 10^{-2} torr doses occurred at convenient rates for kinetic investigation between ambient temperature and 100°C. However, rates of reaction below 60°C were not readily reproducible. Therefore kinetic studies were restricted to the temperature range between 60°C and 105°C. Figures (III-20) and (III-21) illustrate the first order dependence of the reaction on reactant concentration for 10^{-2} torr doses.

Rate reproduciblity is illustrated in figure (III-20) where duplicate runs were performed for the four higher temperatures at which the reaction was studied.

Arrhenius plots for the two sets of reaction data from figures (III-20) and (III-21) are shown in figure (III-22). Calculation of the line slopes for these two plots resulted in an apparent activation energy of 20.6±0.6 kcal./mole and 20.8±0.7

FIGURE (III - 20)

Disappearance of n-Propyl Fluoride

Plotted as a First Order Reaction

for $P_o = 10^{-2}$ torr

○ - 63°C

□, ▽ - 70°C

△, ● - 78.5°C

■, ▲ - 85°C

▼, ◆ - 93°C

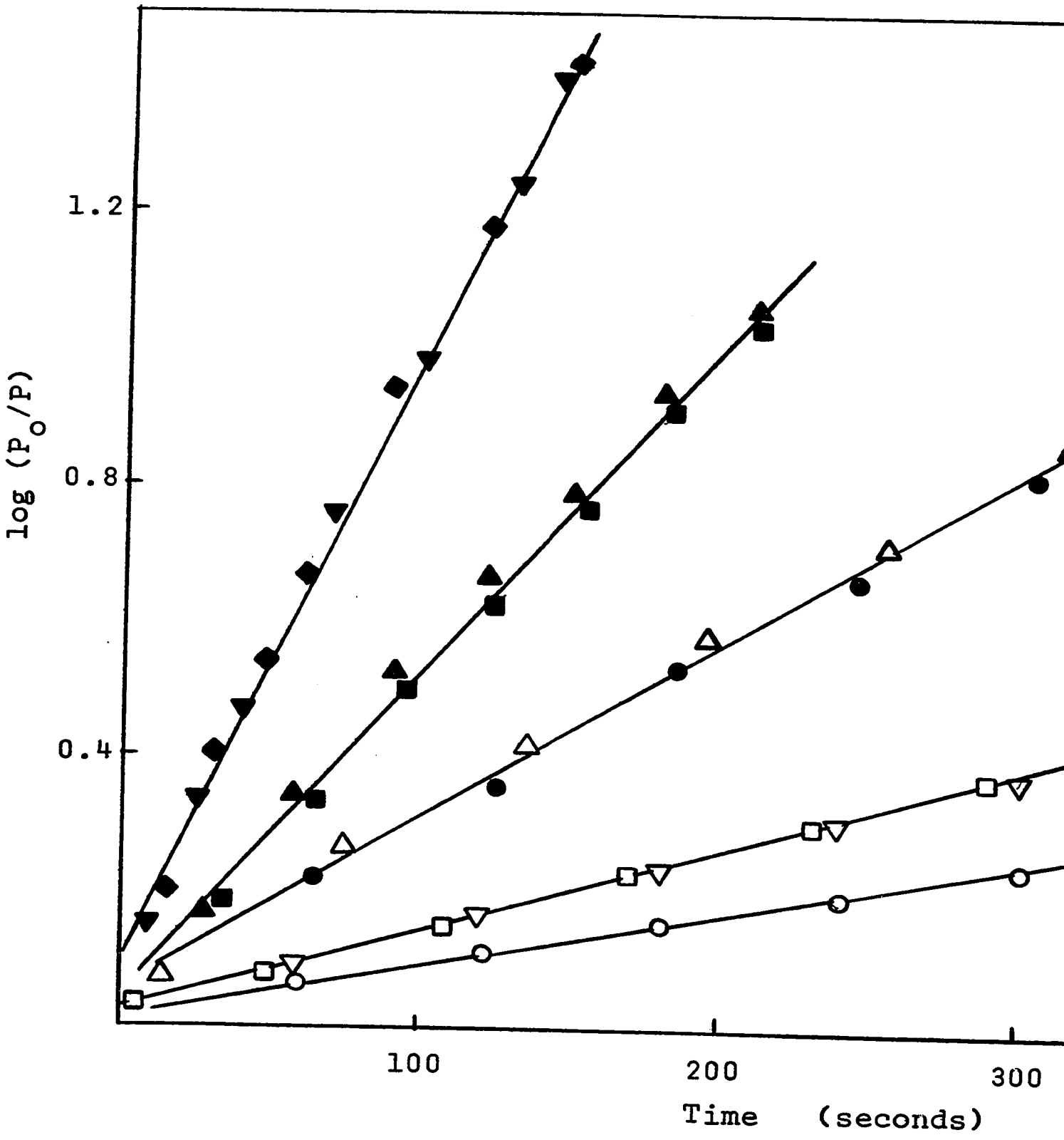
1.2
0.8
0.4
log (P_o/P)
100
200
300
Time (seconds)

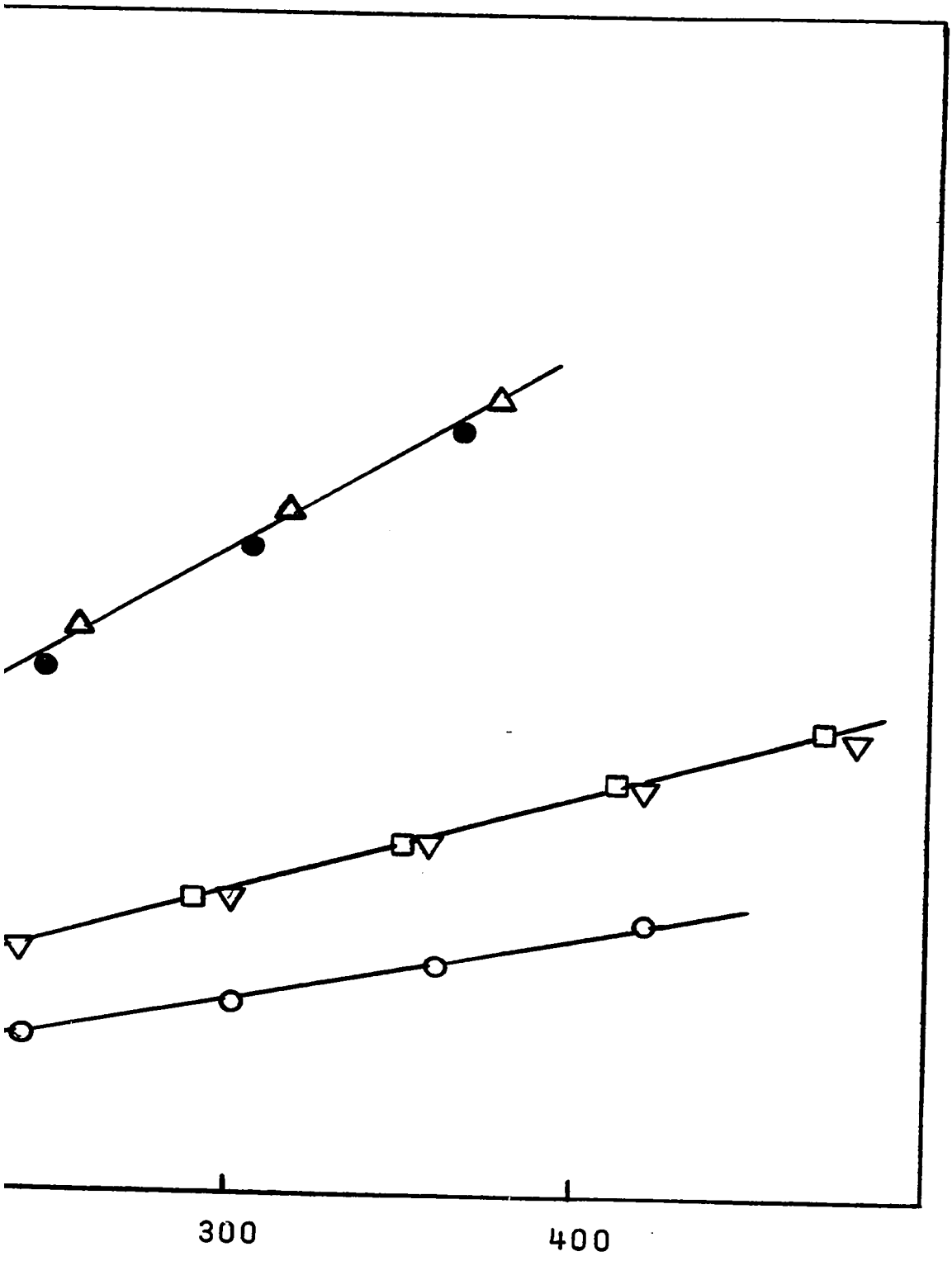
300
400
(seconds)

FIGURE (III - 21)

Disappearance of n-Propyl Fluoride

Plotted as a First Order Reaction

for $P_o = 10^{-2}$ torr

○ - 86°C

□ - 91°C

◇ - 99°C

▽, △ - 104.5°C

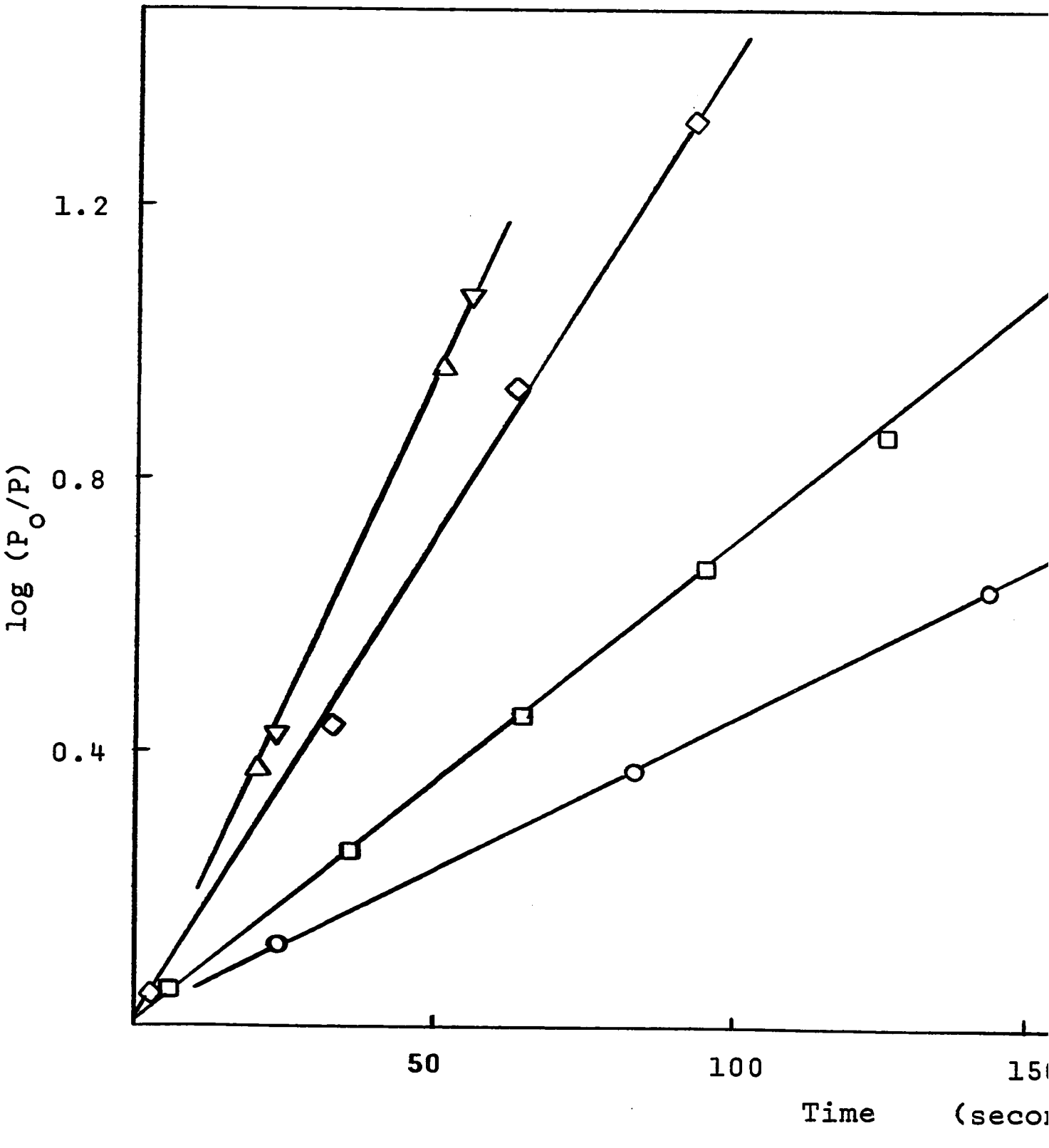
1.2
0.8
0.4
log (P$_o$/P)
50
100
Time
(seco

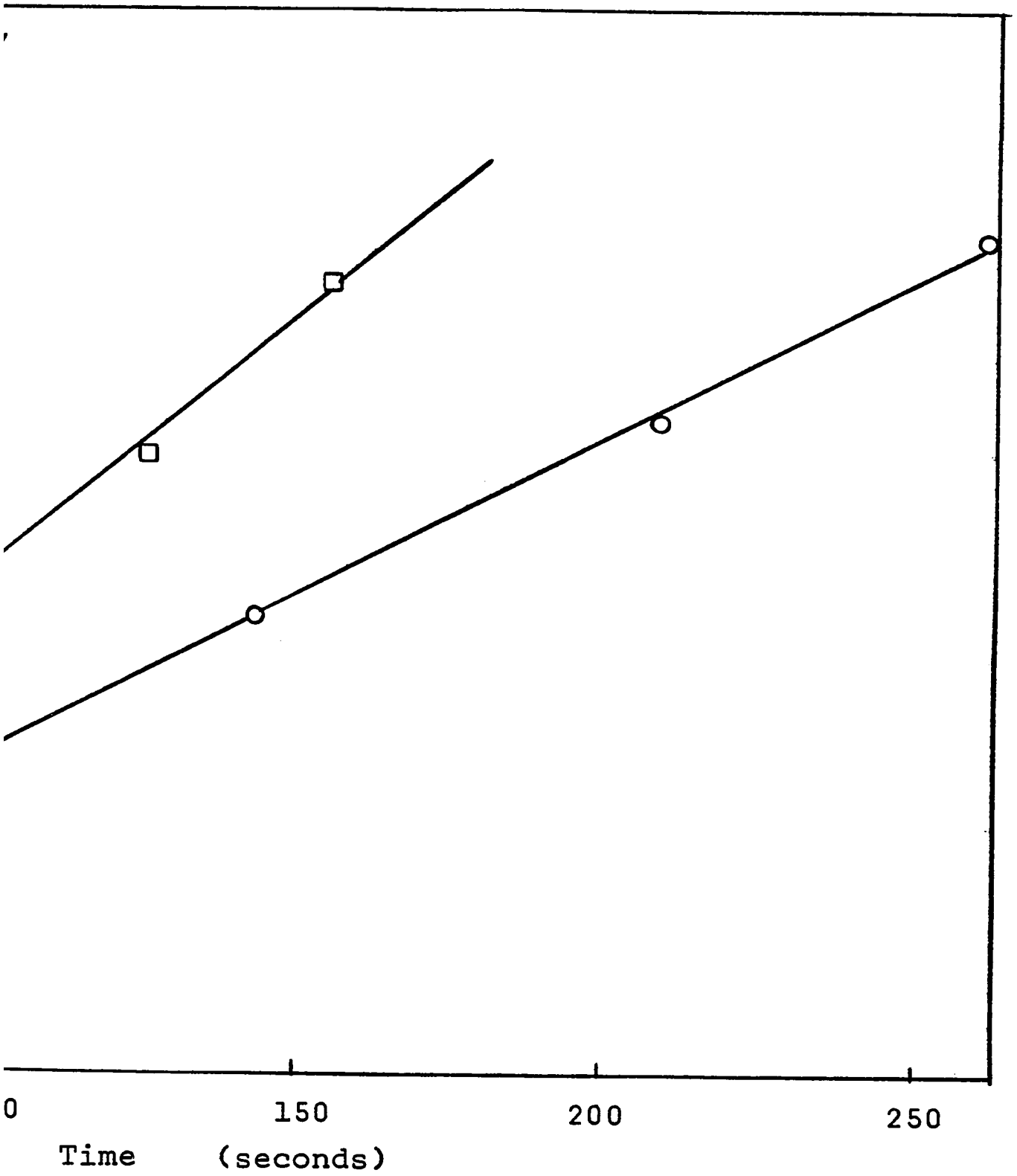
0
150
200
250
Time (seconds)

FIGURE (III - 22)

Arrhenius Plots of Rate Data from First Order Disappearances

of n-Propyl Fluoride

△- Figure (III-20)

O- Figure (III-21)

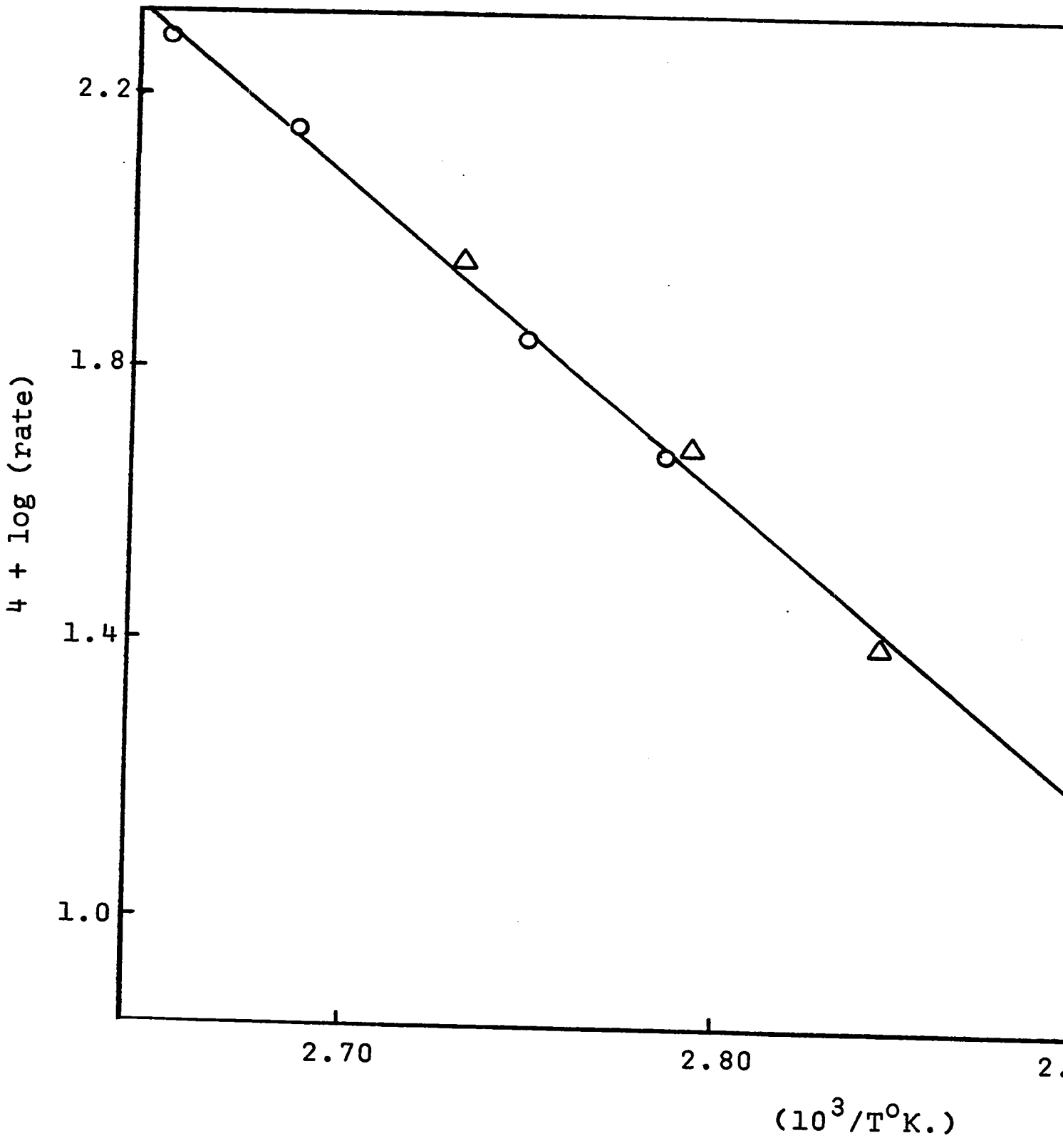
2.2
1.8
1.4
1.0
4 + log (rate)
2.70
2.80
(10³/T°K.)

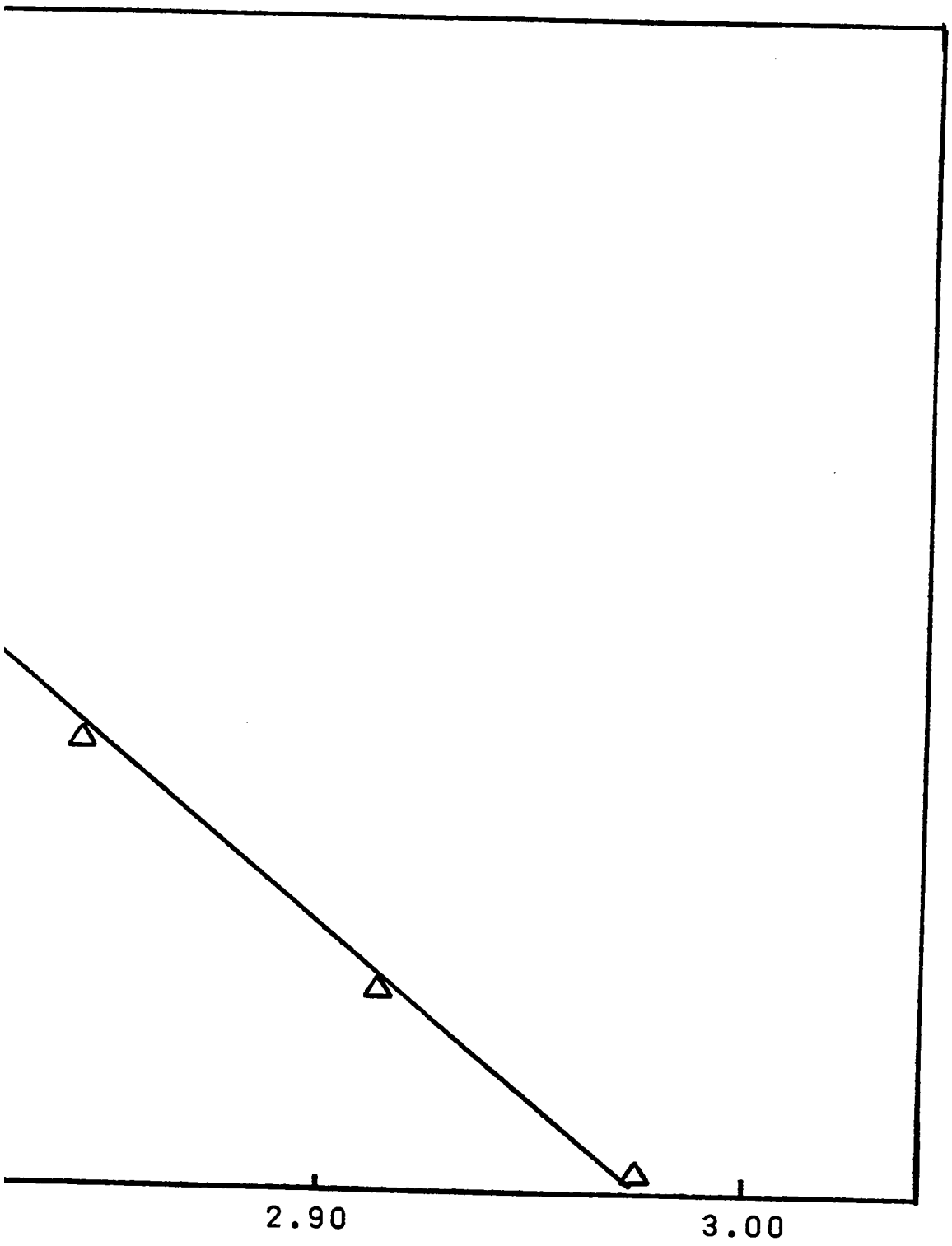

$0^3/T^oK.)$

kcal./mole respectively.

No dependence of propane:propylene ratio on initial reactant pressure was found within the temperature range of the kinetic studies. This lack of dependence is illustrated by figure (III-23). However, a study of the propane:propylene product ratio when a reaction temperature of 200°C was used did show a dependence. The reactions at this temperature were too rapid to follow kinetically so that only final product ratios could be obtained. At 200°C, a reactant pressure of 10^{-2} torr gave a 10:90 propane:propylene ratio. A reactant pressure of 10^{-1} torr gave a 20:80 propane:propylene ratio.

b) α-Methyl Series

i) Ethyl Chloride

The reaction of ethyl chloride at elevated temperatures with previously reacted titanium films, followed the pattern of the n-propyl chloride reaction. Reproducible rates were observed through many monolayer equivalents of reactant which disappeared with half order kinetics and gave a mixture of ethylene and ethane as products. No hydrogen or hydrogen chloride were detected, and no loss of carbon to the films was observed.

The reaction of 10^{-2} torr, 2.5×10^{-2} torr and 5×10^{-2} torr doses occurred at convenient rates for kinetic investigation between 210°C and 240°C. Figures (III-24) and (III-26) show the half order dependence of the reaction on reactant pressure for $P_o = 10^{-2}$ torr on different films. Figures (III-27) and (III-28) illustrate the half order dependence for $P_o = 2.5 \times 10^{-2}$

FIGURE (III -23)

Dependence of Mole Percent Propane Generated on Mole Percent n-Propyl Fluoride Reacted for Various Initial Pressures of n-Propyl Fluoride at $0^{o}C$

Δ - $P_o = 10^{-2}$ torr

O - $P_o = 10^{-1}$ torr

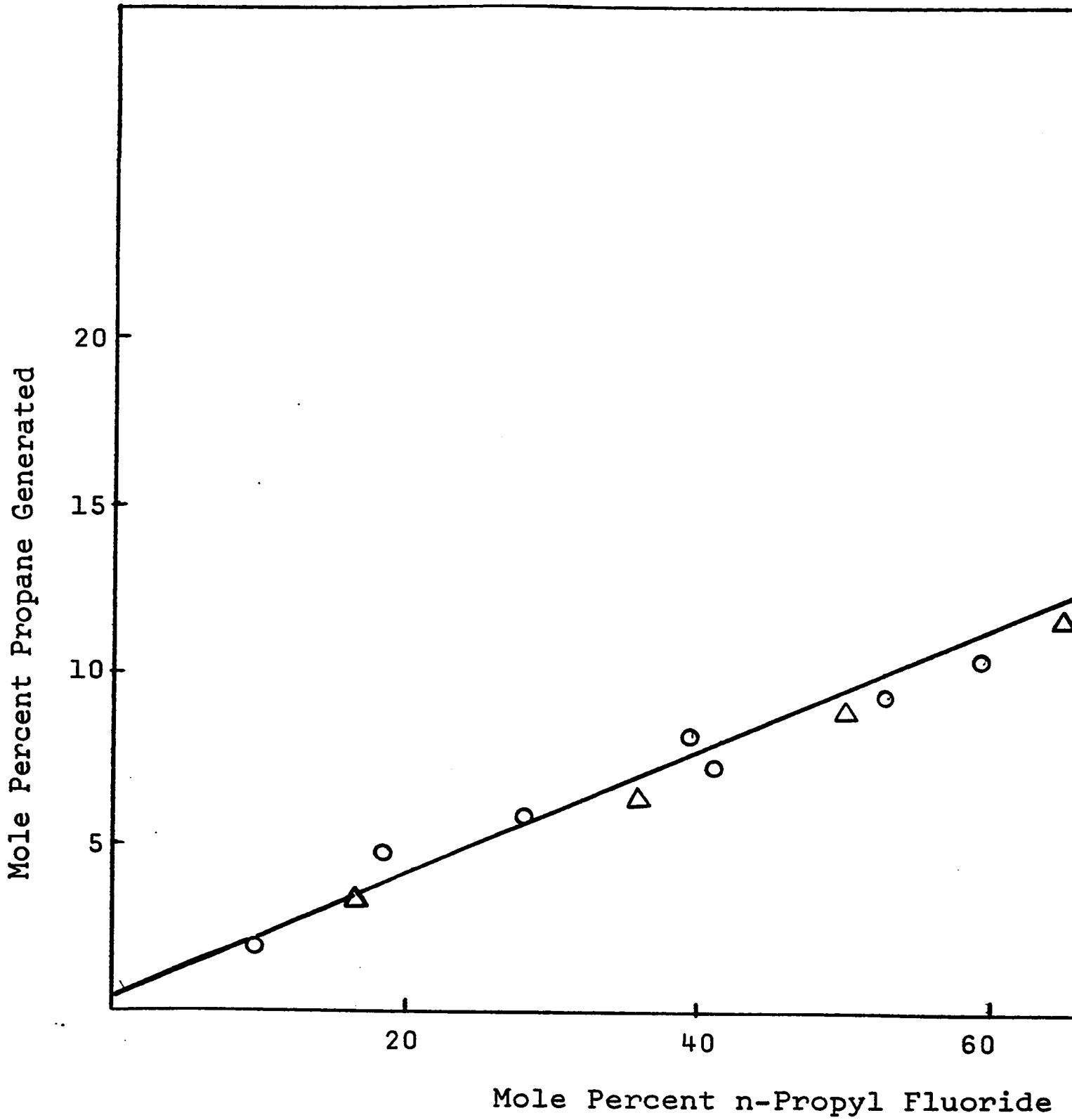
Mole Percent Propane Generated
20
15
10
5
20
40
60
Mole Percent n-Propyl Fluoride

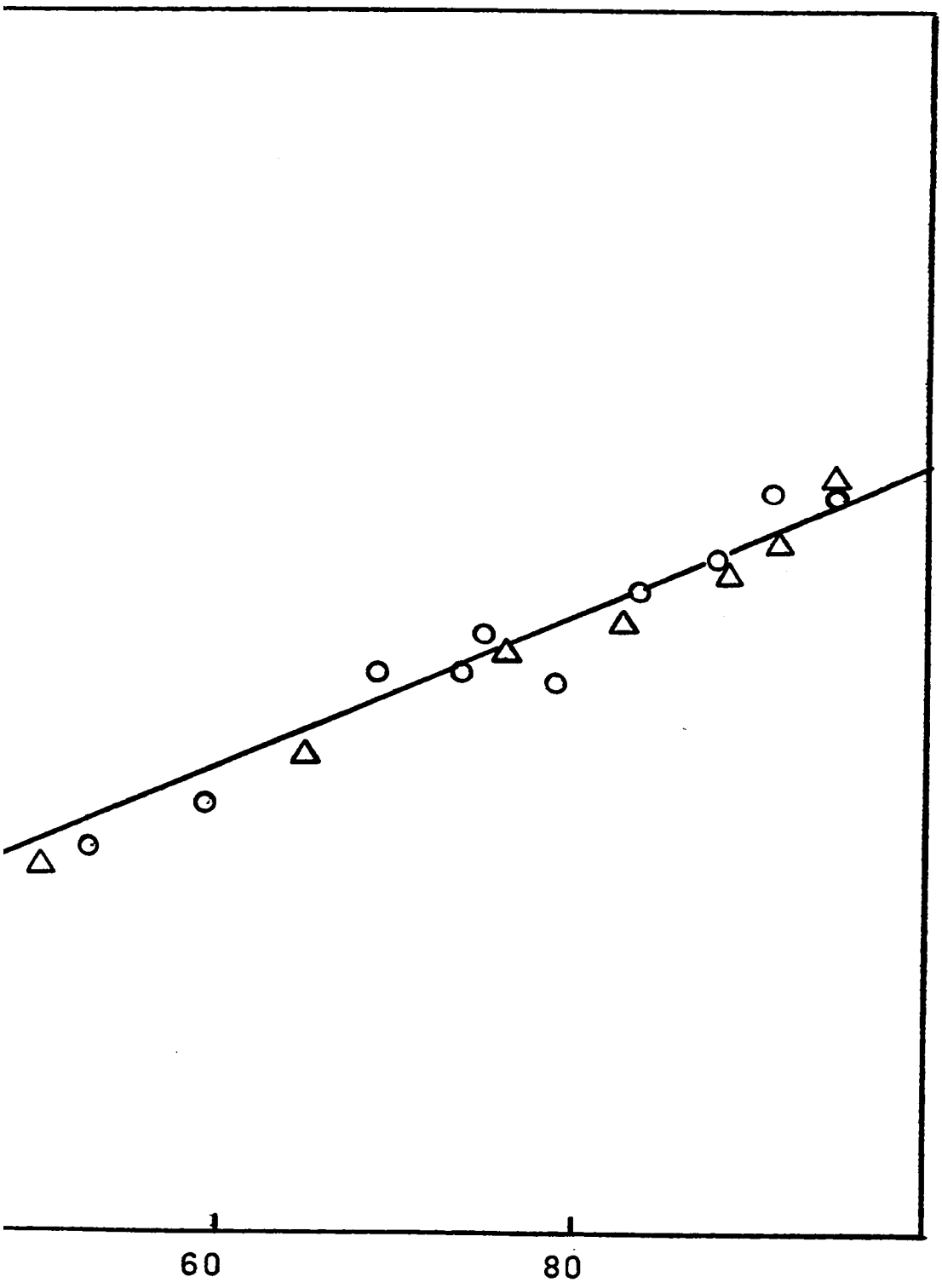

opyl Fluoride Reacted

torr and $P_o = 5x10^{-2}$ torr respectively. Rate constants for the two sets of reactions with initial reactant pressures of 10^{-2} torr are almost identical. Rate constants for the reaction of $2.5x10^{-2}$ torr doses are somewhat greater than for the reaction of the 10^{-2} torr doses. However, the first $2.5x10^{-2}$ torr dose reacted has a period of activation similar to that seen in the n-propyl chloride reactions {compare figure (III-27) with figure (III-8)}. Rate constants for the reaction of $5x10^{-2}$ torr doses are somewhat less than those for 10^{-2} torr or $2.5x10^{-2}$ torr doses. The rate constant for a 10^{-1} torr dose decreased even further. Reaction at this initial pressure was investigated only at 240°C. Rate constants for reactions on the same film at different initial reactant pressures are summarized in Table (III-6).

TABLE (III - 6)

Initial Reactant Pressure (torr)	Apparent Rate Constant at 240°C. ($torr^{\frac{1}{2}}/sec.^{-1}$)
$1.0x10^{-2}$	$5.88x10^{-5}$
$2.5x10^{-2}$	$7.35x10^{-5}$
$5.0x10^{-2}$	$4.72x10^{-5}$
$1.0x10^{-1}$	$2.45x10^{-5}$

Figure (III-25) is the Arrhenius plot for the kinetic data from figure (III-24). Figure (III-29) shows the Arrhenius plots for figures (III-26), (III-27) and (III-28). The slopes

FIGURE (III - 24)

Disappearance of Ethyl Chloride

Plotted as a Half Order Reaction

for $P_o = 10^{-2}$ torr

◇ - 200°C

○ - 210°C

△ - 220°C

□ - 230°C

▽ - 241°C

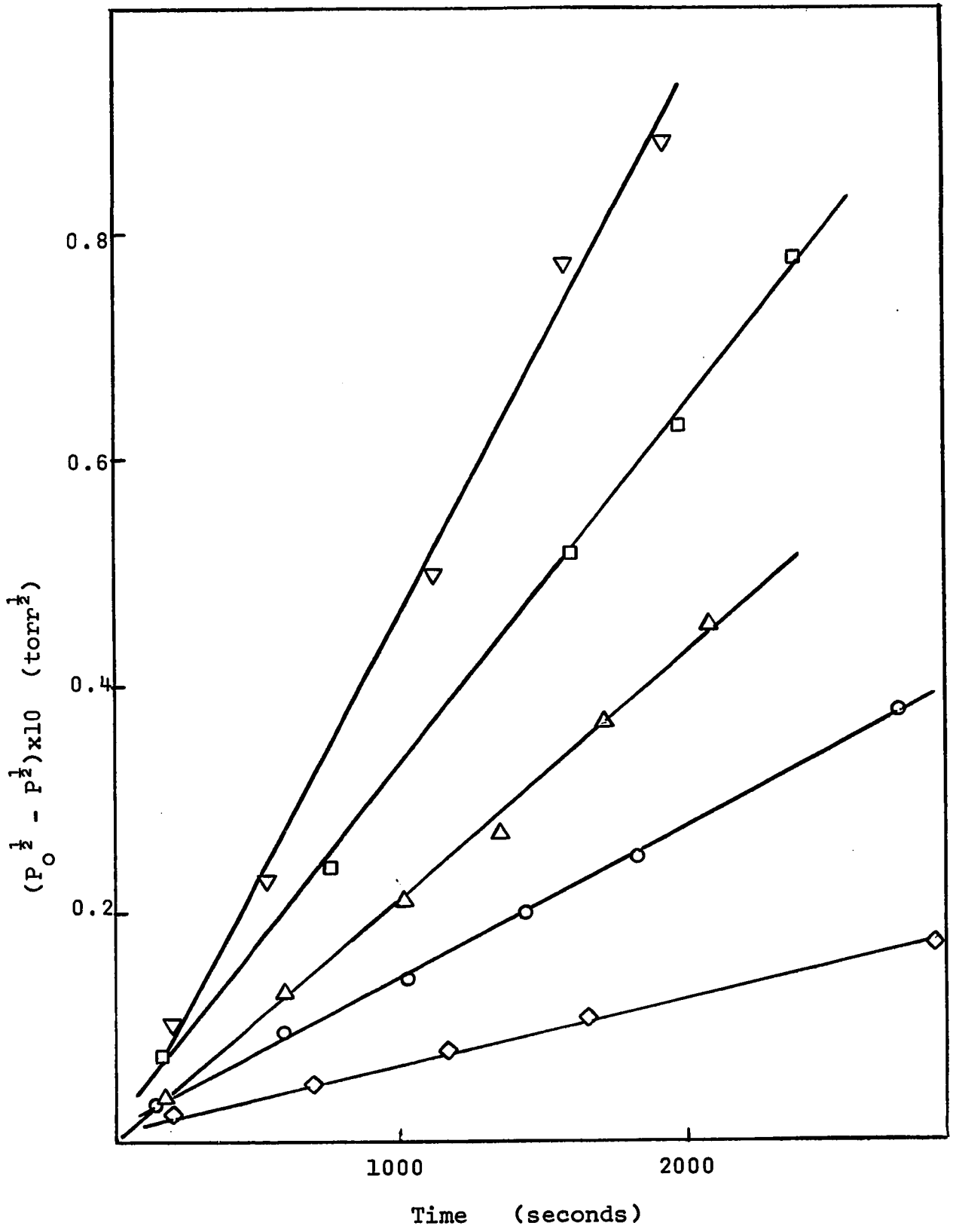
0.8
0.6
0.4
0.2
$(P_o^{\frac{1}{2}} - P^{\frac{1}{2}}) \times 10$ (torr$^{\frac{1}{2}}$)
1000
2000
Time (seconds)

FIGURE (III -25)

Arrhenius Plot of Rate Data from Half Order Disappearance of Ethyl Chloride in Figure (III-24)

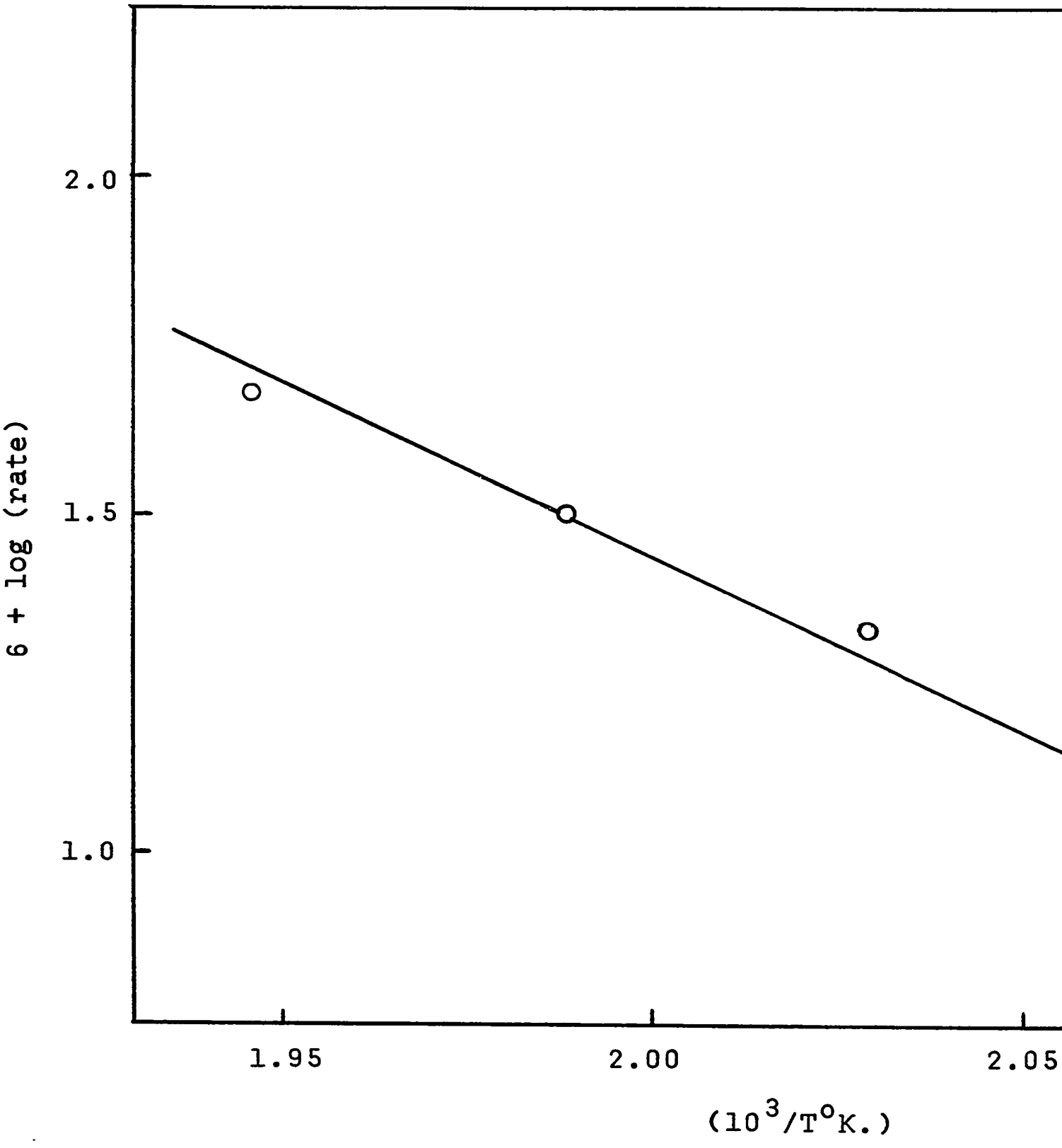
2.0
1.5
1.0
6 + log (rate)
1.95
2.00
2.05
(10³/T°K.)

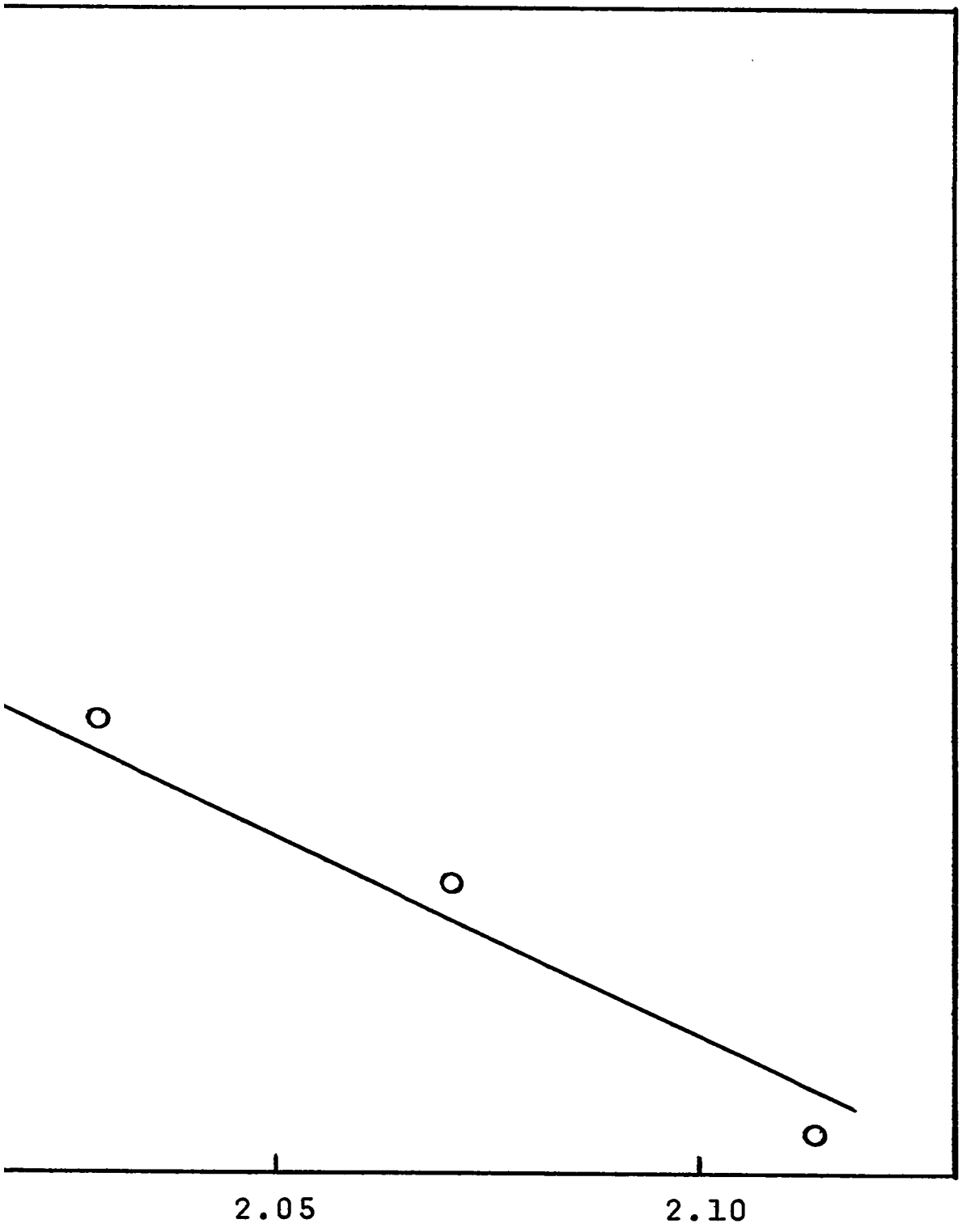
2.05
2.10
/T°K.)

FIGURE (III - 26)

Disappearance of Ethyl Chloride

Plotted as a Half Order Reaction

for $P_o = 10^{-2}$ torr

△- 210°C

○- 220°C

□- 230°C

▽- 240°C

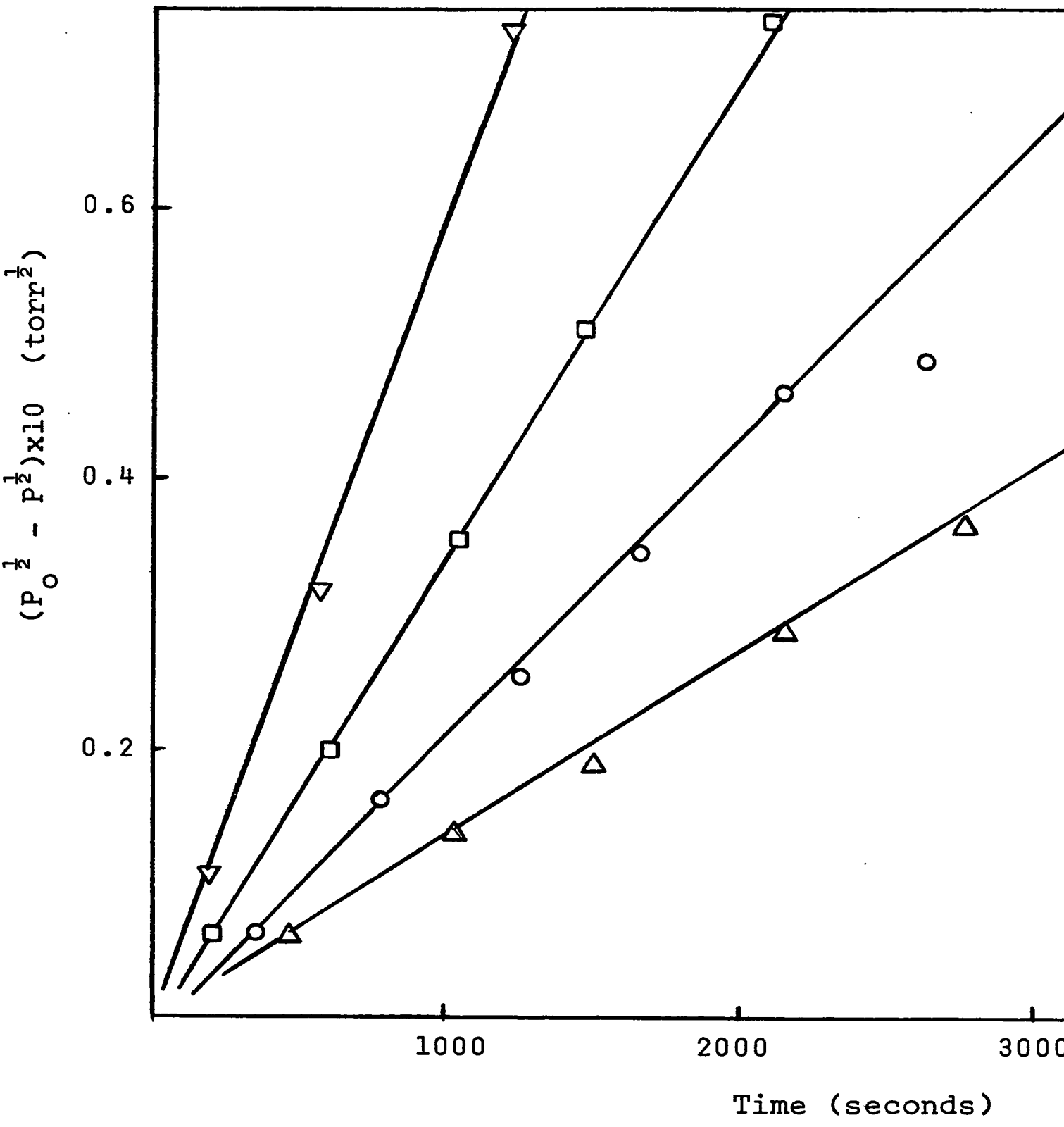
0.6
0.4
0.2
$(P_o^{\frac{1}{2}} - P^{\frac{1}{2}})x10$ (torr$^{\frac{1}{2}}$)
1000
2000
3000
Time (seconds)

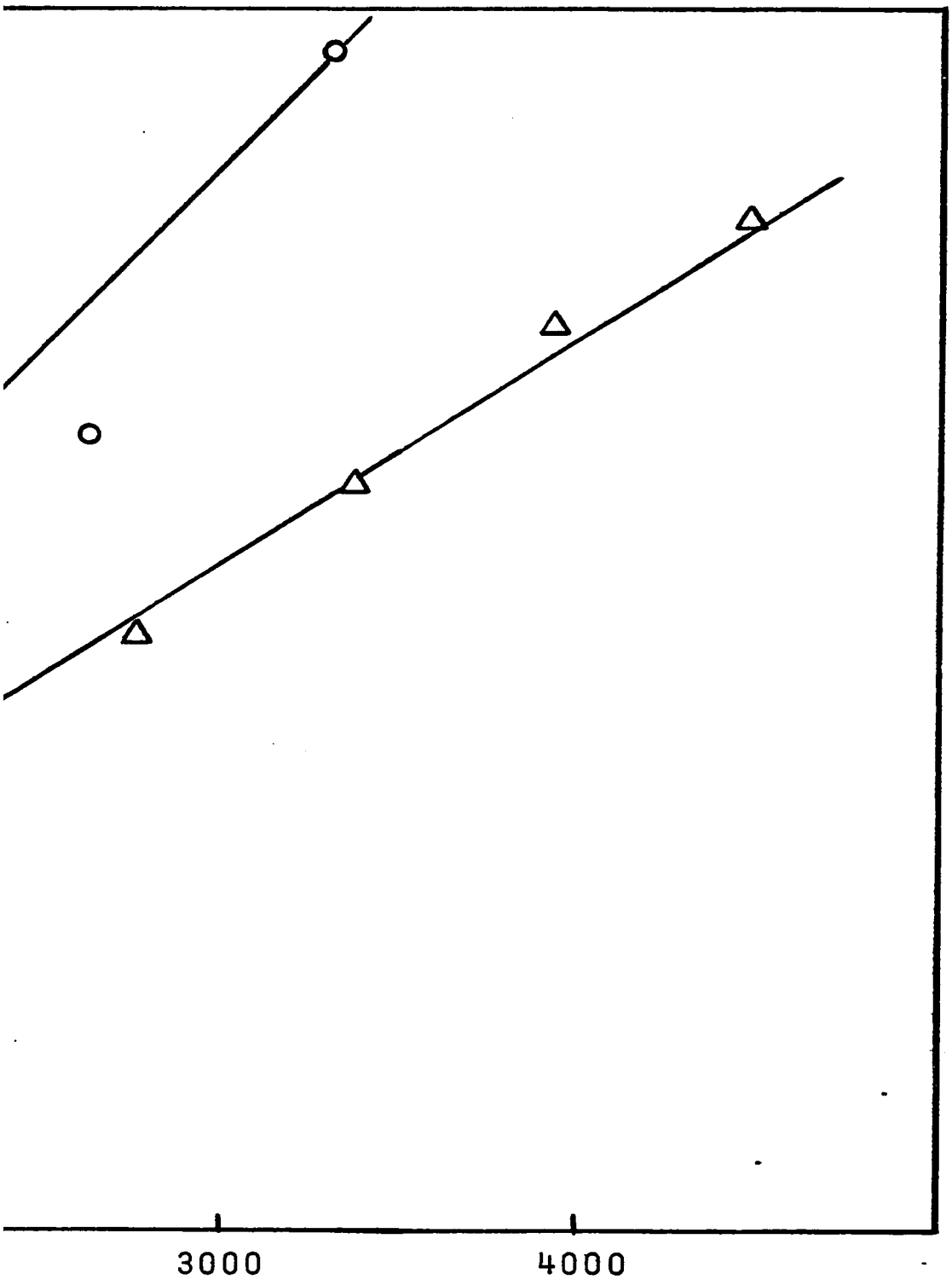

seconds)

FIGURE (III - 27)

Disappearance of Ethyl Chloride

Plotted as a Half Order Reaction

for $P_o = 2.5 \times 10^{-2}$ torr

▽ - 210°C

○ - 220°C

□ - 230°C

△ - 240°C

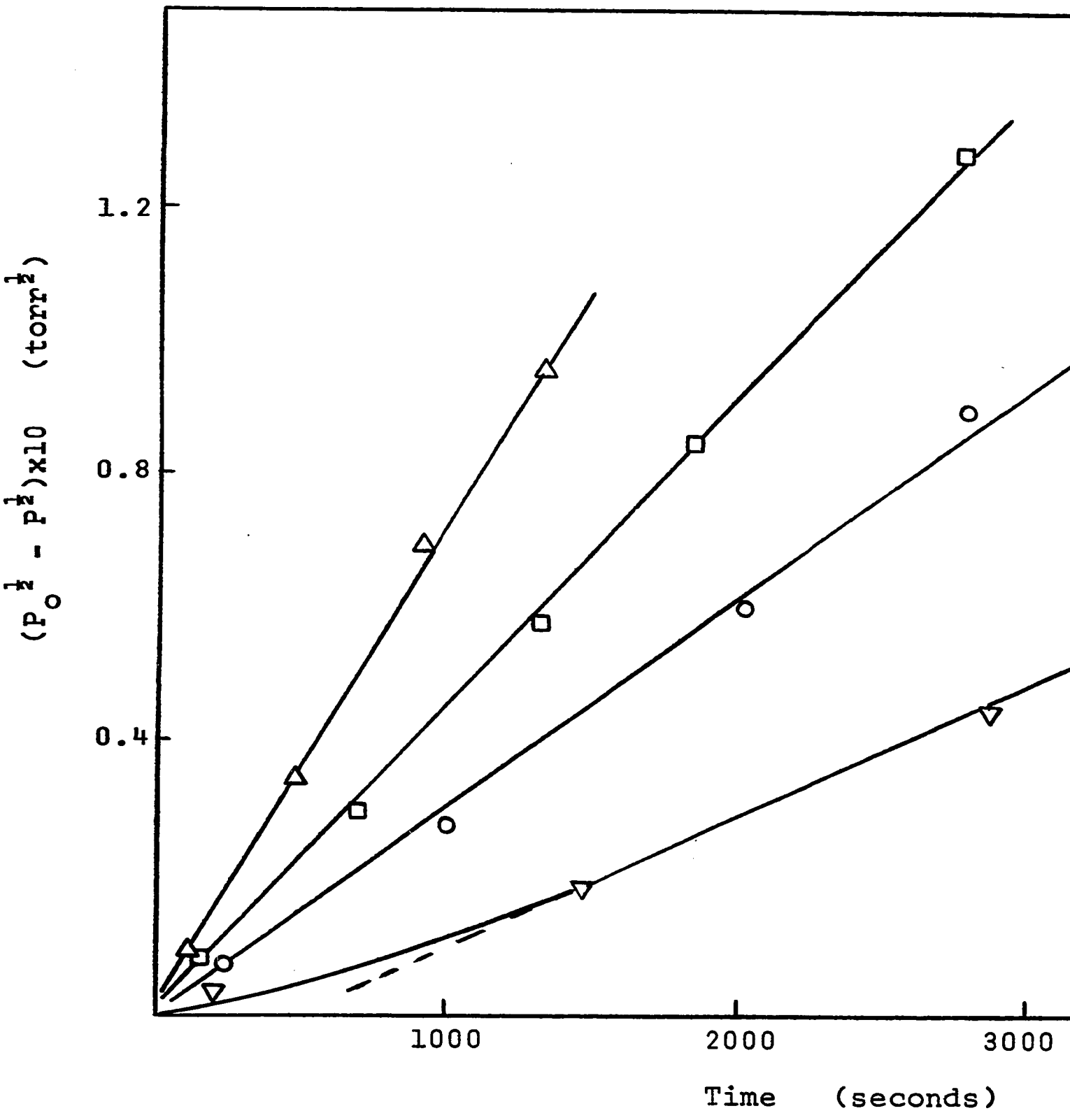
1.2
0.8
0.4
$(P_o^{\frac{1}{2}} - P^{\frac{1}{2}})x10$ $(torr^{\frac{1}{2}})$
1000
2000
3000
Time (seconds)

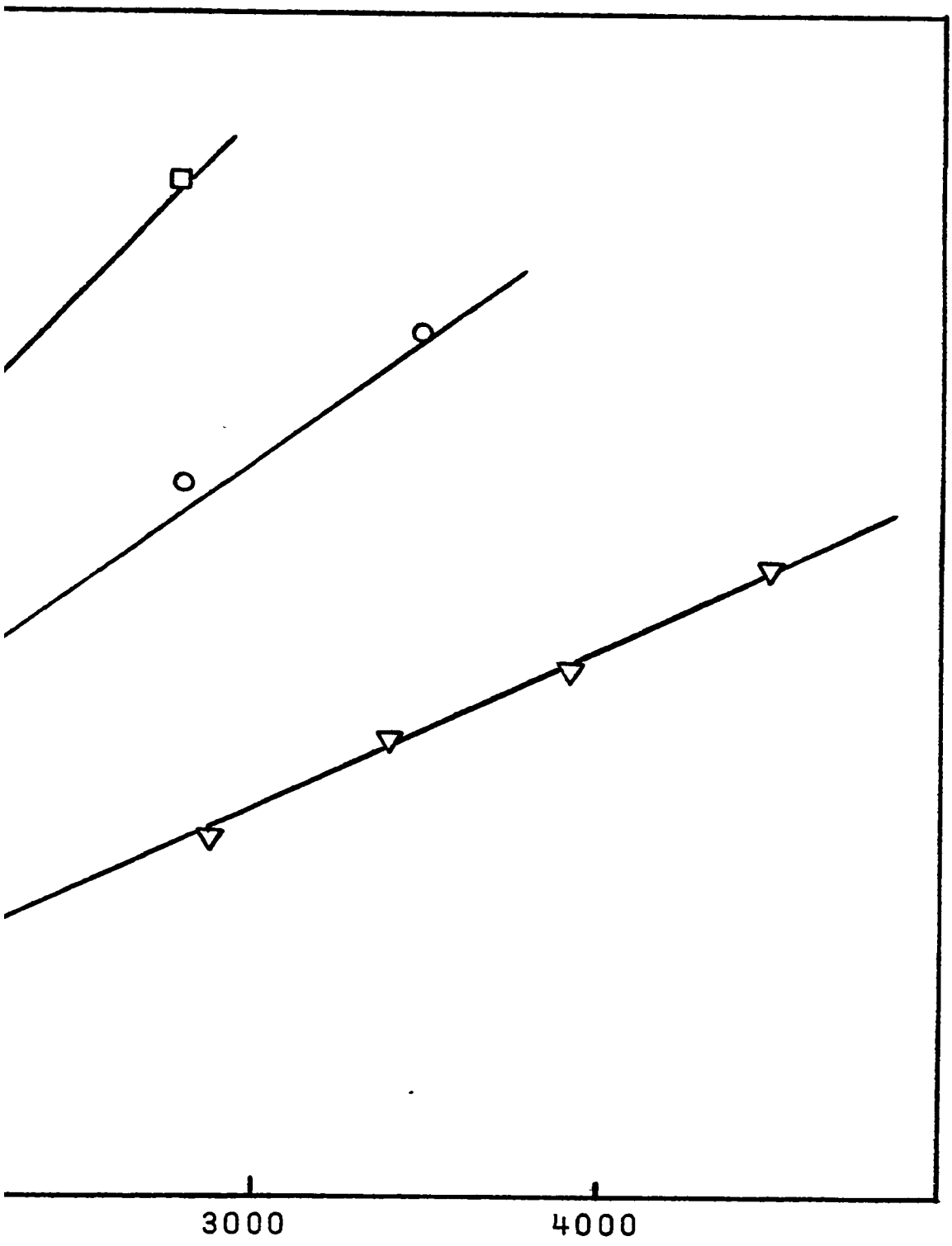
3000
4000
(seconds)

FIGURE (III - 28)

Disappearance of Ethyl Chloride

Plotted as a Half Order Reaction

for $P_o = 5 \times 10^{-2}$ torr

▽ - 210°C

○ - 220°C

△ - 230°C

□ - 240°C

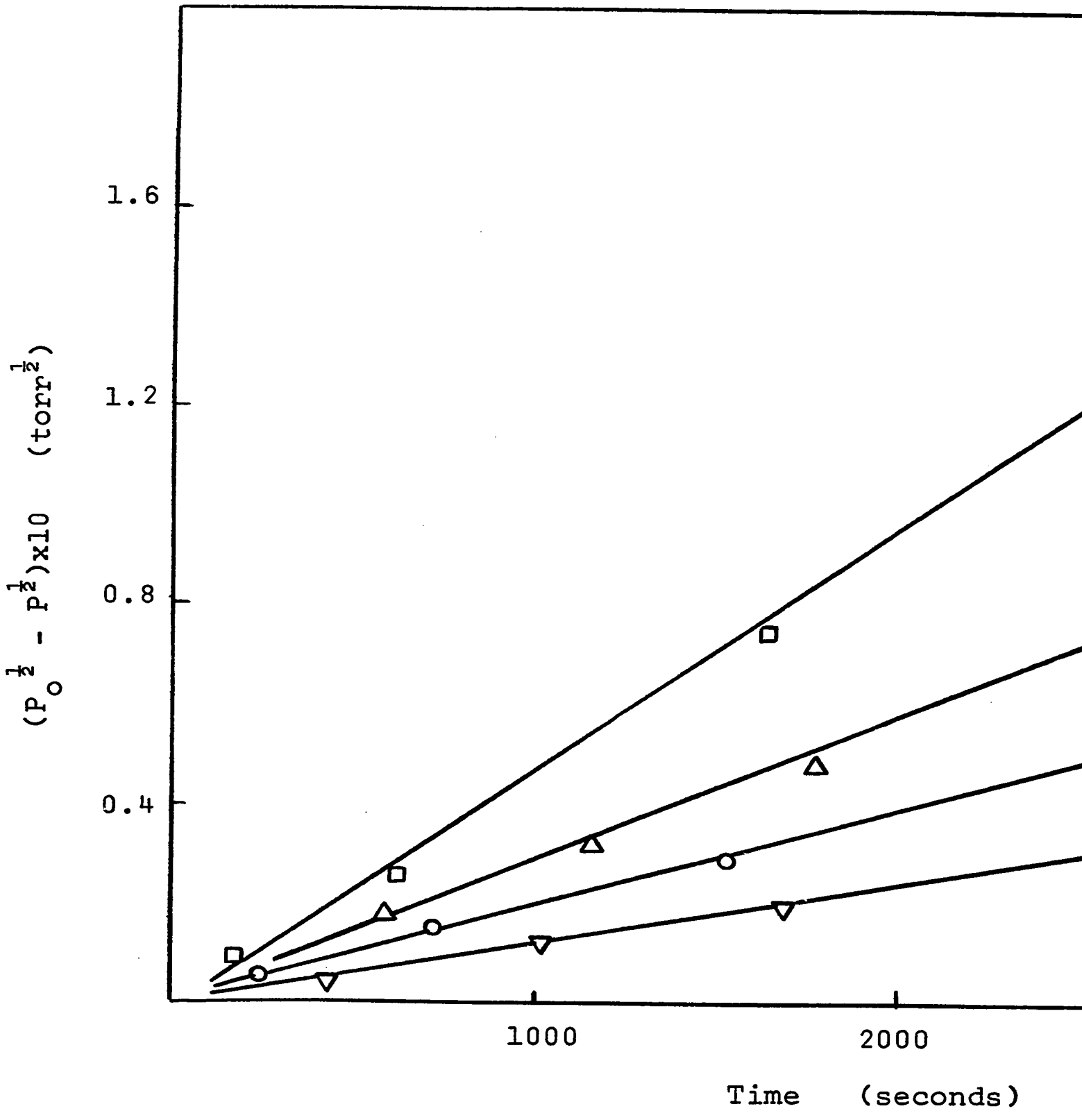
1.6
1.2
0.8
0.4
$(P_o^{\frac{1}{2}} - P^{\frac{1}{2}})x10$ (torr$^{\frac{1}{2}}$)
1000
2000
Time (seconds)

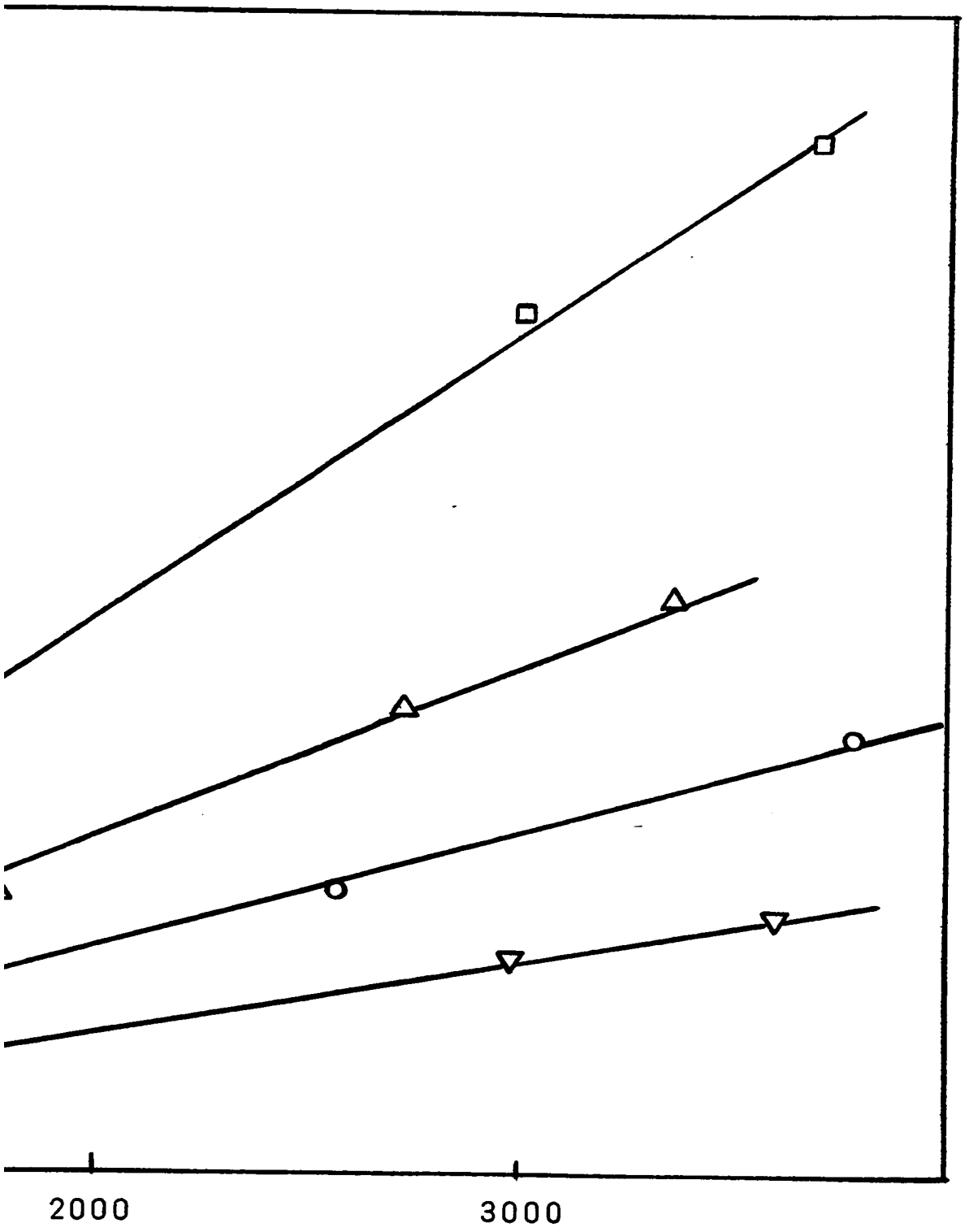
2000
3000
(seconds)

FIGURE (III - 29)

Arrhenius Plots of Rate Data from Half Order Disappearances of Ethyl Chloride

□ - Figure (III-26)

○ - Figure (III-27)

△ - Figure (III-28)

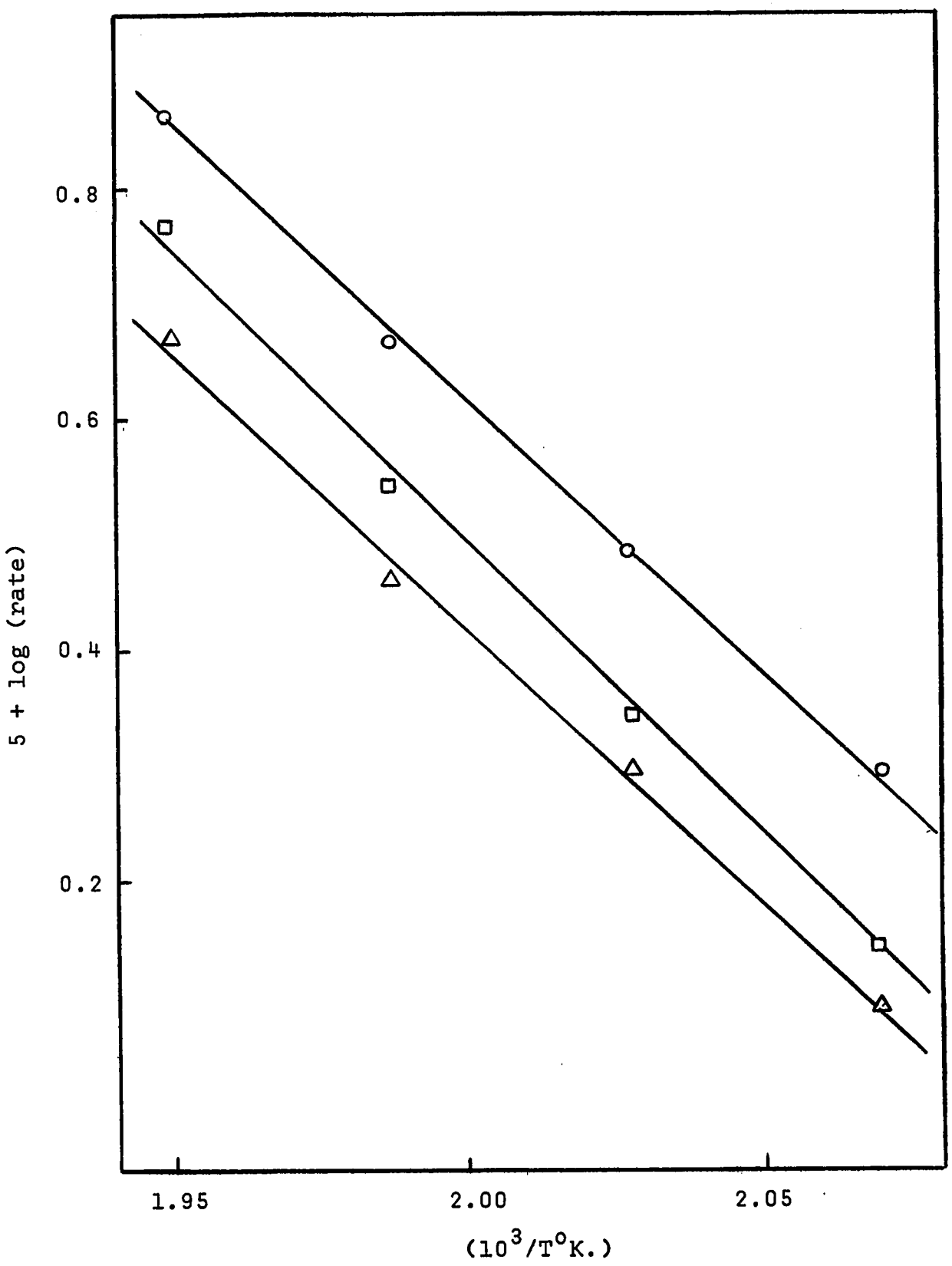
0.8
0.6
0.4
0.2
5 + log (rate)
1.95
2.00
2.05
(10³/T°K.)

of the Arrhenius plots were calculated and gave an apparent activation energy for the reaction of ethyl chloride as 23.5±1.5 kcal./mole, 21.4±0.4 kcal./mole and 21.9±0.7kcal/mole respectively.

As with the n-propyl halides, it was found that increased initial reactant pressure resulted in enhanced paraffin production (ethane in this case). It was also found that the more extensively reacted films produced larger quantities of ethane than those less extensively reacted. These effects are both illustrated in figure (III-30), which also shows a direct proportionality between percent ethane generated and percent ethyl chloride reacted. This means that product ratio remains invariant as reactant is consumed. Within the limits of this study, no variation of product ratio with temperature was found.

A study of the possible inhibiting effect of ethylene on the reaction of ethyl chloride was undertaken. The reaction of 10^{-2} torr of ethyl chloride was not inhibited by the presence of $5x10^{-2}$ torr of ethylene. In addition, it was noted that the presence of the ethylene had no effect on the olefin:paraffin product ratio.

ii) Isopropyl Chloride

The reaction of isopropyl chloride differed markedly from the reactions which have been considered up to this point. After only a few 10^{-2} torr doses of isopropyl chloride had been reacted at elevated temperature, gaseous hydrogen chloride was detected. After reacting a 10^{-1} torr dose, the reaction of

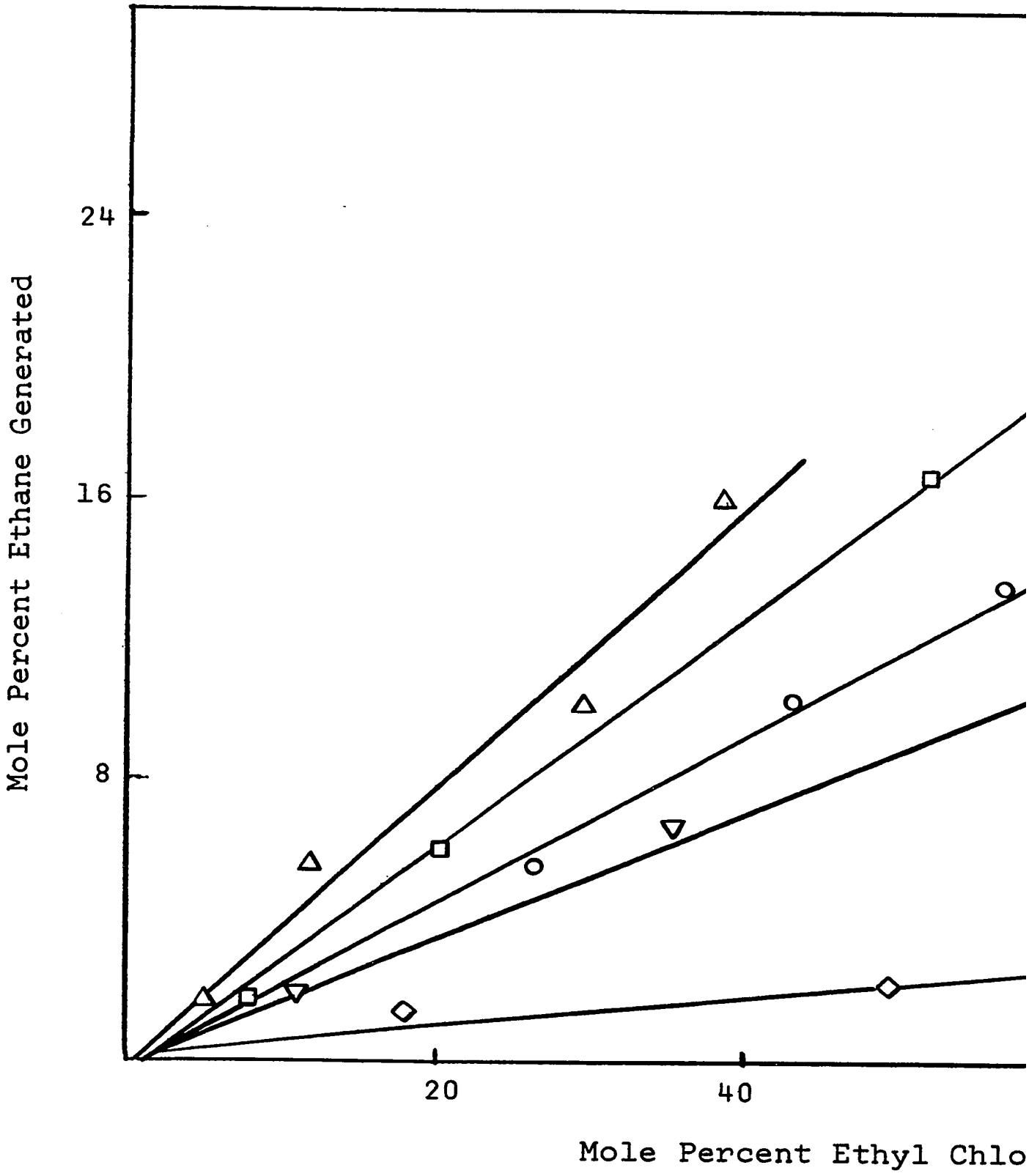
24
16
8
Mole Percent Ethane Generated
20
40
Mole Percent Ethyl Chlo

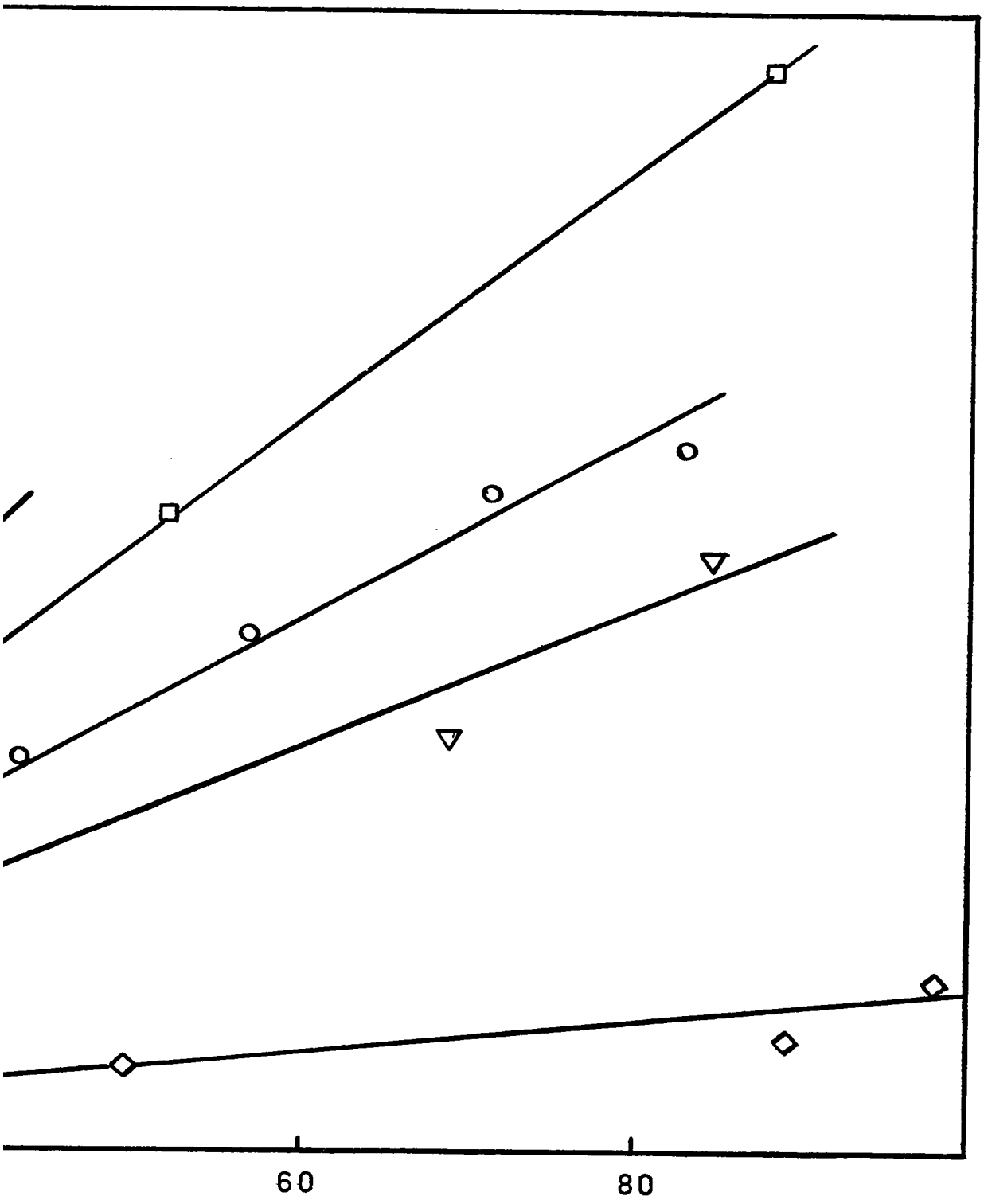

nt Ethyl Chloride Reacted

isopropyl chloride to give propylene and hydrogen chloride became stoichiometric. The reaction was followed either by disappearance of isopropyl chloride or by appearance of hydrogen chloride and occurred with first order kinetics. Convenient rates for kinetic investigation occurred between 100°C and 180°C.

Sets of reactions were studied for $P_o = 10^{-2}$ torr, $5x10^{-2}$ torr and $2.5x10^{-1}$ torr, and are illustrated by figures (III-31), (III-32) and (III-33) respectively. Good first order kinetic plots were obtained in all cases. Dependence of the apparent activation energy on initial reactant pressure was observed. Arrhenius plots for the three sets of reactions at different P_o's are shown in figure (III-34). Calculation of the apparent activation energy from these plots gives 8.7±0.4 kcal./mole for $P_o = 10^{-2}$torr, 12.2±0.1 kcal./mole for $P_o = 5x10^{-2}$ torr and 15.2±0.7 kcal./mole for $P_o = 2.5x10^{-1}$ torr. Levelling of the Arrhenius plot at high temperature for $P_o = 2.5x10^{-1}$ torr is attributed to the limiting response rate of the reaction system {which was discussed in section (II-2, g)}.

The reaction of isopropyl chloride on the titanium films remained completely catalytic only below a certain temperature ceiling. Beyond this temperature, formation of appreciable amounts of two side products occurred. The most important side product was propane. Smaller quantities of diisopropyl were also detected. No hydrogen was observed at any time. Organic product ratios obtained from the reaction of

FIGURE (III - 31)

Disappearance of Isopropyl Chloride

Plotted as a First Order Reaction

for $P_o = 10^{-2}$ torr

◇ - 100°C

□ - 118°C

○ - 134.5°C

▽, △ - 157°C

● - 180°C

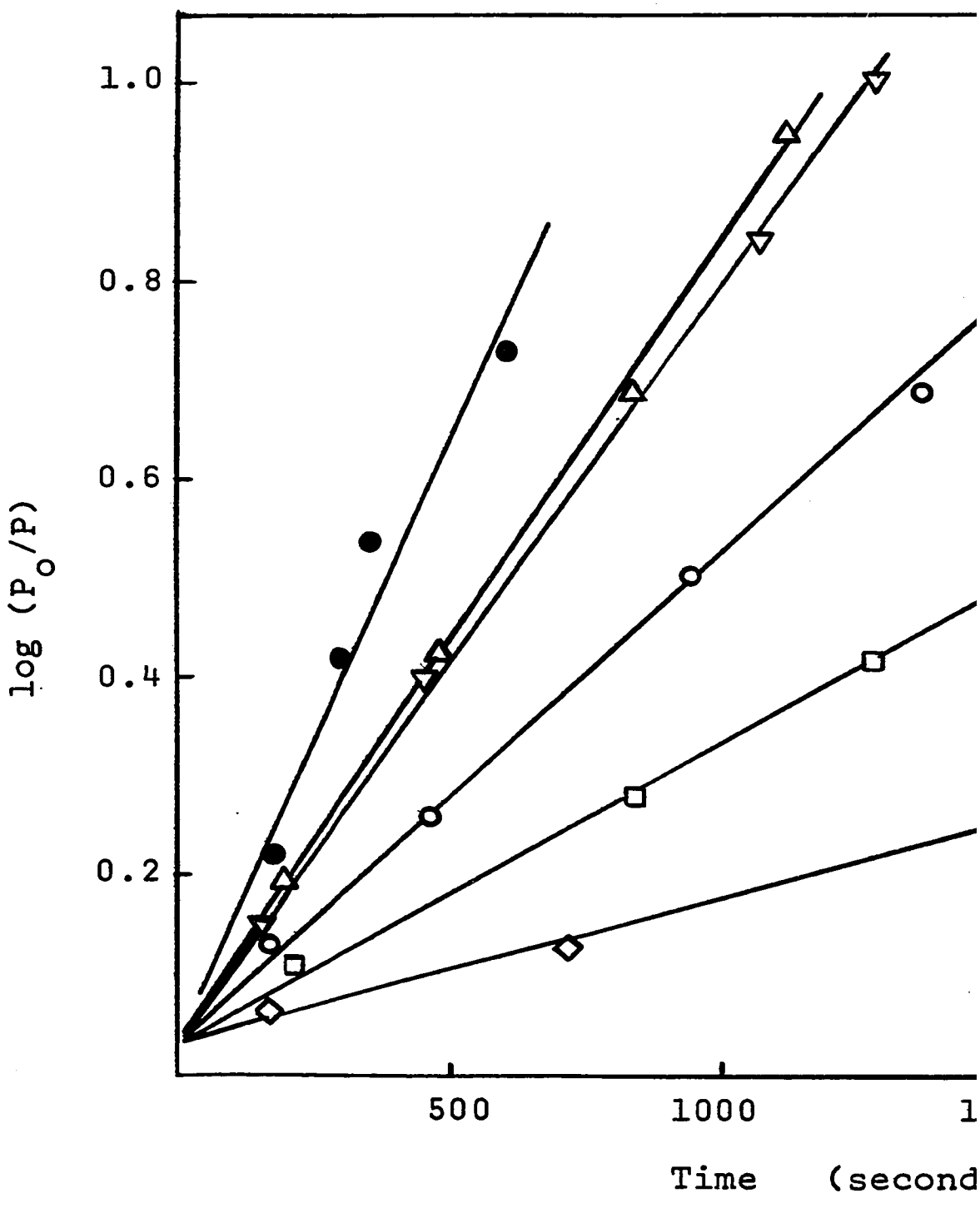
1.0
0.8
0.6
0.4
0.2
log (P$_o$/P)
500
1000
1
Time (second

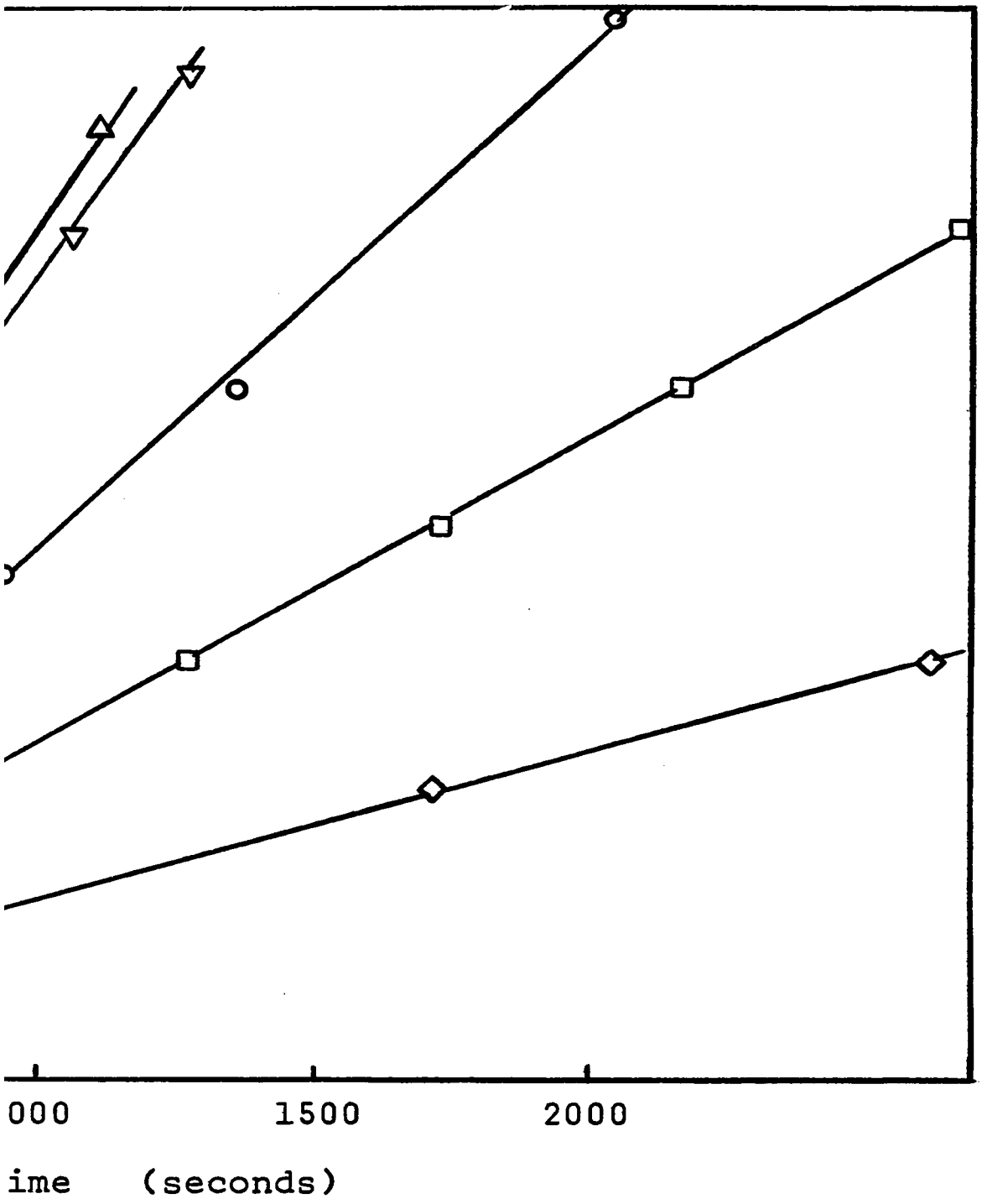
000
1500
2000
ime (seconds)

FIGURE (III - 32)

Disappearance of Isopropyl Chloride

Plotted as a First Order Reaction

for $P_o = 5 \times 10^{-2}$ torr

● - 109°C

▽, △ - 131°C

◇ - 152°C

○, □ - 168°C

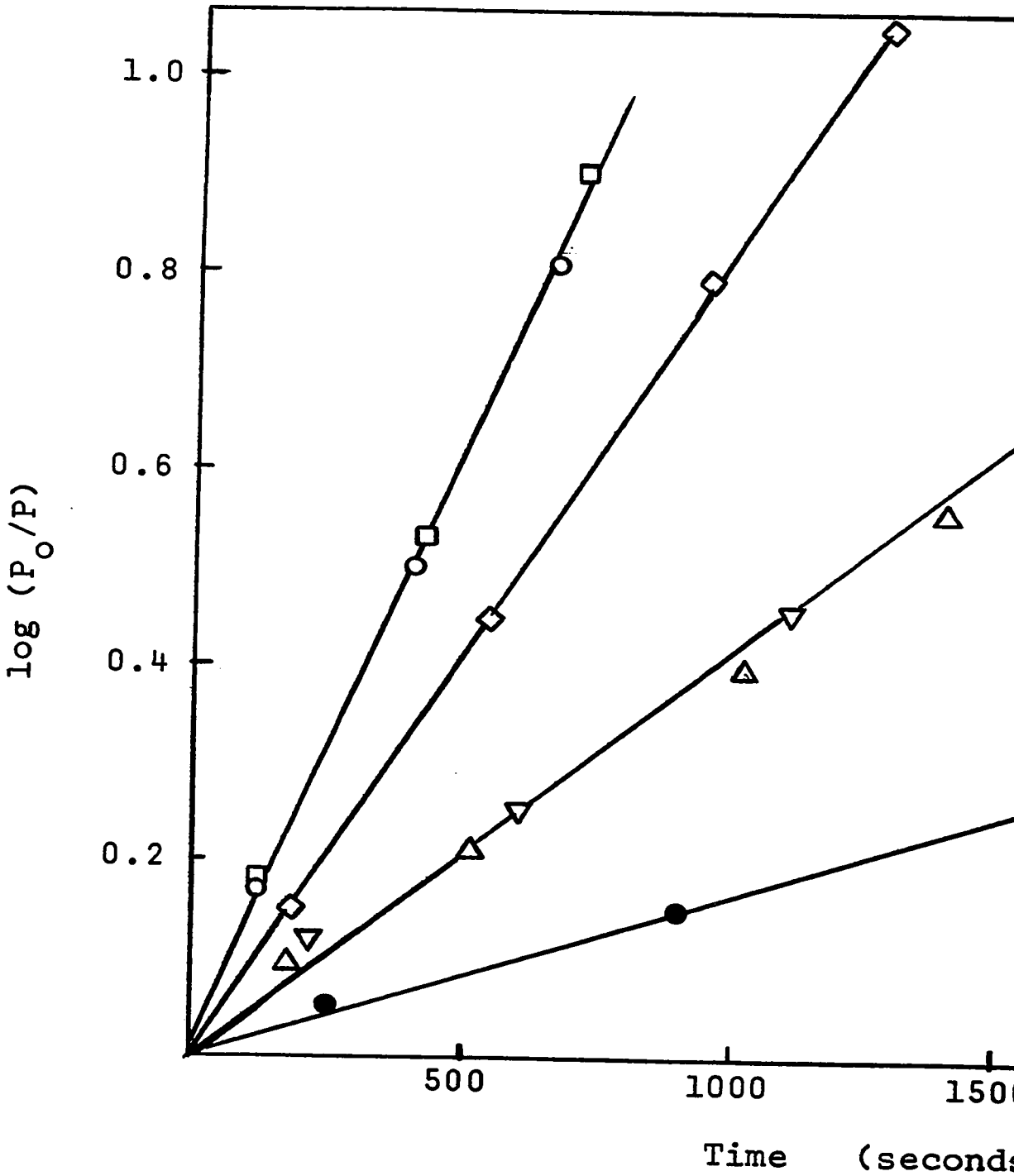
1.0
0.8
0.6
0.4
0.2
log (P_o/P)
500
1000
Time (seconds

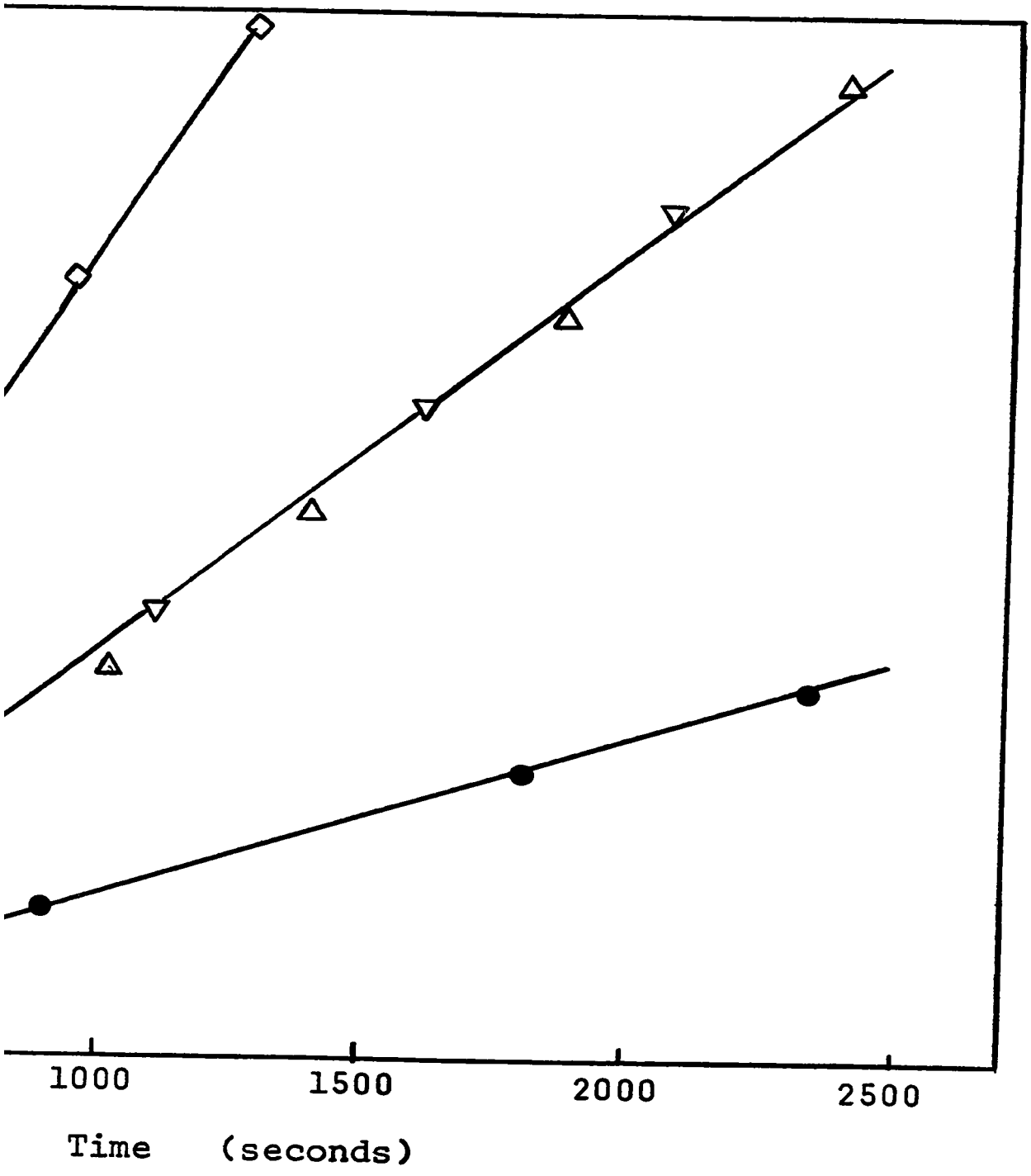
1000
1500
2000
2500
Time (seconds)

FIGURE (III - 33)

Disappearance of Isopropyl Chloride

Plotted as a First Order Reaction

for $P_o = 2.5 \times 10^{-1}$ torr

▽ - 116°C

△ - 125.5°C

◇ - 132.5°C

● - 142°C

▲ - 155°C

○, □ - 170°C

■ - 180°C

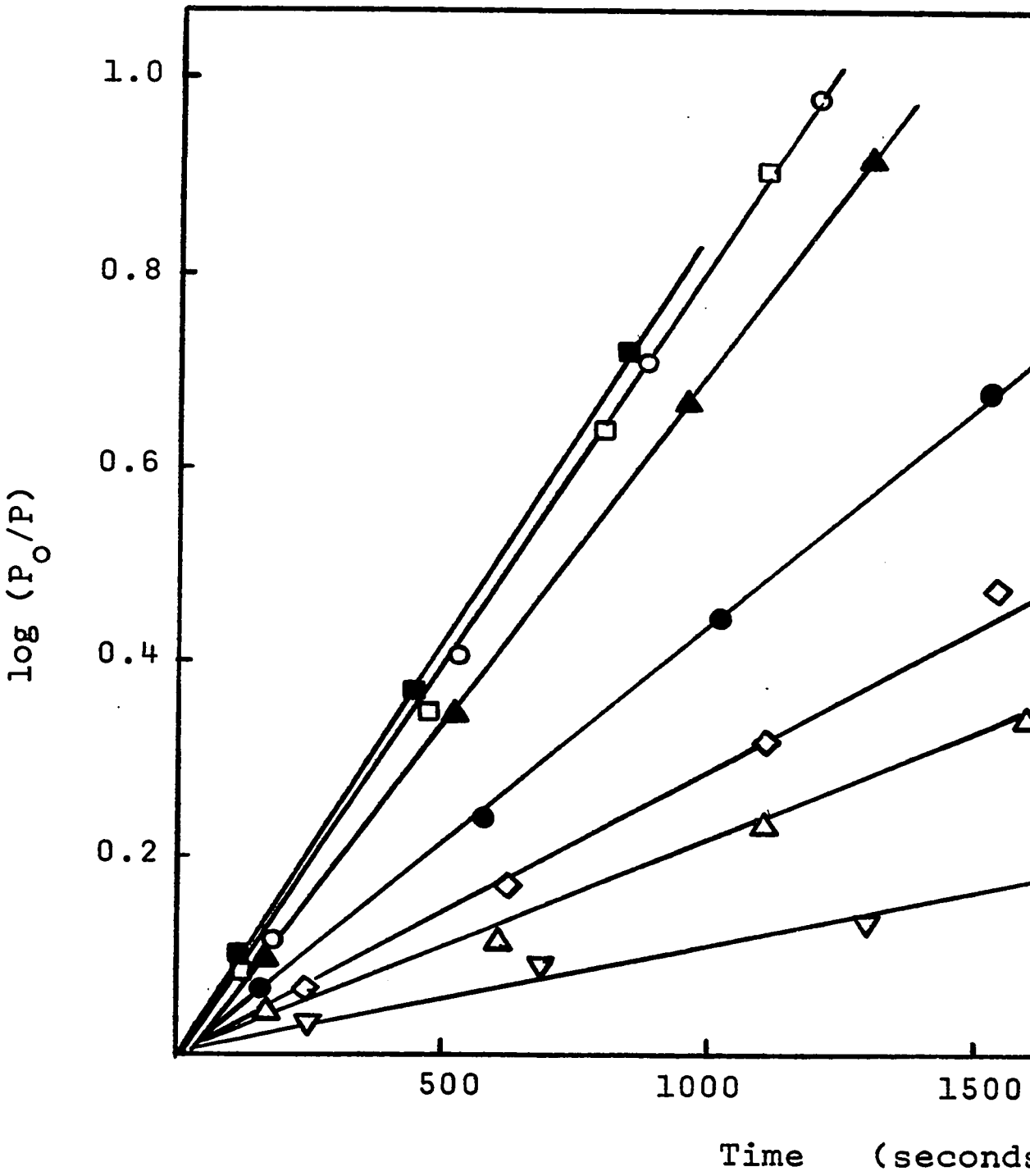
1.0
0.8
0.6
0.4
0.2
log (P_o/P)
500
1000
1500
Time (seconds

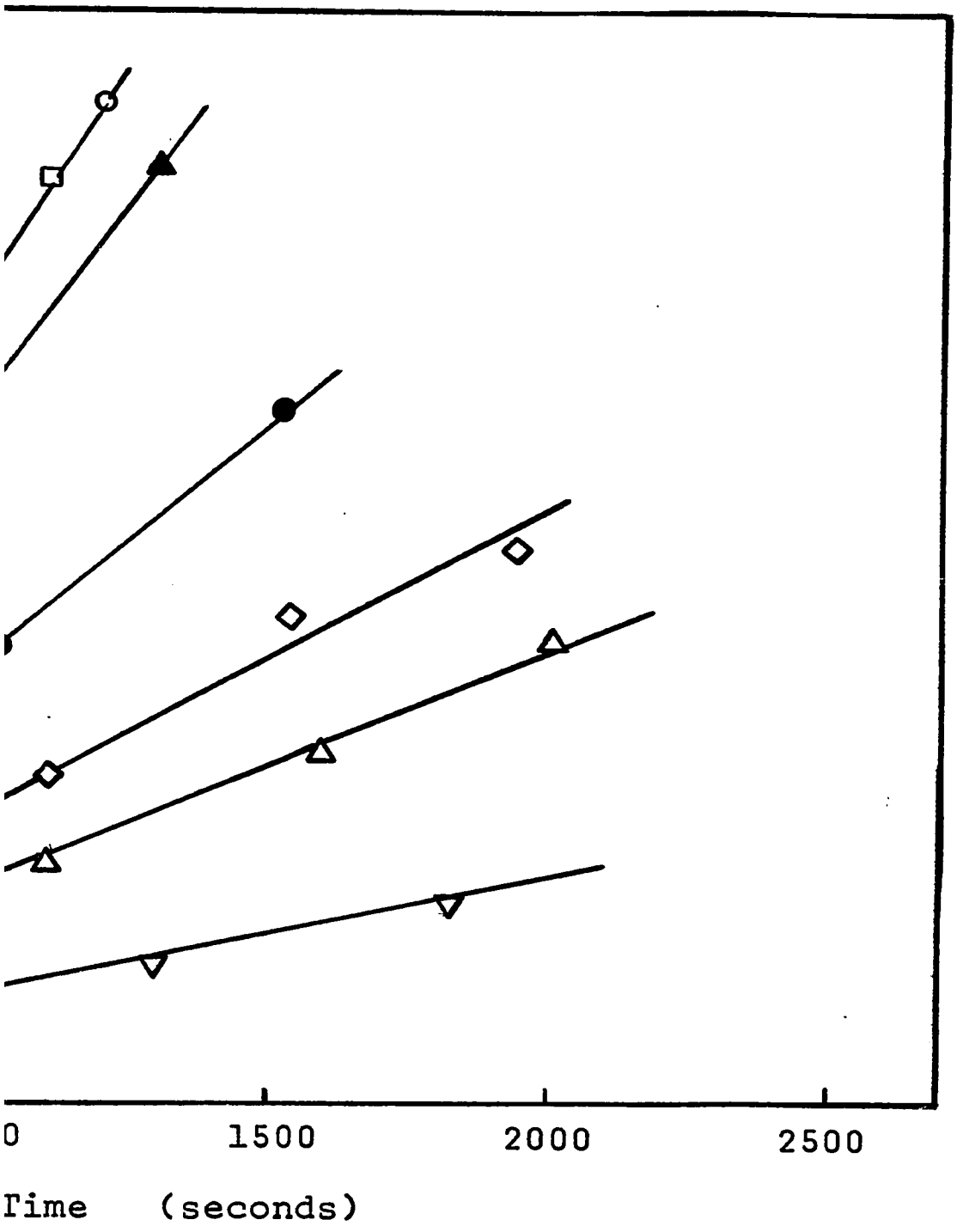
0
1500
2000
2500
Time (seconds)

FIGURE (III - 34)

Arrhenius Plots of Rate Data for First Order Disappearances of Isopropyl Chloride

O - Figure (III-31)*

□ - Figure (III-32)

Δ - Figure (III-33)

* For purposes of clarity, these points have been displaced positively by 0.2 units on the Y - axis.

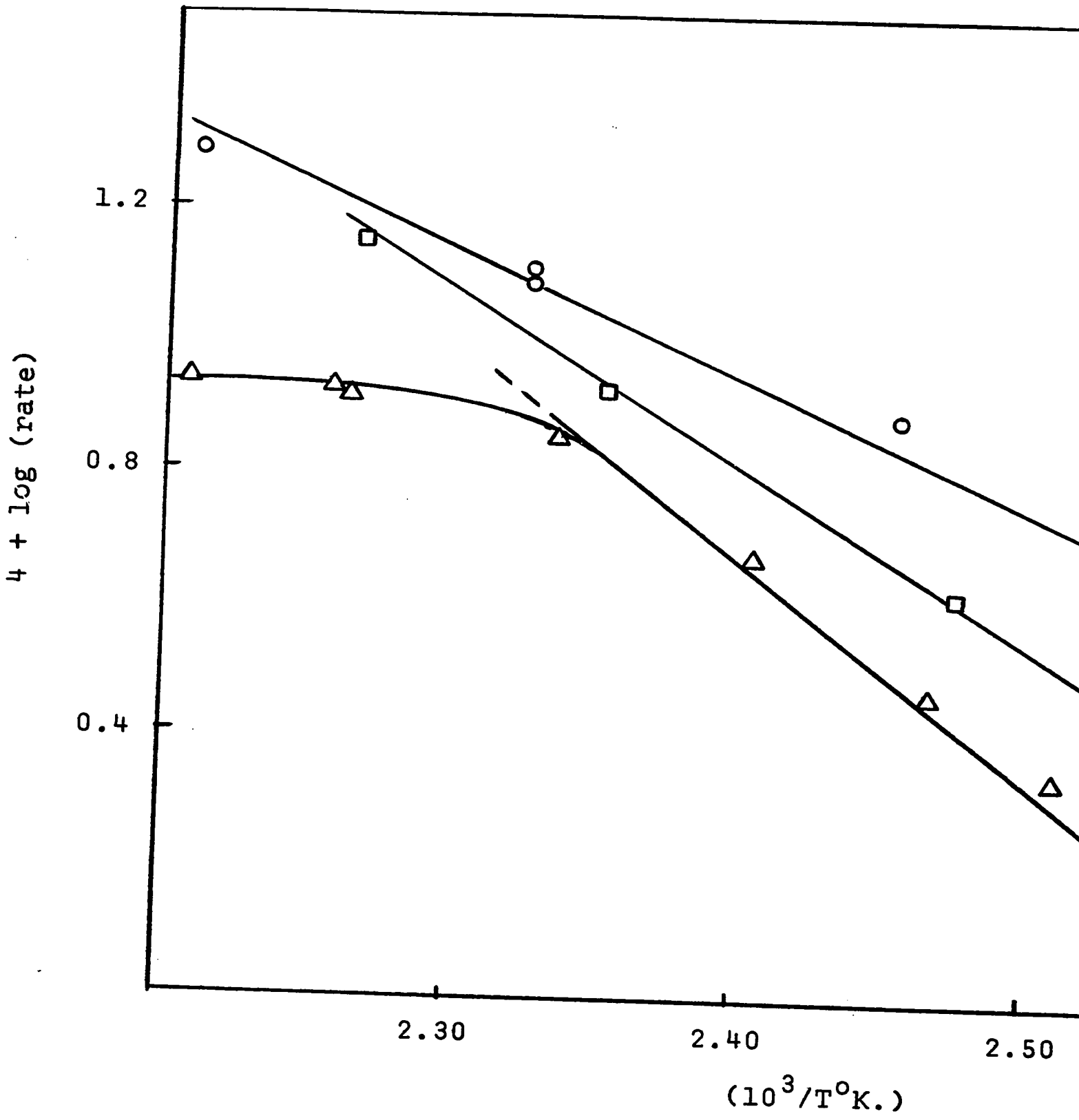
1.2
0.8
0.4
4 + log (rate)
2.30
2.40
2.50
(10³/T°K.)

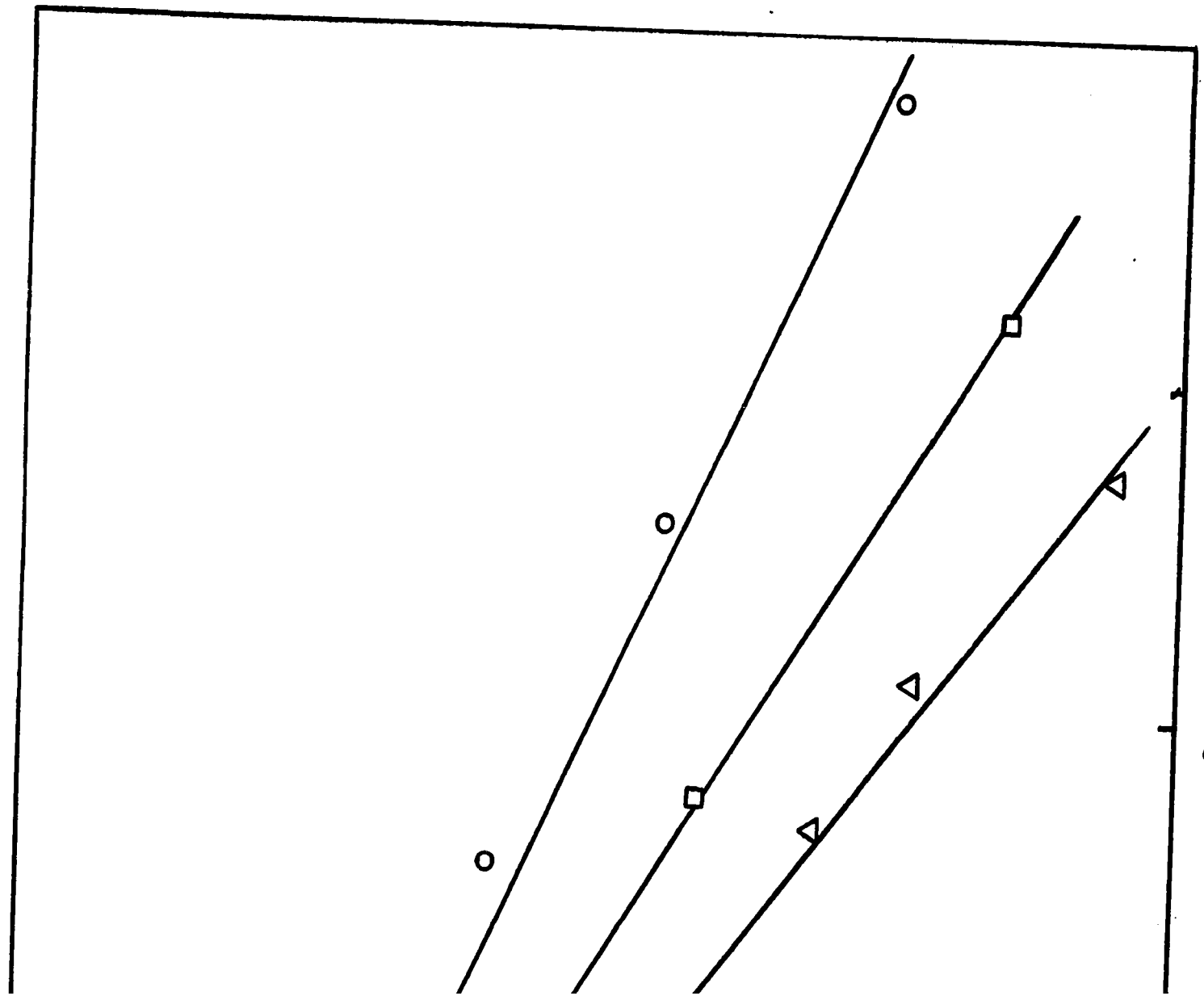
2.60
2.50
$10^3/T^\circ K.$)

10^{-2} torr doses of isopropyl chloride at various reaction temperatures are summarized in Table (III-7).

TABLE (III - 7)

Reaction Temp. °C	Mole Percent Propylene	Mole Percent Propane	Mole Percent Diisopropyl
248	76.5	19.0	4.5
222	86.0	10.0	4.0
195	97.5	1.5	1.0
180	100.0	0.0	0.0

iii) Tertiary Butyl Chloride

The reaction of t-butyl chloride followed the same pattern as isopropyl chloride. As might be expected, it was much more reactive than isopropyl chloride and gaseous hydrogen chloride was first detected during initial low temperature studies of the reactant on a fresh film.

The reaction of t-butyl chloride occurred with first order kinetics and produced isobutylene and hydrogen chloride. Convenient rates for kinetic investigation occurred between 30°C and 70°C. A set of reactions for $P_o = 2.8 \times 10^{-2}$ torr were studied and are illustrated by figure (III-35). Calculation of the slope of the Arrhenius plot of this rate data, which is illustrated by figure (III-36), gave an apparent activation energy of 15.4±0.5 kcal./mole between 33°C and 67.5°C. Levelling of the activation energy to zero above 67.5°C is attributed

FIGURE (III - 35)

Disappearance of t-Butyl Chloride

Plotted as a First Order Reaction

$P_o = 2.8 \times 10^{-2}$ torr

▲ - 33.5°C

■ - 42°C

● - 51.5°C

◇ - 56.5°C

▽ - 67.5°C

□ - 80°C

○ - 93.5°C, 100°C

△ - 148°C, 164°C, 188°C

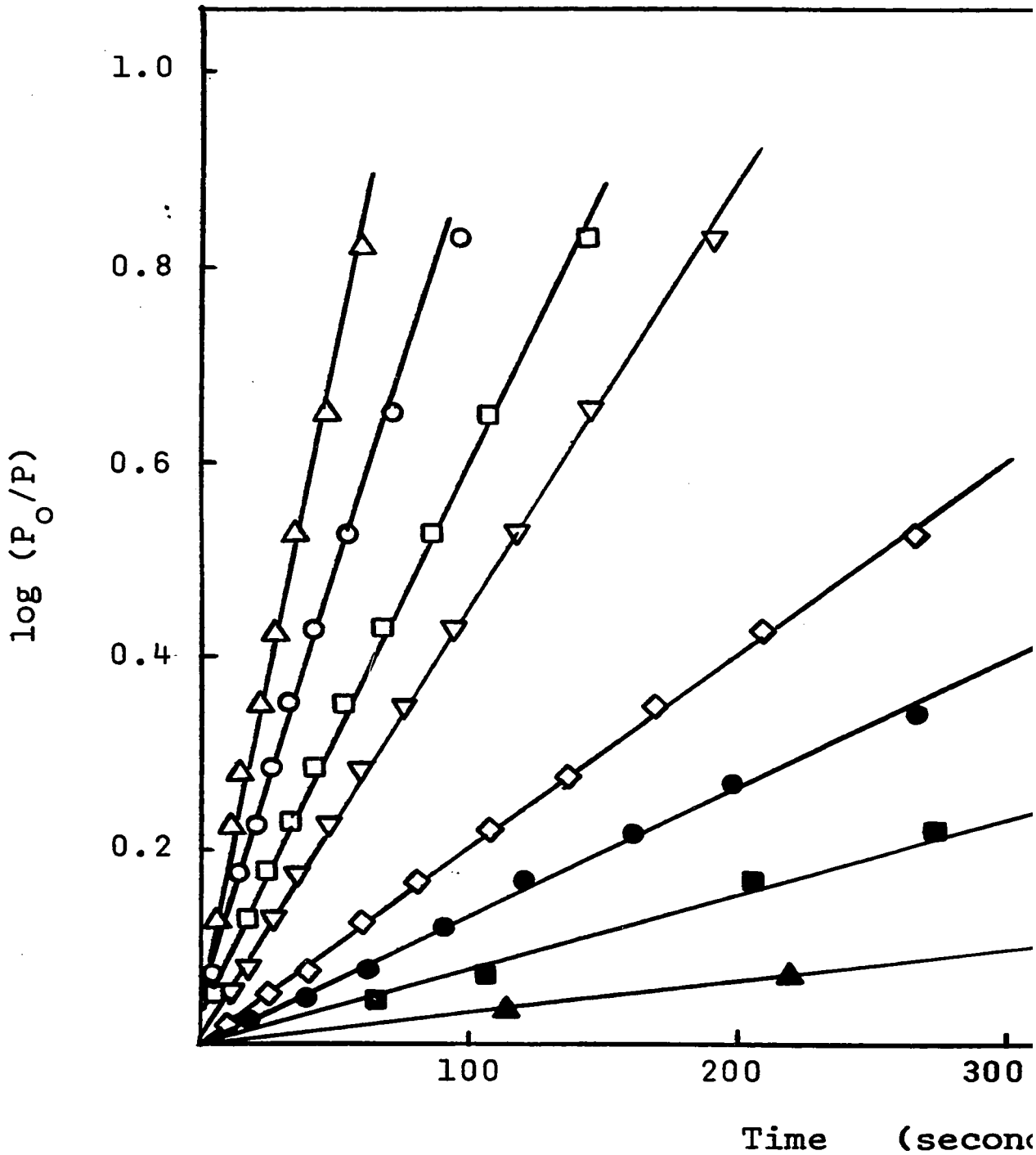
1.0
0.8
0.6
0.4
0.2
log (P_o/P)
100
200
300
Time (second

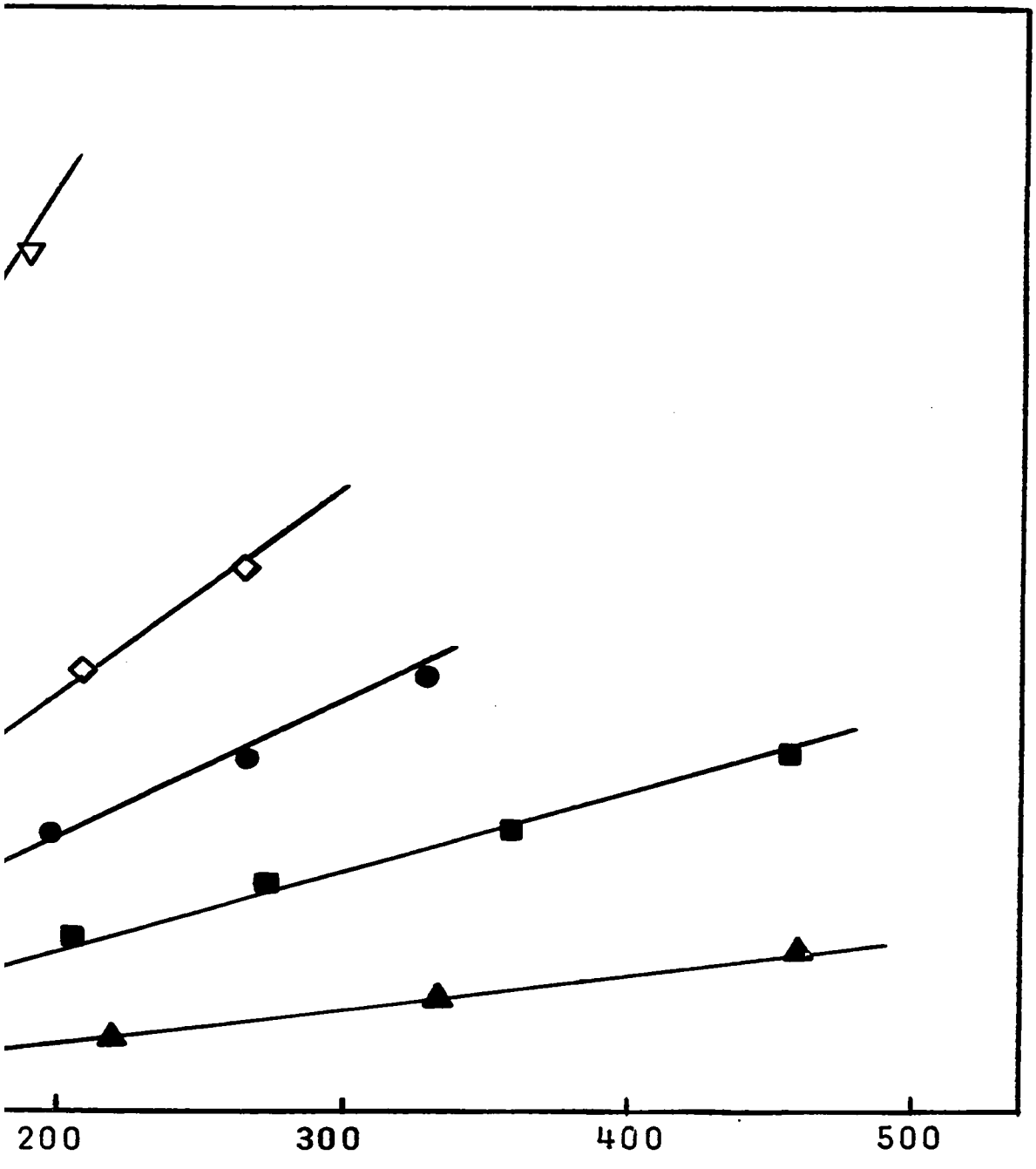
200
300
400
500
Time (seconds)

FIGURE (III - 36)

Arrhenius Plot of Rate Data for First Order Disappearance of

t-Butyl Chloride in Figure (III-35)

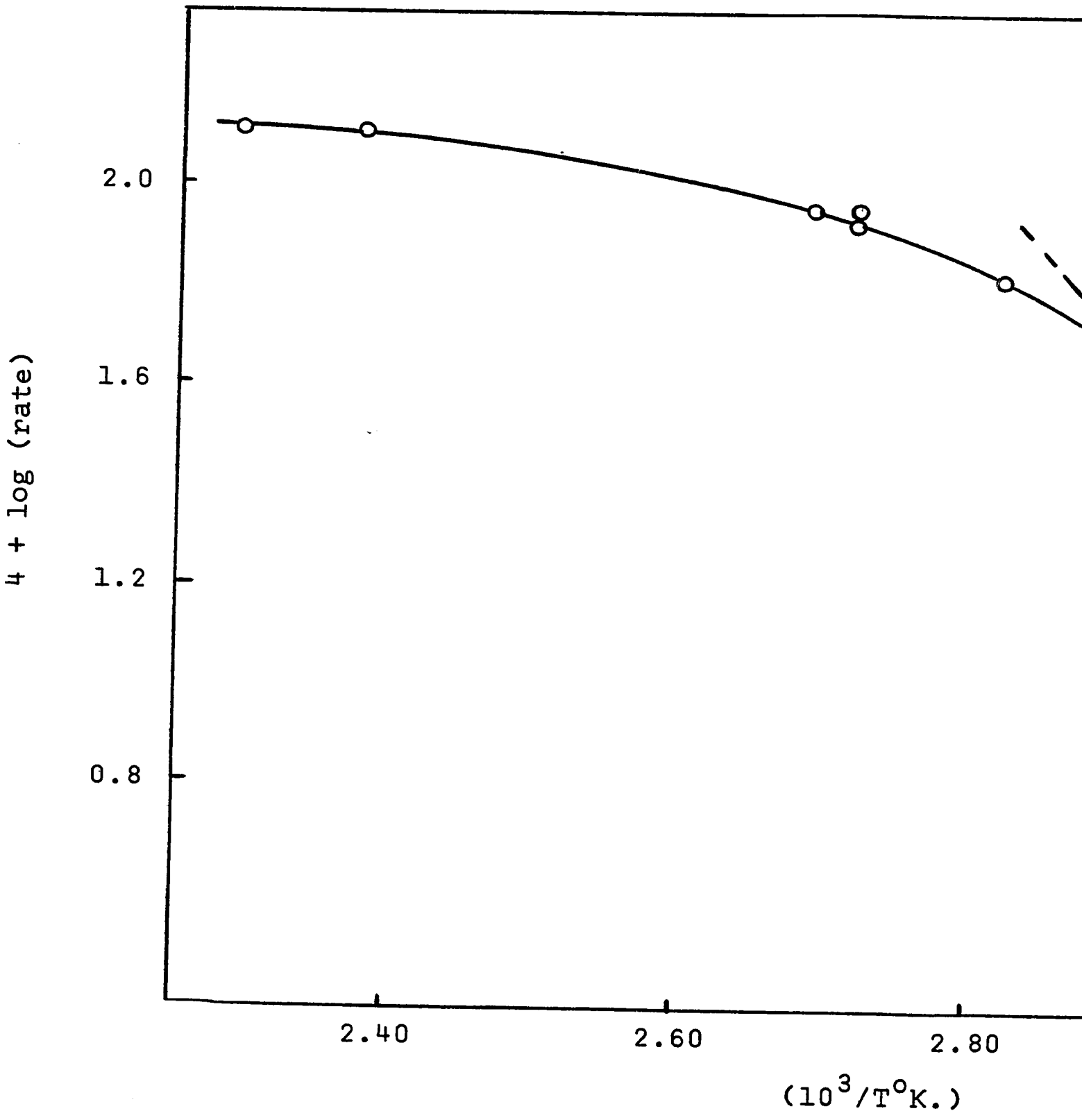
2.0
1.6
1.2
0.8
4 + log (rate)
2.40
2.60
2.80
(10³/T°K.)

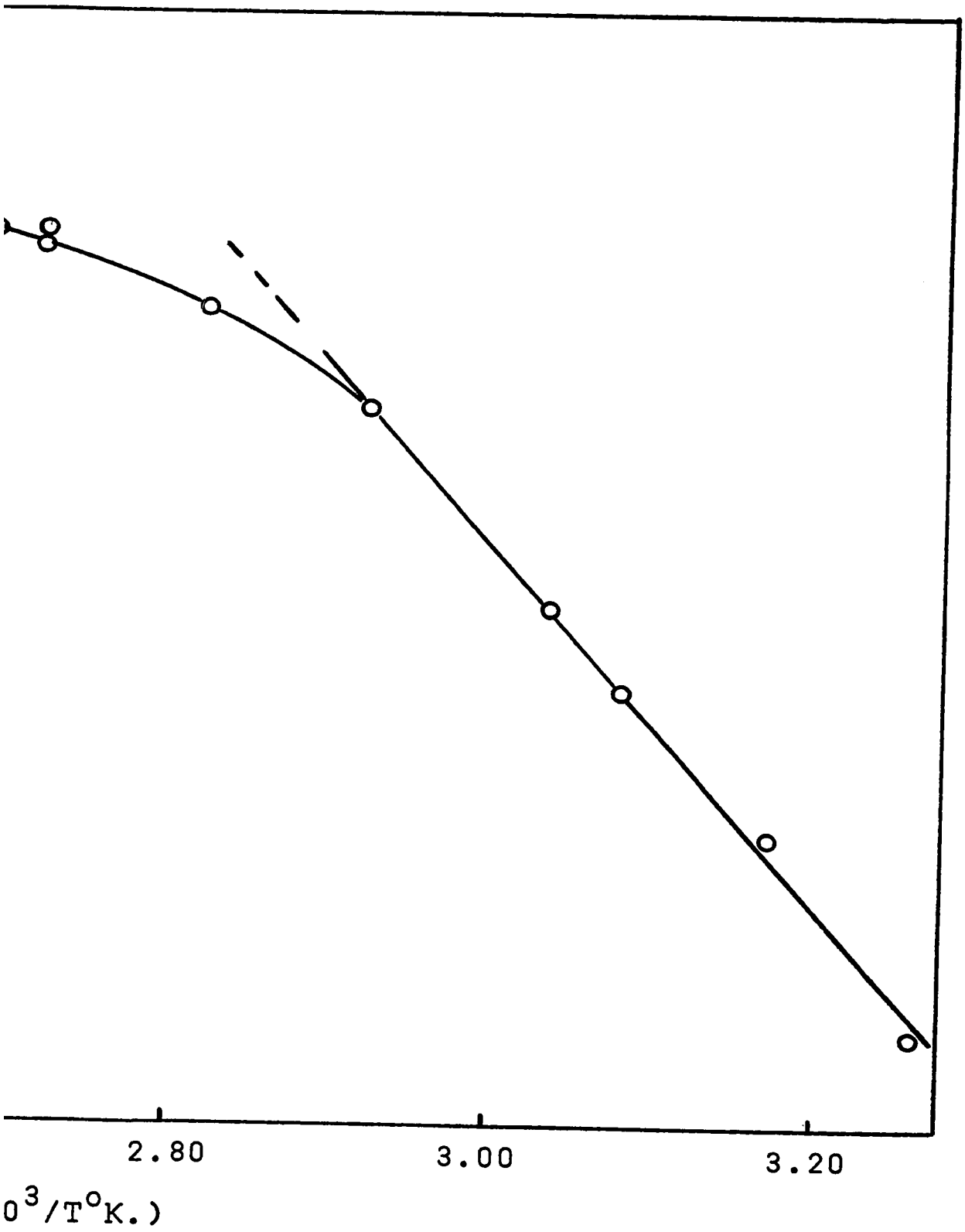
2.80
3.00
3.20
$0^3/T^oK.$)

to the limiting response rate of the reaction {which was discussed in section (II-2, g)}.

Neither isobutane nor hydrogen were detected during any of the reactions which were studied.

Because of the corrosive effect of this reactant on the metal parts of the vacuum system, runs to determine activation energies at other reactant pressures were not performed.

c) β-Methyl Series

i) Ethyl Chloride

Studies of this reactant have been presented in the α-methyl series.

ii) n-Propyl Chloride

Studies of this reactant have been presented in the n-propyl halide series.

iii) Isobutyl Chloride

The reaction of isobutyl chloride followed the pattern established for isopropyl chloride. After the reaction of a few monolayer equivalent doses of reactant, the film became a catalyst for dehydrochlorination. The products of the reaction of isobutyl chloride were isobutylene and hydrogen chloride. The reaction obeyed a first order dependence for all reactant pressures studied. Convenient rates for kinetic investigations occurred between 120°C and 210°C.

Kinetic data for the first order disappearance of isobutyl chloride for $P_o = 10^{-2}$ torr is illustrated by Figure (III-37), and for $P_o = 5 \times 10^{-2}$ torr by Figures (III-39) and

(III-41). Arrhenius data from these kinetic investigations are plotted in figures (III-38), (III-40) and (III-42) respectively. At $P_o = 10^{-2}$ torr an apparent activation energy of 12.6±0.8 kcal./mole was calculated, and at $5x10^{-2}$ torr apparent activation energies of 15.9±0.2 kcal./mole and 15.2±0.8 kcal./mole were calculated.

Neither hydrogen nor isobutane were observed during these reactions. Reactions at higher pressures, $5x10^{-1}$ torr or 1.0 torr, resulted in a trace peak in the product spectra at m/e = 57 which was indicative of the presence of t-butyl chloride.

The kinetics of the early reactions of isobutyl chloride are illustrated in figure (III-43) and show a trend from a noncatalytic half order reaction at a slow rate to a catalytic first order reaction at an increased rate. These initial, high temperature studies were performed at 218°C.

iv) Neopentyl Chloride

Even though neopentyl chloride lacks a β-hydrogen, it follows the reaction pattern established for isopropyl chloride, and undergoes catalytic dehydrochlorination. As with isobutyl chloride, the initial 10^{-2} torr dose reacted slowly and non-catalytically. Subsequent reactions began to release gaseous hydrogen chloride and then after the reaction of only a few more doses, stoichiometric amounts of hydrogen chloride were produced. The reaction followed first order kinetics and convenient rates for kinetic investigation occurred between 150°C

FIGURE (III - 37)

Disappearance of Isobutyl Chloride

Plotted as a First Order Reaction

for $P_o = 10^{-2}$ torr

◇ - 162°C

▽ - 175.5°C

□ - 187°C

△ - 198°C

○ - 207°C

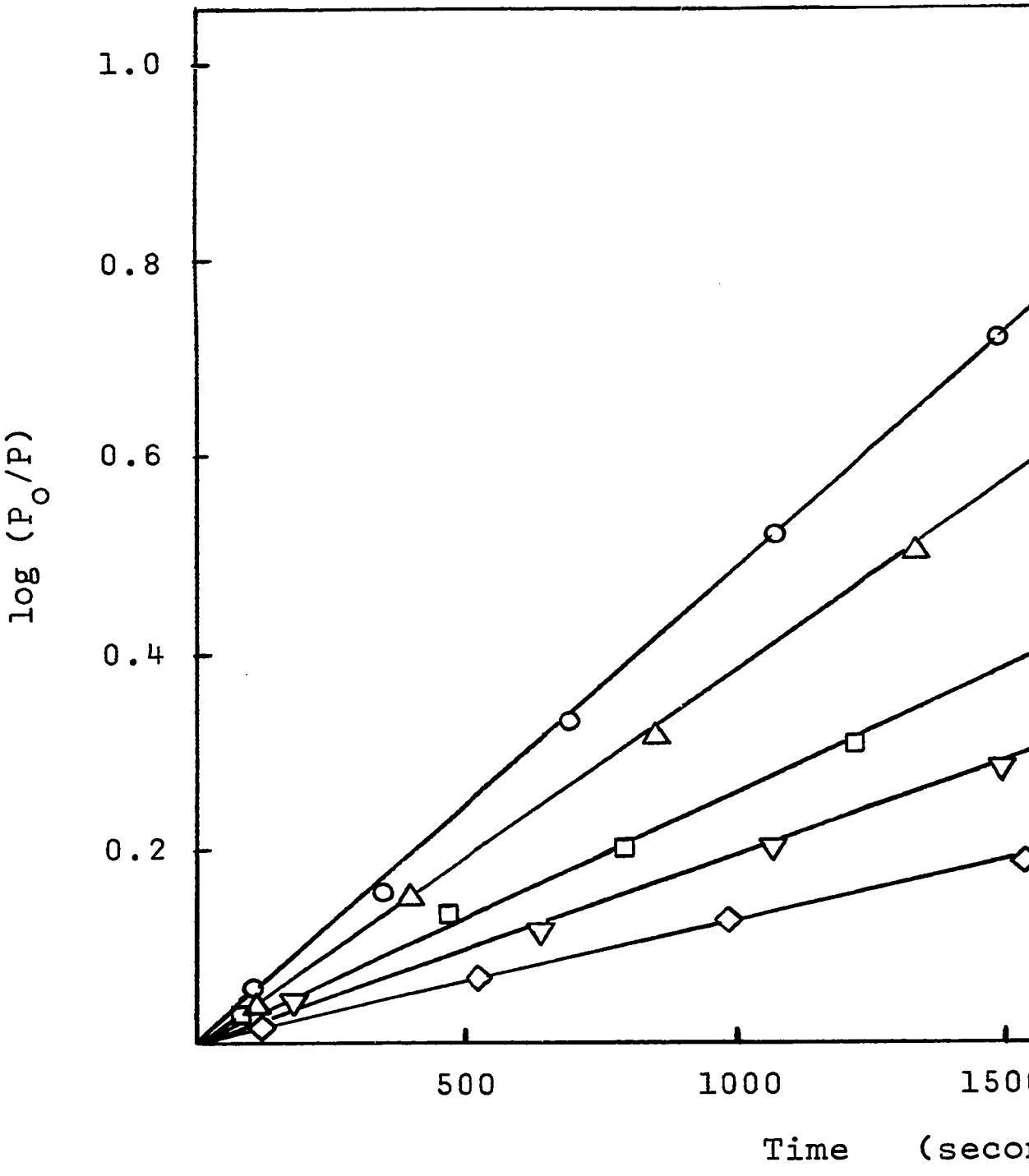
1.0
0.8
0.6
0.4
0.2
log (P_o/P)
500
1000
Time (seco

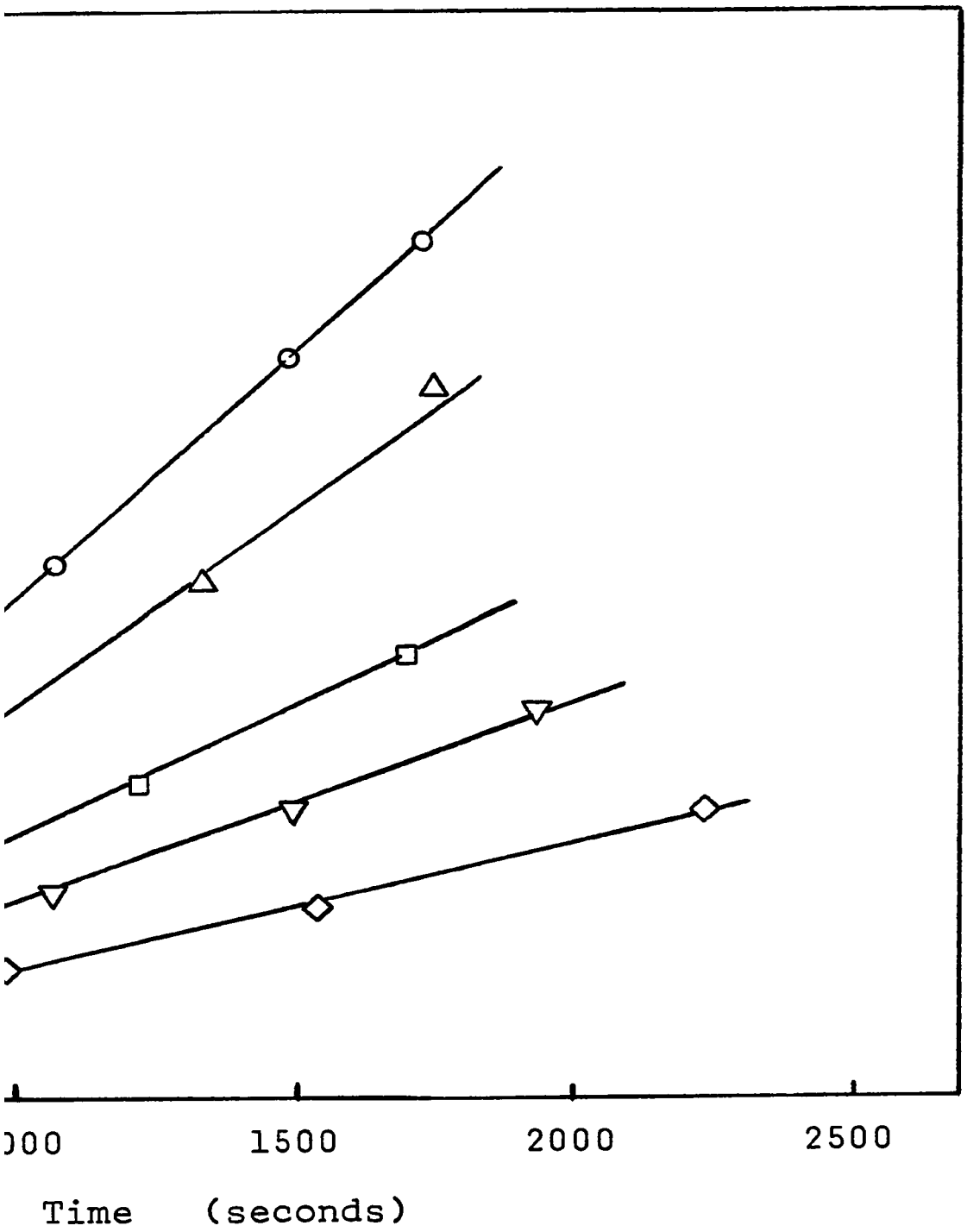
)00
1500
2000
2500
Time (seconds)

FIGURE (III - 38)

Arrhenius Plot of Rate Data for First Order Disappearance of

Isobutyl Chloride in Figure (III-37)

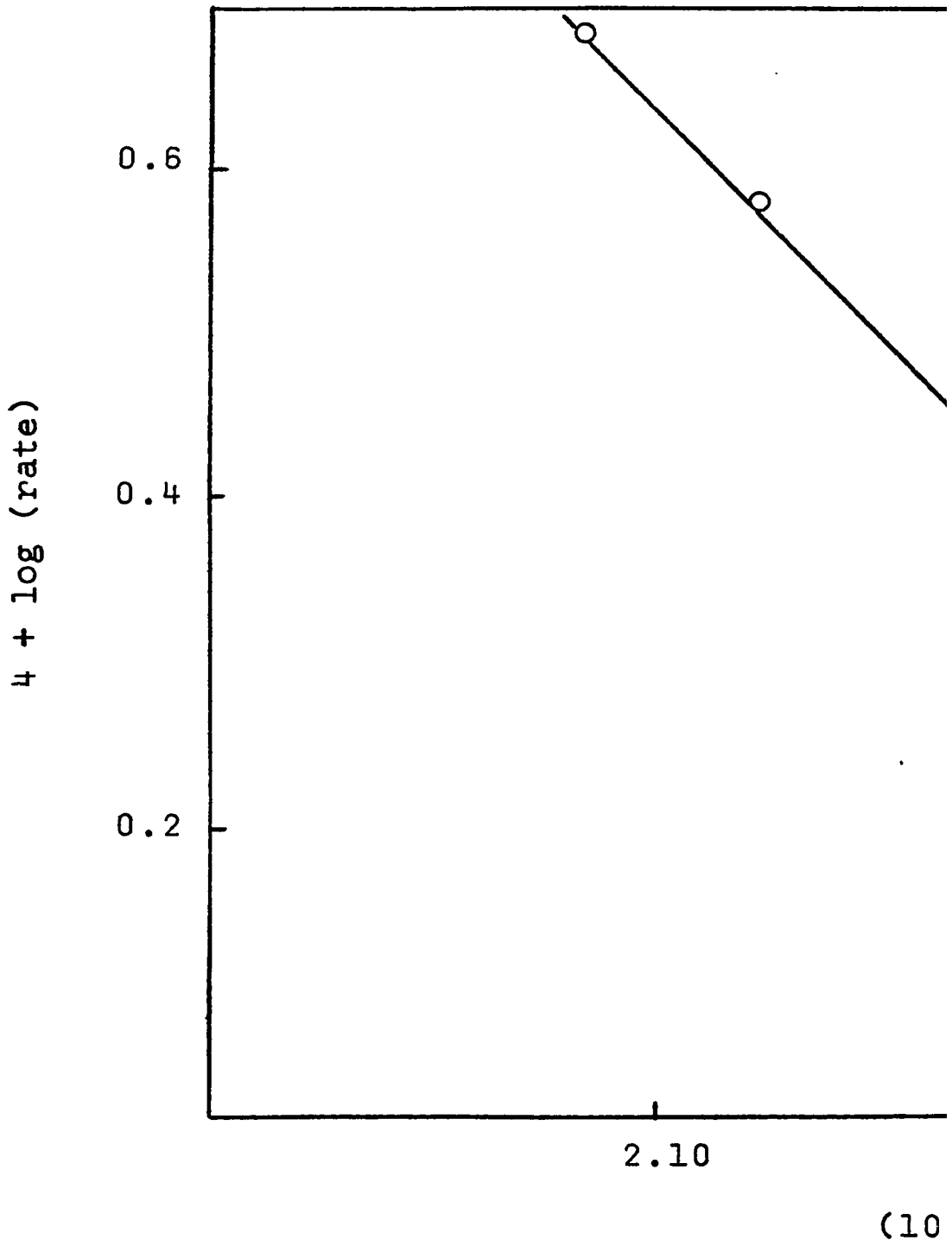
0.6
0.4
0.2
4 + log (rate)
2.10
(10

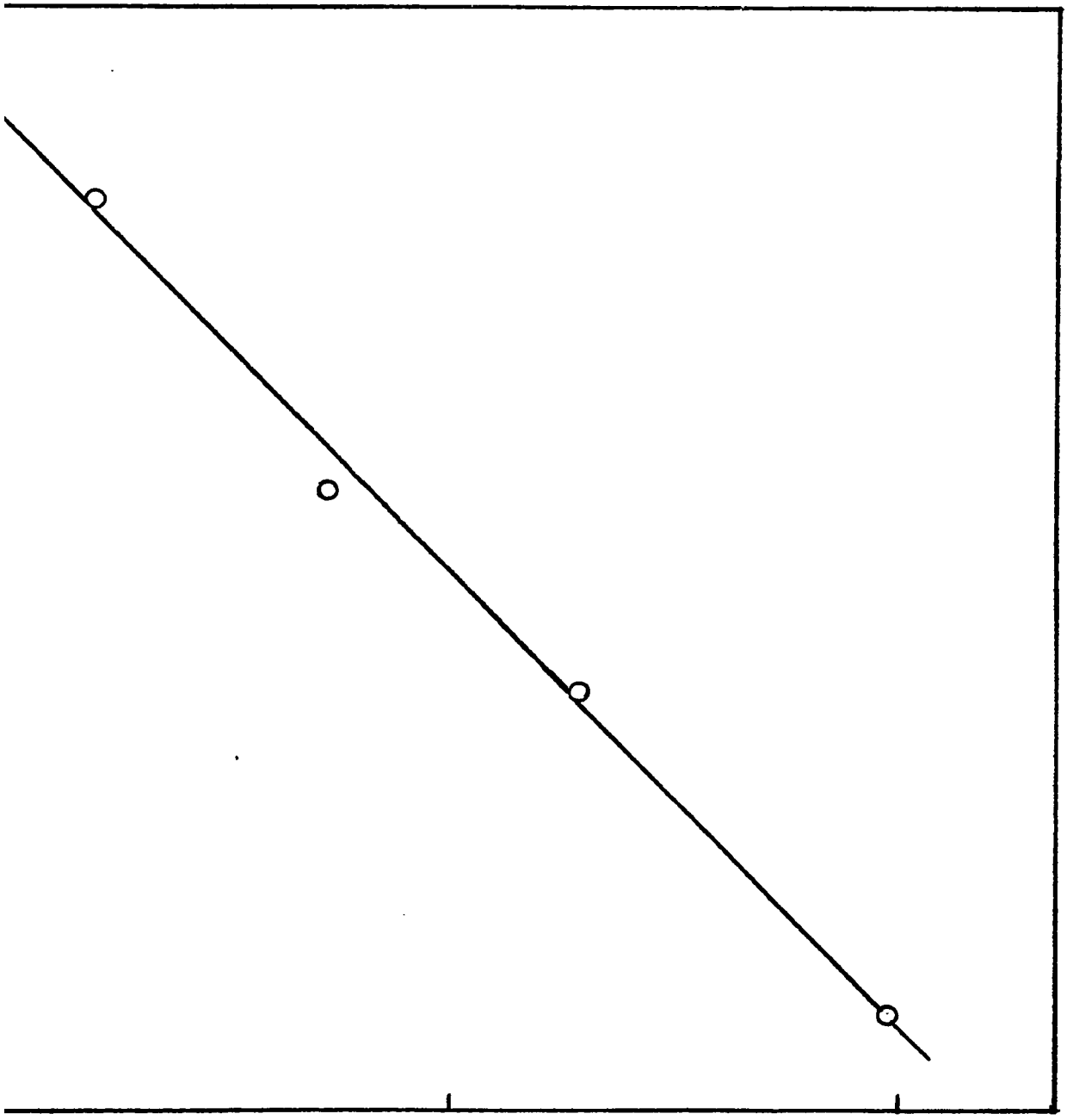
10
2.20
2.30
(10³/T°K.)

FIGURE (III - 39)

Disappearance of Isobutyl Chloride

Plotted as a First Order Reaction

for $P_o = 5 \times 10^{-2}$ torr

● - 143.5°C

▽ - 153.5°C

◇ - 160°C

△ - 167°C

○ - 176.5°C

□ - 178°C

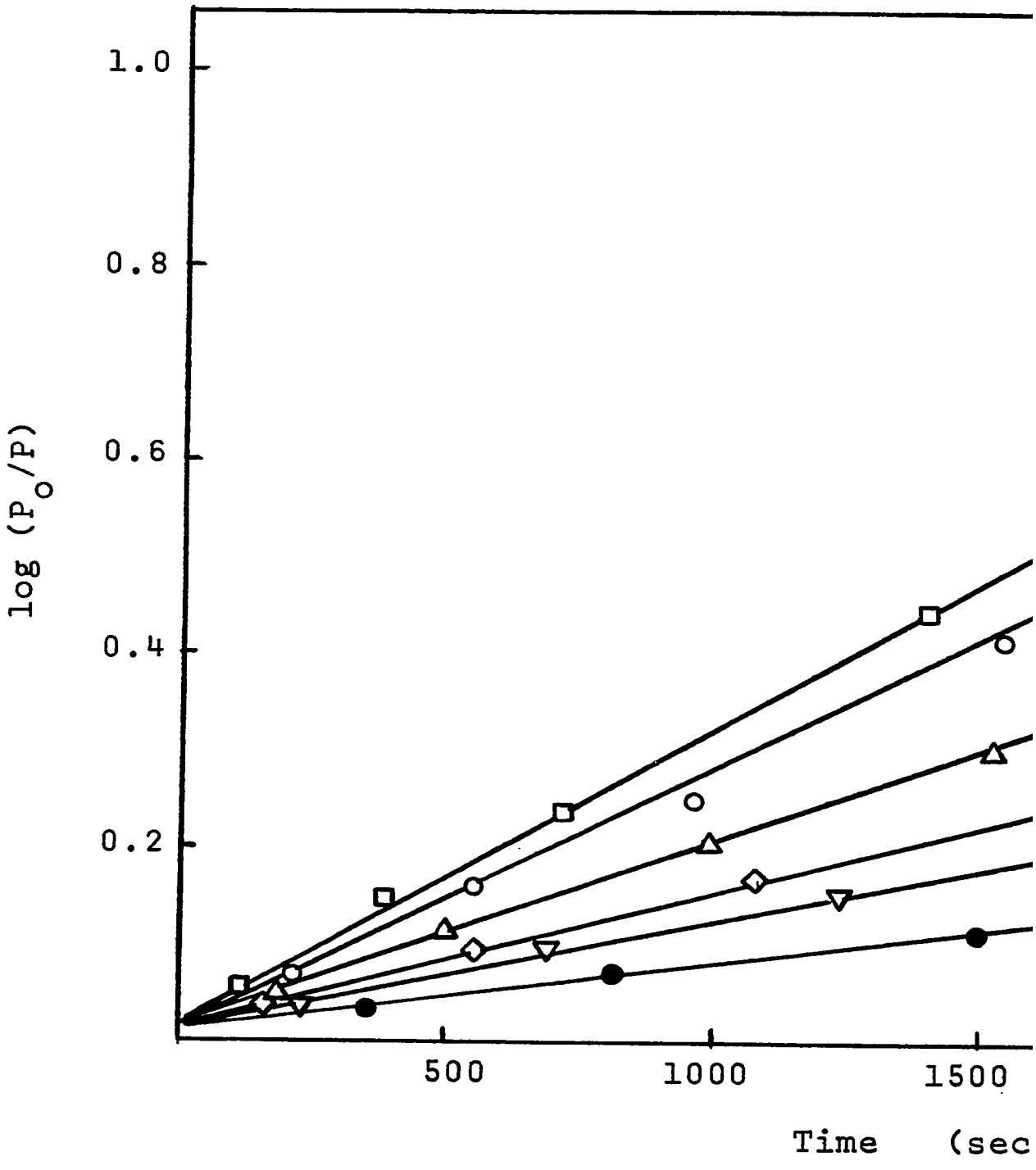
1.0
0.8
0.6
0.4
0.2
log (P$_o$/P)
500
1000
1500
Time (sec

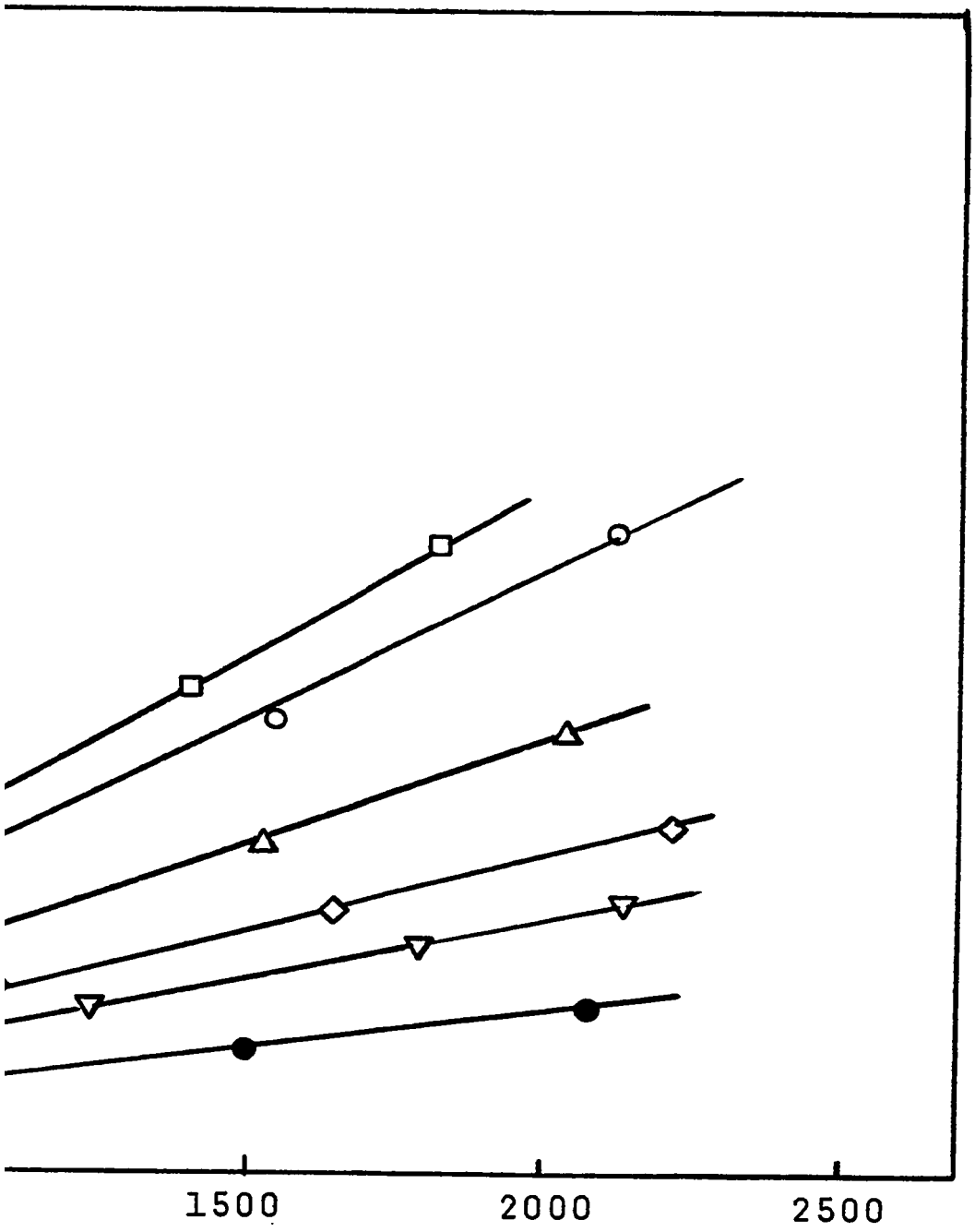
1500
2000
2500
Time (seconds)

FIGURE (III - 40)

Arrhenius Plot of Rate Data for First Order Disappearance of Isobutyl Chloride in Figure (III-39)

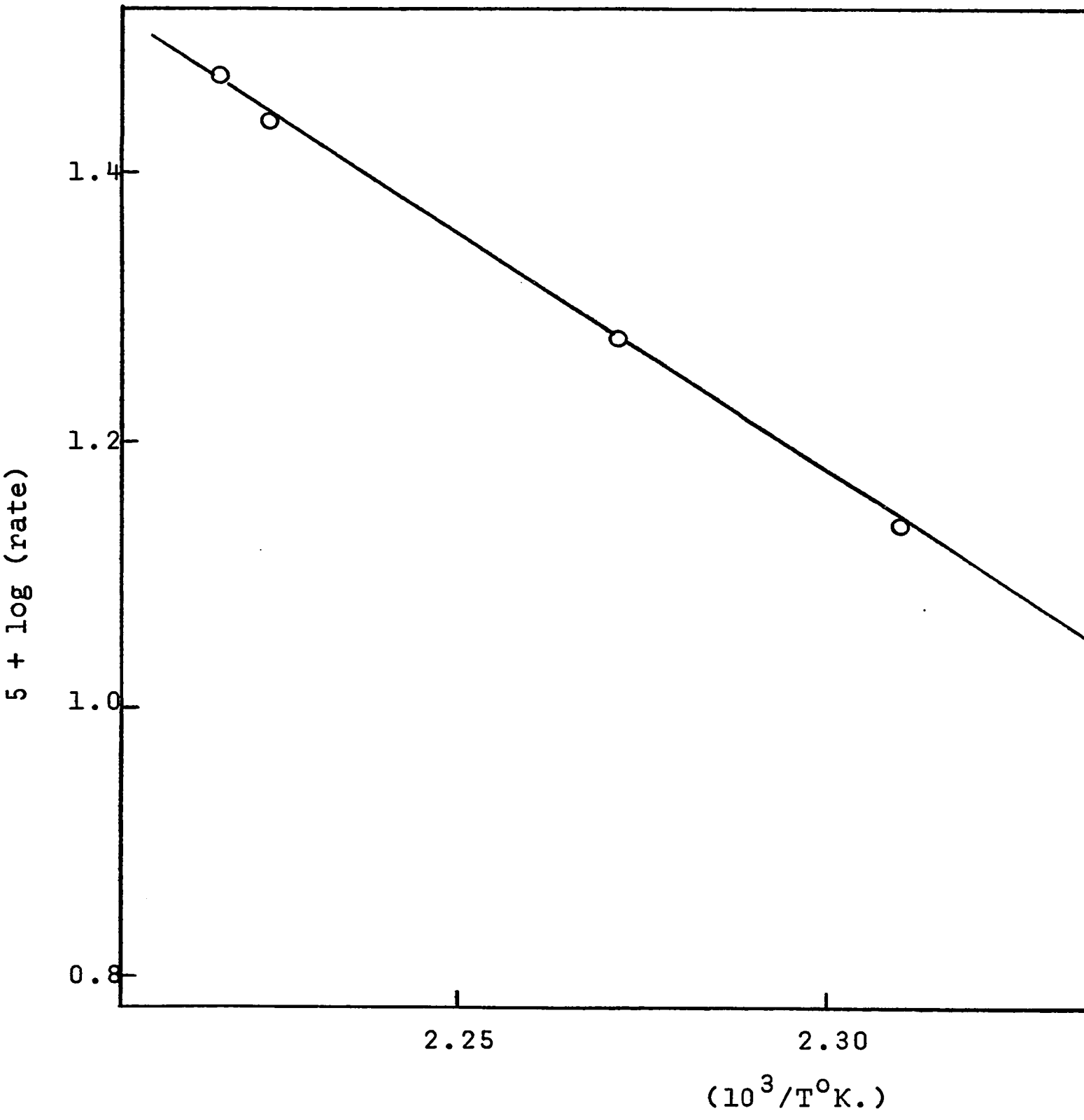
1.4
1.2
1.0
0.8
5 + log (rate)
2.25
2.30
(10^3/T°K.)

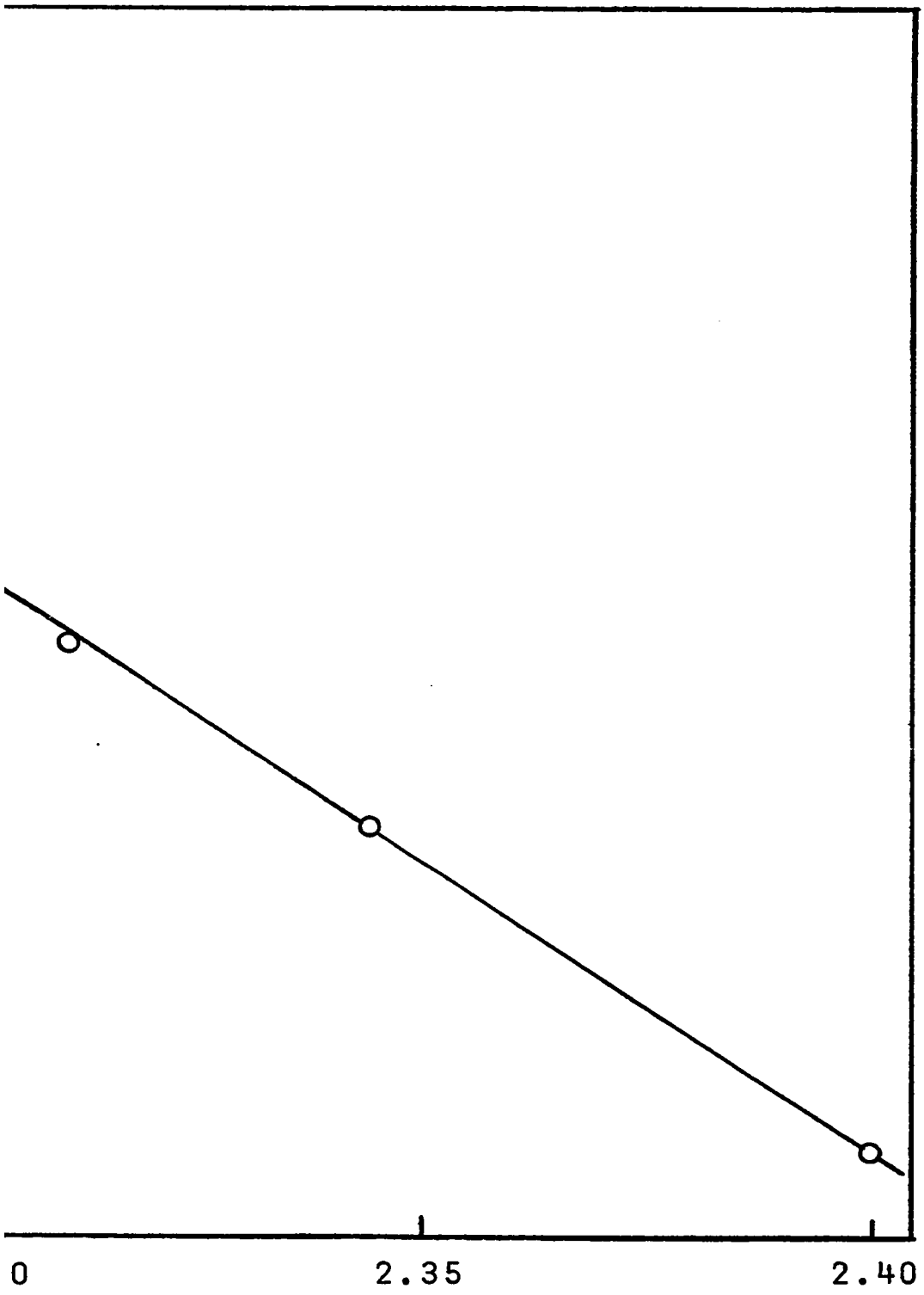
0
2.35
2.40

FIGURE (III - 41)

Disappearance of Isobutyl Chloride

Plotted as a First Order Reaction

for $P_o = 5 \times 10^{-2}$ torr

◇ - 128.5°C

▽, △ - 150°C

□ - 174.5°C

○ - 199.5°C

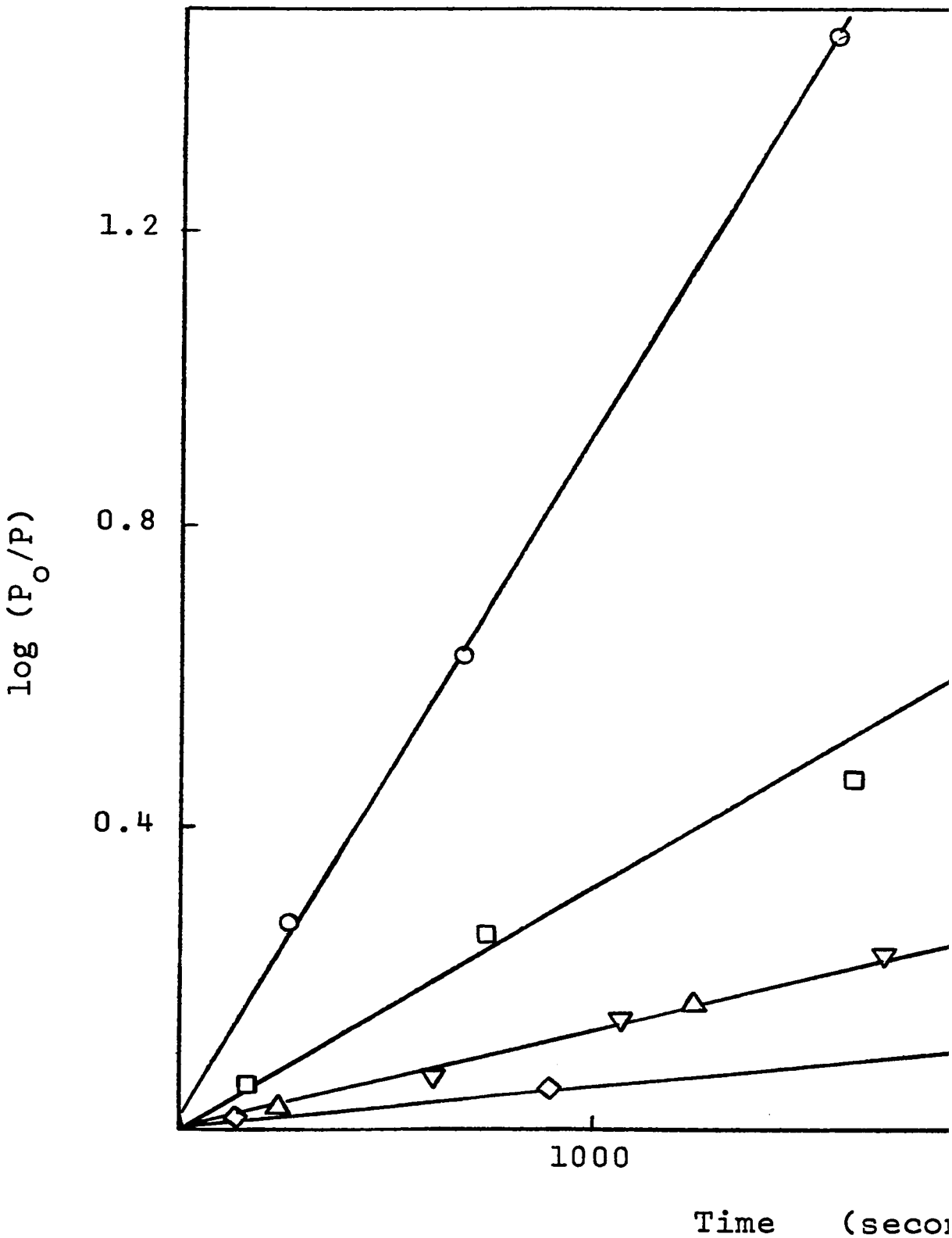
1.2
0.8
0.4
log (P_o/P)
1000
Time (seco

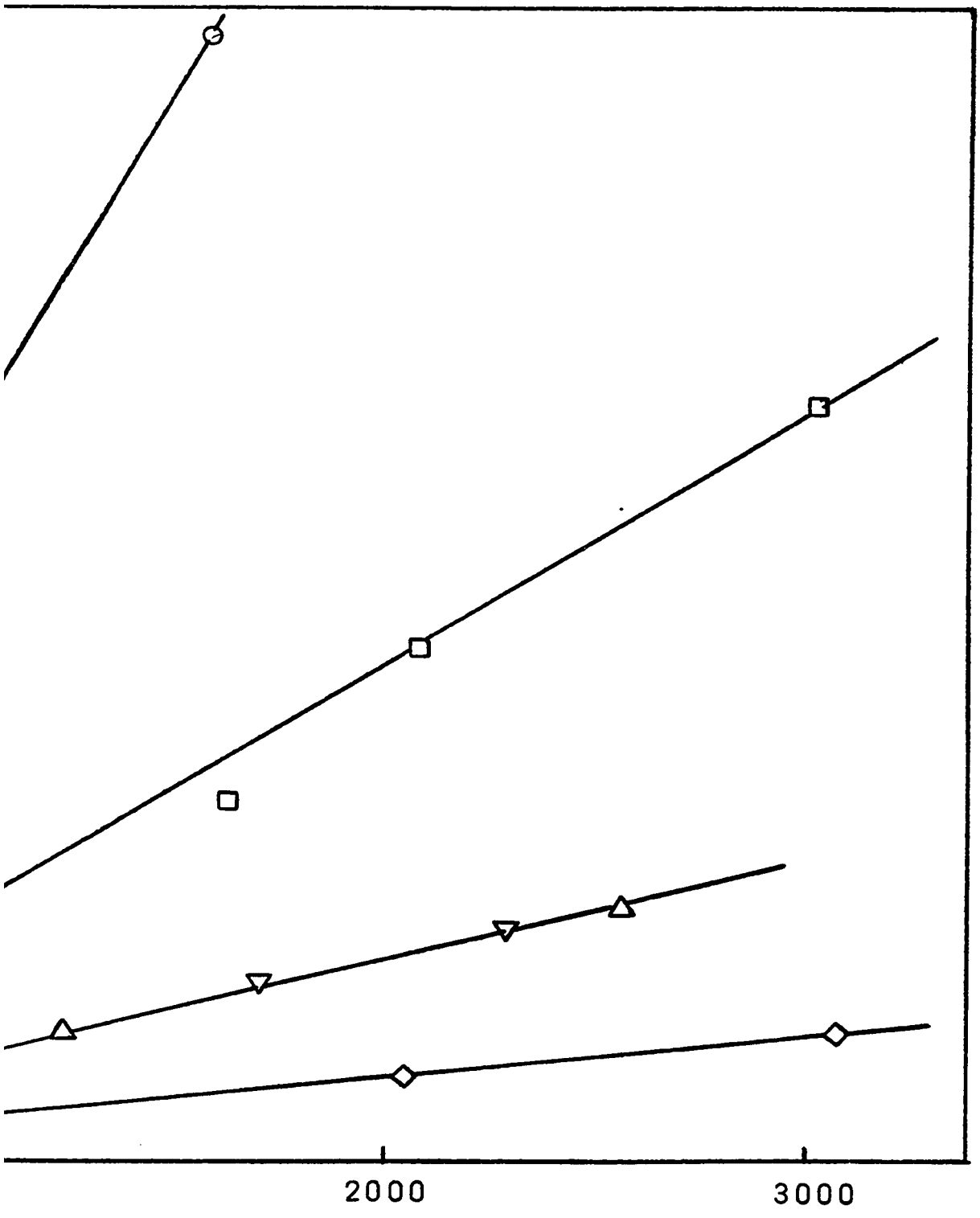
2000
3000
Time (seconds)

FIGURE (III - 42)

Arrhenius Plot of Rate Data for First Order Disappearance of

Isobutyl Chloride in Figure (III-41)

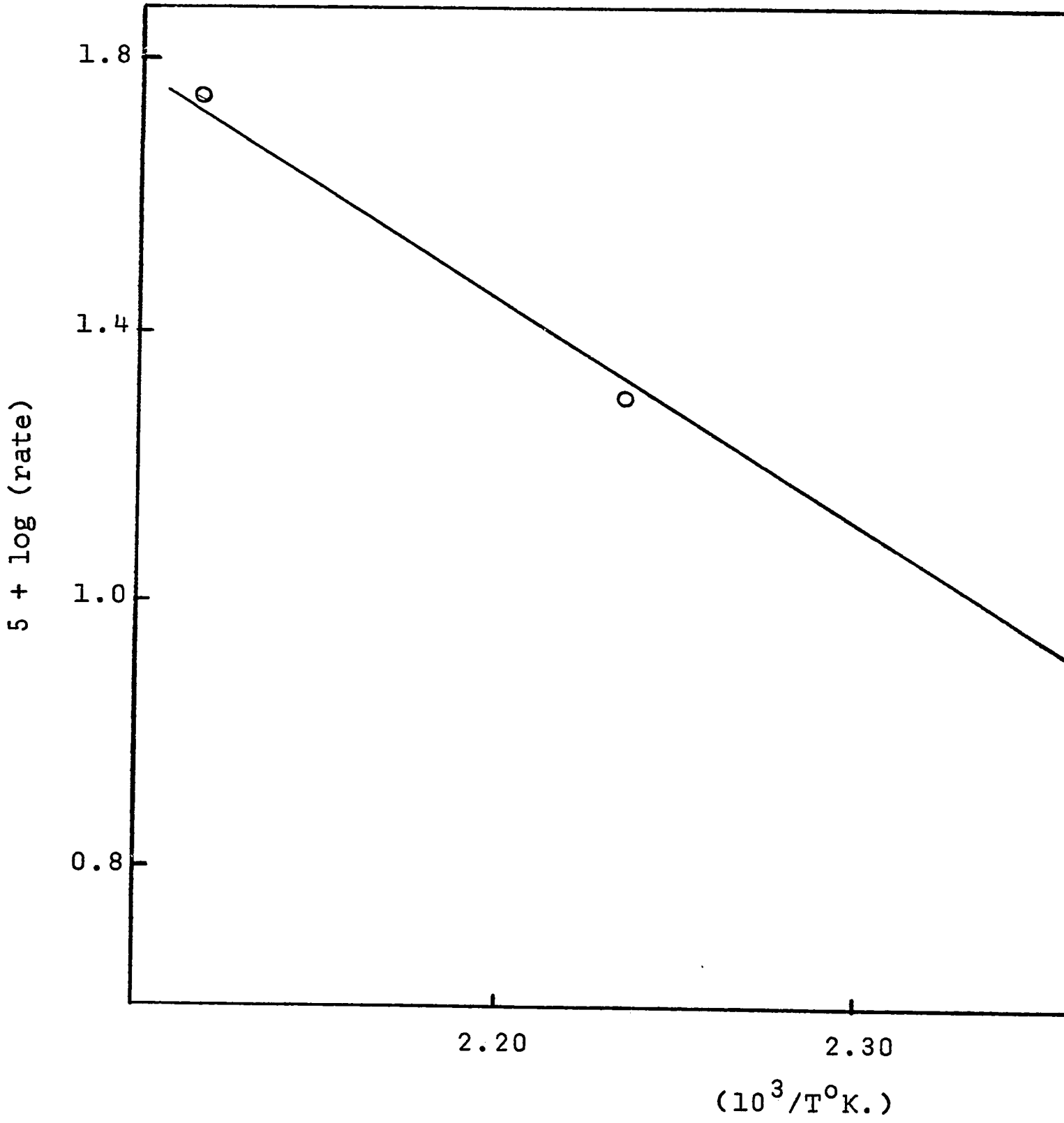
1.8
1.4
1.0
0.8
5 + log (rate)
2.20
2.30
(10³/T°K.)

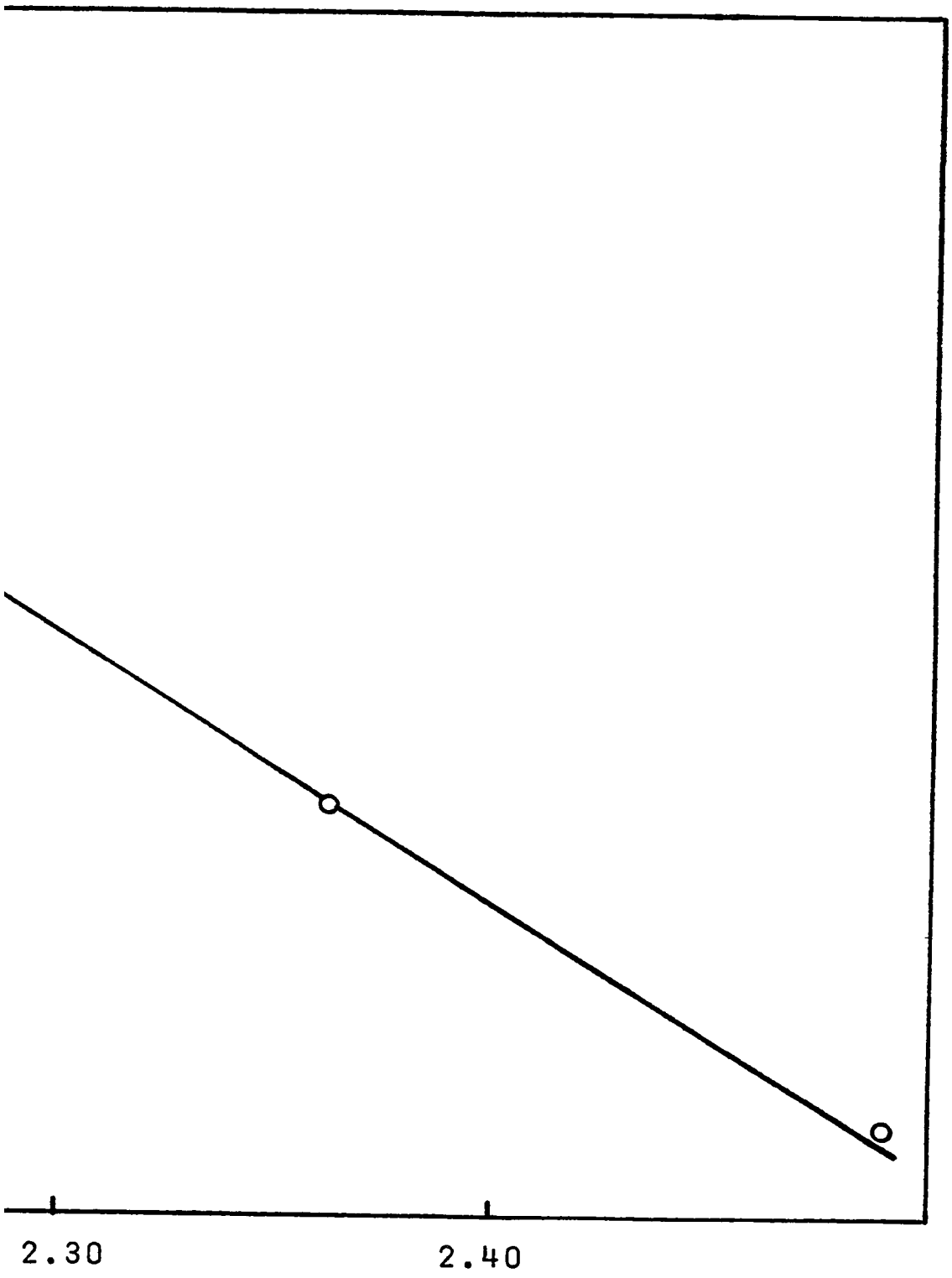
2.30
2.40
T°K.)

FIGURE (III - 43)

Comparison of Half and First Order Plots of Initial High Temperature ($218^{o}C$) Reactions of 10^{-2} torr of Isobutyl Chloride

□ - First Dose; Half Order Plot

○ - First Dose; First Order Plot

△ - Later Dose; Half Order Plot

◇ - Later Dose; First Order Plot

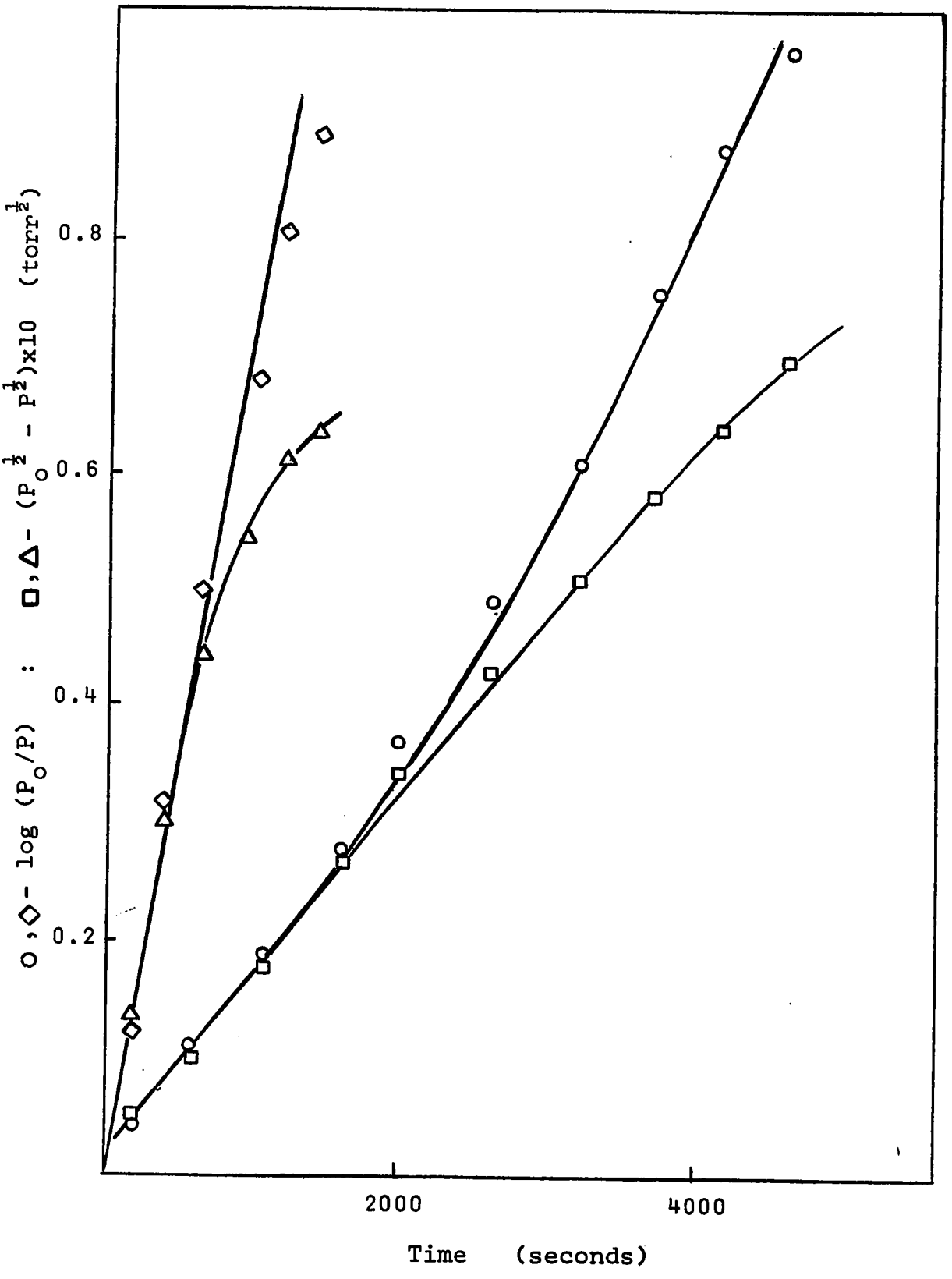
0.8
0.6
0.4
0.2
2000
4000
Time (seconds)
O ,◇- log (P$_o$/P) : □,Δ- (P$_o^{\frac{1}{2}}$ - P$^{\frac{1}{2}}$)x10 (torr$^{\frac{1}{2}}$)

and 230°C. The first order disappearance of neopentyl chloride is illustrated in figure (III-44) for $P_o = 10^{-2}$ torr and in figure (III-46) for $P_o = 2.5 \times 10^{-2}$ torr. Arrhenius plots for these two sets of data are shown in figures (III-45) and (III-47) respectively. The apparent activation energy calculated from these Arrhenius plots is 13.9±0.2 kcal./mole for $P_o = 10^{-2}$ torr and 15.0±0.5 kcal./mole for $P_o = 2.5 \times 10^{-2}$ torr.

The organic product resulting from the dehydrochlorination of neopentyl chloride was identified as 2-methylbutene-2. Because the mass spectra of 2-methylbutene-2 and 2-methylbutene-1 are so similar, it was uncertain whether traces of the latter were also present. Neither neopentane nor hydrogen were detected as products.

Side reactions were not readily induced by increased temperature as in the case of isopropyl chloride. However, use of increased pressures did produce side reactions and resulted in product mixtures which were not readily resolvable by mass spectrometry.

Reaction of 10^{-2} torr of neopentyl chloride with a virgin film at 200°C occurred without apparent adsorption of reactant. After rapid, initial product formation, the reaction proceeded extremely slowly, but with increasing velocity as it progressed. The course of this reaction is illustrated in figure (III-48) and is compared to the course of a typical catalytic reaction on the same surface after extensive chloriding of the film. The prime product of the slow part of the reaction

FIGURE (III - 44)

Disappearance of Neopentyl Chloride

Plotted as a First Order Reaction

for $P_o = 10^{-2}$ torr

● - 160°C

▽ - 170°C

◇ - 183.5°C

□, ∠ - 199°C

○ - 210°C

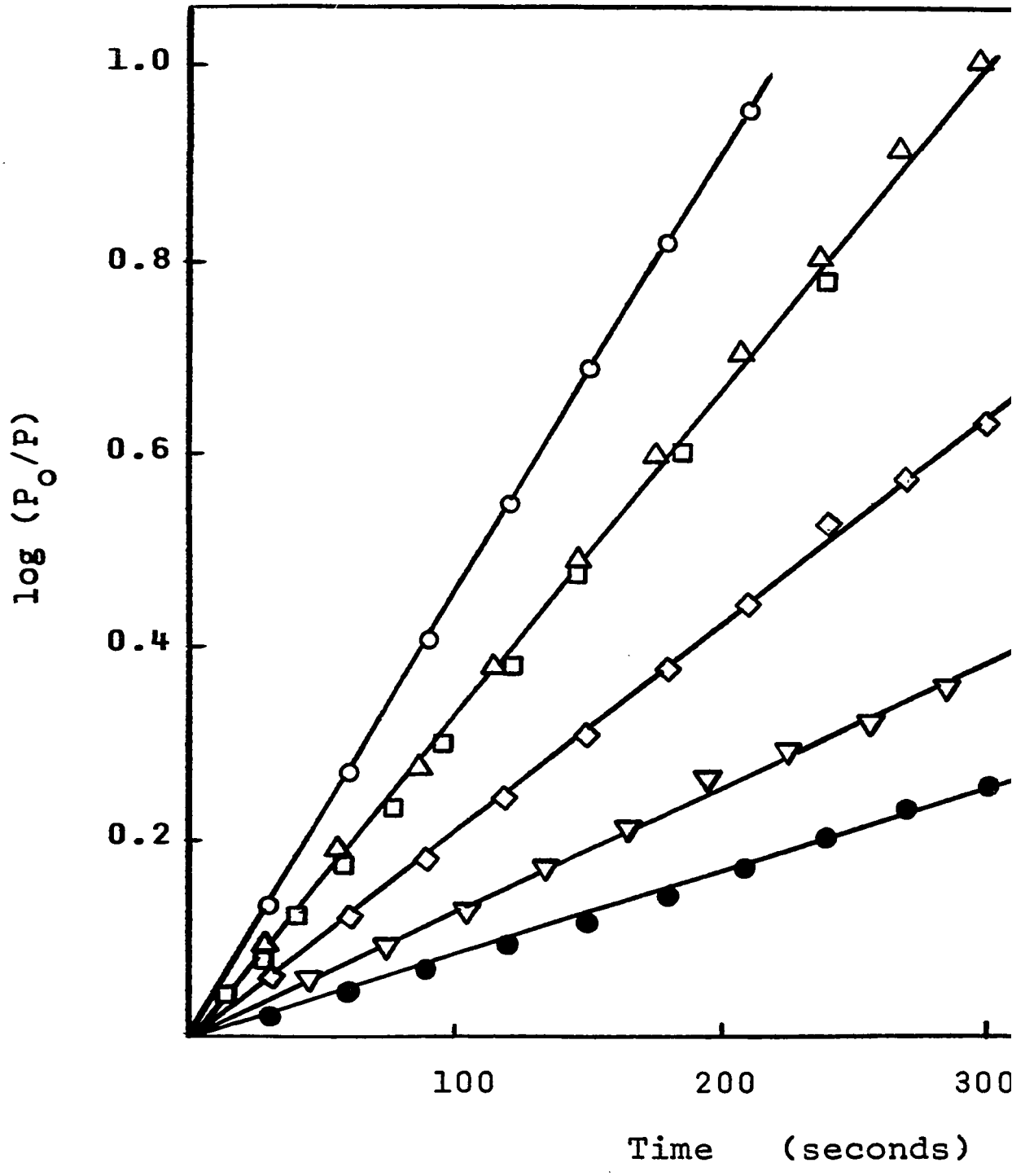
1.0
0.8
0.6
0.4
0.2
log (P_o/P)
100
200
300
Time (seconds)

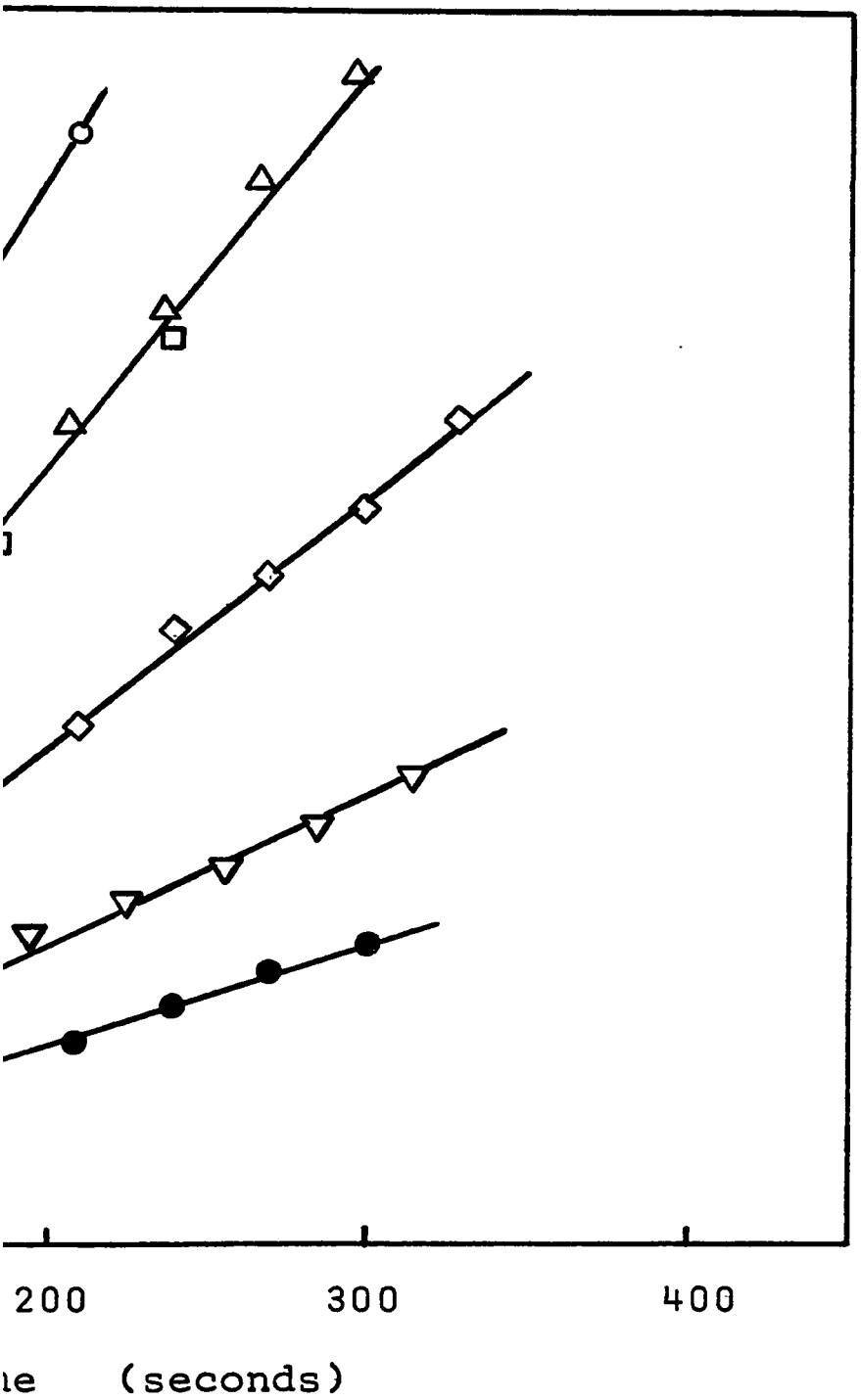
200
300
400
ıe (seconds)

FIGURE (III - 45)

Arrhenius Plot of Rate Data for First Order Disappearance of Neopentyl Chloride in Figure (III-44)

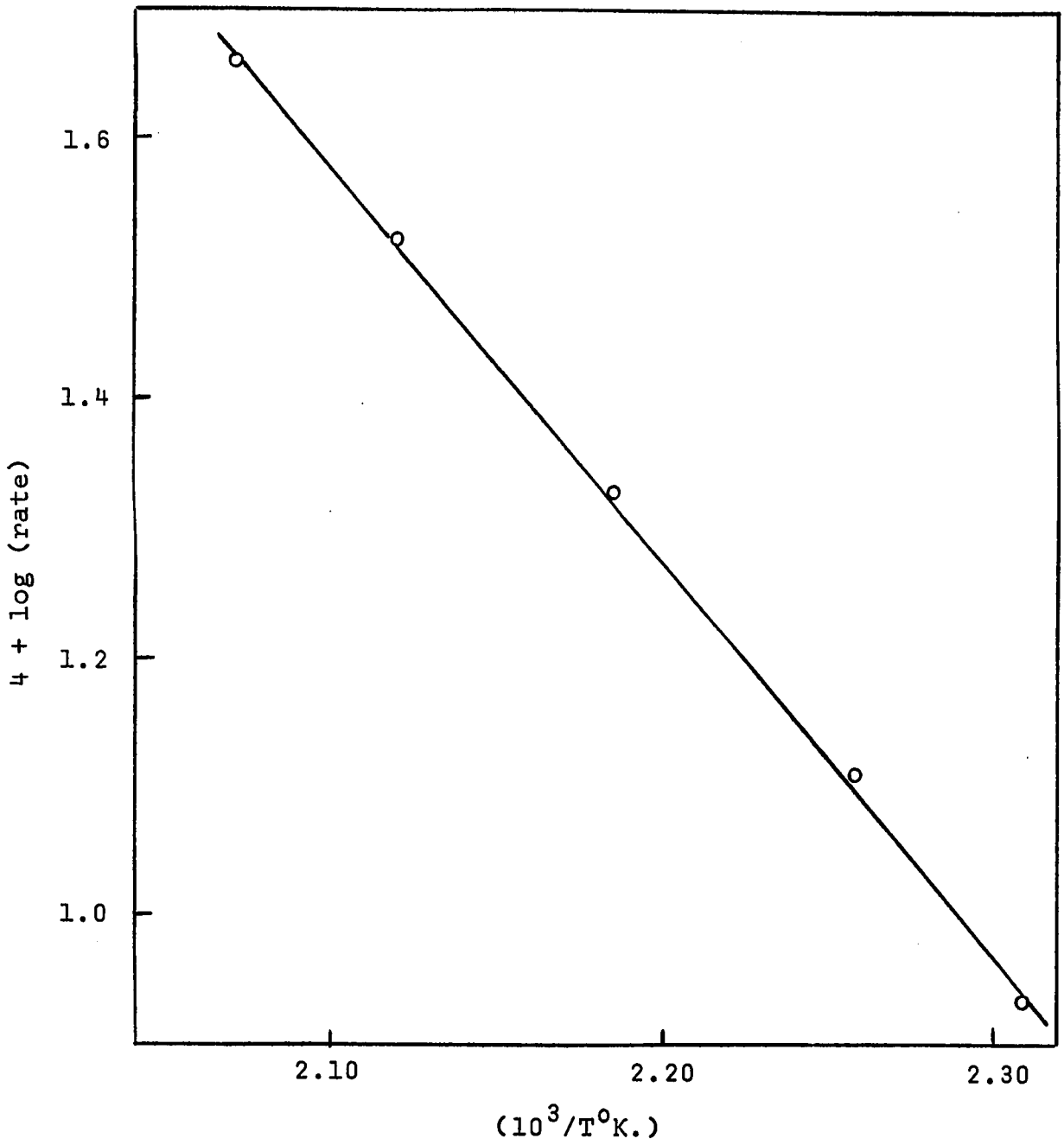
1.6
1.4
1.2
1.0
4 + log (rate)
2.10
2.20
2.30
(10³/T°K.)

FIGURE (III - 46)

Disappearance of Neopentyl Chloride

Plotted as a First Order Reaction

for $P_o = 2.5 \times 10^{-2}$ torr

● - 185°C

▽ - 200°C

◇ , △ - 215°C

◑ , □ - 230°C

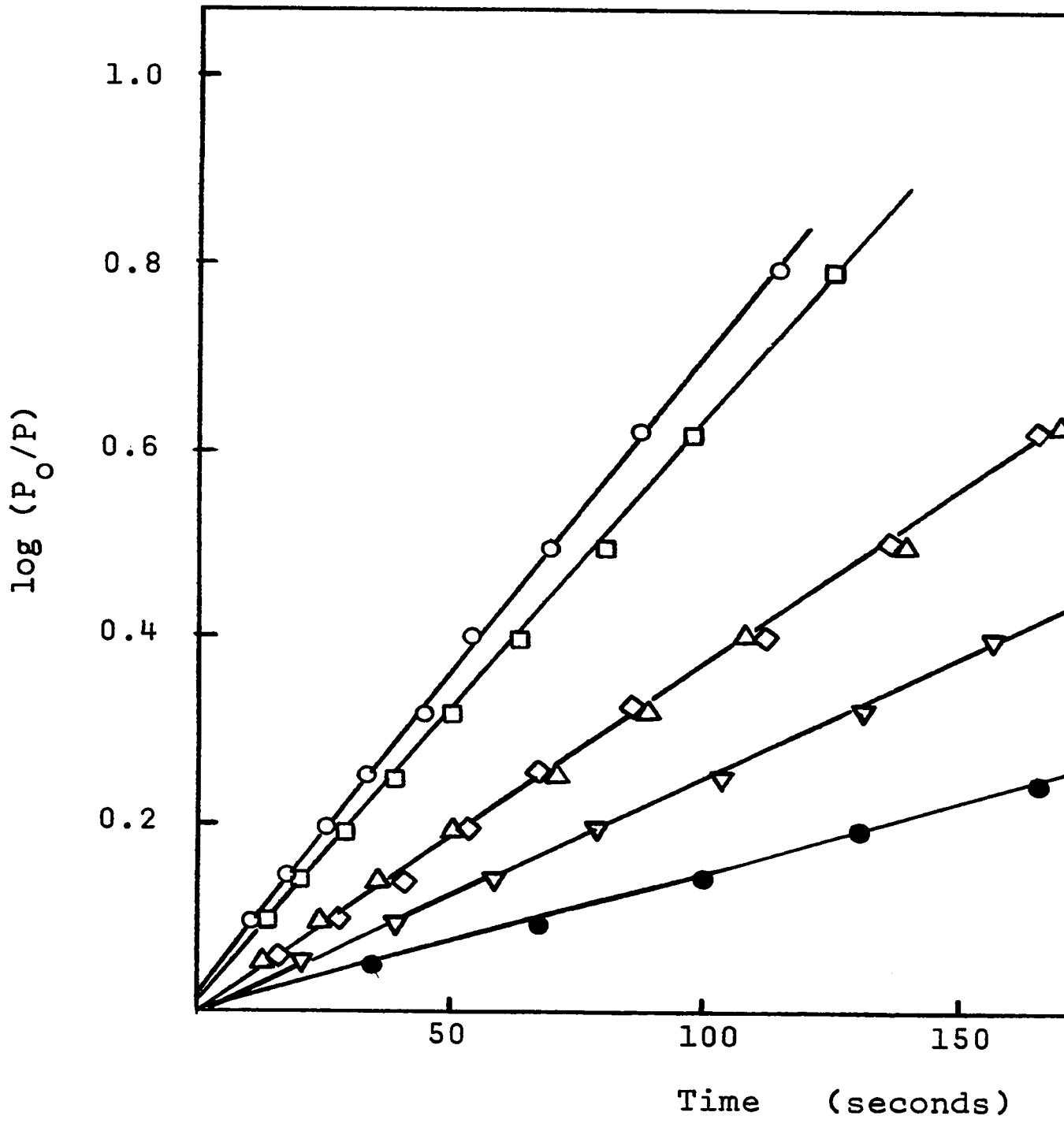
1.0
0.8
0.6
0.4
0.2
log (P$_o$/P)
50
100
150
Time (seconds)

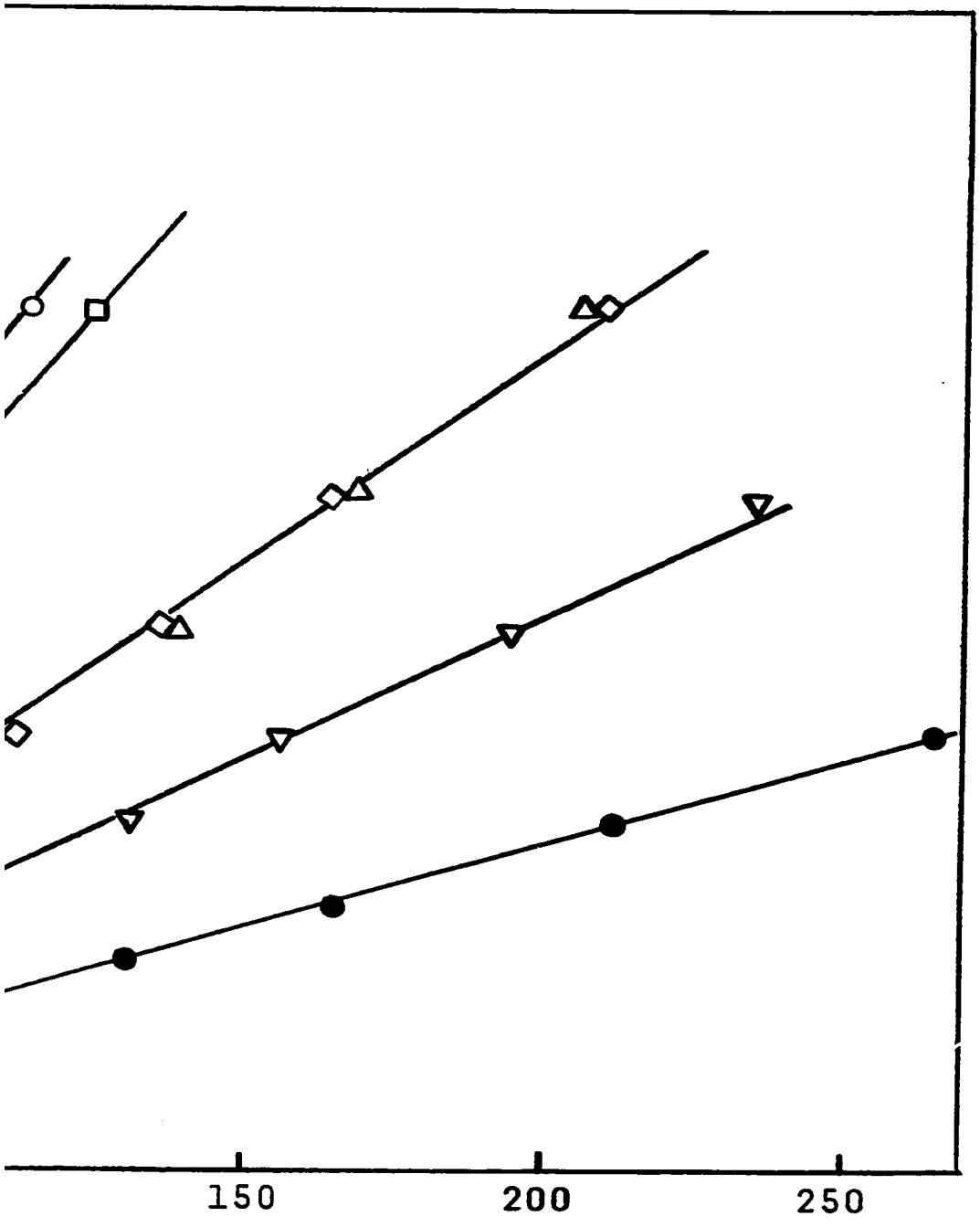
150
200
250
(seconds)

FIGURE (III - 47)

Arrhenius Plot of Rate Data for First Order Disappearance of

Neopentyl Chloride in Figure (III-46)

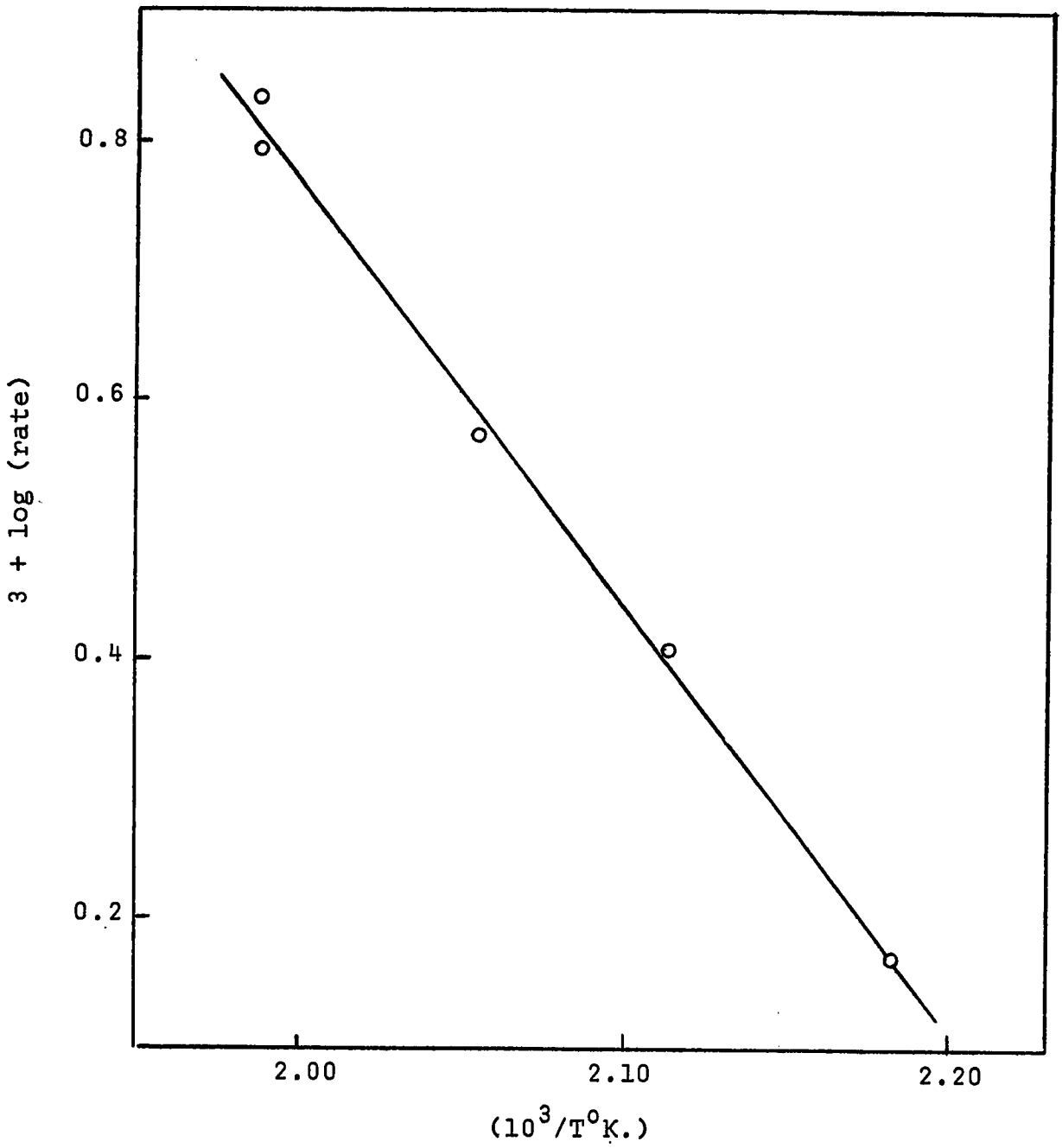
0.8
0.6
0.4
0.2
3 + log (rate)
2.00
2.10
2.20
(10³/T°K.)

FIGURE (III - 48)

Comparison of Progress of Reactions of

Neopentyl Chloride at 200°C and $P_o = 10^{-2}$ torr

∠ - Noncatalytic reaction on virgin film

O - Catalytic reaction on chlorided film

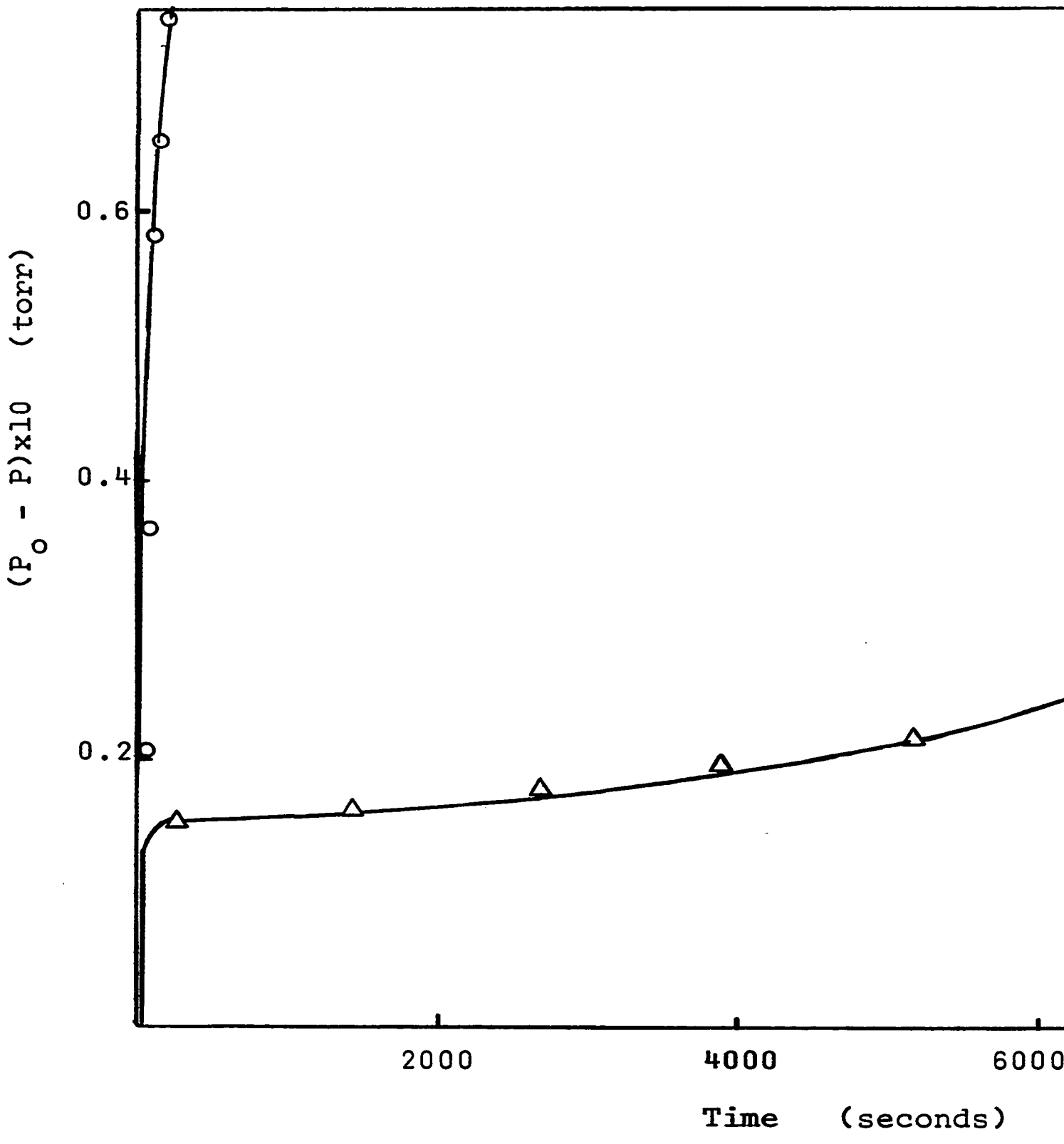
0.6
0.4
0.2
$(P_o - P)x10$ (torr)
2000
4000
6000
Time (seconds)

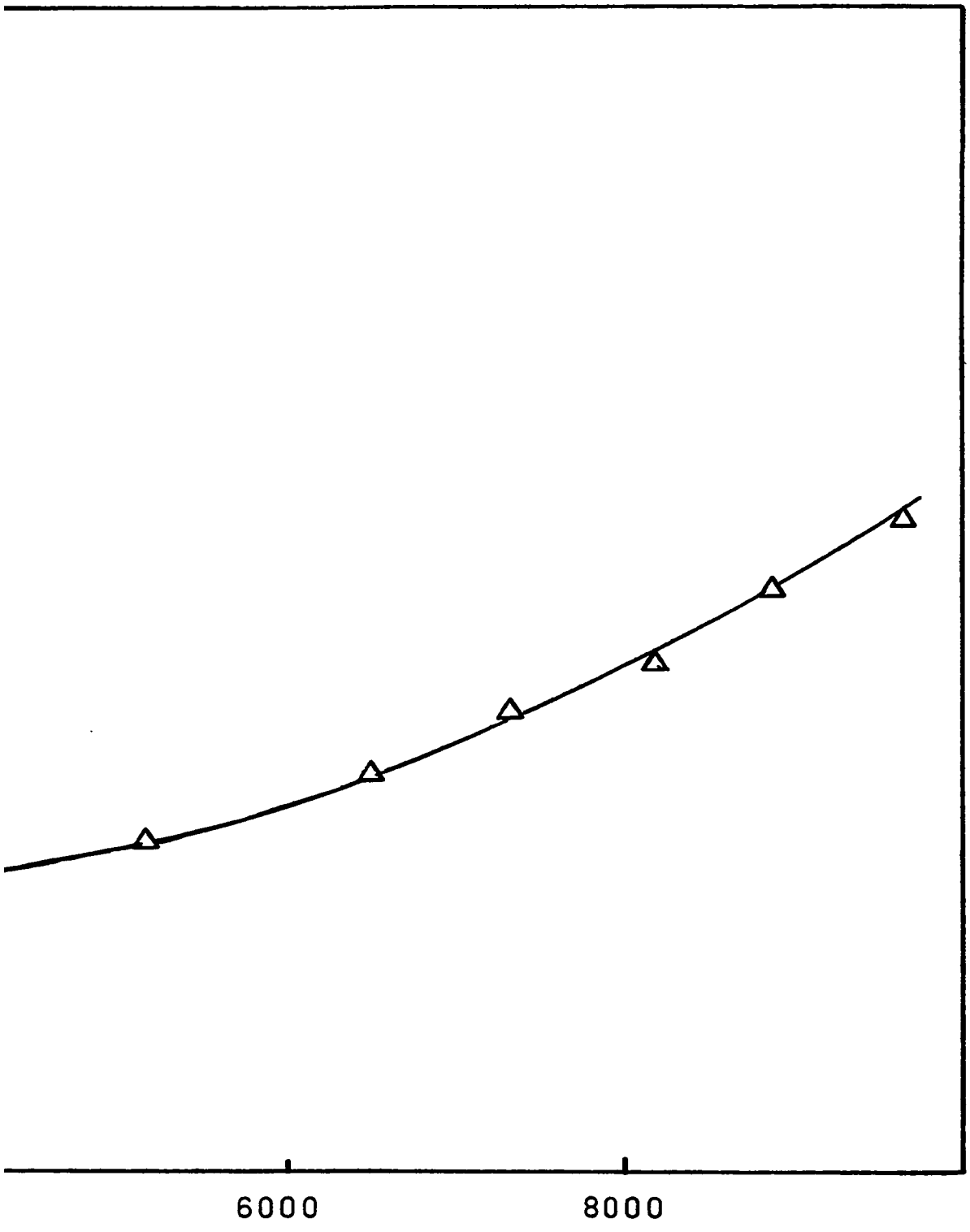
6000
8000
(seconds)

was 2-methylbutene-2, that of the initial, rapid reaction was a mixture, principally neopentane, and minor amounts of isobutylene

d) Dichloro- Series

i) 1,2-Dichloropropane

The reaction of 1,2-dichloropropane at elevated temperatures, with previously reacted titanium films, occurred smoothly through many monolayer equivalents of reactant and with reproducible rates. Only propylene was observed as a product gas. The reactant disappeared with half order kinetics and the reaction occurred at convenient rates for kinetic investigation between 165°C and 205°C.

Figure (III-49) illustrates the half order dependence of the reaction for 10^{-2} torr reactant doses. An Arrhenius plot of the kinetic data generated by figure (III-49) is illustrated in figure (III-50). Calculation of the line slope of this plot results in an apparent activation energy of 24.1±1.4 kcal./mole.

ii) 1,3-Dichloropropane

The reaction of 1,3-dichloropropane at elevated temperatures with previously reacted titanium films, occurred in the same manner as that of 1,2-dichloropropane.

Mixtures of cyclopropane and propylene were observed as reaction products. The principal product was cyclopropane. The product ratio did not vary with temperature or pressures between 10^{-2} torr and 10^{-1} torr, but did vary slightly with extent of film reaction. The more extensively reacted the film,

FIGURE (III - 49)

Disappearance of 1,2-Dichloropropane

Plotted as a Half Order Reaction

for $P_o = 10^{-2}$ torr

● ,▽ - 165°C

◇ - 179.5°C

△ - 184.5°C

□ - 193.5°C

○ - 204°C

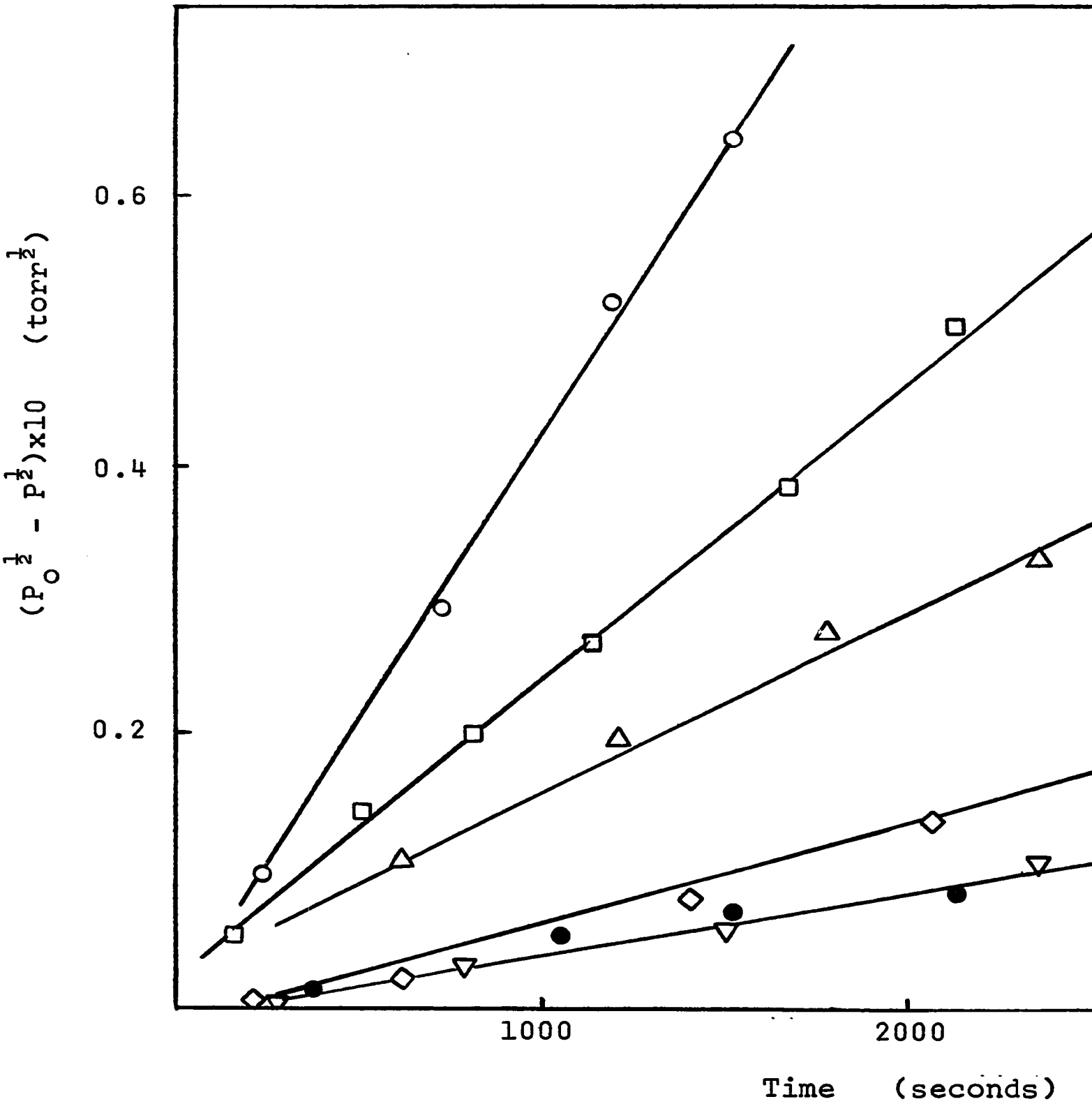
0.6
0.4
0.2
$(P_o^{\frac{1}{2}} - P^{\frac{1}{2}})x10$ (torr$^{\frac{1}{2}}$)
1000
2000
Time (seconds)

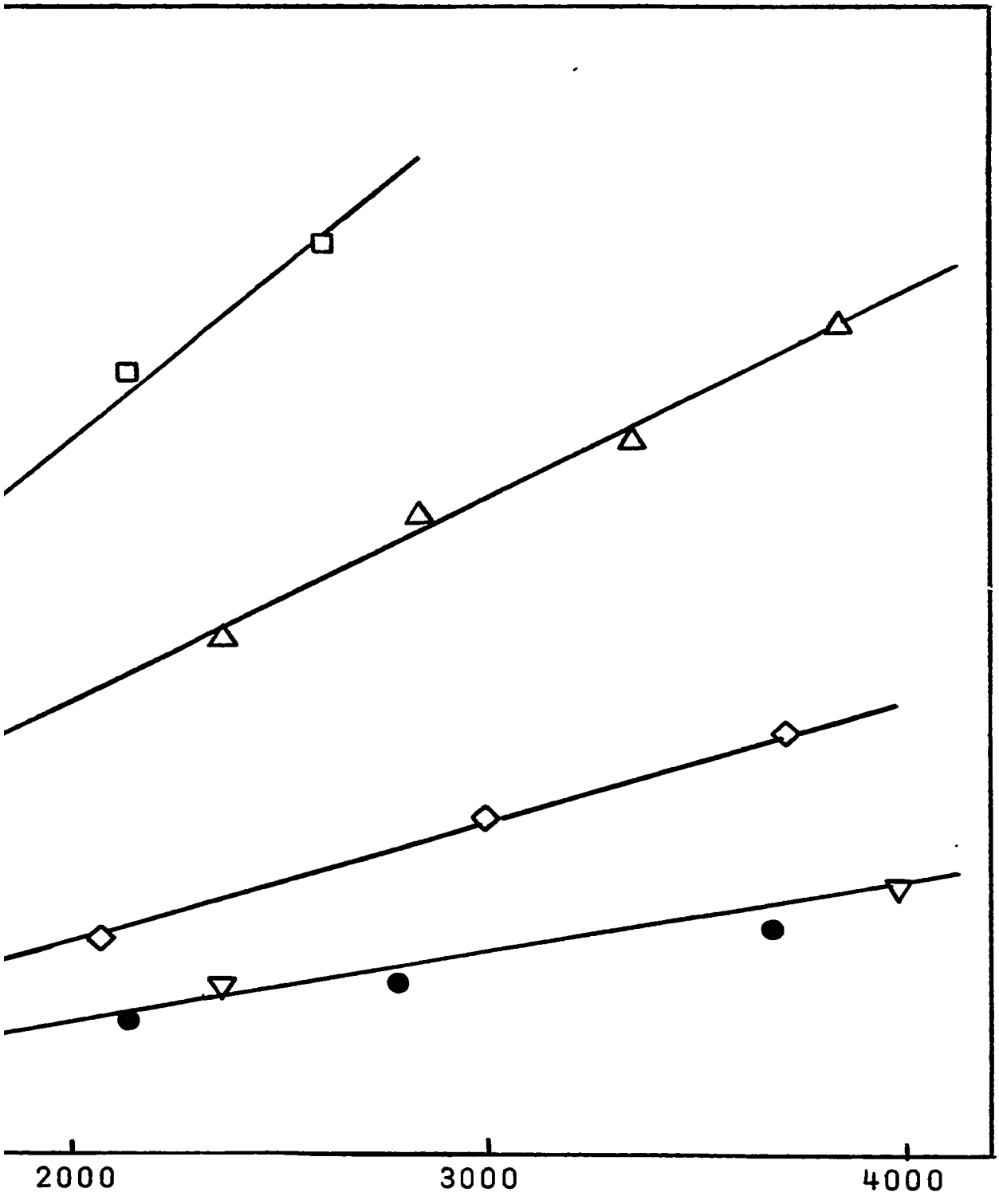
2000
3000
4000
(seconds)

FIGURE (III - 50)

Arrhenius Plot of Rate Data for Half Order Disappearance of 1,2-Dichloropropane in Figure (III-49)

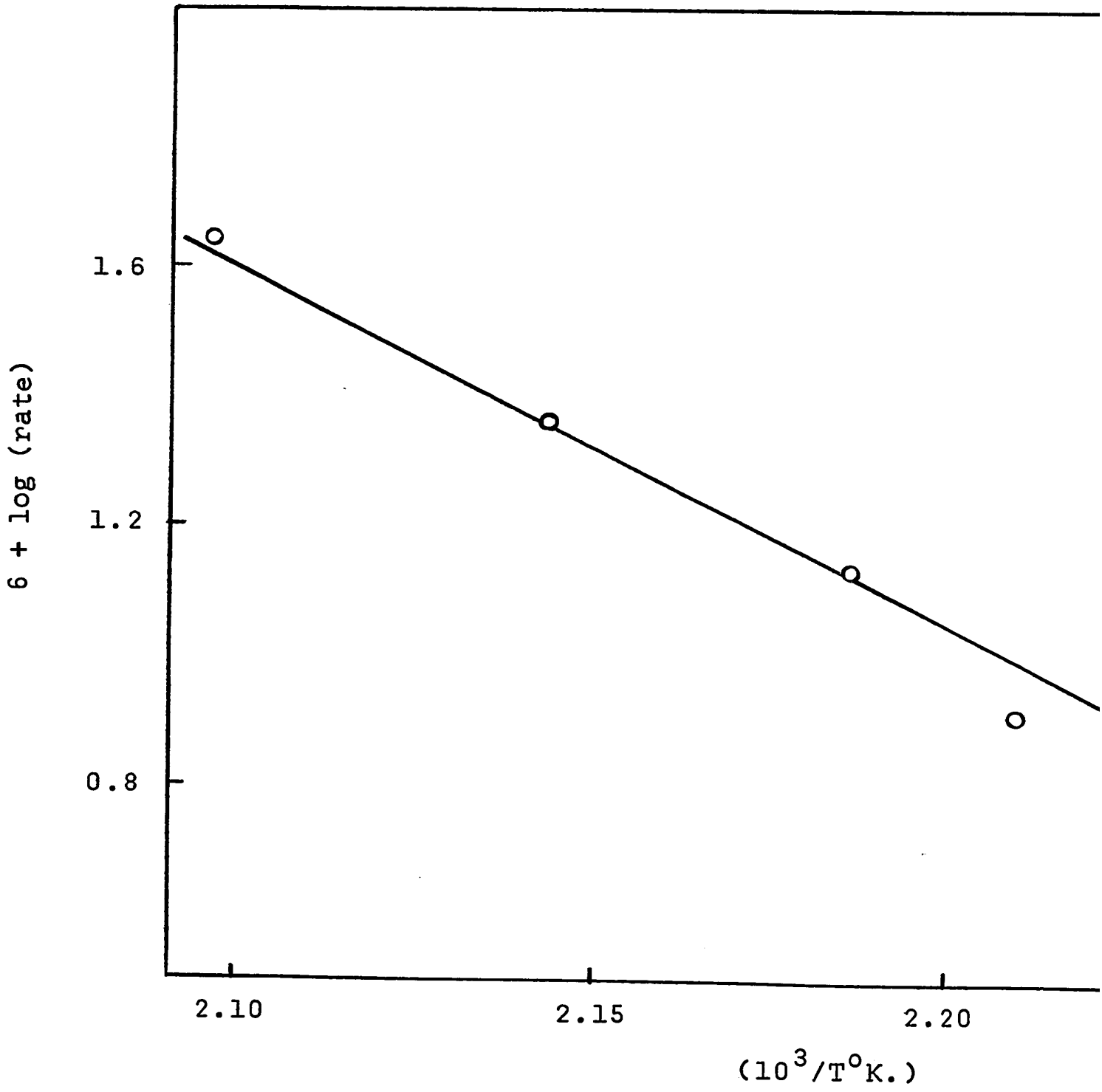
6 + log (rate)
1.6
1.2
0.8
2.10
2.15
2.20
(10³/T°K.)

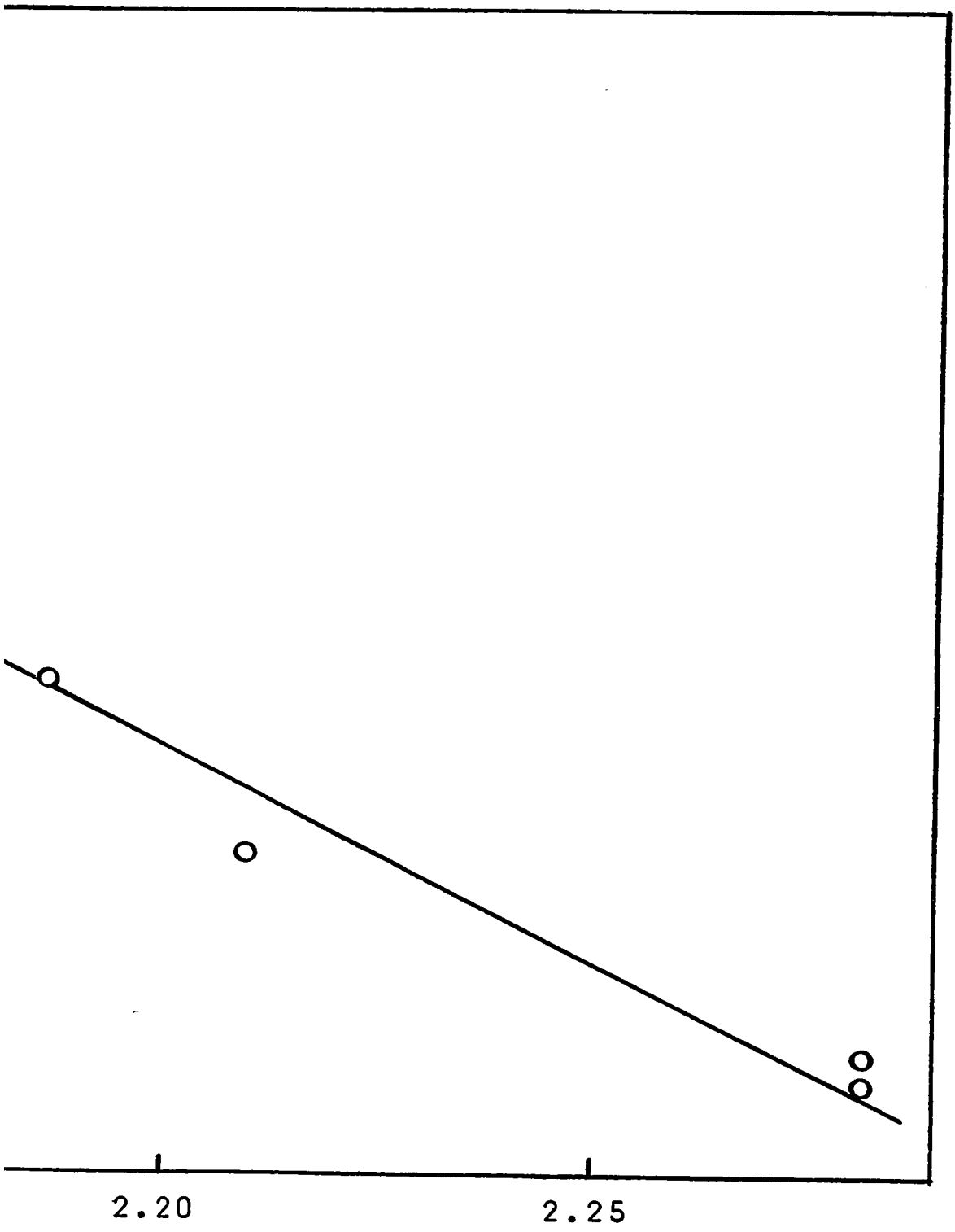
2.20
2.25
/T°K.)

the more enhanced became the production of cyclopropane. A newer film produced as much as 20 mole percent propylene. This value decreased to 10 mole percent as the extent to which the film was chlorided progressed.

The reactant disappeared with half order kinetics and the reaction of 10^{-2} torr doses occurred at convenient rates for kinetic investigation between 200°C and 230°C. The half order dependence of the reaction is illustrated in figure (III-51). An Arrhenius plot of the kinetic data generated by figure (III-51) is shown in figure (III-52). Calculation of the line slope of this plot results in an apparent activation energy of 27.7±1.0 kcal./mole.

iii) 1,3-Dichloro-2,2-dimethylpropane

The reaction of this compound was not pursued in any detail. Gaseous hydrogen chloride was observed during the reaction of this material and it was determined that the hydrogen chloride appeared with first order kinetics. This is illustrated in figure (III-53). Appearance of two moles of hydrogen chloride per mole of reactant was never observed, although the appearance of greater than one mole was observed. Mixtures of C_5H_{10} and C_5H_8 compounds were detected, but no attempt was made to resolve the product mass spectra. At lower reaction temperatures, more C_5H_8 and hydrogen chloride were observed than at higher temperatures. At higher temperatures, the C_5H_{10} product was more extensively produced.

FIGURE (III - 51)

Disappearance of 1,3-Dichloropropane

Plotted as a Half Order Reaction

for $P_o = 10^{-2}$ torr

●, ▽ - 202°C

◇ - 212.5°C

□ - 222.5°C

○, △ - 231.5°C

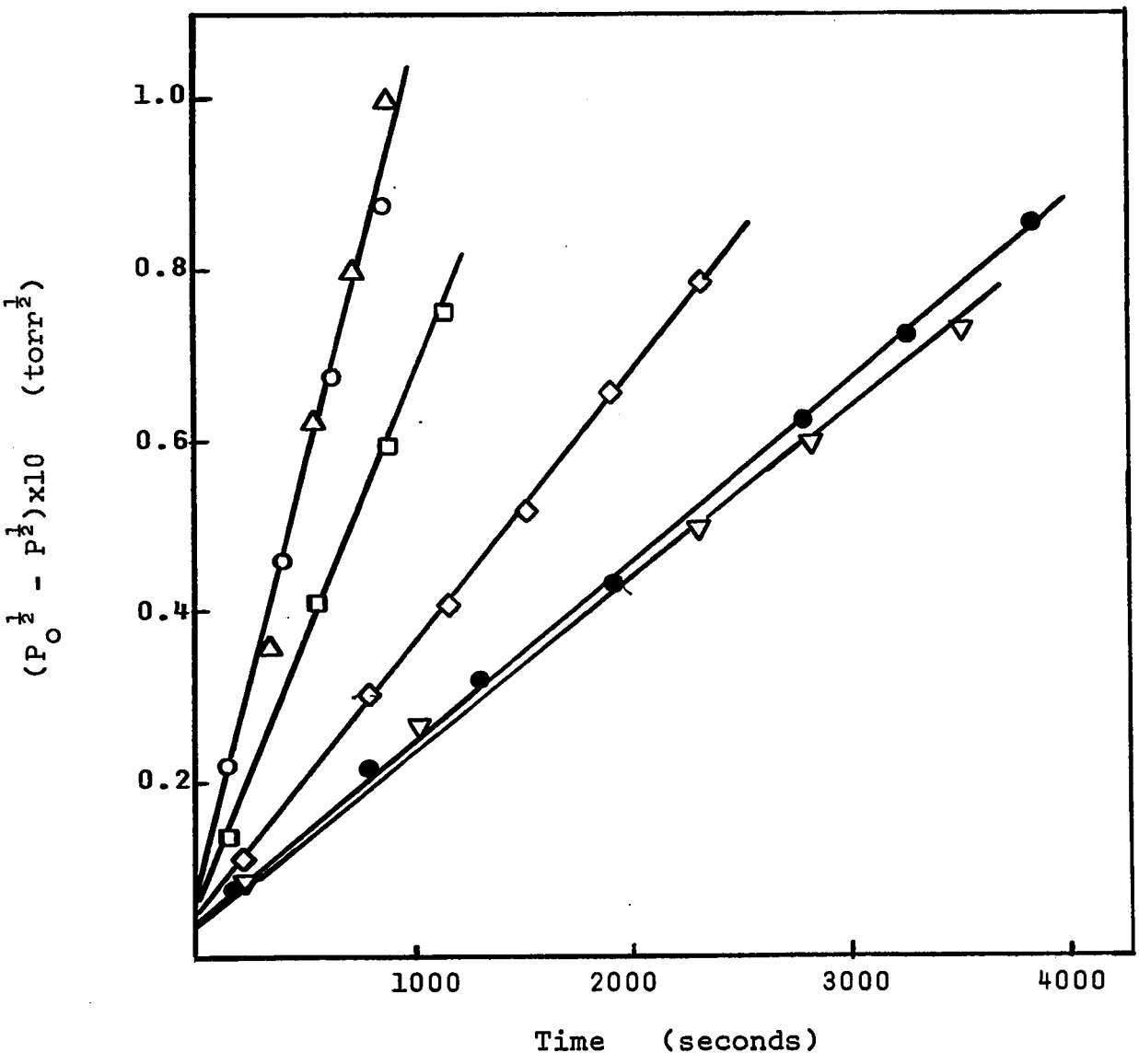
1.0
0.8
0.6
0.4
0.2
1000
2000
3000
4000
Time (seconds)
$(P_o^{\frac{1}{2}} - P^{\frac{1}{2}})x10$ (torr$^{\frac{1}{2}}$)

FIGURE (III - 52)

Arrhenius Plot of Rate Data for Half Order Disappearance of

1,3-Dichloropropane in Figure (III-51)

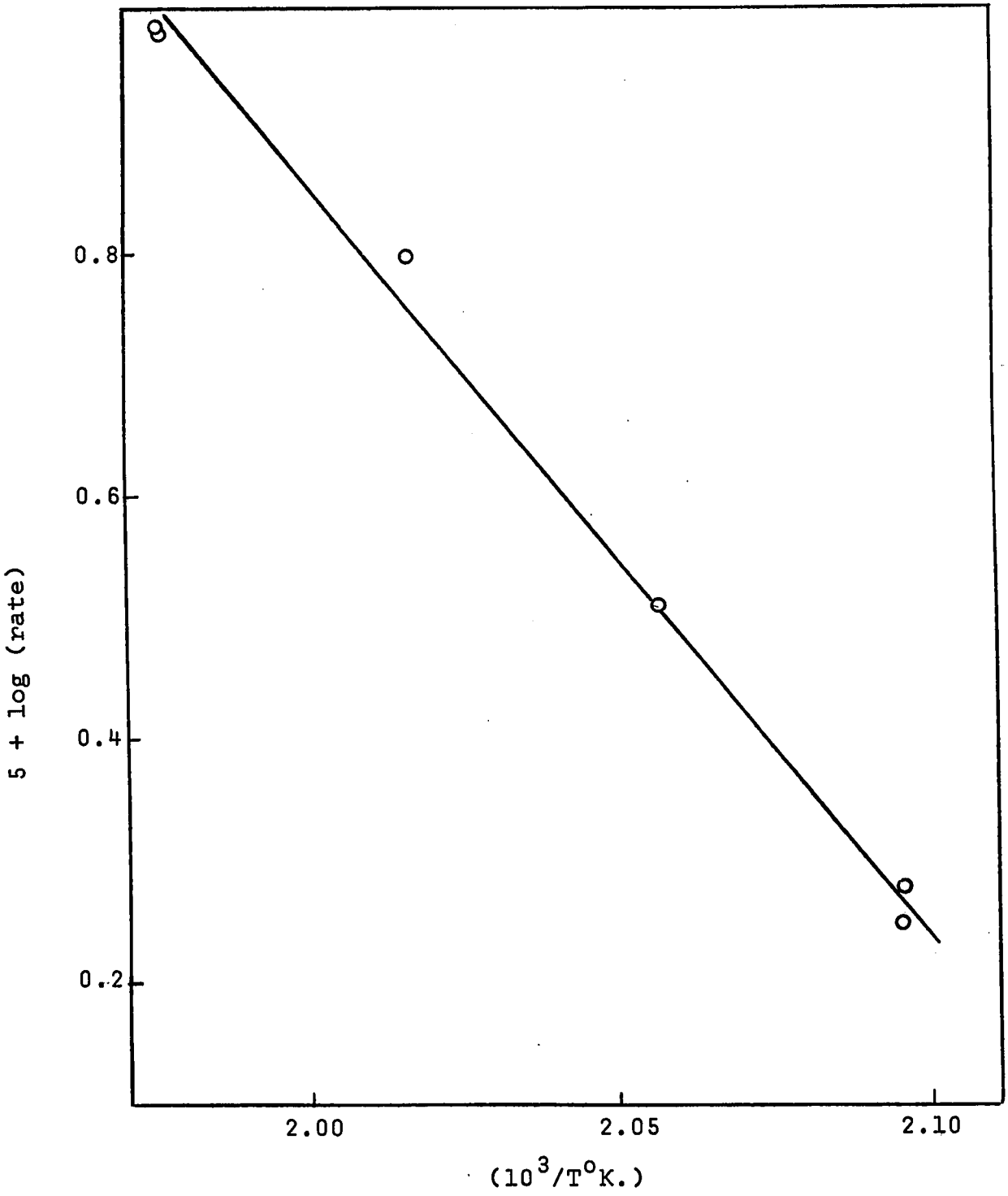
0.8
0.6
0.4
0.2
5 + log (rate)
2.00
2.05
2.10
(10³/T°K.)

FIGURE (III - 53)

Appearance of Hydrogen Chloride during Disappearance

of 10^{-2} torr 1,3-dichloro-2,2-dimethylpropane at $243^{o}C$

Plotted as a First Order Reaction

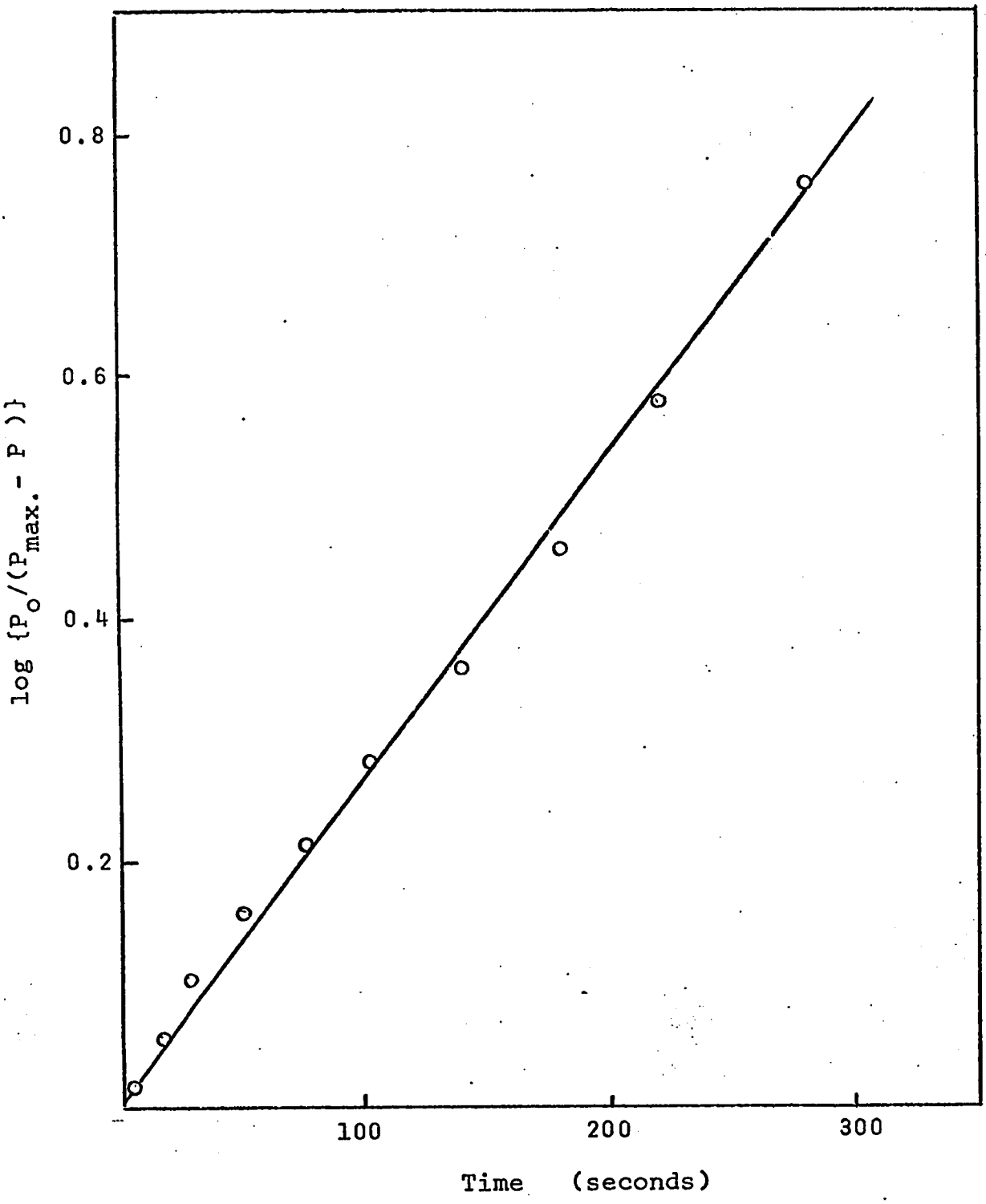
0.8
0.6
0.4
0.2
log {P_o/(P_max. - P)}
100
200
300
Time (seconds)

e) Miscellaneous Series

i) Hydrogen Chloride

The reaction of hydrogen chloride was not pursued in detail. It was determined that hydrogen chloride did not react readily with previously reacted titanium films, at elevated temperatures. It was, in fact, markedly less reactive than any of the alkyl halides studied.

At 235°C, 10^{-2} torr reacted slowly with first order kinetics giving hydrogen as a product. The kinetics of this reaction are illustrated in figure (III-54). Less than 0.5 moles of hydrogen per mole of hydrogen chloride reacted, was detected.

ii) Methyl Chloride

The reaction of methyl chloride with a previously reacted titanium film gave approximately 0.75 moles of methane per mole of reactant at 200°C and $P_o = 5 \times 10^{-3}$ torr. Methyl chloride was considerably less reactive than any of the other alkyl halides that have been studied.

The reaction of methyl chloride caused film deactivation for subsequent reactant doses. No attempt was made to obtain meaningful kinetic data for determination of activation energies. The reaction of the 5×10^{-3} torr dose of methyl chloride with the titanium film occurred with zero order kinetics. Figure (III-55) illustrates the progress of this reaction.

FIGURE (III - 54)

Disappearance of Hydrogen Chloride at 235°C Plotted as a First Order Reaction

$P_o = 10^{-2}$ torr

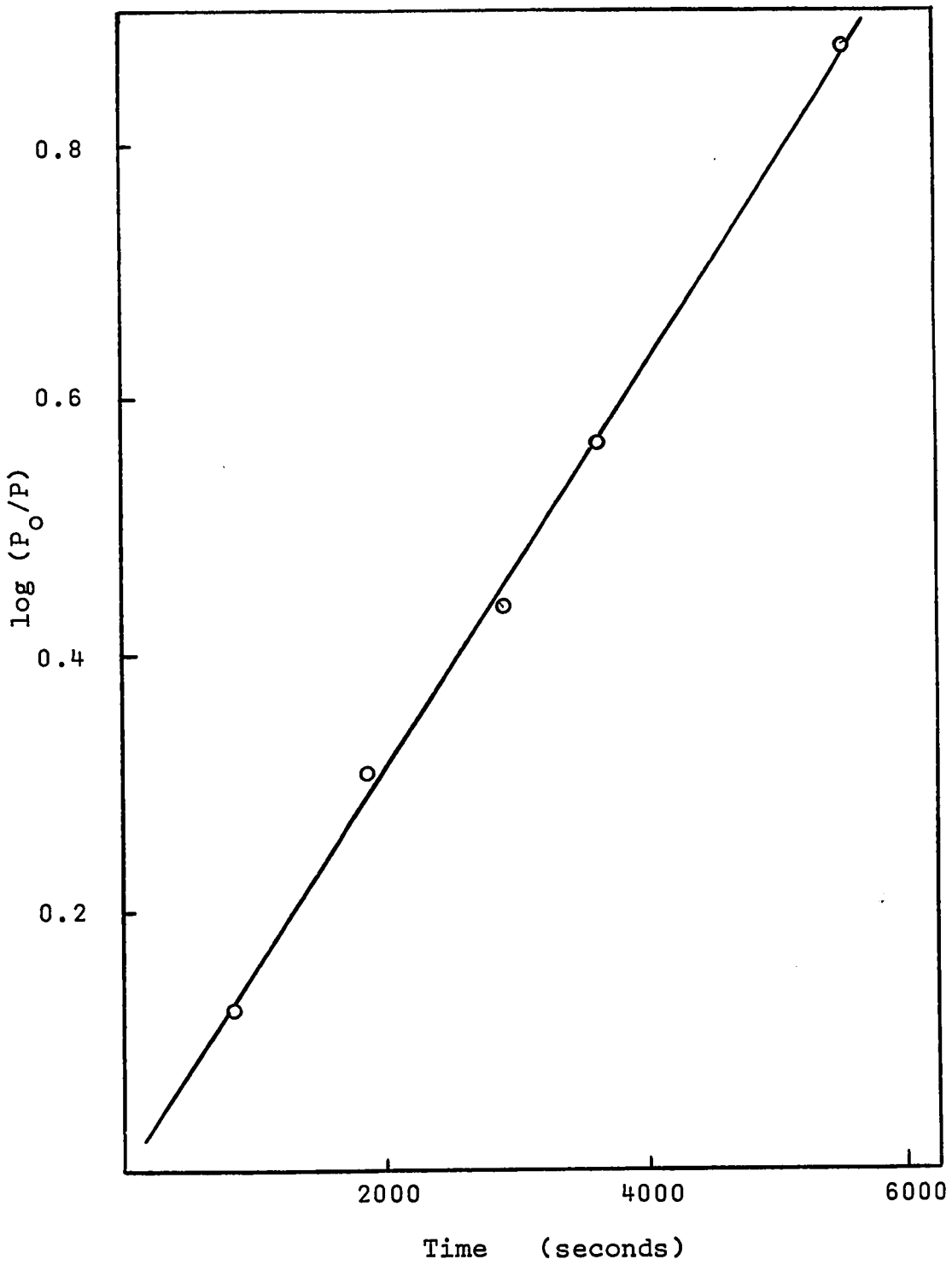
0.8
0.6
0.4
0.2
log (P_o/P)
2000
4000
6000
Time (seconds)

FIGURE (III - 55)

Disappearance of Methyl Chloride at 200°C Plotted as

a Zero Order Reaction

$P_o = 5 \times 10^{-3}$ torr

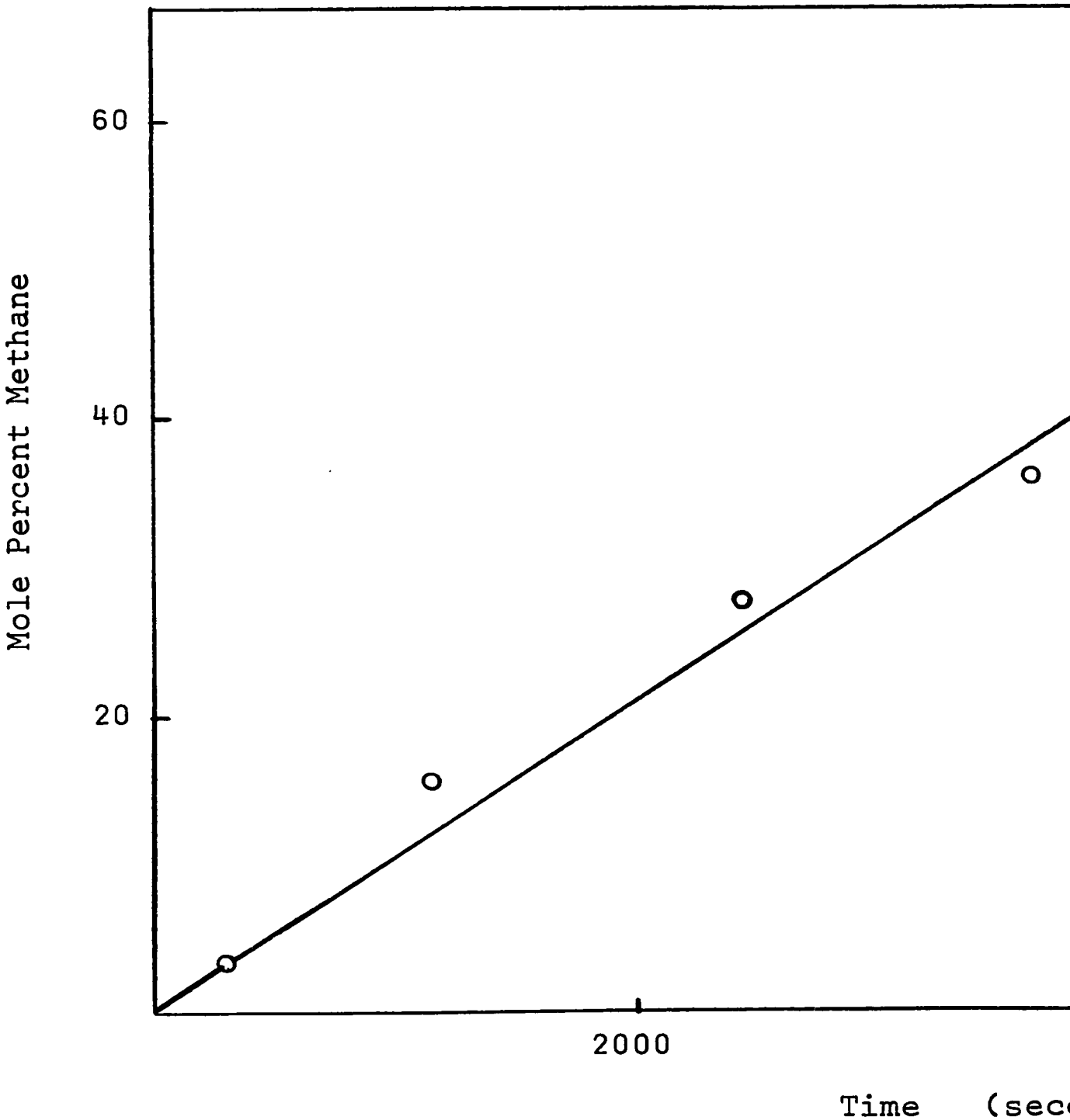
60
40
20
Mole Percent Methane
2000
Time (sec

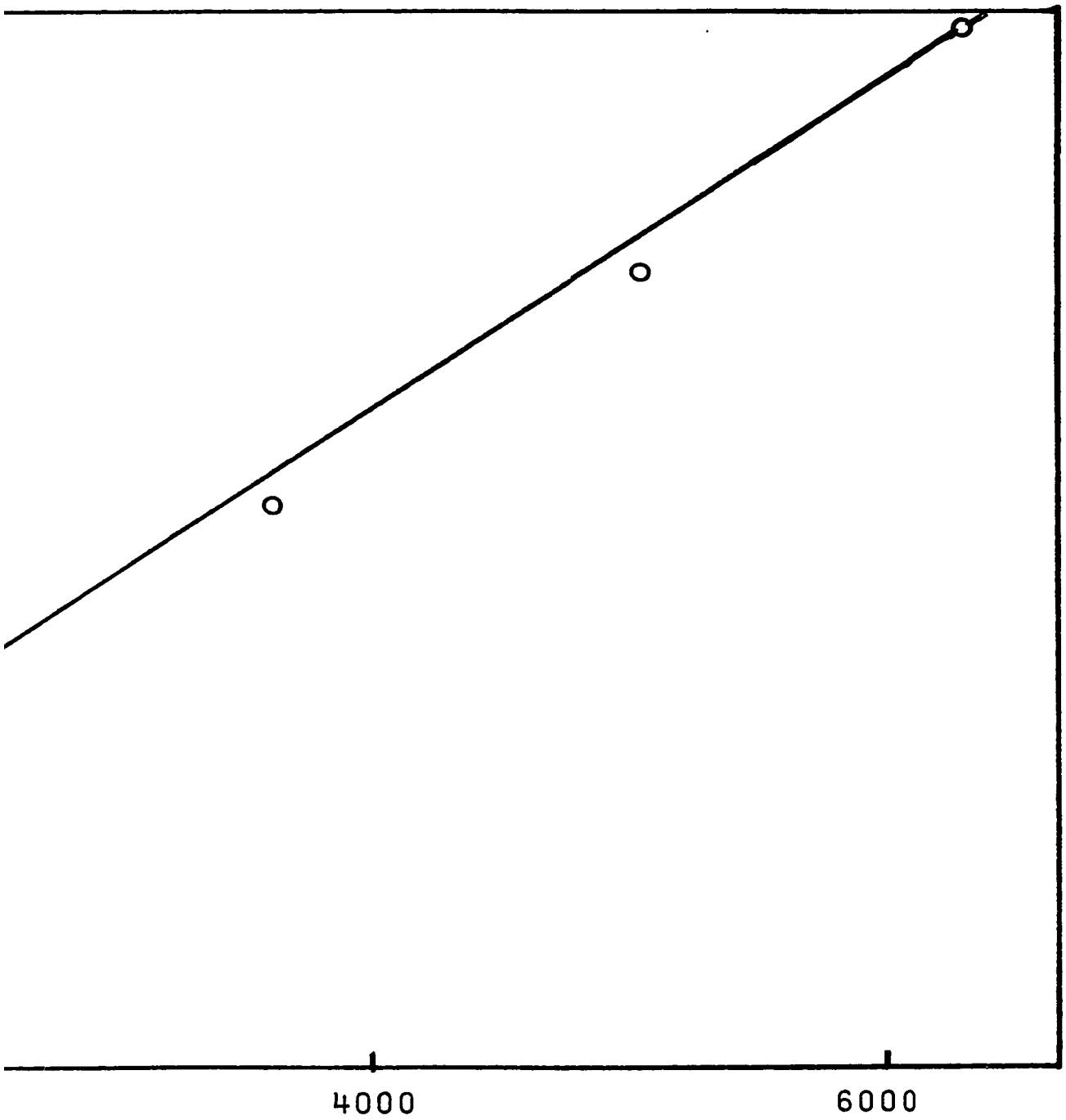
4000
6000
Time (seconds)

III - 5. Summary of Results

Two tables of data are presented as a summary of the experimental results.

The approximate, relative reactivities of the various reactants and whether they reacted catalytically or noncatalytically are summarized in table (III-8). The reaction order, the products and the apparent activation energies for all the reactions for which data are available, are presented in table (III-9). The experimental standard deviations of the activation energies are also included in this table.

TABLE (III - 8)*

Reactant	Relative Reactivity	Reaction Type
Hydrogen Chloride	1	Noncatalytic
Methyl Chloride	10	"
Ethyl Chloride	50	"
n-Propyl Chloride	50	"
n-Propyl Bromide	50	"
n-Propyl Iodide	50	"
1,2-Dichloropropane	50	"
1,3-Dichloropropane	50	"
n-Propyl Fluoride	10^8	"
Isopropyl Chloride	10^3	Catalytic
Isobutyl Chloride	150	"
t-Butyl Chloride	10^9	"
Neopentyl Chloride	500	"
1,3-Dichloro-2,2-dimethylpropane	500	---

* Figures for the more active reactants are based on calculated reaction rates assuming no change in activation energy. Comparison is based on time required for 90% completion of reaction.

TABLE (III - 9)

Reactant	Reaction Order	Apparent $E_a \pm \sigma$	Gaseous Products
Hydrogen Chloride	First	---	Hydrogen
Methyl Chloride	Zero ?	---	Methane
Ethyl Chloride	Half	23.5±1.5	Ethylene, Ethane
"	"	23.5±0.6	" "
"	"	21.4±0.4	" "
"	"	21.9±0.7	" "
n-Propyl Chloride	Half	23.4±0.9	Propylene, Propane
"	"	22.6±1.3	" "
n-Propyl Bromide	Half	25.8±0.4	Propylene, Propane
"	"	27.3±0.6	" "
"	"	27.9±0.2	" "
n-Propyl Iodide	Half	28.9±0.3	Propylene, Propane
"	"	29.8±0.3	" "
n-Propyl Fluoride	First	20.8±0.7	Propylene, Propane
"	"	20.4±0.6	" "

I - 9)

eous Products	$P_o x10^2$ (torr)	App. log A	Ch. III Figure #
n	1.0	---	54
	0.5	---	55
e, Ethane	1.0	11.718	25
"	1.0	10.749	29
"	2.5	9.984	29
"	5.0	9.982	29
ıe, Propane	1.0	11.957	5
"	1.0	11.036	7
ıe, Propane	1.0	12.796	14
"	1.0	13.773	14
"	3.3	13.972	14
ıe, Propane	1.0	13.701	18
"	3.3	14.044	18
ıe, Propane	1.0	14.382	22
"	1.0	14.185	22

TABLE (III -9) Conti

Reactant	Reaction Order	Apparent $E_a \pm \sigma$	Gaseous Produc
Isopropyl Chloride	First	8.7±0.4	Propylene, HCl
"	"	12.2±0.1	" "
"	"	15.2±0.7	" "
Isobutyl Chloride	First	12.6±0.3	Isobutylene, HCl
"	"	15.9±0.2	" "
"	"	15.2±0.8	" "
t-Butyl Chloride	First	15.4±0.5	Isobutylene, HCl-
Neopentyl Chloride	First	13.9±0.2	2-Methylbutene-2, I
"	"	15.0±0.5	"
1,2-Dichloropropane	Half	24.1±1.4	Propylene
1,3-Dichloropropane	Half	27.7±1.0	Cyclopropane, Propy
1,3-Dichloro-2,2-dimethylpropane	---	---	C_5H_{10}, C_5H_8, HCl

LE (III -9) Continued

Gaseous Products	$P_o x10^2$ (torr)	App. log A	Ch. III Figure #
opylene, HCl	1.0	5.322	34
" "	5.0	7.199	34
" "	25.0	8.641	34
obutylene, HCl	1.0	6.641	38
" "	5.0	9.217	40
" "	5.0	8.986	42
obutylene, HCl	2.8	11.554	36
Methylbutene-2, HCl	1.0	7.954	45
" "	2.5	7.307	47
opylene	1.0	12.642	50
clopropane, Propylene	1.0	12.965	52
H_{10}, C_5H_8, HCl	1.0	---	53

DISCUSSION

The reactions of alkyl halides with titanium films, as indicated in the introduction to the experimental section, can be divided into two major groups. These are most readily classified as; a) reactions of alkyl halides with virgin films, and b) subsequent, high temperature reactions.

In all cases except one, the reactions of alkyl halides with virgin films were not unlike the reactions of most gaseous oxidants with clean, metal surfaces where an inert, nonporous product layer is formed. Subsequent reactions fall into two subgroups. In one subgroup, catalytic elimination of hydrogen chloride was observed. In the other, noncatalytic reactions involving the bulk metal of the film occurred. These reactions however, did not exhibit diffusional control.

IV - 1. Reactions on Virgin Films

In general, the reaction on virgin, titanium films followed a fairly typical pattern. An extremely rapid reaction occurred when the surface was first exposed to reactant gas, followed by a large rate deceleration until the rate levelled to zero or some value very near zero. The amount of reactant gas consumed usually corresponded to less than a monolayer equivalent. This behaviour is indicative of the formation of a cohesive, unreactive product layer over the reactive metal surface, and was observed for all primary alkyl halide reactants

except n-propyl fluoride. Mindel and Pollack have observed this type of behaviour for the reaction of oxygen with titanium films (24). Stout and Gibbons have observed an initially linear uptake of oxygen by titanium, followed by a change to a diffusion controlled loss of oxygen which obeyed the parabolic, time dependent, rate law (78).

In the present investigation, the reaction and adsorption of the first dose of reactant isopropyl chloride went to completion immediately at $0^{o}C$. The second and third doses were observed to obey a diffusion controlled, parabolic rate law, {see figure (III-3)}.

The rate and extent of the reaction of isopropyl chloride was considerably greater than that of the primary alkyl halides. This leads to the conclusion that the reactions of the primary alkyl halides at low temperatures (excepting n-propyl fluoride), are limited by lack of reactivity of the carbon-halogen bond with the halided surface, and not by the absolute impermeability of the halide layer. The carbon-chlorine bond of t-butyl chloride was so reactive that the catalytic dehydrochlorination reaction began at low temperatures and interfered with the possibility of observing any diffusion controlled reaction for this reactant.

Because the initial doses of reactants were reacted so rapidly, no detailed kinetic data are available for the virgin film reactions. However, by following these reactions during the period of rate deceleration and observing reaction products and product ratios, certain conclusions may be drawn.

The reaction of n-propyl fluoride was quite unique. With this reactant, no rate deceleration was apparent until after the consumption of many monolayer equivalents of reactant. It is thought that the small size of the fluoride anion (comparable to the size of the hydride anion and smaller than that of the oxide anion) greatly facilitated its loss into the titanium metal lattice. High heats of formation for the titanium fluorides would also enhance this step.

The reaction of the other n-propyl halides are constrasted sharply with n-propyl fluoride, not only by their more normal diffusion limited behaviour, but also by their different gaseous product ratios. The initial reaction products resulting from the reaction of n-propyl chloride, bromide or iodide were an equimolar mixture of propylene and propane. This product mixture most likely results from the formation of n-propyl surface radicals with a high concentration of adjacent species which undergo disproportionation reactions. For each of these reactants the carbon-halogen bond is weaker than a carbon-hydrogen bond, and therefore one might expect that this would be the first bond to break. However, this is not true of n-propyl fluoride and the product ratio resulting from reaction of this compound is signifigantly different from the equimolar ratio found for the other n-propyl halides. In fact, the olefin:paraffin ratio of n-propyl fluoride is almost identical to that of isopropyl chloride and ethyl chloride. Enhanced olefin production in all these cases may result from the formation of a 1,2-diradical

surface species in competition with a simple alkyl species. The diradical would be identical to an adsorbed olefin molecule. Such a surface species might be formed for n-propyl fluoride by the breaking of a carbon-hydrogen bond with, or before, the breaking of the carbon-fluorine bond.

The significant difference in products resulting from the reaction of neopentyl chloride on a virgin film and on a halided film is good evidence that fundamental mechanistic differences exist in these two cases. Although some carbon-carbon bond breaking occurs with this reactant, and results in small amounts of isobutylene and methane, no carbon-carbon bond making, via intermolecular methyl transfer for example, was found. More importantly, no skeletally rearranged products were found.

Little can be learned about the nature of the surface species from the reactants which gave only unsaturated organic products. These include isobutyl and t-butyl chloride which gave only isobutylene, 1,2-dichloropropane which gave only propylene, and 1,3-dichloropropane which gave cyclopropane and some propylene.

In general, reactions of the alkyl halides with virgin films to give gaseous products occurred more readily at lower film temperature. This may be due to the more ready adsorption of the reactant molecule at lower temperature, or perhaps is due to a loss of the more reactive sites by sintering when film temperature was increased.

IV - 2. Nature of the Surface Sites

A considerable body of evidence derived from boundary lubrication studies (25, 26, 27, 28) indicates that a titanium diiodide species is formed on a titanium surface when it is exposed to iodine vapours or iodine in solution. Thermochemical calculations, based on standard heats of formation, are in agreement with the formation of the diiodide when excess titanium is present. They also suggest that a dibromide and a dichloride would be expected, but that the trifluoride rather than the difluoride should be formed. In fact, thermochemical considerations predict that titanium difluoride would be expected to disproportionate to titanium trifluoride and titanium. These calculations are presented in Appendix (III).

Formation of tetrahalides by reaction of bulk titanium with halogen atmospheres has been cited by Barksdale (79). The reaction occurs with fluorine slightly above ambient temperature, with chlorine at 350°C, with bromine at 360°C and with iodine at 400°C. Since halogens generally might be regarded as stronger oxidizing agents than alkyl halides, there is no reason to expect formation of the tetrachloride, tetrabromide or tetraiodide as products of alkyl halide reactions on titanium films in the present study. The formation of the tetrafluoride also should not be expected. The strong oxidizing power of the fluorine molecule is, in large part, a result of its low bond energy. The high carbon-fluorine bond energy of alkyl

fluorides make them poor oxidizing agents relative to fluorine. Therefore, the formation of dichloride, dibromide, diiodide and trifluoride surface species might be expected.

The considerable difference in reactivity of alkyl halides with virgin films and with reacted films also supports the hypothesis that the active sites on the surface of a reacted film are different from those on a virgin film. The sites on a virgin film must be zero-valent titanium.

IV - 3. Induction Periods

Since part of the initial reactant doses were lost via adsorption, it follows that part of the surface must have been contaminated by organic residues. The induction periods during noncatalytic reactions were never pronounced and may simply represent a period of surface decontamination. However, induction periods after an initial, rapid reaction on a virgin film were more pronounced for alkyl halides which eventually reacted catalytically. This was especially true when the film temperature was high so that adsorption on the virgin film was not permitted. A very notable induction period was observed during neopentyl chloride reactions, {see figure (III-48)}. In these cases the induction period may be the result of the formation of active sites which, in turn, participate in the dehydrochlorination reaction.

IV - 4. Subsequent Reactions

a) Kinetics

i) Introductory Comments

It is necessary to note several general points about the reactions which have been studied before beginning detailed kinetic arguments. The most important point, which can not be overemphasized, is that the noncatalytic reactions must have resulted in a cohesive titanium halide layer over the metal surface. The reactions however, exhibited no dependence on the thickness of this product layer. This means that reaction rate control was not the diffusion of metal cations or halide anions through this product layer. The rate of growth of this product layer must have occurred more readily than some other slow phase-boundary step. Details of the possible nature of this slow step will be discussed in a later section which follows the presentation of a mechanism for reactions exhibiting half order kinetics.

Several points should be noted about the production of paraffin during the noncatalytic reactions. The production of paraffin increased as the extent of film reaction was increased. This indicates that surface hydride increased as bulk hydride increased. Reaction rates, however, did not decrease, for a constant P_o, as the amount of surface hydride increased. Thus, the surface alkyl concentration was not reduced by increased surface hydride. This suggests that hydride is not competing for the same surface sites as the halide or alkyl species.

This conclusion was also reached by McConkney and Anderson during hydrogenolysis studies of methyl chloride on titanium films and for the same reason. They observed no change in hydrogenolysis rates with large increases in hydrogen pressure (45).

One other point must be stressed about the appearance of paraffin. The olefin:paraffin ratio was invariant during the course of any reaction. This invariant ratio is good evidence that both products are generated from some common intermediate and by mechanisms which have a common reaction order.

ii) Noncatalytic Half Order Reactions

The half order noncatalytic reactions of alkyl halides with halided titanium films may be explained by the following reaction sequence.

A rapid dissociative adsorption, associative desorption equilibrium is postulated as the initial step.

$$R\text{-}CH_2CH_2\text{-}X + 2\ S \underset{k_{-1}}{\overset{k_1}{\rightleftarrows}} R\text{-}CH_2CH_2\text{-}S + X\text{-}S \qquad (IV - 1$$

In equation (IV-1, 'S' is a nondesignated univalent surface site. It is assumed that subsequent reactions do not disturb this equilibrium. This condition is generally satisfied if the equilibrium is rapid (80).

Olefin is produced by the reactive desorption of the surface alkyl by β-hydride elimination, as shown in equation (IV-2.

$$R\text{-}CH_2CH_2\text{-}S + * \xrightarrow{k_2} R\text{-}CH{=}CH_2 + S + *\text{-}H \qquad \text{(IV - 2}$$

The '*' represents a surface site that selectively adsorbs hydride so that hydride adsorption is not competitive with halide or alkyl adsorption.

Excess surface halide is lost by formation of a bulk metal halide phase. Its disappearance is assumed to have a first order dependence.

$$S\text{-}X \xrightarrow{k_3} S + X_{(lattice)} \qquad \text{(IV - 3}$$

Excess surface surface hydride also must be lost into the metal lattice. However, discussion of how this may occur will be postponed to the latter part of this kinetic argument.

Several mechanisms must be considered for the formation of paraffin. These include; a) reactive desorption of two, adjacent surface alkyls (i.e. disproportionation),

$$2\ R\text{-}CH_2CH_2\text{-}S \xrightarrow{k_{4a}} R\text{-}CH_2CH_3 + R\text{-}CH{=}CH_2 + 2\ S \qquad \text{(IV - 4}$$

b) quasisorbed reaction of olefin and two surface hydrides, (equivalent to a Rideal mechanism),

$$R\text{-}CH{=}CH_2 + 2\ *\text{-}H \xrightarrow{k_{4b}} R\text{-}CH_2CH_3 + S + * \qquad \text{(IV - 5}$$

c) quasisorbed reaction of alkyl halide and surface hydride,

$$R\text{-}CH_2CH_2\text{-}X + *\text{-}H + S \xrightarrow{k_{4c}} R\text{-}CH_2CH_3 + S\text{-}X + * \qquad \text{(IV - 6}$$

d) associative desorption of surface hydride and surface alkyl,

(equivalent to a Hinschelwood mechanism).

$$R\text{-}CH_2CH_2\text{-}S + *\text{-}H \xrightarrow{k_{4d}} R\text{-}CH_2CH_3 + S + * \qquad \text{(IV - 7}$$

Generation of paraffin by disproportionation of surface alkyls is most unlikely. This mechanism would require a substantial surface alkyl concentration, which is not indicated by experimental observations. It can not explain the experimentally observed increase in paraffin production as the extent of film reaction is increased, and can not rationalize the invariant olefin:paraffin product ratio during the reactions.

The production of paraffin by the quasisorbed reaction of olefin with two surface hydrides can also be discounted. It has been shown that the reaction of ethyl chloride in the presence of excess ethylene does not result in enhanced ethane production. In addition, if paraffin production were occurring by this mechanism, then a continuing reaction of olefin and surface hydride after complete consumption of alkyl halide should have been observed, but was not. Indeed, the probability of finding two adjacent surface hydride species in a hydrogen deficient system should be low.

The quasisorbed reaction of alkyl halide and surface hydride also can be discounted. The probability of this reaction occurring in competition with the proposed rapid equilibrium must be small. Moreover, this mechanism postulates a first order dependence on alkyl halide for production of paraffin. However, it has been demonstrated that both paraffin and olefin production

occurs with half order kinetics.

The production of paraffin by the associative desorption of surface alkyl and surface hydride is the remaining possibility and will be shown to be a plausible alternative in the following elaboration of this kinetic scheme.

The rapid dissociative equilibrium of alkyl halide allows a mass balance to be written for the surface halide and surface alkyl species which is based on the rates at which they disappear.

$$k_2(R\text{-}CH_2CH_2\text{-}S) + k_{4d}(R\text{-}CH_2CH_2\text{-}S)(*\text{-}H) = k_3(S\text{-}X) \qquad \text{(IV - 8}$$

Reaction rate control can be ascribed to the concerted rate of appearance of surface sites so that the rate of disappearance of alkyl halide can be equated to half the rate of appearance of surface sites.

$$-\frac{d(R\text{-}CH_2CH_2\text{-}X)}{dt} = \tfrac{1}{2}\frac{d(S)}{dt} = \tfrac{1}{2}\{k_2(R\text{-}CH_2CH_2\text{-}S) + k_3(S\text{-}X) + k_{4d}(R\text{-}CH_2CH_2\text{-}S)(*\text{-}H)\} \qquad \text{(IV -9}$$

Substituting equation (IV-8 into equation (IV-9 gives

$$-\frac{d(R\text{-}CH_2CH_2\text{-}X)}{dt} = \{k_2 + k_{4d}(*\text{-}H)\}(R\text{-}CH_2CH_2\text{-}S) \qquad \text{(IV - 10}$$

Internal consistancy exists in this kinetic scheme since the same result is obtained by

$$-\frac{d(R\text{-}CH_2CH_2\text{-}X)}{dt} = \frac{d(R\text{-}CH{=}CH_2)}{dt} + \frac{d(R\text{-}CH_2CH_3)}{dt} \qquad \text{(IV - 11}$$

The initial equilibrium postulate, equation (IV-1, gives the following equality.

$$(S\text{-}X)(R\text{-}CH_2CH_2\text{-}S) = \frac{k_1}{k_{-1}}(R\text{-}CH_2CH_2\text{-}X)\ (S)^2 \qquad \text{(IV - 12}$$

Substituting equation (IV-8 into equation (IV-12, rearranging, and taking square roots, gives equation (IV-13.

$$(R\text{-}CH_2CH_2\text{-}S) = \left(\frac{k_1k_3}{k_{-1}\{k_2 + k_{4d}(*\text{-}H)\}}\right)^{\frac{1}{2}}(S)(R\text{-}CH_2CH_2\text{-}X)^{\frac{1}{2}} \qquad \text{(IV - 13}$$

Substitution of equation (IV-13 into equation (IV-10 gives equation (IV-14.

$$-\frac{d(R\text{-}CH_2CH_2\text{-}X)}{dt} = \left(\frac{k_1k_3\{k_2 + k_{4d}(*\text{-}H)\}}{k_{-1}}\right)^{\frac{1}{2}}(R\text{-}CH_2CH_2\text{-}X)^{\frac{1}{2}}(S) \qquad \text{(IV - 14}$$

In this expression, if $k_{-1} >> k_1$, then surface coverage will be small and (S) will be effectively a constant.

The matter of surface hydride must now be considered. The reaction of any one dose of alkyl halide will not cause an appreciable change in lattice hydride (or interstitial hydride) concentration. If a rapid equilibrium exists between surface hydride and lattice hydride, then the reaction of any one dose of alkyl halide, which causes no appreciable change in lattice hydride concentration, also will cause no appreciable change in surface hydride concentration. Under these conditions, (*-H) may be regarded as a constant. Larger reactant doses increase the surface alkyl concentration, and thereby increase the probability that a surface alkyl will be adjacent to a surface hydride. This, in turn, would increase paraffin production. As the interstitial hydride concentration slowly increases with increasing extent of film reaction, the equilibrium

surface hydride concentration will also slowly increase. This explains increased paraffin production with increased extent of film reaction.

If one does not assume that hydride surface sites are different from halide or alkyl sites, then these same kinetic arguments can be developed and will result in the same rate expression except that (*-H) is replaced by (S-H). However, if this were the case, rate decreases might be expected as the surface hydride concentration increased. For any given P_o, no rate decreases were observed as extent of film reaction was increased. In either case, exact half order kinetics exist for disappearance of reactant.

If the surface hydride, lattice hydride equilibrium assumption is not made, then the kinetic rate expression, equation (IV-14, must be modified by expressing (*-H) or (S-H) in terms of the reactant concentration. This is accomplished by proposing a steady state condition for surface hydride. This proposal is not unreasonable since it is known that hydride is lost into the film bulk extremely rapidly in the n-propyl fluoride reactions. In fact, both Trapnell (22) and Roberts (23) have suggested that surface hydride may diffuse into a titanium lattice. This postulate is also supported by the well documented ability of titanium to react with hydrogen (81, 82).

The rate of appearance of hydride is therefore equated to its rate of disappearance. Loss of hydride into the film

is expressed by equation (IV-15.

$$(*\text{-H}) \xrightarrow{k_5} (*) + H_{(lattice)} \qquad \text{(IV - 15}$$

The steady state hypothesis gives equation (IV-16.

$$k_2(\text{R-CH}_2\text{CH}_2\text{-S})(*) = k_{4d}(\text{R-CH}_2\text{CH}_2\text{-S})(*\text{-H}) + k_5(*\text{-H}) \qquad \text{(IV - 16}$$

It is assumed that the number of hydride surface sites remains large compared to the surface hydride concentration so that (*) is effectively a constant and then $k_2(*) = k_{2a}$. Increased paraffin production with increasing extent of film reaction is explained by a diffusion controlled loss of surface hydride. Hydride is lost less rapidly into the film as the product layer thickness increases and therefore is increasingly available for reaction with surface alkyls.

When equation (IV-16 is substituted into equations (IV-10 and (IV-13, equations (IV-17 and (IV-18 result. These equations, which are presented on the following page, are not readily soluble in terms of reactant concentration as a function of the rate of disappearance of reactant. It is apparent that when $k_5 >> k_{4d}(\text{R-CH}_2\text{CH}_2\text{-S})$, that is, when no paraffin is formed, that equation (IV-17 reduces to equation (IV-19.

$$-\frac{d(\text{R-CH}_2\text{CH}_2\text{-X})}{dt} = \left(\frac{k_1 k_2 k_3}{k_{-1}}\right)^{\frac{1}{2}} (\text{R-CH}_2\text{CH}_2\text{-X})^{\frac{1}{2}}(S) \qquad \text{(IV - 19}$$

When $k_{4d}(\text{R-CH}_2\text{CH}_2\text{-S}) >> k_5$, that is, when maximum paraffin is formed, equation (IV-17 reduces to equation (IV-20.

$$-\frac{d(\text{R-CH}_2\text{CH}_2\text{-X})}{dt} = \left(\frac{2k_1 k_2 k_3}{k_{-1}}\right)^{\frac{1}{2}} (\text{R-CH}_2\text{CH}_2\text{-X})^{\frac{1}{2}}(S) \qquad \text{(IV - 20}$$

$$-\frac{d(R\text{-}CH_2CH_2\text{-}X)}{dt} = k_{2a}(R\text{-}CH_2CH_2\text{-}S)\left[1 + \frac{k_{4d}(R\text{-}CH_2CH_2\text{-}}{k_5 + k_{4d}(R\text{-}CH_2CH}\right.$$

$$(R\text{-}CH_2CH_2\text{-}X) = \frac{k_{-1}}{k_1k_3(S)^2}\, k_{2a}(R\text{-}CH_2CH_2\text{-}S)^2\left[1 + \frac{k_{4d}(R\text{-}}{k_5 + k_{4d}(}\right.$$

$$\frac{+d(R\text{-}CH_2CH_2\text{-}S)}{k_{4d}(R\text{-}CH_2CH_2\text{-}S)}\Bigg) \qquad \text{(IV - 17}$$

$$+ \frac{k_{4d}(R\text{-}CH_2CH_2\text{-}S)}{k_5 + k_{4d}(R\text{-}CH_2CH_2\text{-}S)}\Bigg) \qquad \text{(IV - 18}$$

We are interested in the region where $k_5 \simeq k_{4d}(R\text{-}CH_2CH_2\text{-}S)$ and moderate amounts of paraffin are formed. This region was investigated by a computer program in which the rate expression was defined by equation (IV-17 and the reactant concentration was defined by equation (IV-18. It was assumed that k_{4d} and k_5 would not be small numbers when compared to $(R\text{-}CH_2CH_2\text{-}S)$. A value of 100 was assigned to k_5, a value of 10,000 was assigned to k_{4d} and values were then assigned to $(R\text{-}CH_2CH_2\text{-}S)$ so that $k_{4d}(R\text{-}CH_2CH_2\text{-}S)$ varied from 0.01 k_5 to 100 k_5. The ratio of $-d(R\text{-}CH_2CH_2\text{-}X)/dt$ and $(R\text{-}CH_2CH_2\text{-}X)^n$ was investigated for various values of 'n' throughout the value range defined for $(R\text{-}CH_2CH_2\text{-}S)$. Values of 'n' less than 0.501 or greater than 0.539 resulted in large and consistent changes in the ratio. Between these values of 'n', the ratio value oscillated through several maxima and minima but maintained a value constant to ±1% throughout reactant concentrations varying from 100 to 10,000 fold. At $n = 0.515$, the maximum variation of the ratio value, throughout the total eight decade reactant concentration range was less than ±5%.

Thus, for a steady state hydride postulate, the reaction order need not vary significantly from 0.50 for various amounts of product paraffin. It is not possible to make a mechanistic distinction between a steady state and an equilibrium surface hydride postulate.

Little or no difference between n-propyl chloride and ethyl chloride rates and apparent activation energies would be

expected on the basis of the rate equations which have been developed, and no significant differences were found. Lack of activation energy dependence on initial pressure, and therefore lack of dependence on olefin:paraffin product ratio suggests that temperature dependence of k_2 and k_{4d} are similar. It also suggests that, if the steady state hydride postulate is correct, k_5 is relatively independent of temperature.

iii) Rate Control in Half Order Reactions

The noncatalytic, half order reactions of n-propyl chloride, bromide, and iodide and of 1,2-dichloro-, 1,3-dichloropropane, and ethyl chloride all occurred with nearly identical rates and in the same temperature region. This, coupled with the similar activation energies, suggests that the reactions are all occurring with the same general mechanism and have the same rate controlling step. This statement is supported by the more rapid catalytic reactions of isobutyl and neopentyl chlorides. These reactants both have primary carbon-chlorine bonds with reactivity and strength similar to the carbon-chlorine bonds of ethyl chloride and n-propyl chloride. The statement is also supported by the much more rapid reaction of n-propyl fluoride. The extremely rapid n-propyl fluoride reaction also excludes reactive desorption of the n-propyl surface radical as the rate controlling step of the half order reactions. This also is supported by the lack of rate difference between the monochloro- and dichloro- compounds where β-chloride or γ-chloride elimination occurs.

Since hydride diffusion into the titanium must be occurring in the n-propyl fluoride reaction as in the other noncatalytic reactions of monohalo- compounds, it must occur rapidly and therefore cannot be the rate controlling step.

Various other phase boundary reaction steps exist and should be examined for applicability to this mechanism. All these steps must involve the reaction of surface halide with bulk metal.

Hauffe and Rahmel (83) have described conditions wherein the reaction of gaseous sulfur (S_2) with nickel proceeds with half order dependence on sulfur pressure and linear dependence on the thickness of the nickel sulfide layer. The mechanism which they propose is identical to a simplified form of the mechanism proposed for the half order reactions described in the present investigation. For this sulfidation reaction, rate control is ascribed to equilibrium dissociative chemisorption of the S_2 molecule. Hauffe notes that incorporation of an S atom into the surface is a step which may be distinguished from chemisorption onto the surface and would result in the same kinetics. The incorporation step may also be distinguished from bulk diffusion which would occur after incorporation.

Further work that suggests that incorporation of chemisorbed species into the gas-metal halide phase boundary may be the rate controlling step has been reported by Stout and Gibbons (78). These workers studied the sorption of oxygen, nitrogen, carbon dioxide, air, water vapour, hydrogen and methane

into titanium metal. They found that gas pressure above the metal decreased linearly with time during sorption of large concentrations of nitrogen and carbon dioxide and for small concentrations of oxygen. In order to account for the linear time, pressure relationship, they postulated a surface barrier limited sorption. It was postulated that the barrier separated a nearly constant number of gas and metal atoms. Under this condition, the rate of combination is constant with time and the entrapped volume of gas increases with zero order kinetics (78). If the number of metal atoms were to exceed considerably the number of gas atoms, then the increase of the entrapped volume of gas should exhibit a rate dependence on gas pressure.

A second phase boundary exists, the metal, metal halide boundary. If rate control were ascribed to abstraction of titanium atoms from the metal lattice with subsequent rapid diffusion through the metal halide layer, then similar rates would exist for the various halides and no diffusion control would be observed. In fact, of the first row transition elements, titanium is the most likely metal to follow this reaction pattern. It has one of the highest metal lattice energies (84) which would make abstraction of atoms from the lattice slow. It also has the lowest metal dihalide lattice energies (85) which might allow lattice disruptions, for example diffusion of titanium cations, to occur relatively easily. In order to maintain a first order disappearance of surface halide, it would be necessary to postulate that the rate of titanium abstraction across this phase boundary

must be proportional to the surface halide population. Precedent for a rate controlling step of this type can be found in sulfidation reactions of silver and copper. Rickert and Wagner have shown that passage of silver cations across the silver, silver sulfide phase boundary was the rate controlling step in the reaction of gaseous sulfur with silver surfaces. In this system, the silver sulfide layer therefore grew with linear time dependence (86, 87)

It has been noted that ionic diffusion occurs more readily when there is a larger number of lattice sites than there are occupants for these sites (88). The Ti^{+2} ions in a titanium dihalide crystal occupies half the available lattice sites. It also has a considerably smaller ionic radius than the halide which would promote its ease of movement in the halide lattice.

An additional phase boundary rate controlling step has been suggested by Hauffe (89). In a protective layer which consists of several distinct phases, transfer of cation or anion from one phase to an adjacent phase, or change of ionic charge with transfer between phases can sometimes be a slow step.

iv) Kinetics for the Noncatalytic Reaction of n-Propyl Fluoride

The reaction of n-propyl fluoride differed from the reactions of the other n-propyl halides. It occurred much more rapidly and with first order kinetics. To account for the different reaction pattern of this compound, it is postulated

that the back reaction in the initial equilibrium step, equation (IV-1, is reduced or has ceased completely and also that the loss of surface halide into the titanium lattice has greatly increased. Both these steps would be the result of the considerably greater heats of formation associated with the production of the titanium fluorides. The increased rate of fluoride loss into the metal lattice also may be attributed to the much smaller size of the anion in this case.

Rate control is attributed to carbon-fluorine bond rupture in equation (IV-21.

$$CH_3CH_2CH_2\text{-}F + 2\ S \xrightarrow{(slow)} CH_3CH_2CH_2\text{-}S + S\text{-}F \qquad (IV - 21$$

All steps subsequent to equation (IV-21 are rapid. Under these conditions, first order kinetics result.

$$-\frac{d(CH_3CH_2CH_2\text{-}F)}{dt} = k_{(slow)}(CH_3CH_2CH_2\text{-}F)(S)^2 \qquad (IV -22$$

Since reactions which regenerate surface sites are rapid, (S) remains essentially constant.

v) Kinetics for the First Order, Catalytic, Dehydrochlorination Reactions

Catalytic dehydrochlorination reactions occurred more rapidly than noncatalytic half order reactions within the temperature limits which were studied.

These reactions may be explained by modification of the noncatalytic half order reaction scheme. The initial, rapid equilibrium step, equation (IV-1, is once again postulated. However, a different reactive desorption step must follow, and

is illustrated by equation (IV-23.

$$R\text{-}CH_2CH_2\text{-}S + S\text{-}X \xrightarrow{k_2} 2\,S + H\text{-}X + R\text{-}CH{=}CH_2 \qquad \text{(IV - 23}$$

As in the noncatalytic reactions, the rate of disappearance of reactant is equal to the rate of appearance of products or to half the rate of appearance of surface sites.

$$-\frac{d(R\text{-}CH_2CH_2\text{-}X)}{dt} = \tfrac{1}{2}\frac{d(S)}{dt} = k_2(R\text{-}CH_2CH_2\text{-}S)(S\text{-}X) \qquad \text{(IV -24}$$

Substituting equation (IV-1 into equation (IV-24 gives the rate of disappearance of reactant as a function of reactant concentration.

$$-\frac{d(R\text{-}CH_2CH_2\text{-}X)}{dt} = \frac{k_1k_2}{k_{-1}}(R\text{-}CH_2CH_2\text{-}X)(S)^2 \qquad \text{(IV - 25}$$

If $k_{-1} >> k_1$, then (S) remains large and constant as was the case in the noncatalytic half order reactions.

vi) Special Cases

Hydrogen Chloride

The extremely slow, first order rate of disappearance of hydrogen chloride, much slower than that of the noncatalytic half order reactions, suggests that bond fission is the rate controlling step in this reaction. Since bond fission is slower than the halide incorporation step, first order kinetics, analogous to those for n-propyl fluoride, are postulated.

Methyl Chloride

Insufficient data has been generated to make meaningful kinetic arguments about this reaction. However, if the appearance of methane is a zero order reaction, as is suggested by

what little data are available this would indicate that rate control is a desorption step. Since McConkney and Anderson (45) have postulated that methane is generated by interaction of two surface methyl radicals, and not by a hydride, methyl interaction, rate control by reactive desorption of two surface methyls to give methane and a methylene radical would seem reasonable. Traces of ethane in the product spectrum would tend to confirm this hypothesis.

b) Arguments to Support the Kinetic Hypotheses

The noncatalytic half order reactions depend on two basic assumptions. The first, that a rapid equilibrium dissociation of the reactant alkyl halide occurs on the active surface, will be examined directly. The second, that the disappearance of surface halide by reaction with the bulk metal of the film to form a metal dihalide layer must be a first order step, has already been examined. (See section IV-a, iii.)

i) Equilibrium Dissociation of Alkyl Halides

Several researchers have studied hydrogenolysis reactions of alkyl halides on metal surfaces. All are in agreement that the initial step of the reaction is the dissociative adsorption of the alkyl halide onto the metal (45 - 49). In their studies of methyl chloride with titanium, McConkney and Anderson suggest that the weaker carbon-chlorine bond might be expected to rupture more readily than a carbon-hydrogen bond (45).

Studies by Kemball and Campbell of the reaction of t-butyl chloride on nickel or iron films to give isobutylene

and hydrogen chloride and of the reverse reaction, supplies indirect proof for the reversibility of carbon-chlorine bond rupture on these surfaces (49).

Coeckelbergs et. al. demonstrated conclusively that methyl chloride or bromide undergo exchange reactions with radioactive adsorbed halides (50 - 53). Although this does not demonstrate a rapid, equilibrium, dissociative adsorption of an alkyl halide, it does indicate that alkyl surface species and halide surface species can combine and re-enter the gas phase. This may be constrasted with the work of McConkney and Anderson who unsuccessfully attempted to scramble isotopes of $CH_3{}^{35}Cl$ and $^{13}CH_3Cl$ on a titanium film at 300°C and concluded that carbon-chlorine bond rupture was irreversible. Immobile surface species or a recombination rate much greater than a surface migration rate or a rapid diffusion of surface chloride into the metal lattice would also explain these results. It is important to note that Coeckelbergs et. al. were working with extensively halided surfaces whereas McConkney and Anderson were not. The large surface halide concentrations used by Coeckelbergs would enhance the probability of exchange.

In solution chemistry the reversible addition of methyl iodide to Vaska's Complex (60) is an example of an equilibrium situation involving carbon-halogen bond rupture. The reaction occurs by a two electron transfer from the metal ion to the addenda.

Other solution chemistry of interest has been described

by Chock and Halpern (90). They investigated the reactions of pentacyanocobaltate(II) with various organic halides. The rate controlling step in these reactions was thought to be the rupture of the carbon-halogen bond by a one electron transfer mechanism;

$$2\ Co(CN)_5^{-3} + R\text{-}X \rightarrow R\text{-}Co(CN)_5^{-3} + X\text{-}Co(CN)_5^{-3} \qquad \text{(IV - 26}$$

It is by this type of one electron transfer that the reactions described in the present investigation are thought to occur.

An example of a rapid equilibrium dissociation of the carbon-halogen bond of an alkyl halide exists in Friedel Crafts chemistry. The dissociation, accomplished by a Lewis acid is heterolytic and results in an ion pair product.

$$Al\text{-}X_3 + R\text{-}X \rightleftarrows R^+\text{-}Al\text{-}X^-_4 \qquad \text{(IV - 27}$$

Nenitzescu has suggested that this equilibrium is rapid and displaced considerably to the left (91). The overall alkylation reaction is third order, having first order dependence on aromatic species, alkyl halide and Lewis acid (92, 93). Both Nenitzescu and Gould have noted that the formation of a free carbonium ion instead of an ion pair would result in half order dependence on alkyl halide and on Lewis acid (92, 93). This behaviour, if it occurred, would be analogous to the formation of separated surface species in the proposed equilibrium dissociation of alkyl halides on halided titanium films.

Evidence for the proposed recombination of titanium alkyl and titanium halide surface species is also contained in the work of Bestian and Beerman (94, 95). They have observed

the catalytic decomposition of alkyltitanium species by titanium chlorides. They also observed that methyltitanium trichloride and titanium tetrachloride reacted rapidly to give methyl chloride and two molecules of titanium trichloride. Adjacent surface alkyls and surface halides might be expected to undergo a similar reaction.

It would be expected that the zero-valent titanium of a virgin film would most likely react with alkyl halides by an electron transfer mechanism. The probability that the halided titanium surface would react with alkyl halides by functioning as a Lewis acid rather than by electron transfer would increase as the oxidation state of the titanium increased. Titanium(IV) species, which most probably are not present, would be more likely to function as Lewis acids than titanium (II) or (III) species.

Lewis acid functionality would most probably follow the order chloride > fluoride > bromide > iodide. In fact, titanium tetraiodide is described by Olah as being of "only limited effect as a Friedel Crafts catalyst" (96).

Since even the highest oxidation state titanium iodide is a poor Lewis acid, the lower oxidation states, thought to be present during these reactions, almost certainly will not function as Lewis acids. The alkyl chloride, bromide and iodide react with the same kinetics and essentially the same rates. It follows that the mechanisms of the reactions are probably the same and therefore, that the titanium halide surface species

are probably reacting by electron transfer rather than by functioning as Lewis acids.

ii) β-Hydride Elimination by Titanium Alkyls

Several examples of olefin elimination from titanium alkyls by β-hydride transfer to metal are known. Brintzinger has observed that mono- and dimethyl complexes of bis(π-cyclopentadienyl)titanium(III) are stable at room temperature. However, corresponding ethyl and isopropyl complexes were unstable and eliminated olefin giving mono- and dihydride complexes (67). From a study of the isomerization of n-propyl and isopropyltitanium trichloride, Razavaev and Lataeva concluded that β-hydride transfer to metal occurred and was a reversible reaction (64).

Transfer of β-hydride to metal with olefin elimination is an accepted termination step during Ziegler catalysis (97). Reaction of this hydride with another titanium alkyl to give paraffin may be another termination step. These two steps, if concerted, would be equivalent to the disproportionation mechanism proposed by deVries (68).

iii) Loss of Hydride into the Titanium Lattice

Diffusion of hydrogen into titanium metal occurs readily, and more extensively than for any other transition metal (81, 82). Both Trapnell and Roberts (22, 23) have postulated hydride diffusion into bulk titanium films as a result of studies of the chemisorption behaviour of hydrocarbons.

Dushman noted that between $0^{o}C$ and $250^{o}C$ one gram of titanium is capable of maintaining 410 $cm.^{3}$ of hydrogen at S.T.P.

in solution (81). This is equivalent to 1.75 gram atoms of hydrogen per gram atom of titanium. Studies of hydrogen adsorption by titanium have shown that solubility is proportional to the square root of gas pressure, that sorption normally begins at 375°C and is rapid above 400°C. Maximum sorption occurs when the metal has been rigourously degassed and sorption is completely reversible (82). Stout and Gibbons have studied hydrogen sorption by titanium specimens which were carefully prepared in the complete absence of oxygen. They reported that extensive sorption of hydrogen occurred (up to 22 atom %) at room temperature. It was proposed, on the basis of their experiments that a small layer of surface oxide on the titanium can effectively seal it from hydrogen attack. This layer would easily account for the failure of other researchers to observe hydrogen sorption below 300°C. Stout and Gibbons also noted that the sorption of hydrogen, unlike that of other gases which they studied, was completely reversible (78). This reversibility is not unexpected since titanium dihydride decomposes at 400°C.

On the basis of these results, it is not suprising that hydrogen did not occur as a reaction product during the reactions of alkyl halides on titanium surfaces which, throughout the present investigation, were prepared in the absence of oxygen. The ready reversibility of hydrogen sorption by titanium which has been observed by several workers, suggests that an equilibrium most probably does exist between surface and bulk hydride. Although no distinction between an equilibrium surface hydride

model and a steady state surface hydride model is possible on the basis of the kinetics presented in the present study, the works of these other researchers support the equilibrium model rather than the steady state model.

iv) Loss of Surface Halide into the Metal Lattice

Work function studies of the adsorption of halogens and oxygen on metal surfaces, including titanium, have indicated that electronegative species may penetrate, at least superficially, into the lattice structure of a metal. It has been shown that the size of the penetrating species and temperature are important parameters (29 - 35). Campbell et. al. have studied the reaction of iodine with tungsten films and reported the formation of a bulk iodide at $300^{o}C$ (28).

When considering the diffusion of halide into the titanium lattice in the half order reactions described in the present investigation, it is important to realize that the totality of reactions on any one film would probably not require reaction of more than ten or fiften mole percent of the titanium which was present. If a conservative roughness factor of five is assumed for the halided surface, then a real film area of 10^{19} square angstroms is available. If as many as fifty 10^{-2} torr doses were reacted to completion on this film, then a total of 1.65×10^{19} molecules of reactant have been used. This number of chloride ions (ignoring hydride) in a close packed array would occupy an area of about 22×10^{19} square angstroms. This implies only about 22 chloride layers (and therefore eleven

titanium layers in a β-$TiCl_2$ layer lattice structure) and a total $TiCl_2$ thickness of about 100 angstroms.

The chloride ions produced by the reaction of one dose of reactant at 10^{-2} torr, in close packed array would occupy $5x10^{18}$ square angstroms or about half the available film area. Thus accomodation of even half a monolayer of chloride ion by diffusion into a halided layer occurs with very great difficulty when compared to the reaction with the unhalided film. This agrees with the observation of Barksdale that hydrochloriding a titanium surface greatly inhibits further corrosion of the metal (98).

The fact that reaction occurs at all and that it is not further inhibited by diffusional control, may be directly attributable to the presence of high diffusivity pathways. These pathways are crystalline defects such as dislocations or grain boundaries (99). Relatively large concentrations of defects are normally associated with vapour deposited metal films (10).

v) Combination of Surface Alkyl and Surface Hydride

Precedent for this type of reaction has been established by several researchers. In particular, McConkney and Anderson have shown that monodeuteriomethane and deuterium chloride are products of the reaction of deuterium and methyl chloride (45). Kemball and Campbell have reported that monodeuterioethane was the principal organic product during the deuteriolyses of ethyl chloride or bromide on nickel or iron films (48).

Olefin hydrogenation in a hydrogen deficient system has been postulated to occur by initial formation of a surface alkyl, by reaction of olefin with a surface hydride and subsequent combination of the alkyl with a second hydride. This type of reaction is known as the Langmuir-Hinschelwood mechanism (100). In hydrogenation reactions following this mechanism, olefin competes with hydride for surface sites. At high olefin pressures, rate decreases occur. In ethylene hydrogenation on nickel surfaces, this expected rate decrease has been observed by Toyama (101) and by Laidler and Townshend (102). It may be concluded, therefore, that these researchers were observing reactions involving combination of surface hydride and surface alkyl.

c) Activation Energies

The activation energies of the catalytic and the non-catalytic reactions differed considerably in magnitude. They also differed in another important respect. The activation energies of the noncatalytic reactions were independent of reactant pressure. However, the activation energies of the catalytic reactions increased as reactant pressure increased. The latter type of behaviour is not uncommon in catalytic surface reactions and may be attributed to decreases in the heat of adsorption of the reactant species as surface coverage is increased with increasing reactant pressure. When θ, the fractional surface coverage of reactant, is zero, the measured activation energy, which is referred to as the apparent activation energy,

is equal to the difference between the true activation energy of the surface reaction and the reactant heat of adsorption. (Product heat of desorption may also contribute positively to the apparent activation energy.) Under these conditions, a first order dependence on reactant pressure is observed. When the reactant θ is equal to one, the measured activation energy is equal to the true activation energy. Under these conditions, a zero order dependence on reactant pressure is observed. For intermediate values of θ, intermediate values of the apparent activation energy and of reaction order should be observed. Since no change in reaction order is found throughout the somewhat limited ranges of reactant pressures which were studied, it may be concluded that the value of θ did not vary appreciably from zero. It should be noted that heats of adsorption may change appreciably for small changes in θ.

The changes in apparent activation energy with reactant pressure were pronounced for isopropyl chloride, marginal for isobutyl chloride and minor for neopentyl chloride. This suggests that the heats of adsorption of the reactant molecules may be decreasing with increasing bulkiness of the alkyl group. This is further established by comparing apparent activation energies for these reactants under isobaric conditions. This comparison is made in table (IV-1). The lack of apparent activation energy dependence on reactant pressure, exhibited by the noncatalytic reactions, may reflect a less sensitive dependence of θ on reactant pressure for these slower reactions.

TABLE (IV - 1)

Reactant	P_o (torr)	Apparent E_a (kcal./mole)
isopropyl chloride	10^{-2}	8.7
isobutyl chloride	10^{-2}	12.6
neopentyl chloride	10^{-2}	13.9
isopropyl chloride	$5x10^{-2}$	12.2
isobutyl chloride	$5x10^{-2}$	15.4

It is interesting to note that the activation energies of the noncatalytic reactions increased with increasing halide size and not with increasing carbon-halogen bond strength. This supports the kinetic hypothesis that the energy barrier to reaction may be a space limited accomodation of the halide species, and not bond fission.

Since the mechanism of the noncatalytic reactions is thought to be complex, {see equation (IV-14}, product formation would contribute to the apparent activation energy value. This would explain the apparent activation energy from reaction of 1,3-dichloropropane to give cyclopropane being greater than that resulting from reaction of 1,2-dichloropropane to give propylene.

d) Rates of Reactions

The rates of the catalytic reactions increase in an expected manner and reflect considerable dependence on the carbon-chlorine bond reactivity. Small but real increases in rates result with β-methylation and large increases result

with α-methylation, {cf. Table (III-8)}. This same type of behaviour is found in unimolecular, gas phase dehydrohalogenation studies (61), and also has been found in hydrogenolysis studies on metal surfaces (47, 48, 49).

e) Products of Reactions

The catalytic and noncatalytic reactions have been treated separately up to this point. These separate treatments have been a matter of convenience. In fact, the catalytic and noncatalytic reactions are most likely competitive. Because the activation energies of the catalytic reactions are lower than those of the noncatalytic reactions, one would expect that the catalytic reaction might be found at low temperature but would be replaced by the noncatalytic reaction at sufficiently high temperature. Generation of significant amounts of propane by the high temperature reaction of isopropyl chloride, although at rates too fast to permit kinetic measurement, supports this hypothesis. Support may also be found by examining the somewhat crude data resulting from the reaction of 1,3-dichloro-2,2-dimethylpropane. A C_5H_{10} product appeared at high reaction temperatures, which indicates a noncatalytic loss of chloride. At lower reaction temperatures, larger amounts of hydrogen chloride appeared, and the C_5H_{10} species concentration was decreased and larger concentrations of a C_5H_8 species appeared.

In general, the reaction products were not unexpected. Chock and Halpern for example, have generated propylene and cyclopropane by reacting 1,2-dichloro- and 1,3-dichloropropane

with pentacyanocolbaltate(II) (90). The same products also result from the reaction of these dichloro- compounds with magnesium (103).

The dehydrochlorination reaction of neopentyl chloride was different from the other catalytic reactions in that it must have occurred via a rearrangement mechanism. Such a rearrangement mechanism would have a formal similarity to the Wagner-Meerwein rearrangement which proceeds by a carbonium ion mechanism in solution (104). It is also one of the postulated unimolecular gas phase decomposition mechanisms for neopentyl chloride (105). However, as pointed out by Anderson and Avery in isomerization studies of neopentane on platinum and palladium surfaces, the possibility of the existence of a carbonium ion as a discrete entity on a metal surface, must be rejected (106).

The probability of these various reactions having occurred by a free radical, or even a mobile surface radical mechanism would seem very low. This assertion is based on the absence of radical dimer products, except for isopropyl chloride reactions at high temperature. Even for isopropyl chloride, the amount of diisopropyl produced remained small at 240°C.

Comment should also be made on the complete absence of any higher molecular weight products which might have been formed by insertion of olefin into a titanium alkyl bond. This is most readily rationalized by postulating that the rate of decomposition of the titanium alkyl species was much faster than the rate of olefin insertion. Polymerization reactions

using alkyltitanium compounds as catalysts, are more normally carried out at lower temperatures and with much greater concentrations of monomer present than was the case in these studies.

IV - 5. Discussion of Errors

When dealing with surface chemistry phenomena, a primary concern is that no changes in the chemical nature of the surface or in the number of surface sites should occur during the course of an investigation. During catalytic processes, this type of concern should be considerably less than during noncatalytic processes where surface site regeneration depends on reactions involving bulk material beneath the surface. The most convenient method for determining whether the surface remains unchanged is simply to check data reproducibility during use of any one film. A method for determining whether any progressive changes are occurring is described in the experimental procedure section and consists of checking Arrhenius plots for unexpected curvatures.

Another important method of checking data is to determine whether experimental scatter can be explained by known experimental variables. In this respect, all Arrhenius data were generated by use of a standard computer program known as 'Curfit'. In addition to giving the best-fit first degree polynomial equation, from which activation energies can be calculated, it also gave the variance of the dependent variable experimental values. This value was converted to a standard deviation figure for the apparent energy of activation. All apparent energies of activation

and their standard deviations, σ, are summarized in Table (III-9).

It is apparent that greater experimental scatter occurs in more of the half order reactions than in the catalytic reactions as was expected. However, even in the cases where scatter is greatest, the largest σ is only about ±6% of the activation energy and, in most cases, is considerably smaller. The greatest σ occurs for an ethyl chloride reaction where app.E_a = 23.5±1.5 kcal./mole. All of the ±6.4% deviation can be accounted for by temperature and pressure uncertainties. Temperature was controlled to ±1°C, or better. For an Arrhenius plot in a temperature range of 200°C, this introduces an error, ξ_x = ±0.004 $K.^{-1}$ units, into the experimental values on the '$(10^3/T^oK.)$' scale. For this reaction, the values on this scale span 0.121 $^oK.^{-1}$ units. The capacitance manometer, which was used to measure pressure of reactant, introduces a maximum uncertainty of 5×10^{-4} torr into a total pressure of 10^{-2} torr, or a rate constant uncertainty of ±2.2% for a half order reaction. This results in an error, ξ_y = ±0.0095 units, for the experimental values on the 'log (rate)' scale of the Arrhenius plot. For this reaction, these values span 0.619 units. The slope of the Arrhenius plot is calculated in equation (IV-28.

$$\begin{aligned} \text{slope} &= (\Delta Y \pm 2\xi_y)/(\Delta X \pm 2\xi_x)/^oK. \\ &= 10^3(0.619\pm0.019)/(0.121\pm0.008)/^oK. \\ &= 10^3(5.15\pm0.50)\,^oK.^{-1} \end{aligned} \qquad \text{(IV - 28}$$

From this slope, the apparent activation energy of the reaction is calculated to be 23.5±2.3 kcal./mole. Thus, it is unnecessary

to postulate that changes in surface area or activity occur during this reaction.

IV - 6. Summary and Conclusions

1) It has been demonstrated that reactions of alkyl halides with titanium films differ depending upon whether the metal is virgin or halided by previous reactions. Differences may be in actual products formed or in the ratios of the products which are formed. The reactions also differ in their rates, their kinetics and their extents.

2) Differences also occur within the group of reactions with halided titanium films. Depending upon the reactant alkyl halide, the halided film functioned as a dehydrochlorination catalyst or reacted noncatalytically with incorporation of halide and some hydride into the bulk metal. These reactions occurred with different activation energies and, in at least two instances, have been observed to occur in competition with each other.

3) Dehydrochlorination reactions apparently required a specific site which is some form of surface titanium chloride species.

4) Similarities between the reactions of surface titanium alkyls and solution titanium alkyls have been noted. These similarities include; a) generation of olefin by transfer of β-hydride to metal, in the case of reactions on halided films, and b) the probable disproportionation of adjacent alkyl species

of certain reactions on virgin films.

5) Dissimilarity in the chemistry of the surface species and that of solution species would include the reaction of an alkyltitanium surface species with surface halide to produce olefin and gaseous hydrogen halide.

6) Certain potential applications have arisen as a result of this investigation. It has been shown that ethyl chloride and n-propyl halides are more reactive, and therefore more corrosive than gaseous HCl. These species should also be more corrosive than any of the alkyl chlorides which react catalytically to produce olefin and gaseous HCl.

As a result of this study, it is possible to suggest that 1,3- or 1,2-dihalopropanes should be considerably better boundary lubricants than any of the n-halopropanes. This suggestion is based on the fact that the n-propyl halides, in addition to transferring halide to the metal surface, also transferred hydride. The presence of hydride introduces a brittle, nonlubricating material. The 1,2-dichloropropane and 1,3-dichloropropane reactants transferred only chloride to the metal, and it is expected that the analogous iodides would react similarly.

SUGGESTIONS FOR FURTHER WORK

The work which has been described in this thesis has answered few questions and has asked many. Although certain hypotheses have been advanced to rationalize the observed results, in many instances, they involve steps which are experimentally untested. Thus, further work should include the testing of these hypotheses.

1) Studies of dehydrochlorination catalysis by titanium dichloride, and in general, of dehydrohalogenation by titanium dihalides, should be initiated to determine whether surface dihalides are the active species in the catalytic reactions.

2) Isotope scrambling experiments, similar to those described by McConkney and Anderson (45), or radiotracer experiments similar to those described by Coeckelbergs (50 - 53), should be undertaken to attempt to establish that an equilibrium dissociation of alkyl halide occurs on the reactive surface.

3) The feasibility of experiments to determine the manner of surface halide incorporation should be examined. These experiments would most likely involve electrochemical studies or electron microscopy studies.

4) A survey of the possible catalytic and noncatalytic reactions of alkyl halides with other transition metals might be undertaken.

5) The study of catalytic dehydrochlorination reactions on titanium films should be extended to studies of alkyl halides

other than chlorides.

6) Studies of the reactions of other compounds, such as ethers or amines might be undertaken.

7) Studies of the use of high boiling, linear halocarbons, particularly diiodoalkanes, as boundary lubricants could prove to be fruitful.

8) Modification of the reaction system so that higher pressures can be monitored, should be considered. The modified system could be used to pursue the original objective of this work, the study of ethylene polymerization by titanium surfaces.

CONTRIBUTIONS TO ORIGINAL KNOWLEDGE

This research constitutes the first systematic investigation of the reactions of gaseous halocarbons with atomically clean titanium surfaces. Two groups of reactions have been found.

Reactions of the first group occurred extremely rapidly on virgin films at low temperature. These reactions normally proceeded to the order of one monolayer equivalent of reactant and, in most cases, proceeded too rapidly to allow meaningful kinetic measurements.

Reactions of the second group occurred subsequent to an initial virgin film reaction and normally proceeded at elevated temperatures. These reactions proceeded through many monolayer equivalents of reactant with reproducible rates and kinetics. This group was divided into two subgroups. The first subgroup consisted of the noncatalytic reactions of alkyl halide to produce mixtures of olefin and paraffin with loss of halide and some hydride into the bulk of the film. However, in no instance did these reactions exhibit diffusional rate control. The second subgroup was the catalytic dehydrochlorination reactions of alkyl chlorides to give gaseous hydrogen chloride and olefin. This group of reactions proceeded more rapidly than the noncatalytic reactions and also exhibited reproducible rates and kinetics.

In the case of certain reactants, these reactions pro-

ceeded on a competitive basis. Kinetics were determined and apparent activation energies were measured for most reactions.

Reactant groups which have been studied include i) all the n-propyl halides, ii) a series of reactants corresponding to the alkyl chlorides generated by successive α-methylation of ethyl chloride, iii) a series of reactants corresponding to the alkyl chlorides generated by successive β-methylation of ethyl chloride and iv) a series of simple dichloro- compounds.

APPENDIX - I

Calculations for Computer Program for Study of the Reaction of n-Propyl Iodide

The base peaks for propane, propylene and n-propyl iodide, the fragmentation values for each of these compounds and the relative sensitivity of the residual gas analyzer to each compound were determined by the calibration procedure which is described in the experimental section.

The following designations were used during calculations and as acceptable variables within the computer program.

n-propyl iodide = halide

propylene = olefin

propane = parfin

Mass # 43 = A

Mass # 41 = B

Mass # 29 = C

Calibration Data

Mass #	Fragmentation Values		
	Halide	Olefin	Parfin
C	0.063	0.010	1.000
B	0.724	1.000	0.110
A	1.000	0.020	0.180
Relative Sensitivities	0.65	1.00	1.84

From the above calibration data, the following set of simultaneous equations are set up;

0.063(0.65)(halide) + 0.010(1.00)(olefin) + 1.000(

0.724(0.65)(halide) + 1.000(1.00)(olfein) + 0.110(

1.000(0.65)(halide) + 0.020(1.00)(olefin) + 0.180(

and simplified to the following,

0.041(halide) + 0.010(olefin) + 1.840(pa

0.471(halide) + 1.000(olefin) + 0.202(pa

0.650(halide) + 0.020(olefin) + 0.331(pa

From this set of simultaneous equations, the follow

Halide	Olefin	Parfin
0.041	0.010	1.840
0.471	1.000	0.202
0.650	0.020	0.331

Solution of the matrix gives the following.

(halide) = (1.838A - 0.033B - 0.327C)/D

(olefin) = (-0.858A + 1.182B - 0.025C)/D

(parfin) = (-0.036A - 0.006B + 0.641C)/D

'D' is the denominator determinant. Values of (hal

and (parfin) are in molar ratios.

olefin) + 1.000(1.84)(parfin) = C

olfein) + 0.110(1.84)(parfin) = B

olefin) + 0.180(1.84)(parfin) = A

lefin) + 1.840(parfin) = C

lefin) + 0.202(parfin) = B

lefin) + 0.331(parfin) = A

:ions, the following matrix is formed.

)lefin	Parfin	
0.010	1.840	C
1.000	0.202	B
0.020	0.331	A

llowing.

33B - 0.327C)/D

182B - 0.025C)/D

006B + 0.641C)/D

Values of (halide), (olefin)

'S' is defined as the sum, (halide) + (olefin) + (parfin) and is equal to (0.944A + 1.143B + 0.339C)/D.
'R' is defined as 'S'xD and therefore is equal to (o.944A + 1.143B + 0.339C).

Mole percent values are obtained by dividing the molar ratio values by 'S' and multiplying by 100%. When this operation is performed, the following equations result.

$$\text{mole \% halide} = (\text{halide})/R = (1.838 - 0.033B - 0.327C)/R$$

$$\text{mole \% olefin} = (\text{olefin})/R = (-0.036A + 1.182B - 0.025C)/R$$

$$\text{mole \% parfin} = (\text{parfin})/R = (-0.036A - 0.006B + 0.641C)/R$$

The computer program which follows is based on these calculations, and allows heights of mass #'s 29, 41 and 43 from any number of spectra to be read in as data. It calculates and prints out mole percent figures for n-propyl iodide, propylene, and propane. It also calculates and prints a value based on mole percent n-propyl iodide, which is proportional to $(P_o^{\frac{1}{2}} - P^{\frac{1}{2}})$.

Computer Program

```
      READ (5,10)N
      WRITE (6,20)
    1 READ (5,30)MSNO,C,B,A
      R=0.944*A+1.143*B+0.339*C
      HALIDE=100*(1.838*A-0.033*B-0.327*C)/R
      OLEFIN=100*(-0.858*A+1.182*B-0.025*C)/R
      PARFIN=100*(-0.036*A-0.006*B+0.641*C)/R
```

```
      ANSWER=10.00-HALIDE**0.50
      WRITE (6,40)MNSO,HALIDE,OLEFIN,PARFIN,ANSWER
      IF (MSNO-N) 1,2,2
    2 STOP
   10 FORMAT (I3)
   20 FORMAT (1H0,1X,44HMSNO   IODIDE   OLEFIN   PARFIN   ANSWER)
   30 FORMAT (I3,3F5.1)
   40 FORMAT (1H ,I5,4F10.2)
      END
```

APPENDIX - II

DATA FOR FIGURES PRESENTED IN EXPERIMENTAL RESULTS*

Figure (III-1)

Change of mole % propylene in product mixture with time during reactions of n-propyl halides with virgin films

Chloride - 0°C		Chloride - 20°C		Bromide - 0°C		Iodide - 0°C	
Mole %	Time	Mole %	Time	Mole %	Time	Mole %	Time
56.5	300	52.5	300	55.5	300	50.0	300
57.3	580	56.5	2100	59.2	970	51.5	900
57.8	1400	57.5	3900	60.0	1660	52.0	1500
57.8	2180	60.0	18900	60.0	2310	52.5	2100
57.8	2900			60.0	2800		

Figure (III-2)

First order disappearance of 0.1 torr n-propyl fluoride at 0°C

log (P_o/P)	Time	log (P_o/P)	Time	log (P_o/P)	Time
0.00	140	0.39	4680	0.78	8480
0.04	620	0.47	5390	0.93	9340
0.09	1240	0.51	5880	0.97	10380
0.14	2150	0.58	6600	1.07	10970
0.22	2770	0.61	6780	1.13	11800
0.23	3250	0.66	7640	1.33	12720
0.32	4080			1.36	13480

* All pressure values quoted in this appendix are based on torr units. All time values quoted are in seconds.

Figure (III-3)

Film deactivation during reactions of isopropyl chloride at 0°C

Second Dose (10^{-2} torr)			Third Dose (10^{-2} torr)		
$(P_o-P)\times10^2$	$(P_o-P)^2\times10^4$	Time	$(P_o-P)\times10^2$	$(P_o-P)\times10^4$	Time
0.049	0.002	180	0.000	0.422	0
0.116	0.013	670	0.007	0.431	190
0.185	0.034	1340	0.039	0.475	1740
0.250	0.063	2280	0.061	0.505	3260
0.324	0.105	3650	0.071	0.522	4100
0.371	0.138	4960	0.108	0.575	5400
0.413	0.171	6060			
0.591	0.349	12520			
0.625	0.391	14370			
0.643	0.416	15790			

Figure (III-4)

Half order kinetic data for reaction of n-propyl chloride, $P_o=10^{-2}$

220°C		210°C		200°C	
$(P_o^{\frac{1}{2}}-P^{\frac{1}{2}})$	Time	$(P_o^{\frac{1}{2}}-P^{\frac{1}{2}})$	Time	$(P_o^{\frac{1}{2}}-P^{\frac{1}{2}})$	Time
0.006	180	0.006	255	0.002	210
0.016	450	0.021	900	0.008	540
0.024	720	0.032	1350	0.013	900
0.041	1425	0.047	1980	0.021	1380
0.054	1425	0.060	2535	0.032	2190
0.067	1815	0.075	3165	0.040	2700
0.089	2295	0.087	3580	0.051	3450

Figure (III-4) Continued

200°C		190°C		180°C	
$(P_o^{\frac{1}{2}}-P^{\frac{1}{2}})$	Time	$(P_o^{\frac{1}{2}}-P^{\frac{1}{2}})$	Time	$(P_o^{\frac{1}{2}}-P^{\frac{1}{2}})$	Time
0.004	240	0.003	300	0.001	600
0.010	660	0.012	1260	0.006	1290
0.022	1560	0.019	2070	0.009	2040
0.032	2040	0.025	2790	0.012	2850
0.048	2970	0.031	3390	0.016	3630
0.060	3720	0.038	3960	0.019	4350

Figure (III-5)

Arrhenius data for half order reaction of n-propyl chloride

$(Rate)\times10^5$ $(torr^{\frac{1}{2}}/sec)$	6 + log (rate)	$(10^3/T^oK.)$	$T^oC.$
3.80	1.580	2.028	220
2.36	1.373	2.070	210
1.47	1.167	2.114	200
1.59	1.200	2.114	200
0.905	0.956	2.160	190
0.438	0.642	2.208	180

Figure (III-6)

Half order kinetic data for reaction of n-propyl chloride, $P_o = 10^{-2}$

175.5°C		182.5°C		190°C		200°C	
$(P_o^{\frac{1}{2}} - P^{\frac{1}{2}})$	Time	$(P_o^{\frac{1}{2}} - P^{\frac{1}{2}})$	Time	$(P_o^{\frac{1}{2}} - P^{\frac{1}{2}})$	Time	$(P_o^{\frac{1}{2}} - P^{\frac{1}{2}})$	Time
0.004	150	0.003	180	0.006	210	0.005	90
0.013	1080	0.011	705	0.015	600	0.033	795
0.021	1590	0.018	1200	0.021	960	0.052	1200
0.029	2250	0.028	1875	0.037	1620	0.063	1500
0.039	3090	0.039	2670	0.049	2085		
0.047	3750	0.045	3225	0.061	2685		
0.057	4530	0.055	3900				
0.068	5520	0.066	4590				

Figure (III-7)

Arrhenius data for half order reaction of n-propyl chloride

$(\text{Rate}) \times 10^5$ $(\text{torr}^{\frac{1}{2}}/\text{sec})$	5 + log (rate)	$(10^3/T^\circ K.)$	$T^\circ C.$
1.15	0.060	2.229	175.5
1.45	0.160	2.194	182.5
2.29	0.359	2.159	190
4.17	0.620	2.114	200

Figure (III-8)

Half order data for initial n-propyl chloride dose at 200°C

$(P_o^{\frac{1}{2}} - P^{\frac{1}{2}})$	Time	$(P_o^{\frac{1}{2}} - P^{\frac{1}{2}})$	Time	$(P_o^{\frac{1}{2}} - P^{\frac{1}{2}})$	Time	$(P_o^{\frac{1}{2}} - P^{\frac{1}{2}})$	Time
0.000	315	0.008	1095	0.030	2820	0.062	4995
0.005	720	0.014	1575	0.042	3675	0.068	5520
		0.019	1965	0.053	4515	0.074	5865

Figure (III-9)

Rate dependence on reactant pressure for n-propyl chloride

1.1×10^{-2} torr		2.5×10^{-2} torr		6.5×10^{-2} torr	
$(P_o^{\frac{1}{2}}-P^{\frac{1}{2}})$	Time	$(P_o^{\frac{1}{2}}-P^{\frac{1}{2}})$	Time	$(P_o^{\frac{1}{2}}-P^{\frac{1}{2}})$	Time
0.007	90	0.023	490	0.015	350
0.023	475	0.042	945	0.024	960
0.041	930	0.060	1400	0.060	1740
0.061	1475	0.097	2440	0.104	3425
0.079	1975	0.113	2885		
0.105	2530				

Figure (III-10)

Mole % propane dependence on mole % n-propyl chloride reacted

1.0×10^{-2} torr		1.1×10^{-2} torr		2.5×10^{-2} torr		6.5×10^{-2} torr	
Mole % C_3H_8	Mole % C_3H_7Cl	Mole % C_3H_8	Mole % C_3H_7Cl	Mole % C_3H_8	Mole % C_3H_7Cl	Mole % C_3H_8	Mole % C_3H_7Cl
1.7	8.0	2.0	12.9	6.1	27.2	2.0	11.1
2.4	19.6	7.0	39.5	10.0	46.9	4.2	17.8
3.0	38.9	11.6	63.0	12.4	62.7	11.2	41.5
4.4	72.8	14.6	94.0	19.0	86.2	21.2	78.3
4.6	83.7	15.6	100.0	18.5	92.5		

Figure (III-11)

Half order kinetic data for n-propyl bromide reaction, $P_o=10^{-2}$

195°C		205°C		214.5°C		224.5°C		224.5°C	
$P_o^{\frac{1}{2}}-P^{\frac{1}{2}}$	Time	$P_o^{\frac{1}{2}}-P^{\frac{1}{2}}$	Time	$P_o^{\frac{1}{2}}-P^{\frac{1}{2}}$	Time	$P_o^{\frac{1}{2}}-P^{\frac{1}{2}}$	Time	$P_o^{\frac{1}{2}}-P^{\frac{1}{2}}$	Time
0.008	195	0.012	220	0.014	145	0.014	90	0.014	95
0.015	485	0.019	460	0.031	425	0.044	380	0.033	300

Figure (III-11) Continued

0.020	760	0.026	745	0.053	845	0.060	585	0.051	515
0.033	1445	0.036	1050	0.067	1100	0.086	940	0.067	725
0.044	2100	0.054	1580	0.083	1480			0.081	940
0.054	2700	0.077	2240						

Figure (III-12)

Half order kinetic data for n-propyl bromide reaction, $P_o=10^{-2}$

$P_o^{\frac{1}{2}}-P^{\frac{1}{2}}$	Time	$P_o^{\frac{1}{2}}-P^{\frac{1}{2}}$	Time	$P_o^{\frac{1}{2}}-P^{\frac{1}{2}}$	Time	$P_o^{\frac{1}{2}}-P^{\frac{1}{2}}$	Time
0.001	215	0.004	240	0.007	170	0.017	200
0.005	830	0.013	780	0.022	650	0.036	500
0.009	1370	0.019	1260	0.032	1000	0.049	740
0.012	1770	0.026	1615	0.042	1370	0.062	975
0.016	2340	0.034	2250	0.056	1880	0.076	1240

Figure (III-13)

Half order kinetic data, n-propyl bromide reaction, $P_o=3.3\times10^{-2}$

$P_o^{\frac{1}{2}}-P^{\frac{1}{2}}$	Time	$P_o^{\frac{1}{2}}-P^{\frac{1}{2}}$	Time	$P_o^{\frac{1}{2}}-P^{\frac{1}{2}}$	Time
0.004	240	0.007	200	0.012	170
0.013	780	0.022	780	0.023	400
0.019	1260	0.032	1200	0.042	740
0.026	1615	0.039	1510	0.054	1010
0.034	2250	0.051	1970	0.068	1275

Figure (III-14)

Arrhenius data for half order reactions of n-propyl bromide

(Rate)x10^5 (torr$^{\frac{1}{2}}$/sec)	6 + log (rate)	(10^3/T°K.)	T°C.
	(P_o = 10^{-2} torr) Figure (III-11) rates		
1.78	1.250	2.136	195
3.05	1.484	2.091	205
5.40	1.732	2.050	214.5
8.55	1.932	2.009	224.5
8.55	1.932	2.009	224.5
	(P_o = 10^{-2} torr) Figure (III-12) rates		
0.705	0.845	2.166	188.5
1.82	1.258	2.100	203
2.78	1.443	2.063	211.5
5.85	1.767	2.013	223.5
	(P_o = 3.3x10^{-2} torr) Figure (III-13) rates		
1.53	1.184	2.100	203
2.58	1.412	2.063	211.5
5.19	1.714	2.013	223.5

Figure (III-15)

Mole % propane dependence on mole % n-propyl bromide reacted

1.25x10^{-2} torr		5x10^{-2} torr		1x10^{-1} torr	
Mole % C_3H_8	Mole % C_3H_7Br	Mole % C_3H_8	Mole % C_3H_7Br	Mole % C_3H_8	Mole % C_3H_7Br
1.4	16.9	1.6	11.6	2.0	11.3
2.7	26.8	5.7	39.2	8.1	46.5
4.5	43.7	9.8	61.2	11.5	63.6
6.4	57.6	10.7	81.1		

Figure (III-15) Continued

8.6	75.7	14.6	94.7	---	---
10.5	94.1				

Figure (III-16)

Half order kinetic data, n-propyl iodide reaction, $P_o=10^{-2}$

218.5°C		207.5°C		198.5°C		191°C	
$P_o^{\frac{1}{2}}-P^{\frac{1}{2}}$	Time	$P_o^{\frac{1}{2}}-P^{\frac{1}{2}}$	Time	$P_o^{\frac{1}{2}}-P^{\frac{1}{2}}$	Time	$P_o^{\frac{1}{2}}-P^{\frac{1}{2}}$	Time
0.014	130	0.007	130	0.005	165	0.002	145
0.029	330	0.023	570	0.015	700	0.012	825
0.046	550	0.034	850	0.029	1290	0.025	1810
0.063	800	0.046	1200	0.044	2015	0.028	2115
0.077	1040	0.065	1715	0.052	2400	0.033	2385

Figure (III-17)

Half order kinetic data, n-propyl iodide reaction, $P_o=3.3\times10^{-2}$

218.5°C		207.5°C		198.5°C		191°C	
$P_o^{\frac{1}{2}}-P^{\frac{1}{2}}$	Time	$P_o^{\frac{1}{2}}-P^{\frac{1}{2}}$	Time	$P_o^{\frac{1}{2}}-P^{\frac{1}{2}}$	Time	$P_o^{\frac{1}{2}}-P^{\frac{1}{2}}$	Time
0.012	160	0.003	145	0.003	190	0.004	550
0.036	530	0.015	445	0.011	670	0.011	1030
0.056	830	0.034	1130	0.021	1270	0.014	1360
0.088	1320	0.061	1845	0.028	1620	0.021	1985
0.110	1690	0.088	2630	0.034	1920	0.026	2395

Figure (III-18)

Arrhenius data for half order reactions of n-propyl iodide

(Rate)x10^5 (torr$^{\frac{1}{2}}$/sec)	5 + log (rate)	(10^3/T°K.)	T°C.
	(P_o = 10^{-2} torr) Figure (III-16) rates		
7.42	0.870	2.034	218.5
3.72	0.570	2.080	207.5
2.08	0.317	2.120	198.5
1.30	0.114	2.154	191
	(P_o = 3.3x10^{-2} torr) Figure (III-17) rates		
6.51	0.812	2.034	218.5
3.33	0.522	2.080	207.5
1.82	0.261	2.120	198.5
1.08	0.031	2.154	191

Figure (III-19)

Mole % propane dependence on mole % n-propyl iodide reacted

1x10^{-2} torr		5x10^{-2} torr		1x10^{-1} torr	
Mole % C_3H_8	Mole % C_3H_7I	Mole % C_3H_8	Mole % C_3H_7I	Mole % C_3H_8	Mole % C_3H_7I
0.6	4.1	1.0	5.8	1.8	8.0
4.1	31.2	4.7	29.5	4.1	16.1
4.5	45.1	7.5	50.6	7.3	30.4
6.4	62.7	10.5	73.2	7.5	38.3
8.3	72.1	12.1	85.6	9.1	44.7
8.9	81.0			11.1	52.4

Figure (III-20)

First order kinetic data, n-propyl fluoride reaction, $P_o=10^{-2}$

93°C		93°C		85°C		85°C		78.5°C	
$\log \frac{P_o}{P}$	Time	$\log \frac{P_o}{P}$	Time	$\log \frac{P_o}{P}$	Time	$\log \frac{P_o}{P}$	Time	$\log \frac{P_o}{P}$	Time
0.206	15	0.156	9	0.020	3	0.172	30	0.085	15
0.404	30	0.337	24	0.196	33	0.346	60	0.274	75
0.549	45	0.477	39	0.348	63	0.535	90	0.426	135
0.675	60	0.758	69	0.502	93	0.686	120	0.584	195
0.946	90	0.986	99	0.630	123	0.787	150	0.722	255
1.176	120	1.243	129	0.773	153	0.935	180	0.868	315
1.410	150			0.904	183	1.063	210	1.010	375

78.5°C		70°C		70°C		63°C	
0.025	5	0.068	50	0.094	60	0.066	60
0.223	65	0.155	110	0.168	120	0.112	120
0.356	125	0.234	170	0.243	180	0.154	180
0.532	185	0.306	230	0.311	240	0.195	240
0.662	245	0.374	290	0.378	300	0.240	300
0.815	305	0.449	350	0.444	360	0.292	360
0.968	365	0.523	410	0.516	420	0.342	420

Figure (III-21)

First order kinetic data, n-propyl fluoride reaction, $P_0=10^{-2}$

104.5°C		99°C		86°C		91°C		91°C cont.	
0.369	21	0.038	3	0.121	24	0.044	6	0.682	96
0.962	51	0.451	33	0.378	84	0.258	36	0.865	126
		0.938	63	0.645	144	0.455	66	1.108	156
0.423	24	1.335	93	0.912	204				
1.073	54			1.193	264				

Figure (III-22)

Arrhenius data for first order reactions of n-propyl fluoride

(Rate)x10^4 (sec^{-1})	4 + log (rate)	($10^3/T^oK.$)	$T^oC.$
	Figure (III-20) rates		
91.4	1.960	2.731	93
48.6	1.687	2.792	85
24.9	1.396	2.843	78.5
12.2	1.087	2.914	70
7.3	0.863	2.976	63
	Figure (III-21) rates		
191.0	2.280	2.648	104.5
145.0	2.155	2.683	99
70.3	1.845	2.746	91
48.2	1.682	2.784	86

Figure (III-23)

Mole % propane dependence on mole % n-propyl fluoride reacted

$P_o=10^{-2}$				$P_o=10^{-1}$					
Mole % C_3H_8	Mole % C_3H_7F	Mole % C_3H_8	Mole % C_3H_7F	Mole % C_3H_8	Mole % C_3H_7F	Mole % C_3H_8	Mole % C_3H_7F	Mole % C_3H_8	Mole % C_3H_7F
3.3	17.0	15.0	82.8	2.0	9.7	9.3	52.6	13.3	78.3
6.4	36.3	16.2	89.1	4.9	18.3	10.5	59.1	15.7	83.4
10.1	49.8	16.9	92.0	5.9	20.1	13.9	69.0	16.1	88.3
11.6	65.3	18.7	94.9	8.4	39.9	13.7	73.4	18.1	91.5
14.4	75.9			7.3	41.1	14.7	75.4	18.1	95.4

Figure (III-24)

Half order kinetic data, ethyl chloride, $P_o = 10^{-2}$

241°C		230°C		220°C		210°C		200°C	
$P_o^{\frac{1}{2}}-P^{\frac{1}{2}}$	Time	$P_o^{\frac{1}{2}}-P^{\frac{1}{2}}$	Time	$P_o^{\frac{1}{2}}-P^{\frac{1}{2}}$	Time	$P_o^{\frac{1}{2}}-P^{\frac{1}{2}}$	Time	$P_o^{\frac{1}{2}}-P^{\frac{1}{2}}$	Time
0.010	210	0.008	165	0.004	180	0.004	150	0.003	210
0.023	540	0.024	765	0.013	600	0.009	585	0.005	705
0.050	1125	0.052	1590	0.021	1020	0.014	1020	0.008	1170
0.078	1575	0.063	1980	0.027	1350	0.020	1440	0.011	1665
0.088	1935	0.078	2385	0.037	1710	0.025	1830	0.013	2250
				0.046	2055	0.038	2745	0.017	2905

Figure (III-25)

Arrhenius data for half order reaction of ethyl chloride

(Rate)x10^6 ($torr^{\frac{1}{2}}$/sec)	6 + log (rate)	($10^3/T°K.$)	T°C.
48.1	1.682	1.945	241
31.6	1.500	1.987	230
21.8	1.338	2.028	220
13.2	1.123	2.070	210
6.2	0.792	2.114	200

Figure (III-26)

Half order kinetic data, ethyl chloride reaction, $P_o = 10^{-2}$

240°C		230°C		220°C		210°C	
$P_o^{\frac{1}{2}}-P^{\frac{1}{2}}$	Time	$P_o^{\frac{1}{2}}-P^{\frac{1}{2}}$	Time	$P_o^{\frac{1}{2}}-P^{\frac{1}{2}}$	Time	$P_o^{\frac{1}{2}}-P^{\frac{1}{2}}$	Time
0.011	200	0.007	205	0.007	370	0.007	485
0.032	585	0.020	625	0.017	800	0.014	1050
0.074	1220	0.036	1065	0.026	1265	0.019	1525

Figure (III-26) Continued

0.097	1630	0.051	1480	0.035	1680	0.029	2185
		0.075	2110	0.047	2155	0.037	2785
				0.049	2655	0.046	3380
				0.073	3310	0.056	3960
				0.088	3800	0.062	4505

Figure (III-27)

Half order kinetic data, ethyl chloride reaction, $P_o = 2.5 \times 10^{-2}$

240°C		230°C		220°C		210°C	
$P_o^{\frac{1}{2}} - P^{\frac{1}{2}}$	Time	$P_o^{\frac{1}{2}} - P^{\frac{1}{2}}$	Time	$P_o^{\frac{1}{2}} - P^{\frac{1}{2}}$	Time	$P_o^{\frac{1}{2}} - P^{\frac{1}{2}}$	Time
0.009	135	0.008	150	0.007	235	0.003	210
0.030	490	0.030	715	0.028	1010	0.019	1445
0.070	925	0.058	1320	0.062	2030	0.046	2880
0.096	1335	0.085	1840	0.091	2795	0.056	3425
		0.129	2790	0.110	3480	0.067	3915
						0.080	4495

Figure (III-28)

Half order kinetic data, ethyl chloride reaction, $P_o = 5 \times 10^{-2}$

240°C		230°C		220°C		210°C	
$P_o^{\frac{1}{2}} - P^{\frac{1}{2}}$	Time	$P_o^{\frac{1}{2}} - P^{\frac{1}{2}}$	Time	$P_o^{\frac{1}{2}} - P^{\frac{1}{2}}$	Time	$P_o^{\frac{1}{2}} - P^{\frac{1}{2}}$	Time
0.009	180	0.018	590	0.006	240	0.004	440
0.025	625	0.032	1160	0.015	720	0.012	1025
0.075	1640	0.048	1770	0.029	1515	0.019	1690
0.148	3000	0.079	2735	0.049	2570	0.038	2980
0.178	3690	0.101	3355	0.075	3785	0.045	3600

Figure (III-29)

Arrhenius data for half order reactions of ethyl chloride

(Rate)x10^5 ($torr^{\frac{1}{2}}$/sec)	5 + log (rate)	(10^3/T°K.)	T°C.
(P_o=10^{-2} torr) Figure (III-26) rates			
5.88	0.769	1.949	240
3.48	0.542	1.987	230
2.22	0.346	2.028	220
1.39	0.143	2.070	210
(P_o=2.5x10^{-2} torr) Figure (III-27) rates			
7.35	0.866	1.949	240
4.67	0.668	1.987	230
3.08	0.488	2.028	220
1.97	0.295	2.070	210
(P_o=5x10^{-2} torr) Figure(III-28) rates			
4.72	0.679	1.949	240
2.90	0.462	1.987	230
1.98	0.296	2.028	220
1.23	0.090	2.070	210

Figure (III-30)

Mole % ethane dependence on mole % ethyl chloride reacted

1.0x10^{-1}		5.0x10^{-2}		2.5x10^{-2}		1.2x10^{-2}		1.0x10^{-2}	
Mole % C_2H_6	Mole % C_2H_5Cl	Mole % C_2H_6	Mole % C_2H_5Cl	Mole % C_2H_6	Mole % C_2H_5Cl	Mole % C_2H_6	Mole % C_2H_5Cl	Mole % C_2H_6	Mole % C_2H_5
1.8	5.0	1.9	8.0	1.9	11.0	1.5	18.1	5.5	26.
5.8	14.7	6.1	20.2	6.9	34.9	2.3	49.6	10.4	42.
10.2	29.4	16.9	52.0	10.9	68.7	3.0	89.0	13.6	56.
16.3	38.3	28.3	87.7	15.4	84.8	4.5	98.7	17.3	71.

Figure (III-31)

First order kinetic data, isopropyl chloride reaction, $P_o=10^{-2}$

log P_o/P	Time	log P_o/P	Time	log P_o/P	Time
180°C		157°C		157°C	
0.218	175	0.149	155	0.194	190
0.420	295	0.398	455	0.426	475
0.538	345	0.839	1060	0.688	840
0.732	600	1.000	1375	0.950	1210
134.5°C		118°C		100°C	
0.130	165	0.111	205	0.071	170
0.260	465	0.279	830	0.127	715
0.502	940	0.414	1275	0.291	1715
0.688	1365	0.553	1730	0.414	2625
1.070	1950	0.687	2175		
		0.853	2685		

Figure (III-32)

First order kinetic data, isopropyl chloride reaction, $P_o=5\times10^{-2}$

168°C		168°C		152°C	
0.143	140	0.176	135	0.150	180
0.449	480	0.501	395	0.450	540
0.756	765	0.809	655	0.795	945
131°C		131°C		1.070	1285
0.097	175	0.120	210	109°C	
0.214	510	0.250	595	0.053	245
0.397	1015	0.456	1090	0.152	890
0.560	1400	0.667	1610	0.296	1800
0.757	1875	0.870	2070	0.377	2335

Figure (III-33)

First order kinetic data, isopropyl chloride, $P_o=25x10^{-2}$

log P_o/P	Time	log P_o/P	Time	log P_o/P	Time	log P_o/P	Time
	180°C		170°C		170°C		155°C
0.098	140	0.116	180	0.092	140	0.092	155
0.371	450	0.408	530	0.352	480	0.346	520
0.721	850	0.710	880	0.638	800	0.667	960
		0.980	1205	0.904	1100	0.921	1300
	142°C		132.5°C		125.5°C		116°C
0.066	160	0.061	245	0.046	170	0.030	255
0.242	575	0.170	630	0.111	610	0.096	685
0.449	1020	0.324	1110	0.236	1110	0.132	1300
0.678	1530	0.481	1545	0.342	1595	0.194	1825
		0.545	1950	0.456	2010		

Figure (III-34)

Arrhenius data for first order reactions of isopropyl chloride

(Rate)x10^4 (sec^{-1})	4 + log (rate)	($10^3/T°K.$)	T°C.
	($P_o=10^{-2}$ torr) Figure (III-31) rates		
12.20	1.086	2.207	180
8.25	0.916	2.325	157
7.75	0.889	2.325	157
5.03	0.701	2.453	134.5
3.06	0.485	2.556	118
1.50	0.176	2.680	100
	(P_o $5x10^{-2}$ torr) Figure (III-32) rates		
14.30	1.155	2.267	168
8.40	0.922	2.352	152

Figure (III-34) Continued

4.09	0.611	2.474	131
1.66	0.220	2.616	109
	(P_o=25x10^{-2} torr) Figure (III-33) rates		
8.49	0.929	2.208	180
8.49	0.929	2.258	170
8.40	0.924	2.258	170
7.25	0.860	2.336	155
4.43	0.678	2.410	142
2.92	0.466	2.466	132.5
2.20	0.342	2.509	125.5
1.20	0.080	2.571	116

Figure (III-35)

First order kinetic data, t-butyl chloride reaction, P_o=2.8x10^{-2}

log P_o/P	Time	log P_o/P	Time	log P_o/P	Time	log P_o/P	Time
188, 164, 148°C		93.5, 100°C		80°C		67.5°C	
0.176	6	0.050	6	0.050	5	0.033	4
0.227	11	0.176	14	0.127	16	0.050	10
0.285	15	0.227	20	0.176	23	0.078	17
0.352	20	0.285	25	0.227	32	0.127	25
0.430	26	0.352	34	0.285	41	0.176	37
0.528	35	0.430	43	0.352	51	0.227	47
0.652	48	0.528	55	0.430	66	0.285	58
0.830	65	0.652	72	0.528	85	0.352	74
		0.830	99	0.652	107	0.430	91
				0.830	144	0.528	115
						0.652	142

Figure (III-35) Continued

56.5°C		51.5°C		42°C		33.5°C	
0.033	5	0.033	14	0.050	65	0.034	115
0.050	22	0.050	40	0.078	105	0.073	220
0.078	39	0.078	62	0.176	206	0.114	335
0.127	57	0.127	90	0.227	273	0.159	460
0.176	81	0.176	121	0.285	360		
0.227	105	0.227	160	0.352	450		
0.285	131	0.285	198				
0.352	163	0.352	265				
0.430	208	0.430	330				
0.528	265						

Figure (III-36)

Arrhenius data for first order reaction of t-butyl chloride

(Rate)x10^4 (sec^{-1})	4 + log (rate)	($10^3/T°K.$)	T°C.
131.	2.116	2.168	188
131.	2.116	2.287	164
131.	2.116	2.374	148
85.0	1.929	2.680	100
85.0	1.929	2.731	93.5
69.5	1.645	2.939	67.5
20.2	1.309	3.033	56.5
13.7	1.136	3.080	51.5
7.80	0.894	3.175	42
3.36	0.526	3.261	33.5

Figure (III-37)

First order kinetic data, isobutyl chloride reaction, $P_o=10^{-2}$

207°C		198°C		187°C		175.5°C		162°C	
$\log \frac{P_o}{P}$	Time	$\log \frac{P_o}{P}$	Time	$\log \frac{P_o}{P}$	Time	$\log \frac{P_o}{P}$	Time	$\log \frac{P_o}{P}$	Time
0.054	100	0.032	95	0.030	90	0.041	175	0.018	120
0.153	345	0.148	395	0.128	470	0.114	640	0.066	520
0.328	680	0.316	845	0.197	795	0.200	1070	0.125	990
0.523	1070	0.506	1335	0.305	1220	0.281	1500	0.183	1540
0.722	1490	0.699	1745	0.432	1710	0.377	1945	0.280	2240

Figure (III-38)

Arrhenius data for first order reaction of isobutyl chloride

(Rate)x10^4 (sec^{-1})	4 + log (rate)	($10^3/T°K.$)	T°C.
4.85	0.685	2.082	207
3.80	0.580	2.122	198
2.55	0.406	2.173	187
1.93	0.285	2.229	175.5
1.23	0.090	2.298	162

Figure (III-39)

First order kinetic data, isobutyl chloride reaction, $P_o=5x10^{-2}$

$\log P_o/P$	Time	$\log P_o/P$	Time	$\log P_o/P$	Time
178°C		176.5°C		167°C	
0.054	125	0.066	215	0.050	175
0.146	395	0.155	560	0.117	495
0.236	730	0.248	965	0.205	990
0.443	1390	0.415	1545	0.301	1525

Figure (III-39) Continued

0.576	1830	0.585	2130	0.398	2075
		0.699	2580		
160°C		153.5°C		143.5°C	
0.036	160	0.037	220	0.036	350
0.094	555	0.092	695	0.073	815
0.165	1080	0.152	1240	0.111	1490
0.237	1645	0.205	1795	0.148	2075
0.310	2215	0.245	2140		

Figure (III-40)

Arrhenius data for first order reaction of isobutyl chloride

(Rate)x10^4 (sec^{-1})	5 + log (rate)	($10^3/T°K.$)	T°C.
3.00	1.475	2.217	178
2.75	1.440	2.224	176.5
1.90	1.279	2.272	167
1.38	1.140	2.308	160
1.075	1.031	2.344	153.5
0.675	0.830	2.400	143.5

Figure (III-41)

First order kinetic data, isobutyl chloride reaction, $P_o=5x10^{-2}$

199.5°C		174.5°C		150°C		150°C		128.5°C	
$\log \frac{P_o}{P}$	Time	$\log \frac{P_o}{P}$	Time	$\log \frac{P_o}{P}$	Time	$\log \frac{P_o}{P}$	Time	$\log \frac{P_o}{P}$	Time
0.277	240	0.053	150	0.031	215	0.064	595	0.004	125
0.724	670	0.258	760	0.169	1325	0.149	1060	0.054	895
1.456	1590	0.453	1630	0.326	2560	0.232	1705	0.112	2040

Figure (III-41) Continued

---	0.673 2075	---	0.304 2275	0.160 3070
	0.987 3020			

Figure (III-42)

Arrhenius data for first order reaction of isobutyl chloride

(Rate)x10^4 (sec^{-1})	5 + log (rate)	($10^3/T^oK.$)	$T^oC.$
9.17	1.962	2.116	199.5
3.23	1.508	2.234	174.5
1.30	1.112	2.363	150
1.30	1.112	2.363	150
0.52	0.707	2.489	128.5

Figure (III-43)

First order and half order data for isobutyl chloride reactions

First reactant dose			Third reactant dose		
$P_o^{\frac{1}{2}}-P^{\frac{1}{2}}$	log P_o/P	Time	$P_o^{\frac{1}{2}}-P^{\frac{1}{2}}$	log P_o/P	Time
0.005	0.045	220	0.013	0.120	150
0.010	0.100	615	0.030	0.310	405
0.018	0.180	1100	0.044	0.500	645
0.027	0.270	1590	0.054	0.680	920
0.035	0.370	2000	0.061	0.810	1205
0.043	0.490	2610	0.073	0.890	1445
0.051	0.610	3215			
0.058	0.755	3700			
0.064	0.880	4155			
0.070	0.960	4620			

Figure (III-44)

First order kinetic data, neopentyl chloride reaction, $P_o=10^{-2}$

log P_o/P	Time	log P_o/P	Time	log P_o/P	Time
210°C		199°C		199°C	
0.133	30	0.096	27	0.038	12
0.271	60	0.197	57	0.079	27
0.411	90	0.276	87	0.125	40
0.549	120	0.379	117	0.176	57
0.687	150	0.487	147	0.234	77
0.815	180	0.602	177	0.301	95
0.952	210	0.704	207	0.380	119
		0.804	237	0.477	146
		0.913	267	0.602	184
		1.005	297	0.777	241
184.5°C		170°C		1.079	326
0.064	30	0.022	15	160°C	
0.120	60	0.058	45	0.021	30
0.185	90	0.090	75	0.045	60
0.245	120	0.128	105	0.068	90
0.310	150	0.171	135	0.095	120
0.380	180	0.213	165	0.117	150
0.446	210	0.265	195	0.146	180
0.530	240	0.296	225	0.172	210
0.572	270	0.324	255	0.206	240
0.635	300	0.358	285	0.236	270
0.711	330	0.405	315	0.258	300

Figure (III-45)

Arrhenius data for first order reaction of neopentyl chloride

(Rate)x10^3 (sec^{-1})	4 + log (rate)	($10^3/T^oK.$)	$T^oC.$
4.55	1.658	2.070	210
3.33	1.522	2.119	199
3.33	1.522	2.119	199
2.12	1.325	2.185	184.5
1.28	1.107	2.257	170
0.856	0.932	2.309	160

Figure (III-46)

First order kinetic data, neopentyl chloride reaction, $P_o=2.5x10^{-2}$

230°C		230°C		215°C		215°C		200°C	
$\log\frac{P_o}{P}$	Time	$\log\frac{P_o}{P}$	Time	$\log\frac{P_o}{P}$	Time	$\log\frac{P_o}{P}$	Time	$\log\frac{P_o}{P}$	Time
0.096	11	0.096	11	0.056	14	0.056	14	0.056	21
0.142	18	0.142	20	0.096	27	0.096	27	0.096	39
0.194	26	0.194	29	0.142	37	0.142	41	0.142	59
0.252	34	0.252	39	0.194	52	0.194	52	0.194	79
0.318	45	0.318	50	0.252	70	0.252	68	0.252	104
0.398	54	0.398	63	0.318	88	0.318	88	0.318	131
0.494	69	0.494	81	0.398	110	0.398	111	0.398	157
0.620	87	0.620	97	0.494	138	0.494	137	0.494	195
0.796	114	0.796	125	0.620	167	0.620	168	0.620	235
				0.796	209	0.796	211	0.796	298

185°C							
0.056	35	0.142	100	0.252	165	0.398	265
0.096	68	0.194	131	0.318	212	0.494	400

Figure (III-47)

Arrhenius data for first order reaction of neopentyl chloride

(Rate)x10^3 (sec^{-1})	3 + log (rate)	($10^3/T^oK.$)	$T^oC.$
6.85	0.835	1.987	230
6.20	0.793	1.987	230
3.74	0.572	2.053	215
3.74	0.572	2.053	215
2.55	0.406	2.113	200
1.48	0.170	2.182	185

Figure (III-48)

Pressure vs. time plot of catalytic and noncatalytic reactions of neopentyl chloride

Catalytic Reaction				Noncatalytic Reaction			
(P_o-P)	Time	(P_o-P)	Time	(P_o-P)	Time	(P_o-P)	Time
0.0020	27	0.0075	177	0.0015	260	0.0026	6490
0.0036	57	0.0080	207	0.0016	1420	0.0029	7290
0.0047	87	0.0084	237	0.0018	2680	0.0032	8200
0.0058	117	0.0088	267	0.0019	3900	0.0035	8860
0.0067	147	0.0090	297	0.0021	5160	0.0039	9640

Figure (III-49)

Kinetic data for half order reaction of 1,2-dichloropropane

$P_o^{\frac{1}{2}}-P^{\frac{1}{2}}$	Time	$P_o^{\frac{1}{2}}-P^{\frac{1}{2}}$	Time	$P_o^{\frac{1}{2}}-P^{\frac{1}{2}}$	Time
204^oC		193.5^oC		184.5^oC	
0.0097	235	0.0056	195	0.0111	625
0.0297	735	0.0143	520	0.0203	1220
0.0526	1180	0.0203	820	0.0293	1785

Figure (III-49) Continued

0.0647	1510	0.0272	1145	0.0337	2355
		0.0388	1585	0.0417	2830
		0.0510	2135	0.0462	3350
		0.0595	2605	0.0542	3840
179.5°C		165°C		165°C	
0.0000	225	0.0000	250	0.0021	410
0.0017	620	0.0030	800	0.0055	1055
0.0075	1420	0.0060	1510	0.0067	1520
0.0140	2080	0.0112	2370	0.0084	2140
0.0219	3000	0.0175	4060	0.0109	2790
0.0279	3720			0.0140	3680

Figure (III-50)

Arrhenius data for half order reaction of 1,2-dichloropropane

(Rate)x10^6 ($torr^{\frac{1}{2}}$/sec)	6 + log (rate)	(10^3/T°K.)	T°C.
43.1	1.635	2.096	204
22.4	1.350	2.143	193.5
13.4	1.120	2.185	184.5
8.12	0.909	2.209	179.5
4.74	0.676	2.282	165
4.13	0.615	2.282	165

Figure (III-51)

Kinetic data for half order reaction of 1,3-dichloropropane

$P_o^{\frac{1}{2}}-P^{\frac{1}{2}}$	Time	$P_o^{\frac{1}{2}}-P^{\frac{1}{2}}$	Time	$P_o^{\frac{1}{2}}-P^{\frac{1}{2}}$	Time
231.5°C		231.5°C		222.5°C	
0.0219	150	0.0224	150	0.0138	140
0.0457	395	0.0358	340	0.0413	550
0.0676	630	0.0625	540	0.0600	875
0.0878	860	0.0799	710	0.0755	1140
		0.1000	880		
212.5°C		202°C		202°C	
0.0114	225	0.0080	210	0.0084	220
0.0304	790	0.0219	790	0.0270	1015
0.0408	1150	0.0322	1290	0.0500	2290
0.0520	1520	0.0434	1910	0.0600	2825
0.0661	1925	0.0626	2780	0.0735	3505
0.0790	2315	0.0726	3260		
		0.0859	3830		

Figure (III-52)

Arrhenius data for half order reaction of 1,3-dichloropropane

(Rate)x10^5 ($torr^{\frac{1}{2}}$/sec)	5 + log (rate)	(10^3/T°K.)	T°C.
9.58	0.981	1.976	231.5
9.58	0.981	1.976	231.5
6.21	0.794	2.016	222.5
3.22	0.507	2.057	212.5
1.76	0.246	2.096	204
1.88	0.275	2.096	204

Figure (III-53)

First order appearance of HCl during reaction of 1,3-dichloro-2,2-dimethylpropane

$\log P_o/(P_{max}-P_o)$	Time	$\log P_o/(P_{max}-P_o)$	Time
0.019	5	0.282	104
0.060	17	0.361	139
0.106	28	0.459	180
0.157	49	0.583	218
0.215	75	0.759	280

Figure (III-54)

First order kinetic data for hydrogen chloride reaction

$\log P_o/P$	Time
0.122	810
0.308	1830
0.435	2935
0.566	3650
0.849	5550

Figure (III-55)

Kinetic data for zero order reaction of methyl chloride

Mole % Methane*	Time
3.4	600
15.8	1500
28.3	2400
36.2	3600
59.6	5100
67.0	6300

* Based on theoretical H; i.e., 100% reaction gives 75 mole % CH_4

APPENDIX - III-A

Standard Heats of Reaction for Titanium with Titanium Halides

Standard Heats of Formation of the Titanium Halides*

X =	F	Cl	Br	I
$Ti-X_2$	-198	-114	-95	-61
$Ti-X_3$	-315	-165	-132	-80
$Ti-X_4$	-370	-179.3	-155	-102

* Values cited are those supplied by the National Bureau of Standards (107), and are in kcal./mole.

Standard Heats of Reaction

$$2\ Ti-X_3 + Ti \rightarrow 3\ Ti-X_2 \qquad \text{(A-3-A - 1}$$

$X = F$, $\Delta H_r = +36$ kcal./mole : $X = Cl$, $\Delta H_r = -12$ kcal./mole

$X = I$, $\Delta H_r = -23$ kcal./mole : $X = Br$, $\Delta H_r = -21$ kcal./mole

$$3\ Ti-X_4 + Ti \rightarrow 4\ Ti-X_3 \qquad \text{(A-3-A - 2}$$

$X = F$, $\Delta H_r = -150$ kcal./mole : $X = Cl$, $\Delta H_r = -122.1$ kcal./mole

$X = I$, $\Delta H_r = -14$ kcal./mole : $X = Br$, $\Delta H_r = -63$ kcal./mole

$$Ti-X_4 + Ti \rightarrow 2\ Ti-X_2 \qquad \text{(A-3-A - 3}$$

$X = F$, $\Delta H_r = -26$ kcal./mole : $X = Cl$, $\Delta H_r = -48.7$ kcal./mole

$X = I$, $\Delta H_r = -20$ kcal./mole : $X = Br$, $\Delta H_r = -35$ kcal./mole

APPENDIX - III-B

Dehydrochlorination Thermodynamics of various Alkyl Chlorides

Using free energy values estimated by the method of Van Krevelin and Chermin (108) and elaborated by Janz (109), calculations have been made which indicate that free energies of reaction are negative above the temperatures listed for the following dehydrochlorination reactions.

Reaction	Temperature at which $\Delta F_r = 0$
$CH_3CH_2\text{-}Cl \rightarrow CH_2{=}CH_2 + HCl$	142°C
$CH_3CH_2CH_2\text{-}Cl \rightarrow CH_3CH{=}CH_2 + HCl$	27°C
$(CH_3)_2CH\text{-}Cl \rightarrow CH_3CH{=}CH_2 + HCl$	31.5°C
$(CH_3)_2CHCH_2\text{-}Cl \rightarrow (CH_3)_2C{=}CH_2 + HCl$	-38.5°C
$(CH_3)_3C\text{-}Cl \rightarrow (CH_3)_2C{=}CH_2 + HCl$	0°C
$(CH_3)_3CCH_2\text{-}Cl \rightarrow (CH_3)_2C{=}CHCH_3 + HCl$	-80.5°C

APPENDIX - IV

Mass Spectral Fragmentation Patterns

A comprehensive presentation of fragmentation patterns for all reactants, pure products and selected, experimentally observed product mixtures is made intractible by the large number of reaction systems which have been studied. Five systems have been selected for inclusion in this appendix. Isopropyl chloride and n-propyl chloride have been included because their reactions are representative of the catalytic and noncatalytic groups of reactants. Neopentyl chloride, n-propyl fluoride and 1,3-dichloropropane have been included because their reactions have exhibited somewhat unique features. The high temperature reaction of isopropyl chloride also has exhibited certain unique features.

Only the important parts of the mass spectra are supplied in the following summaries of peak heights. Mass #28 has not been recorded because this peak had an appreciable and variable background contribution.

n-Propyl Chloride System

	Calibration Spectra			Experimental Spectra	
Mass #	$n\text{-}C_3H_7\text{-}Cl$	C_3H_6	C_3H_8	A	B
27	65.5	46.1	36.8	78.5	62.8
29	59.4	1.0	100.0	100.0	34.0
30	1.6	--	2.1	1.0	0.7
35	2.3	--	--	2.0	0.7
36	14.8	2.1	--	11.5	5.5
37	5.6	11.1	2.1	7.5	12.4
38	10.0	15.3	3.2	15.5	17.3
39	22.8	69.6	11.1	48.5	67.1
40	7.0	26.4	--	12.6	26.0
41	32.8	100.0	9.6	73.0	100.0
42	100.0	58.9	3.2	96.0	74.8
43	14.1	--	17.3	22.5	9.7
44	1.6	--	20.7	13.0	6.9
50	2.3	--	--	1.0	--
52	0.8	--	--	--	--
Rel. Sens. (C_3H_6=1.0)	1.0	1.0	1.84		

A - Reaction of 10^{-2} torr at 0°C on a virgin film, spectrum after 300 seconds. Molar ratios are C_3H_6=30.5, C_3H_8=27.3, $n\text{-}C_3H_7\text{-}Cl$=45.9.

B - Reaction of 10^{-2} torr at 200°C on an extensively reacted film, spectrum after 2685 seconds. Molar ratios are C_3H_6 =74.2, C_3H_8=8.2, $n\text{-}C_3H_7\text{-}Cl$=17.6.

Isopropyl Chloride System

	Calibration Spectra				Experimental Spectra		
Mass #	$i\text{-}C_3H_7\text{-}Cl$	C_3H_6	C_3H_8	$-(i\text{-}C_3H_7)_2$	A	B	C
27	54.5	47.0	35.5	27.0	83.0	46.0	58.0
29	2.0	1.5	100.0	13.0	21.4	2.0	37.5
30	--	--	2.5	--	0.4	1.4	1.0
35	3.5	--	--	--	2.8	14.5	4.1
36	14.5	--	2.0	2.5	19.4	100.0	46.2
37	4.5	13.5	3.0	1.0	11.5	15.5	12.4
38	10.5	17.0	4.5	1.5	19.4	44.2	28.6
39	22.0	75.5	12.5	16.5	54.0	63.0	72.3
40	6.0	28.5	2.5	3.5	17.3	22.8	24.8
41	39.0	100.0	10.5	36.0	82.4	83.0	100.0
42	14.0	58.5	3.5	86.5	39.8	47.5	64.0
43	100.0	2.5	16.5	100.0	100.0	10.5	18.4
44	4.5	--	17.5	6.0	8.2	1.0	6.1
55	--	--	--	4.0			0.5
63-65	6.5	--	--	--			0.2
71	--	--	--	3.0			0.2
Rel. Sens.	1.02	1.0	1.95	2.05			

A - Reaction of 10^{-2} torr at 20°C on a virgin film, spectrum after 300 seconds. (C_3H_6=29.0, C_3H_8=6.5, $i\text{-}C_3H_7\text{-}Cl$=64.5)

B - Catalytic reaction of 10^{-2} torr at 157°C, spectrum after 2685 seconds. (C_3H_6=90.0, $i\text{-}C_3H_7\text{-}Cl$=10.0, note large 35, 36 and 38 peaks for HCl)

C - Reaction of 10^{-2} torr at 222°C. (C_3H_6=86.0, C_3H_8=9.5, $i\text{-}C_3H_7\text{-}Cl$=2.6, $-(i\text{-}C_3H_7)_2$=4.2, note reduced HCl relative to B).

n-Propyl Fluoride System

	Calibration Spectra			Experimental Spectra	
Mass #	$n\text{-}C_3H_7\text{-}F$	C_3H_6	C_3H_8	A	B
27	56.0	44.3	37.0	55.0	52.0
29	35.0	1.5	100.0	43.0	39.5
30	--	--	2.5	1.5	1.1
33	10.5	--	--	--	4.0*
36	3.0	2.1	--	2.1	1.1
37	8.0	11.3	2.0	10.7	11.7
38	11.0	15.3	3.2	16.7	16.7
39	43.0	70.5	12.0	69.5	68.5
40	14.5	25.9	2.0	25.8	26.0
41	64.5	100.0	11.0	100.0	100.0
42	35.4	58.8	4.0	59.0	60.0
43	9.0	1.4	18.4	9.6	8.8
44	17.5	--	22.0	14.0	13.4
45	5.0	--	--	--	--
46	27.0	--	--	--	--
47	100.0	--	--	--	2.2
Rel. Sens.	0.56	1.0	1.84		

A - Reaction of 10^{-2} torr at $0^{\circ}C$ on a virgin film, spectrum after 300 seconds. (C_3H_6=80.4, C_3H_8=19.6, $n\text{-}C_3H_7\text{-}F$=0.0)

B - Reaction of 10^{-2} torr at $70^{\circ}C$ on an extensively reacted film, spectrum after 965 seconds. (C_3H_6=79.4, C_3H_8=17.3, $n\text{-}C_3H_7\text{-}F$=3.3)

* - Throughout the course of the n-propyl fluoride reactions with previously reacted films, abnormally large mass #33 peaks remained after reaction.

1,3-Dichloropropane System

Mass #	Calibration Spectra			Exp'tl. Spectrum
	$Cl-CH_2CH_2CH_2-Cl$	Cyclo-propane	C_3H_6	A
27	65.5	47.0	46.1	42.4
29	--	1.0	1.0	--
30	--	--	--	--
35	10.0	--	--	--
36	variable	5.3	2.1	5.0
37	9.0	11.5	11.1	10.5
38	variable	15.5	15.3	14.5
39	37.0	78.5	69.5	73.2
40	16.0	34.0	26.4	31.6
41	100.0	100.0	100.0	100.0
42	15.0	99.0	58.9	94.0
49	16.5	--	--	--
51	4.7	--	--	--
63	6.0	--	--	--
78	17.5	--	--	--
80	5.0	--	--	--
Rel. Sens.	0.58	0.87	1.0	

A - Reaction of 10^{-2} torr at 245°C on an extensively reacted film, spectrum after 2905 seconds. (1,2-dichloropropane =0.0, propylene = 10.0, cyclopropane = 90.0)

Neopentyl Chloride System

	Calibration Spectra				Exp'tl. Spectra	
Mass #	Neopentyl-Cl	Neopentane	Isobutylene	2-Methyl-butene-2	A	B
27	48.0	30.0	19.1	54.5	44.0	56.0
29	93.0	79.5	12.7	60.8	74.0	58.0
30	1.0	2.0	--	2.6	0.2	2.6
35	2.5	--	--	--	0.5	16.0
36	23.5	1.5	1.8	5.0	10.3	100.6
37	3.0	1.5	3.6	6.5	3.2	10.3
38	13.0	3.0	5.8	12.0	6.6	38.0
39	42.5	25.0	44.5	79.0	41.0	63.5
40	6.0	--	10.9	13.0	5.9	8.5
41	92.5	83.0	100.0	78.5	100.0	73.0
42	8.2	8.8	2.7	59.0	9.4	54.2
43	8.5	8.0	--	7.5	10.2	8.8
53	3.5	1.0	--	14.0	1.0	14.0
55	51.5	4.0	12.3	100.0	44.2	100.0
56	--	--	22.5	--	8.0	--
57	100.0	100.0	--	--	94.0	--
70	--	--	--	10.0	--	12.0
Rel. Sens.	1.0	1.67	1.5	1.49		

A - Reaction of 10^{-2} torr at 20°C on a virgin film, spectrum after 300 seconds. (neopentyl chloride≈90, isobutylene≈10)

B - Reaction of 5×10^{-2} torr at 200°C on an extensively reacted film. Product spectrum essentially is 2-methylbutene-2 and HCl.

REFERENCES

1. A.S. Matlack and D.S. Breslow, J. Polym. Sci., Part A-3, 2583 (1965).

2. G.C. Ray and F.N. Ruehlen, U.S. Patent 3177188 (1965).

3. K. Ziegler, Belgium Patents 533362, 534792 and 534888 (1954); cited in, R. Feld and P.F. Cowe, "The Organic Chemistry of Titanium", Butterworths, London, 1965, Chapter 11.

4. F.G. Allen, J. Eisinger, H.D. Hagstrum and J.T. Law, J. Appl. Phys., 30, 1563 (1959).

5. R.W. Roberts and T.A. Vanderslice, "Ultrahigh Vacuum and its Applications", Prentice Hall Inc., Englewood Cliffs, New Jersey, 1963, p 3.

6. R.W. Roberts and L.E. St. Pierre, Science, 147, 1529 (1965).

7. P.A. Anderson, Phys. Rev., 47, 958 (1935).

8. R.T. Bayard and D. Alpert, Rev. Sci. Instrum., 21, 571 (1950).

9. R.W. Roberts, General Electric Co., Research and Development Report #67-C-087, Schenectady, New York, (1967).

10. J.R. Anderson, R.B. Baker and J.V. Sanders, J. Catal., 1, 443 (1962).

11. P.E. McElligot and R.W. Roberts, J. Chem. Phys., 46, 273 (1967).

12. J.R. Anderson and R.B. Baker, J. Phys. Chem., 66, 482 (1962).

13. P.J. Estrup and J. Anderson, J. Chem. Phys., 46, 567 (1967).

14. G. Ehrlich, Disc. Faraday Soc., 41, 7 (1966).

15. R.L. Burwell Jr., Chem. and Eng. News, 44, (34), 56 (1966).

16. G.C. Bond, "Catalysis by Metals", Academic Press, London, 1962, Chapters 8 - 10.

17. R.W. Roberts and R.S. Owens, J. Science, 2, 69 (1966).

18. N. Cabrera and F.N. Mott, Rep. Progr. Phys., 12, 163 (1949)

19. G.C. Bond, "Catalysis by Metals", Academic Press, London, 1962, Chapter 20.

20. G.C. Bond, "Catalysis by Metals", Academic Press, London, 1962, Chapters 11 - 19.

21. B.M.W. Trapnell, Proc. Roy. Soc., Ser. A, 218, 566 (1953).

22. B.M.W. Trapnell, Trans. Faraday Soc., 52, 1618 (1956).

23. R.W. Roberts, Brit. J. Appl. Phys., 14, 485 (1963).

24. M.J. Mindel and S.R. Pollack, J. Phys. Chem. Solids, 30, 993 (1969).

25. R.W. Roberts and R.S. Owens, Nature, 200, 357 (1963).

26. G.W. Rowe, Brit. J. Appl. Phys., 7, 152 (1956).

27. R.W. Roberts, R.S. Owens and E.D. Brown Jr., Proc. Instrum. Mech. Eng., 182, 407 (1968).

28. J.S. Campbell, R.L. Moss and C. Kemball, Trans. Faraday Soc., 56, 1481 (1960).

29. M.J. Duell, B.J. Davis and R.L. Moss, Disc. Faraday Soc., 41, 43 (1966).

30. M.J. Duell and R.L. Moss, Trans. Faraday Soc., 56, 1487 (1960).

31. J. Anderson, J. Phys. Chem. Solids, 16, 291 (1960).

32. J. Anderson and J. Gani, J. Phys. Chem. Solids, 23, 1087 (1962).

33. R. Kh. Burshtein and M.D. Surova, Dokl. Akad. Nauk S.S.S.R. 61, 75 (1948).

34. R. Kh. Burshtein and N.A. Shurmovskaya, Surface Sci., 2, 210 (1964).

35. C.M. Quinn and M.W. Roberts, Trans. Faraday Soc., 60, 899 (1964).

36. R.G. Jones and H. Gilman, Chem. Rev., 54, 835 (1954).

37. E. Frankland, a) Ann. Chem., 71, 171 (1849).
b) Ann. Chem., 71, 213 (1849).

38. D.T. Hurd and E.G. Rochow, J. Amer. Chem. Soc., 67, 1057 (1945).

39. F.A. Cotton, Chem. Rev., 55, 551 (1955).

40. G.E. Coates and F. Glocking, in "Organometallic Chemistry", H. Zeiss, Ed., Reinhold, New York, N.Y., 1960, p 426.

41. E.O. Fischer and G. Buerger, Z. Naturforsch., B, 16, 702 (1961); cited in, M. Dub, Ed., "Organometallic Compounds", Springer-Verlag Inc., New York, N.Y., 1966, Vol I, p 671.

42. V.A. Shushunov and A.P. Aurov, J. Russ. Phys. Chem., (English Translation), 23, 1197 (1949).

43. E. Wiberg and R. Bauer, Chem. Ber., 85, 593 (1952).

44. J.R. Anderson and B.H. McConkney, J. Catal., 9, 263 (1967).

45. J.R. Anderson and B.H. McConkney, J. Catal., 11, 54 (1968).

46. J.R. Lacher, A. Kianpour, F. Oelting and J.D. Park, Trans. Faraday Soc., 52, 1500 (1956).

47. J. Addy and G.C. Bond, Trans. Faraday Soc., 53, 377 (1957).

48. J.S. Campbell and C. Kemball, Trans. Faraday Soc., 57, 809 (1961).

49. J.S. Campbell and C. Kemball, Trans. Faraday Soc., 59, 2583 (1963).

50. R. Coeckelbergs, A. Frennet, P.A. Gosselain and M.J. Van der Venne, J. Chem Phys., 23, 1731 (1955).

51. R. Coeckelbergs, P.A. Gosselain and A. Frennet, Bull. Soc. Chim. Belges, 65, 229 (1956).

52. R. Coeckelbergs, A. Crucq, A. Frennet and G. Lienard, J. Chim. Phys., 56, 967 (1959).

53. R. Coeckelbergs, P.A. Gosselain and M.J. Van der Venne, Bull. Soc. Chim. Belges, 64, 798 (1955).

54. R.P. Eischens, S.A. Francis and W.A. Pliskin, J. Phys. Chem., 60, 194 (1956).

55. C.H. Amberg, in "The Solid-Gas Interface", E.A. Flood, Ed., Marcel Dekker Inc., New York, N.Y., 1967, Vol. II, p 869.

56. J.J. Rooney, J. Catal., 2, 57 (1963).

57. J.P. Collman, Accounts of Chem. Res., 1, 136 (1968).

58. L. Vaska, Accounts of Chem. Res., 1, 315 (1968).

59. L.R. Burwell Jr. and J.B. Peri, Ann. Rev. Phys. Chem., 15, 131 (1964).

60. G.E. Coates, M.L.H. Green, P. Powell and K. Wade, "Principles of Organometallic Chemistry", Methuen and Co. Ltd., London, 1968, p 14.

61. A. Maccoll, Advan. Phys. Org. Chem., 3, 91 (1965).

62. D.F. Herman and W.K. Nelson, J. Amer. Chem. Soc., 74, 2693 (1952).

63. D.F. Herman and W.K. Nelson, J. Amer. Chem. Soc., 75, 3877 (1953).

64. G.A. Razuvaev and V.N. Latyaeva, Organometal. Chem. Rev., 2, 349 (1967).

65. H.J. Berthold and G. Groh, Z. Anorg. Allg. Chem., 319, 230 (1963).

66. C. La Lau, Rec. Trav. Chim., 84, 429 (1965).

67. H.H. Brintzinger, J. Amer. Chem. Soc., 89, 6871 (1967).

68. H. de Vries, Rec. Trav. Chim., 80, 866 (1961).

69. I.A.M. Rodriguez and H.M. VanLooy, J. Polym. Sci., Part A-4, 1951 (1966).

70. P. Cossee, J. Catal., 3, 80 (1964).

71. R.W. Roberts and T.A. Vanderslice, "Ultrahigh Vacuum and its Applications", Prentice Hall Inc., Englewood Cliffs, New Jersey, 1963, pp 122 - 134.

72. S. Dushman, "Scientific Foundations of Vacuum Technique", J. Wiley and Sons, New York, N.Y., 1962, pp 673 - 688.

73. R.W. Roberts, Brit. J. Appl. Phys., 14, 537 (1963).

74. H. Ishii and K. Nakayama, Trans. Nat'l. Vac. Symp. 8th, 1, 519, (1962).

75. A.E. de Vries and P.K. Rol, Vacuum, 15, 135 (1965).

76. R.W. Dekker, J. Appl. Phys., 25, 441 (1954).

77. S. Dushman, "Scientific Foundations of Vacuum Technique", J. Wiley and Sons, New York, N.Y., 1962, p 709.

78. V.L. Stout and M.D. Gibbons, J. Appl. Phys., 26, 1488 (1955).

79. J. Barksdale, "Titanium, its Occurrence, Chemistry and Technology", Ronald Press, New York, N.Y., 1966, p 60.

80. K.J. Laidler, "Chemical Kinetics", McGraw-Hill Book Co., 1965, p 267.

81. A.L.G. Rees, "Chemistry of the Defect Solid State", Methuen and Co. Ltd., London, 1954, p 11.

82. S. Dushman, "Scientific Foundations of Vacuum Technique", J. Wiley and Sons, New York, N.Y., 1962, p 544.

83. K. Hauffe and A. Rahmel, Z. Phys. Chem., 199, 152 (1952).

84. R.S. Nyholm, Proc. Int. Congr. Catal., 3rd, 1, 25 (1964).

85. T.M. Dunn, D.S. McClure and R.G. Pearson, "Some Aspects of Crystal Field Theory", Harper and Row Inc., New York, N.Y., 1965, p 78.

86. H. Rickert, Z. Phys. Chem. (N.F.), 23, 355 (1960).

87. H. Rickert and C. Wagner, Z. Phys. Chem. (N.F.), 31, 32 (1961).

88. J. Kummer and M.E. Milberg, Chem. and Eng. News, 47, (21), 90 (1969).

89. K. Hauffe, "Oxidation of Metals", Plenum Press, New York, N.Y., 1965, p 255.

90. P.B. Chock and J. Halpern, J. Amer. Chem. Soc., 91, 582 (1969).

91. C.D. Nenitzescu, Rev. Roum. Chim., 9, 5 (1964).

92. H.C. Brown and M. Grayson, J. Amer. Chem. Soc., 75, 6825 (1953).

93. E.S. Gould, "Mechanism and Structure in Organic Chemistry", Holt, Rinehart and Winston Inc., New York, N.Y., 1959, p 449.

94. C. Beerman and H. Bestian, Angew. Chem., 71, 618 (1959).

95. C. Beerman, German Patent 1089382 (1961).

96. G.A. Olah, "Friedel-Crafts and Related Reactions", Interscience Publishers, New York, N.Y., 1963, Vol. I, p 263.

97. L. Reich and A. Schindler, "Polymerization by Organometallic Compounds", Interscience Publishers, New York, N.Y., 1966, p 307.

98. J. Barksdale, "Titanium, its Occurrence, Chemistry and Technology", Ronald Press, New York, N.Y., 1966, p 67.

99. P.B. Shewman, "Diffusion in Solids", McGraw-Hill Book Co., New York, N.Y., 1963, Chapter 6.

100. K.J. Laidler, "Chemical Kinetics", McGraw-Hill Book Co., New York, N.Y., 1965, p 265.

101. O. Toyama, Rev. Phys. Chem. Japan, 11, 153 (1937).

102. K.J. Laidler and R.E. Townshend, Trans. Faraday Soc., 57, 1590 (1961).

103. J.D. Roberts and M.C. Caserio, "Basic Principles of Organic Chemistry", W.A. Benjamin Inc., New York, N.Y., 1964, p 355.

104. F.C. Whitmore, F.C. Whittle and A.H. Popkin, J. Amer. Chem. Soc., 54, 3431 (1932).

105. A. Maccoll and E.S. Swinbourne, J. Chem. Soc., 149 (1964).

106. J.R. Anderson and N.R. Avery, J. Catal., 5, 446 (1966).

107. F.D. Rossini, D.D. Wagman, W.H. Evans, S. Levine and I. Jaffe, "Selected Values of Chemical Thermodynamic Properties, Circular of the National Bureau of Standards, #500", U.S. Dept. of Commerce, N.B.S., Washington, D.C., 1951, pp 305 - 307.

108. D.W. Van Krevelin and H.A.G. Chermin, Chem. Eng. Sci., 1, 66 (1951).

109. G.J. Janz, "Estimation of Thermodynamic Properties of Organic Compounds", Academic Press Inc., New York, N.Y., 1958, p 60.